University of Venda
Creating Future Leaders

UNIVERSITY OF VENDA

THOHOYANDOU, LIMPOPO PROVINCE



SCHOOL OF MATHEMATICAL AND NATURAL SCIENCES

DEPARTMENT OF CHEMISTRY

COMPUTATIONAL STUDY OF ANTIMALARIAL PYRAZOLE ALKALOIDS FROM *NEWBOULDIA LAEVIS IN VACUO AND IN SOLUTION*

BY

KABUYI MIREILLE BILONDA

This thesis is submitted in fulfillment of the requirements for the degree of Master in Chemistry.

SUPERVISOR: PROF. LILIANA MAMMINO

Department of Chemistry, University of Venda, Thohoyandou, South Africa

CO-SUPERVISOR: Dr. CATERINA GHIO

Institute for Physico-Chemical Processes Molecular Modelling Lab, Pisa, Italy

February 2014

© University of Venda

University of Venda
Creating Future Leaders

Declaration

I, Kabuyi Mireille Bilonda hereby declare that the thesis for the Master degree submitted by me has never previously been submitted for a higher degree or diploma at this or any other University. And that to the best of my knowledge and belief, the thesis contains no material previously published or written by another person except where due reference is made in the thesis itself.

Signature..... Date..01-03-2014

Student number 11629612

Signature..Liliana Mammino..... Date..01-03-2014

Supervisor: Prof. Liliana Mammino

Signature..... Date..01-03-2014

Co-supervisor: Dr. Caterina Ghio

© University of Venda

University of Venda
Creating Future Leaders

Abstract

This thesis is concerned with the computational study of pyrazole alkaloids having anatimalarial propperties by means of electronic structure methods. The pyrazole alkaloids studied in the present work are the following: withasomnine (3-phenyl-5,6-dihydro-4H-pyrrolo[1,2-b]pyrazole) and newbouldine (3-phenyl -3a,5,6-tetrahydro-3H-pyrrolo[1,2-b]pyrazole) with their corresponding p-hydroxy and p-methoxy. They were isolated from the root-bark of *Newbouldia laevis* (an endemic plant in DR Congo traditionally used for the treatment of malaria, diarrhoea and other disease). The antimalarial activity of these compounds is intriguing because it appears rarely in alkaloids containing pyrazole groups. This makes their computational study particulary interesting to search for information thay may contribute to a better understanding of their biological activity and to the design of molecular structures with enhanced biological activity. This is the reason of focusing the efforts on the investigation of chemical and physical properties of these alkaloids molecules.

The molecules were firstly studied *in vacuo* and secondly in three different solvents. These solvents (chloroform, acetonitrile and water) are characterized by different polarities and different H-bonding abilities. The octanol/water partition coefficients of these molecules suggest a non-negligible presence in media with broad polarity-range. Experimental studies on the withasomnine and 4'-hydroxywithasomnine nitro derivatives have shown an enhancement in antimalarial activity of these molecules, therefore the studies were extended on these nitro derivatives.

Wave functions and electron density methods (HF,DFT/B3LYP,MP2) combined with different basis sets (6-31G(d,p), 6-31+G(d,p), 6-31++G(d,p), 6-311G(d,p), 6-311+G(d,p), 6-311++G(d,p) were utilised to compare their performance for compounds of this type, also in view of a future study extending to other compounds of the same class. Quantum chemical calculations on these molecules in solution were carried out using the polorisable contininuum model (PCM). The study in water solution was complemented by the study of adducts with explicit water molecules, because of the presence of atoms (e.g: O, N) capable of forming hydrogen bonds with water molecules.

The results provide a comprehensive picture of the molecular properties of these compounds, such as conformational preferences in *vacuo* and in solution, bond rotational scans, harmonic

© University of Venda

University of Venda
Creating Future Leaders

vibrational frequencies, solvent effects, preferred interactions with explicit water molecules. The results in solution show the influence of the solvent on the molecular structures (including the characteristics of the intramolecular hydrogen bond) and the energy aspects of the solution process. The results of the study of adducts with explicit water molecules show possible preferred arrangements of water molecules around the studied pyrazoles alkaloids moleculeand may facilitate the interpretation of the results in water solution.

Different computational methods (HF, MP2 and DFT) were utilised, depending on the affordability considerations for the structural sizes, in order to allow to obtain an assessment of the performance of less expensive methods like HF or DFT, in view of their utilisation for other classes of alkaloids structures for which more sophisticated methods (like MP2) remain unaffordable.

Keywords: antimalarials of natural origin, conformational preferences of pyrazoles alkaloids, electronic structure methods, *Newbouldia Laevis*, Polarizable Continuum Model (PCM), solute-solvent interactions, withasomnine.

© University of Venda

University of Venda
Creating Future Leaders

Dedication

To all people suffering of malaria disease may find in this master work a relief and my compassion to their pain.

To my dear husband Tshishimbi Muya, Jules-Christophe for your presence beside me and your continuous encouragement during my master study.

I dedicate this work

Mireille, K Bilonda

© University of Venda

University of Venda
Creating Future Leaders

Acknowledgements

First of all, I would like to express my sincere gratitude to my mentor, Professor Dr. Liliana Mammino for giving me the opportunity of doing my research in computational chemistry unit and for giving me nice place in her computational chemistry lab at the University of Venda. Her advices, strictness, availability and guidance were of great importance in the accomplishment of this work. Without her help the realization of this master thesis should not be possible. I appreciate her acknowledge and her time taking for correcting this master thesis.

I am grateful to my co-supervisor Dr. Caterina Ghio of the Institute for Physico-Chemical Processes – Molecular Modelling Lab (Pisa), for her interest in this work.

I owe special thanks to all staff members of the Department of Chemistry at the University of Venda, especially Mr.P. MOJAPELO, for all they have done to make my life easier at the University of Venda.

I owe thank to all the professors of the Department of Chemistry at the University of Kinshasa. I am grateful to all colleagues and friends who help me to be inserted in the social live at Venda, especially to Tshiwawa Tendamuzimu, Sedzani Netavani, Isabelle Kouame and Zongo Kom.

Especially, I would like to give my deep thanks to my family for their unconditional support and encouragement.

Mireille Bilonda

© University of Venda

University of Venda
Creating Future Leaders

Acronyms

ACE:	Alternating Conditional Expectation
AM1:	Austin Method, version 1
AMBER:	Assisted Model Building with Energy Refinement
ACT:	Artemisinin-based Combination Therapy
AO:	Atomic Orbital
B3LYP:	Becke 3-Parameter (Exchange), Lee, Yang and Parr
BSSE:	Basis Set Superposition Error
CC:	Coupled Cluster
CNDO/2	Complete Neglect of Differential Overlap, *version2*
CI:	Configuration Interactions
CP:	Counterpoise
DFT:	Density Functional Theory
GGA:	Generalized Gradient functionals
GTO:	Gaussian Type Orbital
HF:	Hartree-Fock
IEF:	Integral Equation Formalism
HOMO:	Highest Occupied Molecular Orbital
LCAO:	Linear Combination of Atomic Orbitals
LDA:	Local Density Functionals
LUMO:	Lowest Unoccupied Molecular Orbital
MM:	Molecular Mecanism
MO:	Molecular Orbital
MP2:	Möller-Plesset second perturbation theory
MCSCF:	Multi-Configurations Self Consistent Field
PES:	Potential Energy Surface
PCM:	Polarizable Continuum Model
PLS:	Partial Least Squares
PM3:	Parametrization Model, version 3
RHF:	Restricted Hartree-Fock
SCF:	Self-Consistent Field
SCRF:	Self-Consistent Reaction Field models

© University of Venda

University of Venda
Creating Future Leaders

STO: Slater Type Orbital

UHF: Unrestricted Hartree-Fock

QSAR: Quantitative Structure Activity Relationships

WHO: World Health Organization)

© University of Venda

University of Venda
Creating Future Leaders

List of figures in text

1. **Figure 1.1:** Some of the most commonly used antimalarial drugs. Page 2
2. **Figure 1.2.** Pyrazole alkaloids isolated from *Newvouldia laevis* and their derivatives. Page 6
3. Figure 2.1. Potential energy surface showing minima, transition-states saddle points, second order saddle point, reaction paths, and a valley ridge inflection point. Page 10
4. **Figure 2.2.** Graphical illustration of the variation of 1ψ (1s) using STO, STO-1G, STO-2G and STO-3G basis sets. Page 18
5. **Figure2.3.** Examples of intramolecular hydrogen bond (a) and intermolecular hydrogen bond (b). Page 32
6. **Figure 4.1.** Optimized geometries of pyrazole alkaloids of natural origin considered in this study and acronyms utilised (A: withasomnine. B: p-hydroxy derivative of withasomnine. D: p-methoxy derivative of withasomnine. E: newbouldine. F: p-hydroxy derivative of newbouldine. G: p-methoxy derivative of newbouldine) computed at MP2/6-31++G(d,p) level. Page 47
7. **Figure4.2.** Nitroderivatives of withasomnine n-A (left) and p-hydroxy derivative of withasomnine n-B (right) considered in this study and acronyms utilised to denote them. Page 48
8. **Figure 4.3.** Atom numbering utilised for all alkaloids and nitroderivatives compounds considered in this study. Page 49
9. **Figure 4.4.** Scan (energy versus C11–C7–C4–C5 torsion angle of the rotation of the C7–C4 bond between the two ring systems in compound A (left) and E (right). HF/6-31G (d,p) (—■—), DFT/B3LYP/6-31G (d,p) (—●—) and MP2/6-31G(d,p) (—▼—) results. Page 51
10. **Figure 4.5.** Scan (energy versus C2 –C1 – O15 – H27 torsion angle of the rotation of the C1 –O27 bond in compound B (left) and scan (energy versus C2 –C1 – O15 – H29 torsion angle) of C1-O15 bond in compound F (right). HF/6-31G (d,p) (—■—), DFT/B3LYP/6-31G(d,p) (—●—) and MP2/6-31G(d,p) (—▼—) results. Page 52
11. **Figure 4.6.** Scan the rotation of OH in phenol. HF/6-31G (d,p) (—■—), DFT/B3LYP/6-31G(d,p) (—●—) and MP2/6-31G(d,p) (—▼—) results. Page 52
12. **Figure 4.7.** Scan (energy versus C2 –C1 – O15 – H27 and C11-C7-C4-C5 torsion angles) of the rotation of the C1 –O15 bond and C7-C4 bonds in compound B computed at HF/6-31G (d,p). Page 53
13. **Figure 4.8**. Scan (energy versus C6–C1–O15–C27 torsion angle) of the rotation of the C27–O15 bond in compound D (left) and Scan (energy versus C6 –C1 – O15 – C29 torsion angle) of the rotation of the C29–O15 bond in compound G (right) in vacuo.HF/6-31G (d,p) (—■—), DFT/B3LYP/6-31G(d,p) (—●—) and MP2/6-31G(d,p) (—▼—) results. Page 54
14. **Figure 4.9.** Scan (energy versus C11–C7– C4–C5 torsion angle of the rotation of the C4–C7 bond in compound n-A. HF/6-31G (d,p) (—■—), DFT/B3LYP/6-31G(d,p) (—●—) results. Page 55
15. **Figure 4.10.** Scan (energy versus C2–C1– N15– O27 torsion angle of the rotation of the C1–N 15 bond in compound n-A. HF/6-31G (d,p) (—■—), DFT/B3LYP/6-31G(d,p) (—●—) and MP2/6-31G(d,p) (—▼—) results. Page 56
16. **Figure 4.11**. Scan rotation of the NO2 in nitrobenzene. HF/6-31G (d,p) (—■—),

© University of Venda

University of Venda
Creating Future Leaders

DFT/B3LYP/6-31G(d,p) (—●—) and MP2/6-31G(d,p) (—▼—) results. Page 56

17. **Figure 4.12.** Scan (energy versus C6 –C1 – O15 – H27 torsion angle) of the rotation of the OH group in compound n-B. HF/6-31G (d,p) (—■—), DFT/B3LYP/6-31G(d,p) (—●—) and MP2/6-31G(d,p) (—▼—) results. Direction of rotation ↻. Page 57
18. **Figure 4.13.**Geometries of the conformers of the compounds having more than one conformer. Page 59
19. **Figure 4.14.** Scan (energy versus C11–C7–C4–C5 torsion angle) of the rotation of the C4–C7 bond between the two rings in compound A *in vacuo* and in the three solvents considered. HF/6-31G(d,p) results in vacuo (—▲—), in chloroform (—▼—), in acetonitrile (—■—), and in water (—●—).Direction of rotation ↻. Page 61
20. **Figure 4.15.** Scan (energy versus C2–C1–O15–H27 torsion angle) of the rotation of the C1–O15 bond in compound B *in vacuo* and in the three solvents considered. HF/6-31G(d,p) results in vacuo (—▲—), in chloroform (—▼—), in acetonitrile (—■—) and in water (—●—). Direction of rotation ↻. Page 61
21. **Figure 4.16.** Scan (energy versus C6–C1–O15–C27 torsion angle) of the rotation of the C27–O15 bond in compound D *in vacuo* and in the three solvents considered. DFT/B3LYP/6-31G(d,p) results in vacuo (—▲—), in chloroform (—▼—), in acetonitrile (—■—) and in water (—●—).Direction of rotation ↻. Page 62
22. **Figure 4.17.** Scan (energy versus C2–C1–N15–O27 torsion angle) of the rotation of the C1–N15 group in compound n-A *in vacuo* and in the three solvents considered. HF/6-31G(d,p) results in vacuo (—▲—), in chloroform (—▼—), in acetonitrile (—■—) and in water (—●—).Direction of rotation ↻. Page 62
23. **Figure 4.18.** Scan (energy versus C6–C1–O15–H27 torsion angle) of the rotation of the OH group in compound n-B *in vacuo* and in the three solvents considered. HF/6-31G(d,p) results *in vacuo* (—▲—), in chloroform (—▼—), in acetonitrile (—■—) and in water (—●—).Direction of rotation ↻. Page 64
24. **Figure 4.19**. Calculated IR spectra of compounds A, B, D, E, F, G, n-A and n-B1 at MP2/6-31G(d,p). Page 66
25. **Figure 4.20**. HOMO-LUMO energy gaps computed using HF and MP2 calculations with different basis sets for compounds A (—■—), B (—●—), D (—▲—), E (—▼—), F (—◆—) and G (—◀—). Page 67
26. **Figure 4.21.** Variation of the total electronic energy with respect to the size of the basis set for A (—■—), B (—●—), D (—▲—), E (—▼—), F (—◆—) and G (—◀—) using the HF method. The HF energy is set to zero for comparison. Page 69
27. **Figure 4.22.** Comparison in stabilization energy between A (—■—), B (—●—), D (—▲—), E (—▼—), F (—◆—) and G (—◀—) compounds in different solvents computed at HF/6-31G(d,p) using HF. Page 70
28. **Figure 4.23**. ΔG_{solv}(a) and G_{el}(b) energies of A, B, D, E, F and G with various methods in chloroform(—▼—), acetonitrile (—■—)and water (—●—)solvent. Solid and doted dashed lines in figures (c-d) correspond to DG solv and DG elec, respectively. Page 71
29. **Figure 4.24**. Optimized geometries of the calculated adducts with explicit water molecules for the compounds considered. Page 73

© University of Venda

University of Venda
Creating Future Leaders

30. **Figure 4.25.** Interaction energy (kcal/mol) of the calculated adducts with explicit water molecules. Page 76
31. **Figure 5.1.** Schemes, names and acronyms of all alkaloids and nitroderivatives investigated. Page 188

© University of Venda

University of Venda
Creating Future Leaders

List of Tables N° page

1. **Table 3.1.** Standard acronyms and abbreviations. 41
2. **Table 4.1.** Bond lengths of the skeleton of the calculated molecules in vacuo, the results of different calculation methods. 78
3. **Table 4.2.** Bond lengths of the skeleton of molecules A, B, D, E, F and G in vacuo, from the results of different calculation methods with 6-311G (d,p) , 6-311+G(d,p) and 6-311++G(d,p) basis sets. 82
4. **Table .4.3.** Bond angles of the skeleton of molecules A, B, D, E, F and G in vacuo, from the results of different calculation methods 85
5. **Table 4.4** Torsion angles of the skeleton of molecules A, B, D, E, F and G in vacuo, from the results of different calculation methods 89
6. **Table 4.5.** Relative energies of the conformers of compounds A, B, D, E, F and G in different media, from the results of different calculation methods. 97
7. **Table 4.6.** Reference energies in Hartree of the conformers of compounds A, B, D, F and G in different media, from the results of different calculation methods. 101
8. **Table 4. 7.** Octanol/water partition coefficients of the compounds considered in this study. 102
9. **Table 4.8.** Relative energy of the two conformers of compound n-B corresponding to the lowest energy orientation of the rings and differing by the presence or absence of the intramolecular hydrogen bond between the OH group and the NO_2 group. Results from different calculations methods, in vacuo and in the three solvents considered.103
10. **Table4.9.** Bond lengths of the skeleton of the calculated molecules in different media and in the results of different calculation methods. 104
11. **Table 4.10.** Parameters of the intramolecular hydrogen bond in the lowest energy conformer of compound n-B, from the results of different calculation methods and in the media considered. 125
12. **Table 4.11.** Dipole moments of the calculated compounds in vacuo and in the three solvents considered. Results from different calculation methods. 126
13. **Table 4.12.** IR frequencies of relevant bonds (harmonic approximation) in different media.The frequencies have been scaled by the following factors: 0.9024^a, 0.92^b, 0.961^a , 0.9857^b and 0.9356^a for respectively HF, HF+, DFT, DFT+ and MP. 130
14. **Table 4.13**. Frequency (harmonic approximation) and Red shifts of the IR frequency (in parentheses) of the OH group in compound n-B in different media. The reference is the frequency of the OH group in compound B.The frequencies have been scaled by the following factors: 0.9024^a, 0.92^b, 0.961^b, 0.9857^b and 0.9356^a for respectively HF, HF+, DFT, DFT+ and MP2. 136
15. **Table 4.14.** HOMO-LUMO energy difference of the calculated compounds in vacuo and in the three solvents considered. Results from different calculation methods. 136
16. **Table 4.15.** Shapes of the frontier orbitals (LUMO and HOMO) and close-to-HOMO molecular orbitals (HOMO-1, HOMO-2, and HOMO-3) for the calculated compounds *in vacuo*, from the results of different calculation methods. 140

© University of Venda

University of Venda
Creating Future Leaders

17. **Table4.16.** Shapes of the frontier orbitals (HOMO and LUMO) and close-to-HOMO molecular orbitals (HOMO-1, HOMO-2, and HOMO-3) for the calculated compounds in different media. HF/6-31G (d,p) results. 155
18. **Table 4.17.** Natural charges (NBO) on the electronegative atoms and the atoms adjacent to them in the calculated compounds, in different media. Results from different calculation methods. 164
19. **Table 4.18.** Solvent effect (ΔG_{solv}) and its electrostatic component (G_{el}) for the calculated compounds in the three solvents considered. Results from different calculation methods. 174
20. **Table 4.19.** Comparison of the geometries of the isolated molecule, of the same molecule in water solution, and when it is the central molecule in an adduct with explicit water molecules. HF/6-31G (d,p) results. 181
21. **Table 4.20.** Comparison of the parameters of the intramolecular hydrogen bond of the lowest energy conformer of compound n-B (conformer n-B1) in the isolated molecule. in water solution and in adducts with explicit water molecules. HF/6-31G (d,p) results. 185
22. **Table 4.21.** Bond length of the intermolecular hydrogen bonds in the calculated adducts with explicit water molecules. HF/6-31G (d,p) results. 183
23. **Table 4.22.** Comparison of the bulk solvent effect (DG_{solv}) and its electrostatic component (G_{el}) for the calculated adducts with explicit water molecules and for the corresponding uncomplexed molecules in water solution. HF/6-31G (d,p) results. 184
24. **Table S 1 Results in vacuo for calculations with the 6-311G (d.p) basis set** The results are compared with the corresponding results from using the 6-31G (d.p) basis sets, with the same methods (HF, MP2 and DFT/B3LYP). considering also the addition of diffuse functions only on the heavy atoms or on both the heavy atoms and the hydrogen atoms. 185

© University of Venda

University of Venda
Creating Future Leaders

TABLE OF CONTENTS

Declaration i

Abstract ii

Dedication iv

Acknowledgements v

Acronyms vi

List of figures in the text vii

List of tables xi

TABLE OF CONTENT xiii

CHAPTER 1 1

INTRODUCTION 1

1.1. Background Information 1

1.1.1. Malaria-disease 1

1.1.2. Currently used antimalarial drugs 1

1.1.3 Resistance to antimalarial drug 3

1.2. Importance of Natural Products 4

1.3. The Molecular Systems that are Objects of this Study 5

1.4 Aim of this Study 5

1.5. Organisation of the Material 7

CHAPTER 2 8

THEORETICAL BACKGROUND AND LITERATURE REVIEW 8

2.1. The Structure of Molecules 8

© University of Venda

University of Venda
Creating Future Leaders

2.1.1. Molecular geometry parameters 8

2.1.2. Conformations and conformational analysis 9

2.1.3. Potential energy surface and geometry optimisation 9

2.2 Electronic Structure Methods 11

2.2.1 The quantum mechanical description of atoms and molecules 11

2.2.2 The Born-Oppenheimer approximation 11

2.2.3 The Hartree-Fock Theory 12

2.2.4. The Linear Combination of Atomic Orbitals 17

2.2.5. Post-Hartree-Fock methods 20

2.2.6. Density functional theory 20

2.3 Calculation of Relevant Molecular Properties 21

2.3.1. Dipole moment 22

2.3.2. Frequencies 22

2.3.3. The frontier Molecular Orbitals (HOMO-LUMO) 24

2.4. The Computational Study of Molecules in Solution 25

2.4.1. Importance of studying molecules in a medium 25

2.4.2. Solvent effects on molecular properties 26

2.4.3. The Polarisable Continuum Model (PCM) 28

2.4.4. Supermolecular structures: adducts with explicit solvent molecules 28

2.5. Hydrogen Bonding 30

2.5.1. Nature and types of hydrogen bonds 30

2.5.2. Effects of hydrogen bonding and its importance in biological systems 32

2.6. Relevance of the Computational Study of Biologically Active Molecules 33

LIBRARY

© University of Venda

University of Venda
Creating Future Leaders

2.7. Brief Overview on Antimalarial Drugs 34

2.7.1. Antimalarial drugs of natural origin 34

2.7.2 Review of theoretical studies of antimalarial drugs 34

CHAPTER 3 38

OVERVIEW ON COMPUTATIONAL METHODS USED 38

3.1 Choice of Computational Methods 38

3.1.1. Computations in vacuo 38

3.1.2. Computation of solvent effects 40

3.1.3. Calculation of adducts with explicit water molecules 42

3.1.4. Frequency calculations 42

3.2. Preparation of Inputs 43

3.2.1. Calculations in vacuo 43

3.2.2. Calculations in solution 43

3.2.3. Adducts with explicit water molecules 43

3.3. Presentation of Results 44

3.3.1. Units used 44

3.3.2. Non-Standard Acronyms Utilised 45

CHAPTER 4 46

RESULTS 46

4.1. Conformational Preferences in vacuo 46

4.2. Conformers' Relative Energies in Different Media 60

4.3. Dipole Moments in Different Media 64

4.4. Vibrational Frequencies in Different Media 65

© University of Venda

University of Venda
Creating Future Leaders

4.5. HOMO, LUMO and close-to-HOMO Molecular Orbitals in Different Media 67

4.6. Natural Charges on the Atoms in Different Media 68

4.7. Total Electronic Energy in Different Media 69

4.8. The Solvent Effect 70

4.9. Adducts with Explicit Water Molecules 72

4.9.1. Geometries of the calculated adducts 72

4.9.2. Geometry characteristics of the central molecule in the adducts 74

4.9.2. The characteristics of the intermolecular H-bonds in the adducts 75

4.9.3. Interaction Energy in the calculated adducts 75

4.9.4. Solvent effects in adducts with explicit water molecule 77

CHAPTER 5 188

DISCUSSION AND CONCLUSION 188

REFERENCES 191

© University of Venda

University of Venda
Creating Future Leaders

CHAPTER 1

INTRODUCTION

1.1. Background Information

1.1.1 Malaria-disease

Malaria remains one of the diseases responsible for most serious health problems with many deaths and huge morbidity in tropical regions [1]. Nearly 225 million cases of malaria and 781.000 [2] deaths were estimated in 2009; 219 million cases and 660.000 deaths in 2010 [3], 207 million cases and 627 000 deaths in 2012 [4]. According to WHO (World Health Organization) reports, 2.23% deaths worldwide are due to malaria. Africa is one of the continents with many malaria-endemic countries (about 45 [5]), and about 90% deaths, mostly children, are related to malaria [3].

Malaria is caused by a mosquito-borne infection of protozoa parasites of the *plasmodium* genus, among which *plasmodium falciparum* is responsible for most of the deaths [6, 7]. The greatest challenge for the treatment of malaria is the fast rate at which *plasmodium falciparum* develops resistance against drugs, just few years after they enter into clinical use. To avoid the onset of a catastrophic situation, it is therefore necessary to develop new viable drugs that can at least keep the pace with the rate of resistance development.

1.1.2. Currently used antimalarial drugs

1.1.2.1 Main antimalarial compounds

Antimalarial drugs currently in clinical use belong to different types of compounds. The most important drugs are shown in figure 1.1: they include artemisinin, amodiaquine, PS (combinations of pyrimethamine and various sulfa-drugs – sulfonamides such as sulfadoxine and sulfalene and the sulfone, dapsone), chloroquine, mefloquin, quinine and quinidine.
In general, drugs act by interfering with cellular or biochemical process through interactions

© University of Venda

University of Venda
Creating Future Leaders

with specific molecules called "targets". The best drugs should exhibit selective and possibly high toxicity for the pathogen and, at the same time, should exhibit minimal toxicity to the host. In the case of malaria, the antimalarial drug should lead to the killing of *plasmodium falciparum* [8, 9]. Different drugs act with different mechanisms. The mechanism of action of chloroquine [8-10] is here utilized as an example of antimalarial drug actions.

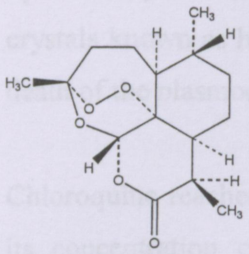

Artemisinin

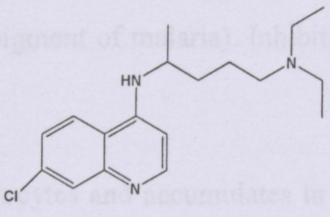

Chloroquine

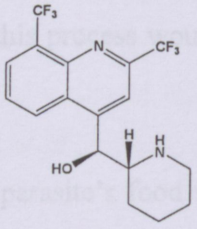

Mefloquine

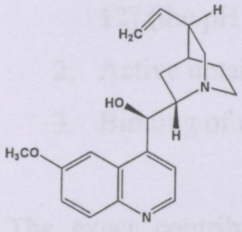

Quinine

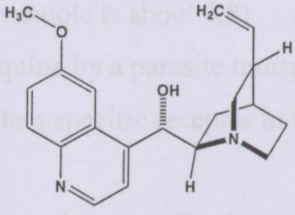

Quinidine

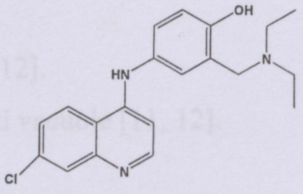

Amodiaquine

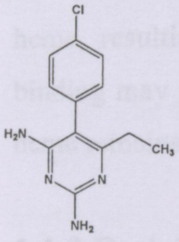

Pyrimethamine

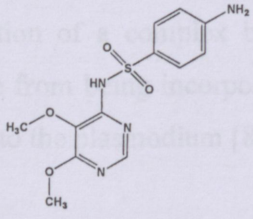

Sulfadoxine

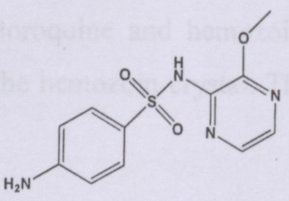

Sulfalene

Figure 1.1: The most commonly used antimalarial drugs

© University of Venda

University of Venda
Creating Future Leaders

1.1.2.2. Mechanism of the chloroquine antimalarial activity

Within the red blood cell (erythrocytes), the plasmodium breaks down haemoglobin. This releases the heme units which, if released in membranes, can cause the generation of reactive oxygen intermediates which will inhibit other processes vital for the plasmodium. Indeed, in the food vacuole, significant quantities of heme are released as a result of the digestion of haemoglobin by the plasmodium [8-12]. The plasmodium detoxifies heme in food vacuoles, by a biocrystallization process in which heme units are sequestered into large insoluble crystals known as hemozoin (pigment of malaria). Inhibiting this process would result in the death of the plasmodium [8].

Chloroquine reaches the erythrocytes and accumulates in the parasite's food vacuole, where its concentration can reach up to 400mM. Three possible mechanisms of this accumulation of chloroquine in the vacuole have been proposed, namely:

1. Protonation and ion trapping of chloroquine due to the low pH of the food vacuole [11, 12] (the pH of the food vacuole is about 4.8).
2. Active uptake of chloroquine by a parasite transporter [12].
3. Binding of chloroquine to a specific receptor in the food vacuole [11, 12].

The exact contribution of these three mechanisms, or the exact mechanism by which chloroquine inhibits hemozoin formation, is not yet clearly established. Nonetheless, it has been demonstrated that chloroquine exerts its antimalarial effect by interfering with the conversion of free heme into hemozoin. It is known that chloroquine can bind to the heme, resulting in the formation of a complex between chloroquine and hemozoin. This binding may prevent the heme from being incorporated into the hemozoin crystal. Thus, the heme remains extremely toxic to the plasmodium [8-12].

1.1.3 Resistance to antimalarial drug

Among currently used antimalarial drugs, artemisinin and its derivatives are the most widely used and appear to have the most rapid action. The artemisinin-based combination therapy (ACT) has been recommended by WHO as the first-line treatment for malaria caused by *plasmodium falciparum* (the most dangerous of the *plasmodium* parasites that infect humans). Chloroquine is still being used for *plasmodium vivax* malaria where the parasite is not

© University of Venda

University of Venda
Creating Future Leaders

resistant, whereas appropriate ACT has to be used in areas where *plasmodium vivax* is resistant to chloroquine.

Resistance of plasmodia to artemisinins has been observed in some countries (e.g., in the Greater Mekong subregion: Cambodia, Myanmar, Thailand and Viet Nam). The 2007 World Health Assembly meeting recommended a progressive removal of monotherapies treatment of artemisinin and their replacement by ACT. However, the treatment with ACT is not always successful in the countries where resistance is developing. In Cambodia, for instance, the parasite resistance against multiple ACTs has been reported and a special provision using a non-artemisinin-based combination (atovaquone-proguanil) has been proposed [13-14].

Another important strategy is fighting malaria vectors by using insecticides. Unfortunately, the elimination of mosquitoes through the use of insecticides has shown some failure. A survey made in 2012 and reported by WHO, revealed that, in 64 of the countries explored, mosquitos show resistance to at least one of the insecticides used [13-14].

It is clear from all this that new drugs with specific modes of action are urgently needed.

1.2. Importance of Natural Products

Set apart chemical products that humans are synthesizing, there is a great number of different molecules that are produced by living organisms and have not yet been discovered [15]. They are referred to as *natural products*. Many natural products have been found to present interesting chemical properties. Natural products represent a potentially immense source of new compounds, with diverse molecular structures and pharmacophores. Among them, there are molecules which exhibit suitable properties as new leads of antimalarial drugs in drug development. Several plants used in traditional medicine were experimentally proved to be active against malaria. This implies that they contain biologically active molecules that are effective against malaria and that are likely different from the drugs already in clinical use. New antimalarial leads may certainly emerge from tropical plant sources [16-17]. As mentioned in the previous section, there is an urgent need of new and accessible compounds having an original mode of action. A systematic exploration of natural products can provide new molecules to effectively address the drug resistance presented by *plasmodium*.

© University of Venda

University of Venda
Creating Future Leaders

Alkaloids are a group of naturally-occurring molecules, including several classes with antimalarial activity. The isolation of these molecules, the study of their activity and the investigation of possible derivatives with enhanced activity are essential steps in the development of new antimalarial drugs [16]. This work focuses on new molecules isolated from some Congolese plants, which have been proved to present biological activity against the malaria parasite.

1.3. The Molecular Systems that are Objects of this Study

The molecules that are the object of this study were isolated from the root bark of *Newbouldia laevi,* (Bignoniaceae), an endemic plant used in various ethnomedicinal preparations in DR Congo and across West Africa to treat diarrhoea, dysentery, worms, sexually transmitted disease, and malaria, to reduce dental caries and as an astringent [18]. Phytochemical analysis of the root bark of *Newvouldia laevis* revealed the presence of four pyrazole alkaloids, namely withasomnine, 4'-hydroxywithasomnine, newbouldine and 4'-hydroxynewbouldine [19]. Several investigations performed by researchers in DR Congo, in the Laboratory of Energetic and Natural products at the University of Kinshasa, have revealed the presence of two others pyrazole alkaloids: 4'-methoxywithasomnine and 4'-methoxynewbouldine. On measuring their biological activities, the half maximal inhibitory concentration (IC_{50}) value was found to be nearly 122.2 mg/ml for the alkaloic totum of those compounds [20-21]. The nitration of withasomnine and 4'-hydroxy-withasomnine has revealed that the activity of nitro-withasomnine derivatives is higher than that of the original molecules [22- 23]. The structures of all these molecules are shown in figure 1.2.

1.4 Aim of this Study

The present study aims at identifying preferential conformers and computable molecular properties of withasomnine, 4'-hydroxy-withasomnine, newbouldine, 4'-hydroxy-newbouldine and the nitro derivatives of withasomnine and 4-hydroxy-withasomnine, in vacuo and in three solvents with different polarities (chloroform, acetonitrile and water). This study provides detailed information on molecular properties that can be related to the biological activity of these compounds and compares the results from different calculation methods and different basis sets, to obtain useful indications for future studies on other alkaloids.

© University of Venda

University of Venda
Creating Future Leaders

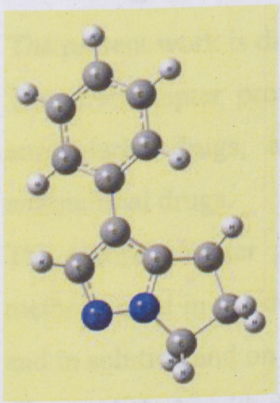

Withasomnine

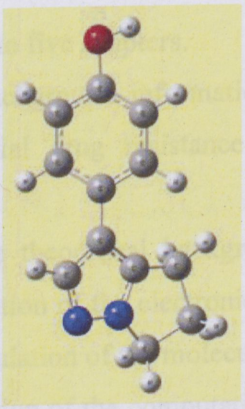

4'-hydroxy-withasomnine

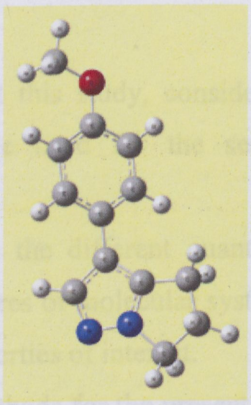

4'-methoxy-withasomnine

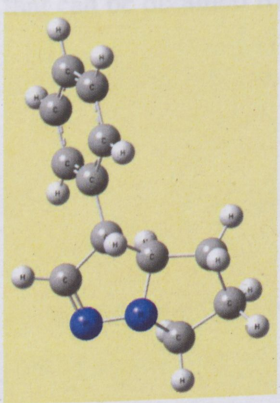

Newbouldine

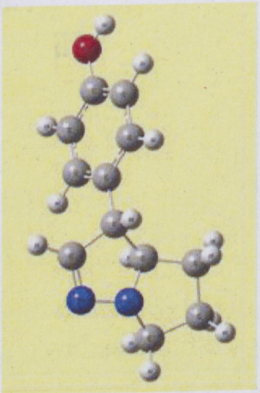

4'-hydroxy-newbouldine

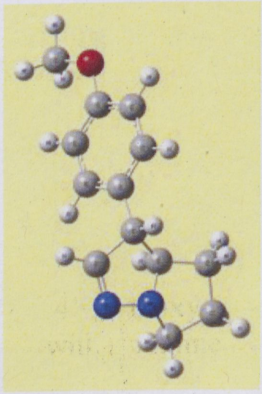

4'-methoxy-newbouldine

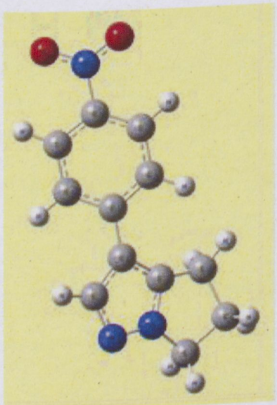

nitro-withasomnine

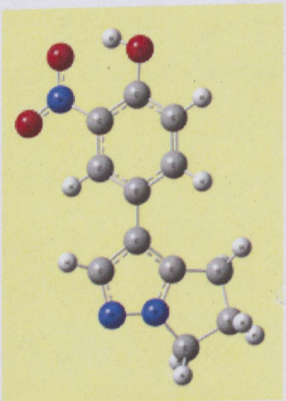

nitro-4'-hydroxy-withasomnine

Figure 1.2. Pyrazole alkaloids isolated from *Newvouldia laevis* and their derivatives

© University of Venda

University of Venda
Creating Future Leaders

1.5. Organisation of the Material

The present work is divided into five chapters.

The first chapter provides background information about this study, considering malaria, antimalarial drugs, antimalarial drug resistance and the need for the search of new antimalarial drugs.

The second chapter gives the theoretical background on the different quantum chemical methods used in the determination of the electronic structures of molecular systems in vacuo and in solution and on the calculation of the molecular properties of interest.

Chapter 3 deals with the selection of the computational methods for the present study. It also describes the approaches for the preparation of inputs.

Chapter 4 presents the results obtained, giving all the details.

Chapter 5 contains a discussion of the results presented in chapter 4 and the main conclusions that can be obtained from them.

© University of Venda

University of Venda
Creating Future Leaders

CHAPTER 2

THEORETICAL BACKGROUND AND LITERATURE REVIEW

This chapter presents the main computational approaches to the investigation of molecular structures and properties, paying particular attention to the methods that are utilized in the current study; it considers various aspects of the theoretical description of molecules and their properties, which are relevant for the current study; it also provides an overview of existing computational studies of other antimalarial drugs.

2.1. The Structure of Molecules

2.1.1. Molecular geometry parameters

Molecules are made of atoms, forming stable groupings with a sequential arrangement specific to each molecule. Atoms inside a molecule have different behaviour compared to isolated atoms. The study of molecules considers the nature and situation of their constituent atoms. The specificities of the chemical bonding of the atoms in a molecule are the basis of the observed physical and chemical properties of that molecule [24]. The spatial distribution of the nuclei of its constituent atoms determines the equilibrium geometry of a molecule. The molecular geometry is characterized by the following parameters:

- bond length – the distance between the nuclei of two consecutive atoms;
- bond angle – the angle between three consecutive atoms;
- dihedral angle – the angle between the plane identified by the first three of four consecutive atoms and the plane identified by the last three.

These parameters, called also *internal coordinates* of the molecule, are spatial coordinates of the molecular system and describe its geometry in space [25]. In theoretical chemistry, the three-dimension structure of the molecule constitutes the starting information, on the basis of which it is possible to determine other relevant information.

© University of Venda

University of Venda
Creating Future Leaders

2.1.2. Conformations and conformational analysis

The geometry of most molecules is not rigid, because the rotation around single bonds is free. The different spatial arrangements of atoms arising from rotation around one or more single bonds of the molecule are termed conformations. Each conformation has a unique geometry, which has a specific energy. The conformations having low energies are those which are experimentally observable and the ones that have non-negligible population. The chemical properties of molecules depend on their conformations [26], mostly on the low energy ones. The computational study aimed at determining the possible conformations of a molecule and the corresponding energies is called *conformational analysis*.

2.1.3. Potential energy surface and geometry optimisation

Each of the geometry parameters of a molecule can be varied (only to a limited extent when rotation is not possible, such as around multiple bonds). Varying geometry parameters generates a mathematical representation of the molecule's energy a as a function of its geometry; this representation is called *potential energy surface* (PES) or *potential energy hypersurface* [27]. Potential energy surfaces constitute valuable sources of information in the study of molecular structures, properties and reactivities [28]. A potential energy surface has stationary points, i.e., points at which the gradient of the electronic energy is zero for all the internal coordinates of the molecule [27]. Stationary points may have different meanings (figure2.1), the most relevant of which are the following:

- minima, corresponding to minimum energy values. The conformations corresponding to minima in the PES are called *conformers* of the given molecule. There can be more than one minimum (often many minima) for a given molecule. The minimum corresponding to the lowest energy value is the *global minimum*; the other minima are called *local minima*.
- saddle points. First order saddle points correspond to transition states (transitions between two minima). There are also higher–order saddle points.

The global minimum corresponds to the most stable geometry of the molecule. This geometry, and other geometries corresponding to sufficiently low local minima to have non-negligible population, are responsible for the properties of the molecule and the substance. Therefore, finding the global minimum and possible low-energy local minima is the first step

© University of Venda

University of Venda
Creating Future Leaders

in the theoretical-chemistry study of many chemical processes [29, 30]. These equilibrium geometries are identified via a geometry optimization procedure [30] – a mathematical

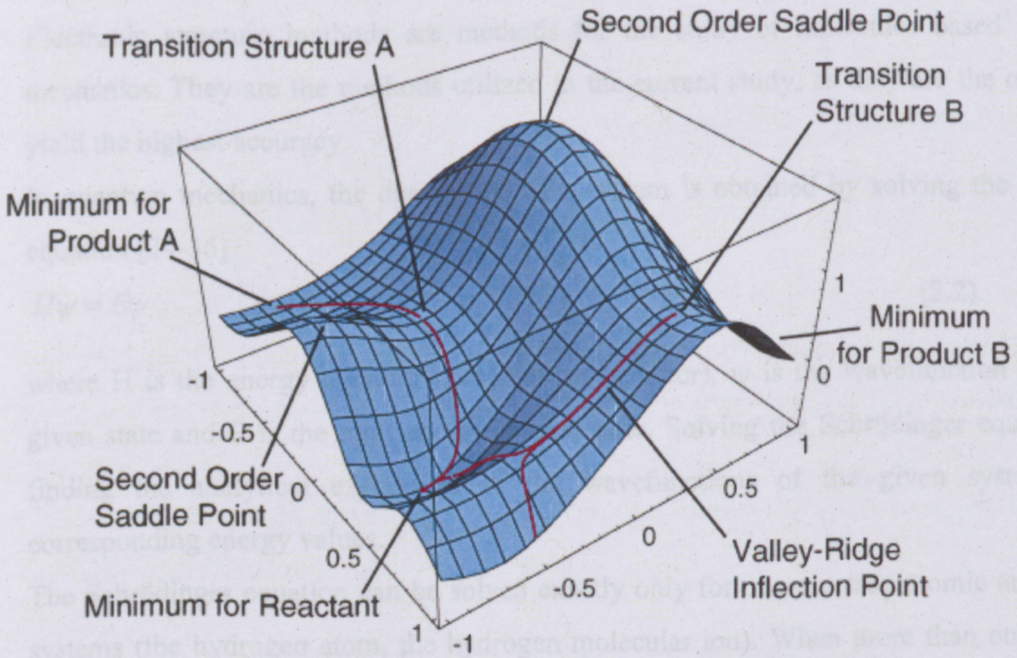

Figure 2.1. Potential energy surface showing minima, transition-states saddle points, second order saddle point, reaction paths, and a valley ridge inflection point [29].

operation or algorithm that searches for the stationary points on the potential energy surface via energy minimization [31], by varying the molecule's parameters. The optimization of the molecular geometry can be summarized through the following expression in matrix form:

$$E(R_q + X) = E(R_q) + G'X + \frac{1}{2}X'HX \quad [32] \qquad (2.1)$$

where R_q represents the initial geometry; X(R) is the displacement vector of moving R_q geometry towards a new R_{q+1} geometrical position on the molecular potential energy surface (change in atomic coordinates in R_q), G(R) is the energy gradient with respect to the atomic displacement, and H(R) is the second derivative of the energies with respect to the change in the atomic positions given in matrix form [32] (Hessian matrix).

Energy minimizations can in principle yield any type of stationary point on the PES. In order to distinguish between minima and saddle points, it is necessary to perform an analysis of the harmonic frequencies of the molecule [31, 33]. Minima correspond to geometries for which all frequencies are real. Transition states (first-order saddle points linking two local minima and defining a static reaction path between them) are identified by the presence of one imaginary frequency.

© University of Venda

University of Venda
Creating Future Leaders

2.2 Electronic Structure Methods

2.2.1 The quantum mechanical description of atoms and molecules

Electronic structure methods are methods for the study of molecules based on quantum mechanics. They are the methods utilized in the current study, as they are the ones that can yield the highest accuracy.

In quantum mechanics, the description of a system is obtained by solving the Schrödinger equation [34-36]

$$H\psi = E\psi \tag{2.2}$$

where H is the energy operator (hamiltonian operator), ψ is the wavefunction describing a given state and E is the total energy of that state. Solving the Schrödinger equation means finding the analytical expression of the wavefunctions of the given system and the corresponding energy values.

The Schrödinger equation can be solved exactly only for one-electron atomic and molecular systems (the hydrogen atom, the hydrogen molecular ion). When more than one electron is present, it is not possible to solve the equation exactly, because of the presence of electron-electron repulsion terms. Therefore, it is solved by using approximate methods. The next sections outline the most important approximations utilized in the theoretical study of molecules.

2.2.2 The Born-Oppenheimer approximation

The Born-Oppenheimer approximation simplifies the Schrödinger equation for molecules by treating the motion of electrons and the motion of nuclei separately. This is justified by the large mass difference between nuclei and electrons, for which electrons move much faster (thousands of times faster) than nuclei [37, 38]. Then, the kinetic energy of the nuclei is considered negligible and the nucleus-nucleus electrostatic repulsion is calculated separately, for specific internuclear distances. The hamiltonian of the molecular system is thus reduced to the hamiltonian of electrons.

For example, the full hamiltonian of a system consisting of M nuclei and N electrons is given by the following expression [39] (using atomic units):

© University of Venda

University of Venda
Creating Future Leaders

$$H = -\sum_{i=1}^{N}\frac{1}{2}\nabla_i^2 - \sum_{A=1}^{M}\frac{1}{2M_A}\nabla_A^2 - \sum_{i=1}^{N}\sum_{A=1}^{M}\frac{Z_A}{r_{iA}} + \sum_{i=1}^{N}\sum_{j>i}^{N}\frac{1}{r_{ij}} + \sum_{A=1}^{M}\sum_{B>A}^{M}\frac{Z_A Z_B}{R_{AB}} \quad (2.3)$$

where Z_A is the nuclear charge of atom A, M_A is the nuclear mass of atom A, R_{AB} is the internuclear distance between atom A and atom B, r_{iA} is the distance between nucleus A and electron i, r_{ij} is the distance between electron i and electron j, Z_B is the nuclear charge of atom B and ∇^2 is the Laplacian operator, having the expression $\frac{\partial^2}{\partial x^2}+\frac{\partial^2}{\partial y^2}+\frac{\partial^2}{\partial z^2}$.

In equation 2.3, the first and second terms describe respectively the kinetic motions of N electrons and M nuclei, the third term is the Coulomb attraction energy between nuclei and electrons, while the two last terms are electron-electron and nuclei-nuclei Coulomb repulsion energies.

Using the Born-Oppenheimer approximation, the motion of the nuclei and the nucleus-nucleus electrostatic repulsion are removed

$$H = -\sum_{i=1}^{N}\frac{1}{2}\nabla_i^2 - \cancel{\sum_{A=1}^{M}\frac{1}{2M_A}\nabla_A^2} - \sum_{i=1}^{N}\sum_{A=1}^{M}\frac{Z_A}{r_{iA}} + \sum_{i=1}^{N}\sum_{j>i}^{N}\frac{1}{r_{ij}} + \cancel{\sum_{A=1}^{M}\sum_{B>A}^{M}\frac{Z_A Z_B}{R_{AB}}} \quad (2.4)$$

The remaining hamiltonian is the electronic Hamiltonian operator H_{el}

$$H_{el} = -\sum_{i=1}^{N}\frac{1}{2}\nabla_i^2 - \sum_{i=1}^{N}\sum_{A=1}^{M}\frac{Z_A}{r_{iA}} + \sum_{i=1}^{N}\sum_{j>i}^{N}\frac{1}{r_{ij}} \quad (2.5)$$

The nucleus-nucleus repulsion is more often taken into account by adding it *a posteriori* to the electronic energy (i.e., it is calculated separately and, after finding the electronic energy, the total energy of the molecule is given by the sum of the electronic energy and the nucleus-nucleus repulsion energy).

2.2.3 The Hartree-Fock Theory

Electrons are fermions, i.e., they are particles whose behaviour is governed by Pauli's exclusion principle. Therefore, a system of electrons is described by an antisymmetric total wavefunction.

The Hartree-Fock method [40, 41] is one of the most familiar approximation methods for determining the electronic energy of atomic and molecular systems. If one considers a

© University of Venda

University of Venda
Creating Future Leaders

molecular system containing N electrons and N_A nuclei, the hamiltonian operator of this system has the following expression [31]:

$$H = \sum_{i=1}^{N} h(i) + \sum_{i=1}^{N} \sum_{j>i}^{N} \frac{1}{r_{ij}} \tag{2.6}$$

where the first term accounts for one electron energy terms (one electron integrals) and the operator $h(i)$ is expressed as [37,39]:

$$h(i) = -\frac{1}{2}\nabla_i^2 - \sum_{A=1}^{N_A} \frac{Z_A}{r_{iA}} \tag{2.7}$$

The second sum appearing in equation (2.6) is the sum of the electron-electron repulsion terms, considering each pair of electrons in the given system; therefore, it also corresponds to the correlation of electron motions. These electron-electron repulsion terms are responsible for the impossibility of solving the Schrödinger equation exactly, because each of them depends on the coordinates of two particles simultaneously, which prevents the separation of variables that would be necessary to be able to integrate the equation. Approximation methods need to find alternative ways of solving the Schrödinger equation, without having to integrate electron-electron repulsion terms

Hartree and Fock [40, 41] proposed an approximation method that is still used today in many quantum chemical studies of multi-electron systems. In this approximation, each electron appears independently, but the influence of the other electrons is taken into account in an average way. The approximated hamiltonian has the following expression

$$H^{app} = \sum_{i}^{N} (h(i) + V^{HF}(i)) \tag{2.8}$$

where $V_i\ (i)$ represents the average potential perceived by the ith electron due to the presence of the other electrons.

As mentioned previously, the wavefunction describing a multielectron system must be antisymmetric. This is obtained by using spin-orbitals ψ_0, constructed as Slater determinants, as shown by the following expression:

© University of Venda

University of Venda
Creating Future Leaders

$$|\psi_0\rangle = |\varphi_1 \ldots\ldots \varphi_N\rangle \tag{2.9}$$

In this expression, the spatial wavefunction ψ_0 is given in Dirac notation [42-43] ($|\psi_0\rangle$: ket vector) as a product of N one-electron spatial wavefunctions φ_i ($\psi_0 = \prod_i^N \varphi_i$) denoted by a vector ket as $|\varphi_1 \ldots\ldots \varphi_N\rangle$. The conjugate function of the spatial wavefunction ψ_0^* is expressed in Dirac notation as a bra vector, $\langle\psi_0|$. The Dirac expression of a scalar product between the wavefunction ψ_0 and its conjugate function ψ_0^*, expressed mathematically by $\int \psi_o^* \psi_o dV$, can be written in Dirac expression as $\langle\psi_o|\psi_o\rangle$ and the integrand describes the N-particle electron density.

If $|\psi_0\rangle$ is normalized, the expectation value of the corresponding energy is given in Dirac notation by the following expression:

$$E_0 = \langle\psi_0|H|\psi_0\rangle \tag{2.10}$$

Each electron i is in motion with a given kinetic energy, and it experiences an attractive potential from the nuclei while repeals the other electrons (equation 2.5).

The electrons are not classical point charges with fixed distances between them. The one-particle probability density $\rho(\mathbf{r})$ to find an electron in the position $\mathbf{r}$, multiplied by the charge of the electron (-1 in atomic units), yields the charge density. $\rho(\mathbf{r})$ is related to the wavefunction amplitude by $\rho(\mathbf{r}_1) = N \int|\Psi(\mathbf{r}_1, \mathbf{r}_2, \ldots \mathbf{r}_N|^2 \, dr_2^3 \, dr_3^3 \ldots dr_N^3$. And to find the wavefunction we need to solve the Schrödinger equation. The wave-like behaviour of the electron makes the formulation of the hamiltonian difficult. To deal with this, one should make a wavefunction guess and solve the Schrödinger equation by self-consistency iterations, i.e., the iterative process continues till a given convergence criteria is satisfied. We cannot get the exact solution but we are looking for the best approximation possible. Let us consider a molecular system of two electrons, (1) and (2). To obey the anti-symmetrical property upon exchange of two electrons, in agreement with the Pauli exclusion principle, the spin orbital wavefunction $\psi(1,2)$ can be written as a Slater determinant, because the use of determinants enforces the antisymmetry of the wave function in a trivial way. For instance, for the He atom in its ground state, containing only two electrons [44]:

$$\psi(1,2) = \frac{1}{\sqrt{2}} \begin{vmatrix} 1s\alpha(1) & 1s\beta(1) \\ 1s\alpha(2) & 1s\beta(2) \end{vmatrix} \tag{2.11}$$

© University of Venda

University of Venda
Creating Future Leaders

where 1s is the 1s atomic orbital, and α and β are the opposite spins of the two electrons. Interchanging the spatial and spin coordinates of the two electrons corresponds to permute two rows of the determinant, with the consequence that the determinant change sign. The

$\psi(2,1) = \frac{1}{\sqrt{2}}(1s\alpha(2)1s\beta(1) - 1s\alpha(1)1s\beta(2))$ wavefunction is the opposite of the

$\psi(1,2) = \frac{1}{\sqrt{2}}(1s\alpha(1)1s\beta(2) - 1s\alpha(2)1s\beta(1))$ wavefunction. Thus $\psi(1,2) = -\psi(2,1)$ and the given function is anti-symmetric. Using this spin wavefunction as guess orbital of the electronic hamiltonian will give

$$\sum_{i=1}^{2}\left(-\frac{1}{2}\nabla_i^2 - \frac{Z}{r_i}\right)\psi(1,2) + \sum_{i<j}^{2}\frac{1}{r_i - r_j}\psi(1,2) = E\psi(1,2) \quad (2.12)$$

$$\left(-\frac{1}{2}\nabla_1^2 - \frac{Z}{r_1}\right)\psi(1,2) + \left(-\frac{1}{2}\nabla_2^2 - \frac{Z}{r_2}\right)\psi(1,2) + \frac{1}{r_{12}}\psi(1,2) = E\psi(1,2) \quad (2.13)$$

Supposing that the wavefunction is orthonormal, the total energy of the system can be obtained by calculating the following integral given in Dirac expression by:

$$E = \langle\psi(1,2)|\left(-\frac{1}{2}\nabla_1^2 - \frac{Z}{r_1}\right)|\psi(1,2)\rangle + \langle\psi(1,2)|\left(-\frac{1}{2}\nabla_2^2 - \frac{Z}{r_2}\right)|\psi(1,2)\rangle + \langle\psi(1,2)|\left(\frac{1}{r_{12}}\right)|\psi(1,2)\rangle$$

(2.14)

The first and second terms are referred to as *one integral energies* of electron (1) and (2), and denoted as h(1) and h(2) respectively.

After replacement of $|\psi(1,2)\rangle$ by $\frac{1}{\sqrt{2}}(1s\alpha(2)1s\beta(1) - 1s\alpha(1)1s\beta(2))$ and rearrangement of the third term, one obtains the following components:

$$J_{12} = \int 1s\alpha(1)1s\beta(2)\frac{1}{r_{12}}1s\alpha(1)1s\beta(2) + \int 1s\alpha(2)1s\beta(1)\frac{1}{r_{12}}1s\alpha(2)1s\beta(1) \quad (2.15)$$

$$K_{12} = -\int 1s\alpha(2)1s\beta(1)\frac{1}{r_{12}}1s\alpha(1)1s\beta(2) - \int 1s\alpha(1)1s\beta(2)\frac{1}{r_{12}}1s\alpha(2)1s\beta(1) \quad (2.16)$$

After a careful examination of the two expressions, one can see that J_{12} is the Coulomb repulsion energy between electron (1) and (2), whereas the second term, K_{12}, has no physical meaning in classical physics; it is called the *exchange energy* and it comes from the anti-symmetric property of the wavefunction with respect to the permutation of the coordinates of

© University of Venda

University of Venda
Creating Future Leaders

any two electrons. The J_{12} and K_{12} terms are also referred to as *Coulomb integral* and *exchange integral*.

Thus, the *Coulomb operator* and the *exchange operator are* defined (in Dirac notation) as:

$$\hat{J}_j(1)\psi_i(1) = \langle \psi_j(2)|\frac{1}{r_{12}}|\psi_j(2)\rangle \psi_i(1) \tag{2.17}$$

$$\hat{K}_j(1)\psi_i(1) = \left(\langle \psi_j(2)|\frac{1}{r_{12}}|\psi_i(2)\rangle\right)\psi_j(1) \tag{2.18}$$

$\hat{J}_j(1)$ and $\hat{K}_j(1)$ are one-particle quantum mechanics exchange operators that have to act on orbital $|\psi_i(1)\rangle$, i.e., an orbital containing electron 1 in orbital $|\psi_i\rangle$, at r_{12} distance from electron 2.

The Fock operator $f(1)$, that combines both the coulomb operator $\hat{J}_j(1)$ and the exchange operator $\hat{K}_j(1)$, is defined as:

$$f(1) = h(1) + \sum_{j}^{Ne}(2J_j(1) - K_j(1)) \tag{2.19}$$

For a molecular system with N_e electrons, the total wave function Ψ can be written as the Slater determinant:

$$\Psi = \frac{1}{\sqrt{N_e!}}\begin{vmatrix} \psi_1(1) & \psi_2(1) & \cdots & \psi_N(1) \\ \psi_1(2) & \psi_2(2) & \cdots & \psi_N(2) \\ \cdot & & & \\ \cdot & \cdot & \cdot & \cdot \\ \cdot & & & \\ \psi_1(N) & \psi_2(N) & \cdots & \psi_N(N) \end{vmatrix}$$

where $\frac{1}{\sqrt{N_e!}}$ is the normalization factor.

The energies of the occupied ψ_μ orbitals are obtained from the Hartree–Fock equation (the subscript μ is used for molecular orbitals, whereas the subscripts i and j are used for atomic orbitals):

$$f\psi_\mu = \varepsilon_\mu \psi_\mu \tag{2.20}$$

where ε_μ is the energy of the orbital ψ_μ. In these equations, the subscript μ is used for molecular orbitals, whereas the subscripts i and j are used for atomic orbitals.

© University of Venda

University of Venda
Creating Future Leaders

The wavefunction ψ_μ can be constructed as a linear combination of a set of Slater determinants ϕ_i, called *basis set*:

$$\psi_\mu = \sum_i c_{ij}\phi_i \qquad (2.21)$$

When written in matrix form, the Hartree-Fock equation is called the Roothaan equation [45] and it is written as:

$$\mathbf{FC} = \mathbf{SCE} \qquad (2.22)$$

where **F** is the Fock operator in matrix form, **S** the orbital overlap matrix, **C** is the matrix of the coefficients in the orbital expansion (equation 2.21) and **E** is the diagonal matrix of the energies of the molecular orbitals. The overlap of atomic orbitals describes the concentration of electrons in the region between two adjacent atoms of the molecular system; mathematically, it is represented by the scalar product between two atomic orbitals, expressed by:

$$S_{ij} = \langle \psi_j(2) | \psi_i(1) \rangle \qquad (2.23)$$

2.2.4. The Linear Combination of Atomic Orbitals

The wavefunctions can be expressed in different ways according to how chemical bonding is modelled. The most widely utilized model is the *molecular orbital theory* (the alternative model is called *valence bond theory*). The molecular orbital theory considers electrons as moving under the influence of the nuclei in the entire molecule [46, 47]; therefore, the wavefunctions (molecular orbitals) extend to the entire molecule. On the other hand, the orbitals of each of the atoms constituting a molecule contribute to chemical bonding. Therefore, each molecular orbital χ_i is written as a sum of atomic orbitals φ_i, i.e., it is a *Linear Combination of Atomic Orbitals* (LCAO) [47]:

$$\chi_i = \sum_i c_i \varphi_i \qquad (2.24)$$

The coefficients c_i are determined by using the variational principle and minimising the energy expectation value.

When introduced into the approximated Hamiltonian proposed by Hartree and Fock (equation 2.10), the molecular orbitals written using Slater determinants generate a new term without

© University of Venda

University of Venda
Creating Future Leaders

physical meaning resulting from the permutation of the determinant elements. This term is called exchange term, K, and referred to as self electron interaction.

The expression of the atomic orbitals (solutions of the Schrödinger equation for the hydrogen atom) proved too complex for the solution of all the integrals needed when solving the Schrödinger equation for a molecule, expressing molecular orbitals through equation 2.24. It turned out to be more convenient to express the molecular orbitals as linear combination of other types of basis functions, still centred on the nuclei of the atoms constituting the molecule. These functions are called *basis sets* [48].

The first basis sets functions different from the actual atomic orbitals were introduced by J. C. Slater. For instance, for 1s basis functions [48, 49]:

$$\text{basis function} = Ne^{-\alpha r} \tag{2.25}$$

where N is a normalisation constant, α an orbital exponent and r the atomic radius (in Å). The expression of the Slater Type Orbital (STO) obtained from expression 2.25 is the following:

$$STO = \frac{2\xi^{3/2}}{r^{0.5}} e^{-\xi r} \tag{2.26}$$

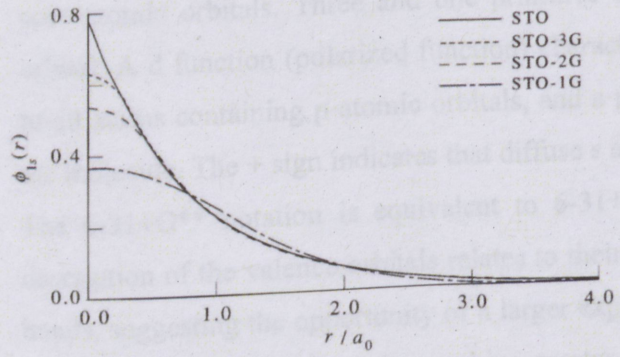

Figure 2.2. Graphical illustration of the variation of 1ψ (1s) using STO, STO-1G, STO-2G and STO-3G basis sets

However, solving the integrals when utilising STO is not easy (three and four center integrals cannot be solved analytically, but must be solved numerically). To facilitate computation, S. F. Boys suggested the Gaussian Type Orbitals (GTO), having the following expression [50]:

$$GTO = \frac{2\chi}{r^{0.75}} e^{-\chi r^2} \tag{2.27}$$

© University of Venda

UNIVERSITY OF VENDA
LIBRARY

University of Venda
Creating Future Leaders

GTOs differ from STOs by the exponent of the exponential term (r^2 instead of r), whose integrals can be solved analytically.

Although making computation easier, GTOs yield a less accurate description of the behaviour of atomic orbitals: with respect to STOs, GTOs lack of cusps at short distances and sharply decay at long distances. To remedy those disadvantages, linear combinations of GTOs, and not individual GTOs, are used in the expansion of the molecular orbital (each linear combination of GTO approximates an atomic orbital). The higher the number of GTOs used in the expansion of the molecular orbital, the more accurate the description of the molecular system [51].

Different types of basis sets utilising GTOs have been proposed, according to the types and number of GTOs utilised for each atomic orbital. Those developed by J.A. Pople and co-workers are very popular because contained in the Gaussian code [145]. A type of widely used basis sets are the *split-valence basis sets*, in which the basis functions are divided in two parts, respectively describing the core electrons and the valence electrons. The valence electrons are described by multiple basis functions and are referred to as double-zeta or triple-zeta split-valence basis sets. For instance, 6-31G+(d,p) represents a Pople-type set of atomic functions to construct molecular orbitals. This kind of functions enables great flexibility in the description of bonds between atoms. It requires 6 primitive functions for the description of core atomic orbitals. Three and one primitive functions are used for each valence atomic orbital. A d function (polarized function) characterized by high angular momentum is added to all atoms containing p atomic orbitals, and a p function is added to all hydrogen atoms in the molecule. The + sign indicates that diffuse s and p functions are added to the heavy atoms. The 6-31+G** notation is equivalent to 6-31+G (d,p). The reason for a more complete description of the valence orbitals relates to their important role in the formation of chemical bonds, suggesting the opportunity of a larger expansion of molecular orbitals. Using a greater number of basis functions also enables greater flexibility, which is important because the valence orbitals may change size (becoming bigger or smaller) when other atoms approach [51-56].

The description of the molecular system becomes more accurate as the number of basis functions increases. For instance, the inclusion of polarization functions into the basis set increases the flexibility of an atom to bond in any direction; this effect enhances the accuracy of the computed molecular properties. Diffuse functions take in account the electron densities in regions further away from the nuclei. Their inclusion in the basis sets improves the

© University of Venda

University of Venda
Creating Future Leaders

description of polarized molecular systems, excited states, anionic molecules and the chemical systems characterised by weak chemical bonds like hydrogen bonding [51-56]. Diffuse functions are also important for the calculation of properties such as dipole moments and polarizabilities [51].

2.2.5. Post-Hartree-Fock methods

The main limitation of the Hartree- Fock (HF) method is the limited way in which it takes into account the correlation of the electronic motions (electron correlation), which is taken into account only partially, in an average way (through the fact that antisymmetry dictates that two electrons with the same spin cannot be in the same molecular orbital). Because of this, in several cases the method does not yield satisfactory evaluations of relevant chemical properties.

A number of methods have been developed which incorporate electron correlation in a better way. Post-Hartree-Fock methods include Møller-Plesset perturbation theory (MPn, where n is the order of correction), Multi-Configurations Self Consistent Field (MCSCF), Configuration Interaction (CI) and Coupled Cluster theory (CC). They are called Post-Hartree Fock methods because they start by computing the Hartree-Fock energy, and then correct this energy by adding the consideration of electron correlation (e.g., MPn), or take the HF orbitals as starting point and then modify them (e.g., MCSCF). Among them, the Møller-Plesset perturbation theory has been utilised in the study reported here and will therefore be described in some detail.

The Møller-Plesset perturbation theory is based on the perturbation theory [57]. A perturbation V is added to the Hartree-Fock Hamiltonian H_o, which takes the role of unperturbed Hamiltonian (V is small in comparison with H_o). Therefore, the Møller-Plesset Hamiltonian has the expression

$$H = H_o + \lambda V \qquad (2.28)$$

where λV represent a perturbing Hamiltonian and λ is the strength of the perturbation and can take any values varying between 0 and 1.

The MP2 energy is the Hartree-Fock energy summed with the second order perturbation correction (formally, the zero-order energy is the sum of the occupied orbital energies; adding

© University of Venda

University of Venda
Creating Future Leaders

the first-order correction gives the HF energy; adding the second-order correction marks an improvement with regard to the HF energy).

2.2.6. Density functional theory

Post-Hartree-Fock methods are based on the wavefunction and are computationally expensive (computer time-demanding). An alternative, less expensive method – not based on the wavefunction – is the *density functional theory* (DFT), which utilises the electron density (ρ) as the key factor of chemical information [58]. Knowing the electron density leads to the knowledge of all the other chemical and physical properties of the molecule.

DFT is based on two theorems called Hohenberg theorems [59, 60]. The energy is considered as a functional of the electron density [59]. The theorems state that each molecular system is characterized by a unique external potential and the ground state energy can be obtained by minimizing the energy functional. The DFT energy is expressed as a sum of functionals of ρ, each corresponding to one of the contributions to the total energy:

$$E_{DFT}[\rho] = T_S[\rho] + E_{ne}[\rho] + J[\rho] + E_{xc}[\rho] \qquad (2.29)$$

where:

T_S is the kinetic energy functional (the subscript S shows that the kinetic energy is obtained from a Slater determinant);

E_{ne} is the electron–nuclear attraction functional;

J is the Coulomb component of the electron–electron repulsion functional;

E_{xc} is the exchange correlation functional, incorporating correlation and exchange energy.

Several exchange correlation functionals have been proposed and are classified as local density functionals (LDA), generalized gradient functionals (GGA) and hybrid functionals. The most popular among them is the hybrid functional called B3LYP (Becke's three parameter exchange and Lee, Yang, Parr correlation) [61, 62]. It is the functional utilised in the present work for DFT calculations.

DFT gives a good balance between results accuracy and computation time. It has fewer variables compared to Post-Hartree-Fock methods and can be used in the calculations of larger molecular systems and in calculations of solid state. It has been validated over a wide range of systems.

© University of Venda

University of Venda
Creating Future Leaders

2.3 Calculation of Relevant Molecular Properties

This section considers some important molecular properties – dipole moment, vibrational modes, and energy gap of the frontier molecular orbitals – and outlines the way in which they are obtained from the analysis of the electronic structure and the geometry of the ground state.

2.3.1. Dipole moment

The dipole moment (μ) is a vector quantity associated with the presence of two opposite charges of magnitude q separated by a distance d. Its magnitude is given by the product of the total positive or negative charge and the distance between the centre of the positive change and the centre of the negative charge:

$$|\mu| = q \times d \tag{2.30}$$

Thus, the magnitude of the dipole moment is directly proportional to the charge and to the distance between the centres of the positive and negative charges. The direction of the vector is conventionally considered from the centre of the negative charges (origin of the vector) to the centre of the positive charges.

In a molecular system, the dipole moment is a measure of the asymmetricity of the charge distribution [30]. Computationally, it is evaluated as the first derivative of the energy with respect to an applied electric field, given by the following equation

$$\mu = \mu_0 + \alpha F + \beta F^2 + \gamma F^3 + ... \tag{2.31}$$

with μ_o is the permanent dipole, α is the (dipole) polarisability, β is the first hyperpolarisability, γ is the second hyperpolarisability.

2.3.2. Frequencies

Molecular systems in the gas phase have translation motion, rotation motion and vibrational motion. The vibration motion is the movement that changes the internal coordinates of the molecular systems. In diatomic molecules, for instance, the vibrational mode is a simple stretching of the unique bond. For a non-linear triatomic molecule, two stretching (symmetric and anti-symmetric) and one bending motions are possible. For a molecule with many atoms, the vibration is complex. The overall vibration of the molecular systems results from some basic vibrational modes. Each vibrational mode is a harmonic motion characterized by a specific frequency, and the atoms involved in the motion are moving in phase passing through the equilibrium position at the same time [63-65]. The number of these fundamental

© University of Venda

University of Venda
Creating Future Leaders

vibrational modes is related to the number of atoms (N) in the molecule, and it is equal to 3N-5 for a linear molecule and to 3N-6 for a non-linear molecule.

Each vibrational mode has its own energy and amplitude. In symmetrical molecules, some vibrational modes have the same energy or the same frequency; they are called degenerate modes. The energy of the vibrational modes is quantised. The amplitude of the vibrational modes changes by absorption or emission of energy, if the energy absorbed or emitted corresponds to the difference between two vibrational energy levels. When a molecule absorbs light at a frequency corresponding to the difference between two energy levels of a vibrational mode, the vibrational energy of the molecule increases. The measurement of the different frequencies at which the different vibrational modes of a given molecule absorb energy yields the vibrational spectrum of that molecule [65].

Vibrational spectra are specific to each molecule and are useful in the characterization of molecules. They provide information regarding the amplitude of the vibrational modes of a molecule and the strength of its chemical bonds. They thus allow characterizing new molecules and also intermediates occurring during a chemical reaction. The molecular vibration energies lie in the infrared (IR) region. Not all vibrational modes are active in IR spectroscopy, but only those that cause a significant change in the molecular dipole moment [66-67].

Theoretically, the frequencies of a molecular system are obtained by solving the following differential equation [65, 68-69] :

$$H\psi = -\frac{h^2}{2\mu}\frac{d^2\psi}{dx^2} + \frac{1}{2}kx^2\psi = E\psi \qquad (2.32)$$

where k is the constant force associated to the vibrational mode, μ is the reduced mass of the atom and x is the displacement of the atom from its equilibrium position. The term ½ kx^2 is the potential of the harmonic oscillator (which is a parabolic potential).

Equation 2.32 has the following solutions [65, 68-69]:

$$\nu = \frac{1}{2\pi}\sqrt{\frac{k}{\mu}} \qquad (2.33)$$

$$E_n = h\nu\left(n + \frac{1}{2}\right) \qquad (2.34)$$

© University of Venda

University of Venda
Creating Future Leaders

where n is the vibrational quantum number and E_n is the energy corresponding to the vibrational level n. The quantum number n is an integer and can also take the 0 value (n = 0, 1, 2, 3, ….). The vibrational energy E_n increases as the quantum number n increases. The energy levels of the harmonic oscillator are equidistant, and the energy separation between neighbouring energy levels is hν. The energy of the harmonic oscillator is never zero, even when the vibrational quantum number n is zero. Each molecular vibration has a *zero point energy* (ZPE) which corresponds to $n = 0$ in equation 2.34. This energy should be added to the computed lowest energy to get the energy of the ground state of the molecule (ZPE-corrected energy), due to the fact that all quantum molecular systems undergo random fluctuations.

The force constants are correlated to molecular vibrational frequencies. The frequency analysis of a molecule allows predicting the IR and Raman spectra of that molecule.

Molecular vibrations are generally approximated to harmonic oscillators, and this option is utilised in this study. However, in real molecules, vibrations are often anharmonic. The energy of an anharmonic potential is written as a series expansion:

$$E_n = h\nu\left(n+\frac{1}{2}\right) - h\nu\left(n+\frac{1}{2}\right)^2 Xe + h\nu\left(n+\frac{1}{2}\right)^3 Ye + \ldots \qquad (2.35)$$

where Xe and Ye are anharmonic constants

The information about thermodynamic quantities, such as internal energy, free energy and entropy can be obtained from the frequency calculations outputs [30, 70, 71]. Computationally, the calculation of the frequencies of molecular vibrations involves the evaluation of the Hessian matrix (second derivatives of the energy with respect to atomic Cartesian coordinates).

As anticipated in section 2.1.3, frequency calculations are a crucial step in the computational study of molecules because they enable the identification of the nature of stationary points on the potential energy surface (whether minima, or saddle points corresponding to transition states, or other types of saddle points).

© University of Venda

University of Venda
Creating Future Leaders

2.3.3. The frontier Molecular Orbitals (HOMO-LUMO)

In a molecule, electrons occupy molecular orbitals (MO) starting from the lowest energy ones and in order of increasing energy. The Highest Occupied Molecular Orbital (HOMO) and the Lowest Unoccupied Molecular Orbital (LUMO) constitute the *frontier* molecular orbitals and have been found to play a crucial role in the prediction of the chemical reactivity of a molecule [72]. For instance, predictions based on the properties of the frontier orbitals have been important in the determination of the stereochemistry and rates of many reactions involving soft electrophiles and nucleophiles [71]. The energy gap between the HOMO and the LUMO is a governing factor in many reactions. For instance, a large HOMO-LUMO energy gap is associated with greater kinetic stability of the molecule whereas a small HOMO-LUMO energy gap is generally associated with greater tendency to undergo chemical reactions (kinetically unstable systems). Furthermore, according to Koopmans' theorem [73], the HOMO and LUMO energies provide an estimation of the first ionization energy and of the electron affinity respectively. The shapes of the highest occupied molecular orbitals were reported by to be useful in interpreting molecular geometry (Walsh's rules) and chemical reactivity (Woodward-Hoffmann rules 11) [74].

The frontier molecular orbitals are listed in the optimization output in the latest computed wavefunction. In fact, the SCF method uses an initial guess wavefunction, and proceeds through several iterations till the changes in total energy and molecular geometry between two successive iterations do not vary significantly. All the molecular orbitals (including the HOMO and LUMO frontier molecular orbitals) of the lowest-energy geometry (optimized geometry) can be visualized with the help of the GaussView program, which also shows their occupancy and lists their eigen-energies (in hartrees). The HOMO is easily identified as the last occupied molecular orbital and the LUMO as the first non occupied molecular orbital in the energy-level diagram of Gauss View.

2.4. The Computational Study of Molecules in Solution

2.4.1. Importance of studying molecules in a medium

Most reactions, including all the reactions in biological systems, take place in a medium. Therefore, it is important to study molecules or molecular ions in solution, to better

© University of Venda

University of Venda
Creating Future Leaders

understand how their properties and behaviour are influenced by the medium. In the case of biologically active molecules, the interaction of a molecule (drug) with the target site may be influenced by the medium in many ways, depending on the properties of the molecule and the properties of the medium [75].

In common practice, a molecule is initially calculated *in vacuo* to determine its properties when it is totally isolated (gas phase), i.e., it is not interacting with an environment. The results obtained from the calculations *in vacuo* are then utilised as a starting point for the calculation of the same molecule in a medium.

2.4.2. Solvent effects on molecular properties

Solvent and solute may interact in many ways: interactions with polarised areas (electrostatic interaction); lyophilic or lyophobic interactions (hydrophilic and hydrophobic when the solvent is water [76]); solute-solvent hydrogen bonds. The type and strength of the interactions depend on the nature of the solute and on the nature of the solvent.

The solute-solvent interactions may influence many properties of the solute molecule. For instance, the presence of the solvent may influence:

- the geometry of the solute molecule(e.g; the influence of solvent on formation of the molecular geometry of [{Fe(salphen)}$_2$O][77]). Two complexes of [{Fe(salphen)}$_2$O] , ([{Fe(salphen)}$_2$O].(C_4H_8SO) and [{Fe(salphen)}$_2$O].($C_4H_8O_2$)) were studied in different solvents in order to investigate the influence of the solvents on the geometry of these complexes.The results shown that the influence of solvents are not important on the molecular geometry and magnetic properties of these complexes.
- the energies of the solute conformers and, therefore, also the conformers' relative energies (e.g. the carbohydrate conformation [78]);
- the spectroscopic properties of the solute (e.g., the absorbance spectra of poly(propylene-oxide)-poly(p-phenylene-ethynylene) blockcopolymers at same concentrations in different solvents (chloroform, hexane, methanol, methanol-water mixture) is not the same. In chloroform, it is at 349 nm, 335 nm in hexanol- methonol and 331 nm in the methanol-water mixture. The solvent tend to decrease the absorbance of the compound [79]);
- the electric charge distribution of the solute molecule (e.g., the solvation of perchlorate ion and nitrate ion in water. Knowing a better charge distribution of those ions gives an idea in how solvent can surround its. The nitrate ion is planar with angles

© University of Venda

University of Venda
Creating Future Leaders

of 120 degre between the three N–O bonds. The charge on each oxygen atom is −0.62 eo while the charge on the central nitrogen atom is 0.86 eo. Whith this planar geometries, all four atoms can be reached by the surrounding water molecules, which make the nitrate ion strongly solvated and the solubility of nitrate salts in water is very high. Due to its tetrahedral structure and it charge distribution, perchlorate fits easily into the water structure in a non-disruptive manner. Each of the oxygen atoms are hydrogen bonded to adjacent water molecules. That justifies the high solubility of LiClO4 and NaClO4 in water. [80]);

- the dipole moment of the solute molecule (e.g., large increase of the dipole moment of the singlet excited state as consequence of the large charge transfer taking place during the excitation of the benzothiazole derivative of 4-(benzothiazol-2-yl)-N,N-diphenylaniline in methanol solvent [81]);
- the solute optical properties (e.g., the optical rotation of glucose in aqueous solution. Eight most abundant structures of glucose in aqueous solution were calculated following the TD-DFT/GIAO approach for the property and the PCM description for the solvent. As results, all α structures give a large positive contribution to the OR property, while the β structures give both positive and negative contributions [82]);
- the intramolecular hydrogen bonds of the solute molecule (e.g., the solvent effects on the electronic absorption and fluorescence spectra. It has been shown that the magnitude of the spectral shifts in various solvents, having different polarities, principally depends on the strength of the intermolecular hydrogen bond(s) between the substituent groups of the spectrally active molecule and the – OH or – NH groups of the solvent molecules and whether the intramolecular hydrogen bonds are present or not. In the molecular systems having intramolecular hydrogen bonds, the spectral shifts are very small. The solvent shifts are well interpreted by the solvent polarity function in the case of absence of the intermolecular hydrogen bonds in all the intramolecular hydrogen bonded systems. [79]

In turn, the properties of the solvent are influenced by the presence of the solute (e.g., changes in bulk solvent structure).

It is not easy to model the interactions between solute and solvent and the changes brought in by the solvent, because a solution is a dynamic ensemble of molecules in continuous motion and with different types of interactions (solvent-solvent and solute-solvent being the most important). Models unavoidably introduce simplifications into this dynamic picture. Several

© University of Venda

University of Venda
Creating Future Leaders

approaches have been suggested. Two of them are based on quantum chemistry *ab initio* formulations: the continuum model approach and the supermolecule approach [84-92]. They are outlined in the next sections because they are both utilised in the study reported here.

2.4.3. The Polarisable Continuum Model (PCM)

In continuum models, the solvent is treated as a structureless continuum dielectric medium or conductor, into which the solute is embedded. The Polarisable Continuum Model (PCM, [86-92] is the most popular of the Self-Consistent Reaction Field (SCRF) models, i.e; models based on the consideration that the solute tends to polarize the continuum solvent and the solvent, in turn, tends to polarize the solute.

In the PCM model, the solvent is considered as an infinite isotropic dielectric into which the solute is embedded; therefore, the solute is modelled as a cavity in the continuum solvent, represented by a distribution of charges on the surface of the cavity. The shape and size of the cavity are determined by modelling the atoms of the solute molecule as intersecting spheres and smoothing the intersections according to the extent to which the solvent molecules can approach it. The cavity surface is generally described in terms of *tesserae* (small finite surface elements); the smaller the size of the *tesserae*, the higher their number and the higher the accuracy of the description. Each *tessera* has an apparent surface charge.

The hamiltonian operator for the solute, H, considers the energy of the molecule *in vacuo* (unperturbed hamiltonian H^0) and a perturbation term V_R accounting for the effects of the solvent:

$$H = H^0 + V_R \tag{2.37}$$

The main energy-quantity considered is the free energy of solvation (ΔG_{solv} – the free energy change accompanying the formation of the solution), often called "solvent effect". ΔG_{solv} comprises two major contributions: electrostatic and non-electrostatic. The non-electrostatic term comprises the following contributions: cavitation energy, dispersion energy and repulsion energy.

The PCM algorithm most commonly utilised in computational software is currently the IEFPCM (PCM utilising the Integral Equation Formalism, [91-92]).

2.4.4. Supermolecular structures: adducts with explicit solvent molecules

The PCM model does not take into explicit account directional, comparatively strong solute-solvent interactions such as solute-solvent hydrogen bonds. When both the solute and the

© University of Venda

University of Venda
Creating Future Leaders

solvent have sites that can form hydrogen bonds, it becomes important to consider adducts of the solute molecule with explicit water molecules situated near the sites of the solute molecule capable of forming solute-solvent hydrogen bonds, in order to obtain more information on the effect of these hydrogen bonds on the solute molecular geometry and properties.

The most important quantity in this case is the interaction energy between the solute molecule and the solvent molecules bonded to it in the adduct. The estimation of this energy needs to take into account whether the solvent molecules are interacting only with the solute molecule or also among themselves. The equations can be illustrated considering adducts with explicit water molecules.

Let $A(H_2O)_n$ denote an adduct in which n water molecules are H-bonded to a central (solute) molecule A, but not to each other. The interaction energy ($\Delta E_{solute-naq}$) between the central molecule A and the water molecules H-bonded to it is calculated through the equation

$$\Delta E_{solute-naq} = E_{adduct} - E_{solute} - nE_{aq} \qquad (2.38)$$

where E_{adduct} is the energy of the adduct, E_{solute} is the energy of the isolated solute molecule and E_{aq} is the energy of an isolated water molecule.

If some of the water molecules are H-bonded to each other, equation (2.38) becomes:

$$\Delta E_{solute-naq} = E_{adduct} - (E_{solute} + nE_{aq}) - \Delta E_{aq-aq} \qquad (2.39)$$

where ΔE_{aq-aq} is the overall interaction energy between water molecules (from water–water H-bonds). ΔE_{aq-aq} can be assessed by performing a single-point calculation on a group of water molecules identical to that in the $A(H_2O)_n$ adduct [93], to find its energy $E_{aq\ (interacting)}$. Then

$$\Delta E_{aq-aq} = E_{aq(interacting)} - nE_{aq(isolated)} \qquad (2.40)$$

where $E_{aq\ (isolated)}$ is the energy of an isolated water molecule.

The adduct with explicit water molecules can be viewed as a complex between the central molecule (A) and the water molecules (B). The interaction energy of this complex may need to be corrected for the basis set superposition error (BSSE, [94, 95]) by means of the so-called counterpoise method (CP, [94, 96]). To explain the meaning of the BSSE, it is easier to consider a complex AB between the solute molecule (A) and one water molecule (B). In fact, the number of functions used to optimize the complex AB is higher than those used to optimize their two components, namely the solute A and the ligand B. By the fact that A

© University of Venda

University of Venda
Creating Future Leaders

interacts with B in the AB complex, A can be stabilized by the near presence of the basis functions of B and B by the presence of basis function of A. Thus, the additional basis functions on B ameliorate the description of A. Similarly, the additional basis functions on A ameliorate the description of B. As a consequence of the improved descriptions, the AB system energy is over-stabilised. Thus the difference in the number of basis functions considered in the optimization of AB and its components yields an error in the appreciation of the interaction energy between A and B in the AB complex. The interaction energy calculated in this way differs from the true binding energy. This energy difference is called basis set superposition error (BSSE), which is due to the effect of the basis functions of one moiety on the calculated energy of the other moiety.

To correct this error, the counterpoise method calculates the energy of each moiety with its own basis function (E'_A, E'_B) and in the presence of the basis function of the entire system ($E_{A[B]}$, $E_{B[A]}$) but without nuclei and electrons of the partner.
The counterpoise energy corrections for A and B (ΔE_A^{CP} , ΔE_B^{CP}) are given by the following equations:

$$\Delta E_A^{CP} = E_{A[B]} - E_A \quad (2.41)$$

$$\Delta E_B^{CP} = E_{B[A]} - E_B \quad (2.42)$$

The total correction to the interaction energy is given by the sum of these counterpoise corrections, $\Delta E_A^{CP} + \Delta E_B^{CP}$, and the counterpoise corrected interaction energy is expressed as [94, 96]:

$$\Delta E_{AB}^{\text{BSSE corrected}} = E_{AB} - E_A - E_B - \Delta E_A^{CP} - \Delta E_B^{CP} \quad (2.43.)$$

2.5. Hydrogen Bonding

2.5.1. Nature and types of hydrogen bonds

The hydrogen bond is defined by the *International Union of Pure and Applied Chemistry.* (IUPAC) as an attractive interaction between a hydrogen atom from a molecule or a molecular fragment X–H in which X is more electronegative than H, and an atom or a group of atoms in the same or a different molecule, in which there is evidence of bond formation [97].

© University of Venda

University of Venda
Creating Future Leaders

Hydrogen bonds (H-bonds) are formed when an electronegative atom (Y) approaches a hydrogen atom bound to another electro-negative atom (X). The latter is called hydrogen bond *donor* and the Y atom is the hydrogen bond *acceptor*. A hydrogen bond situation can be described as X–H···Y, where X–H represents the donor, Y represents the acceptor and the three dots represent the hydrogen bond.

Hydrogen bonds are described by the following parameters: the H···Y bond length, the X···Y distance and the XĤY bond angle. According to the strength of the interaction between the donor and the acceptor, hydrogen bonds can be strong, moderate or weak. This strength is evaluated by the energy of the hydrogen bond. Strong hydrogen bonds are those which resemble covalent bonds in most of their proprieties, weak hydrogen bonds have energy close to the range of van Der Waals interactions; intermediate situation correspond to moderate hydrogen bonds [97-99]. The shorter the hydrogen bond length, the stronger the hydrogen bond. This may be used as reference for the classification of hydrogen bonds. According to the classification in [100], the H···Y bond length is 1.2–1.5 Å for strong hydrogen bonds, 1.5–2.2 Å for moderate hydrogen bonds and 2.2–3.3 Å for weak hydrogen bonds; the X···Y distance is 2.2–2.5 Å for strong hydrogen bonds, 2.5–3.2 Å for moderate hydrogen bonds and more than 3.2 Å for weak hydrogen bonds; the XĤY angle is 170–180° for strong hydrogen bonds, 130–150° for moderate hydrogen bonds and more than 90–120° for weak hydrogen bonds.

Hydrogen bonds are classified as intermolecular hydrogen bonds and intramolecular hydrogen bonds depending on whether X and Y belong to different molecules or to the same molecule respectively (figure 2.3).

Intermolecular hydrogen bonds form between different molecules, i.e., the X and Y atoms belong to different molecules of the same compound or of different compounds. The XĤY angle is often linear. They contribute to stabilize the condensed phases of compounds in which they are possible, such as water and other compounds containing O–H or N–H bonds [97,100–105].

Intramolecular hydrogen bonds form within one single molecule, i.e., the X and Y atoms belong to the same molecule. They can form it if X and Y are in positions in which they can

© University of Venda

University of Venda
Creating Future Leaders

interact. The XĤY bond angle is often considerably less than 180°. Intramolecular hydrogen bonds increase the stability of the conformers in which they are present.

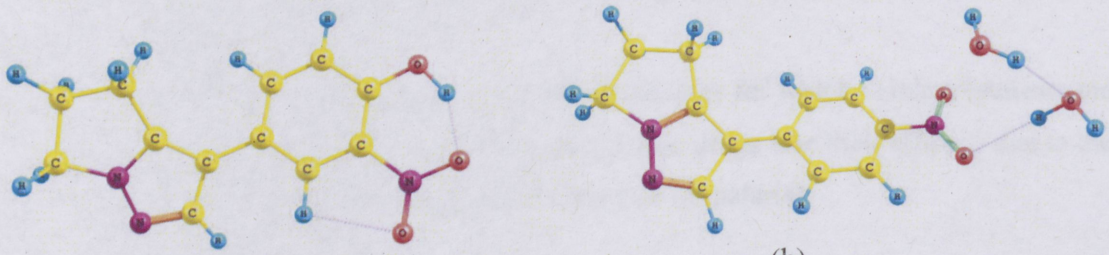

(a) (b)

Figure2.3. Examples of intramolecular hydrogen bonds (a) and intermolecular hydrogen bonds (b).

The hydrogen bonds are represented by dotted segments. Model (a) shows two intramolecular hydrogen bonds in the same molecule. Model (b) shows two intermolecular hydrogen bonds, one between a solute molecule and a water molecule and one between two water molecules.

When a substance dissolves in solvents capable of forming solute-solvent intermolecular hydrogen bonds, there may be competition between intramolecular hydrogen bonds and intermolecular hydrogen bonds. It appears that intramolecular hydrogen bonds present in the solid state remain in solution, as their stabilising effect tends to prevent major changes from an increase in temperature or the addition of a solvent [106].

2.5.2. Effects of hydrogen bonding and its importance in biological systems

Hydrogen bonding plays important roles in determining the structure and properties of a large number of chemical systems ranging from inorganic to biological systems [97, 101–110]. Hydrogen bonding influences macroscopic properties such as melting and boiling points, enthalpies of fusion and enthalpies of vaporization, dielectric constants, surface tension, and molecular properties such as electronic density distribution, vibrational frequencies, and chemical shifts. It defines the structure and properties of the condensed states of water and other solvents capable of forming intramolecular hydrogen bonds. It determines the secondary structure of proteins. It holds together the two strains of DNA [109]. It plays important roles in the mechanism of biological reactions, such as the interactions between a biologically active molecule and its receptor.

LIBRARY

© University of Venda

University of Venda
Creating Future Leaders

2.6. Relevance of the Computational Study of Biologically Active Molecules

A molecule has a biological activity when it is able to produce some demonstrable effects in the living of organisms [111].

The search for new drugs is very important both for diseases for which viable treatments are not yet available and for diseases for which currently used drugs lose their efficacy due to the development of resistance by the pathogen (as is the case of malaria).

The biological activity of a compound is related to its molecular properties. For many years, researchers have attempted to identify relationships between molecular properties and activity, or Quantitative Structure Activity Relationships (QSAR). The initial attempts consisted primarily of statistical correlations of structural descriptors with biological activities. The development of high-speed computers and of software for molecular computations and visualizations (molecular graphics) has enabled the development of what is often termed *rational drug design* or *computer-assisted drug design* [70, 112].

Nowadays, computational studies constitute a powerful source of information for drug development, as they provide information about the molecular properties of the compounds considered and may also help predict the properties of compounds that have not yet been synthesized. This restricts the number of compounds that are to be studied experimentally, because only the promising ones will be synthesized and investigated through microbiological tests and, if these are successful, through the other steps of trials *in vivo*. Since computational studies are less expensive and less time-consuming compared to experimental studies, this enables substantial cost-savings [70].

Rational drug design utilises different approaches, such as the identification of the pharmacophore (the part of the molecule that is responsible for the given activity [113]), or the investigation of how existing molecules can bind to a known receptor site (target) or how to build new molecules that will fit into that site and inhibit its activities.

© University of Venda

University of Venda
Creating Future Leaders

2.7. Brief Overview on Antimalarial Drugs

2.7.1. Antimalarial drugs of natural origin

Compounds of plants origin have played important roles in the development of antimalarial drugs. Therefore, it can be anticipated that new antimalarial leads may likely emerge from tropical plant sources [114].

The natural compounds (from plants) possessing antiplasmodial and antimalarial properties belong mainly to the following classes: alkaloids, terpenes, limonoids, flavonoids, chromones, xanthones and anthraquinones [115- 116].

Among them, a prominent role is played by alkaloids, because most antimalarial drugs of natural origin, including quinine, belong to that class. According to the literature reported between 1990 and 2000, nearly one hundred alkaloids extracted from plants were found to have significant antimalarial activity; some of them were more potent than chloroquine [116]. Alkaloids comprise several classes, such as bisbenzylisoquinolines, phenolic aporphine-benzylisoquinolines, naphtylisoquinolines, flavopereirine, and β-carboline alkaloids [116-133]. The activity of alkaloids and of the so-called biogenetic alkaloids (expressed in term of IC_{50}) was correlated with their structural classes. Another class of alkaloids showing antimalarial activity is that of pyrazole alkaloids (section 1.3, figure 1.2), which constitute the object of the current study.

2.7.2 Review of theoretical studies of antimalarial drugs

The biological activity of drugs is generally related to their molecular properties. Computational studies are important both in order to understand the activity of existing drugs and to predict the possible activities of compounds that have not yet been synthesised (e.g., derivatives of drugs currently in clinical use). This section presents a brief overview of computational studies of antimalarial drugs available in literature.

Quinine was the first antimalarial drug, and is still the "ultimate resort" in cases of resistance to all the other drugs. A study of its potential energy surface using molecular mechanics (MM) and the AM1 and PM3 quantum mechanical semi-empirical methods identified six distinct low-energy conformers; it also identified the transition states between them [134].

© University of Venda

University of Venda
Creating Future Leaders

The theoretical results of this study were found to be in good agreement with experimental information.

Theoretical and experimental studies on the enantioselective interaction of carbamoylated quinine and (S)-3,5-dinitrobenzoyl alanine by means of circular dichroism (CD), and the interaction between tert-butylcarbamoylquinine selector and (S)-3,5-dinitrobenzoyl alanine selectand by chiroptical methods, have been reported and the dissimilarities in interactions between chiral molecules were clarified combining experimental and the calculated DFT circular dichroism spectra [135]. These authors assert that density functional theory (DFT) is a reliable quantum chemical method that can deal even with more complicated systems interacting via multiple interactions of different nature.

Joshi et *al.* [136] estimated the magnitude of the dipole moment of the quinine sulphate dication (QSD) using B3LYP functional and absorption and fluorescence spectra. They obtained the ground-state dipole moment of QSD from quantum mechanical calculations (B3LYP) and estimated the excited state dipole moment of QSD from Bakhshiev's and Kawski-Chamma-Viallet's equations by means of solvatochromic shift method (however, these equations are validated only for neutral species). Further, A.K. Bhattacharjee [137] studied the electrostatic potential profiles of antimalarials chloroquine and mefloquine in order to elucidate the cation–pi interaction and the equilibrium geometry for metal–aromatic complexes in these antimalarials. They observed a significant difference in bonding energy, geometry and site of interaction between chloroquine $-Na^+$ and mefloquine-Na^+ complexes, implying two different mechanistic paths for this type of non-covalent interaction. The electrostatic potential profiles of uncomplexed molecules were suspected to play a crucial role in determining the cation–pi non-covalent interaction for the computed equilibrium geometries.

Bhattachajee et *al.* [138] studied 17 compounds using AM1 semi-empirical methods to elucidate the chloroquine resistance reversal. The stereoelectronics properties computed via AM1 were in good agreement with the electrostatic potential profiles model. A correlation between the resistance reversal activity and the intrinsic basicity of the nitrogen atom, the frontier molecular orbital energies, and the lipophilicity of the set of compounds has been proposed.

© University of Venda

University of Venda
Creating Future Leaders

A Quantitative Pharmacological Analysis of Structure-Activity Relationships for mefloquine antimalarial drugs using optimal transformations was investigated by Cong et *al.*[139] using an alternating conditional expectation (ACE) to study the relationship between electrostatic structures and antimalarial activity of mefloquine and its substituted derivatives. The electronic structure of these molecules was modelled by using atomic net charges evaluated on the basis of CNDO/2 molecular orbital calculations. The authors claimed that ACE can be a good technique for predicting pharmacological activity of compounds and establishing quantitative structure activity relationships (QSAR).

In the search for new artemisinin derivatives, Cardoso et *al.* [140] have studied artemisin derivatives with potent activity against *Plasmodium falciparum* malaria using *ab initio* and Partial Least Squares (PLS) methods. The molecular structures obtained experimentally were compared with the optimized geometries from Hartree-Fock calculations using the 3-21G (d,p), 3-21G and 6-31G basis sets. The computed values of bond lengths were found close to experimental data. Based on some quantum descriptors such as the LUMO+1 energy, atomic charges, total surface area, bond angles formed, and maximal electrotopological positive difference, a significant regression model was established by PLS method for those artemisinin derivatives with antimalarial activity. A new artemisinin derivative was predicted, with antimalarial activity higher than that of compounds reported in literature [140].

Pinheiro and co-workers [141] also studied the antimalarial activity of artemisinin derivatives using the regression model obtained by PLS, based on the following quantum descriptors: LUMO+1 energy, atomic charges, number of hydrogen atoms and the radial distribution function RDF030m. The increasing antimalarial activity against *Plasmodium falciparum* was found to arise from higher values of LUMO+1 combined with high negative charges on the C and O atoms, high number of hydrogen atoms and lower values of RDF030m (a radial distribution function centered at 3.0 a interatomic distance and weighted by atomic masses).

On investigating 26 well-known anti-malarial agents and 1730 novel compounds showing strong anti-malarial activity, low toxicity and structural dissimilarity, Sullivan *et al.* [142] reported that the gradient's metric modelling approach and the electron-density molecular representations are potentially powerful tools in the discovery and design of novel anti-malaria drugs. Fernandez et al. [143] have compared the bioactivity of a series of endoperoxide compounds with the natural drug artemisinin. Several endoperoxides molecules

© University of Venda

University of Venda
Creating Future Leaders

were found more efficient than artemisinin and the activity of those molecules were correlated with the stability of O-O bonds. According to the authors, quantum chemical calculations on six-membered cycles, using B3LYP with 6-311++G(d,p) and 6-31+G(d) basis sets, revealed the following stability order: 1,2-dioxane > 1,2,4-trioxane >1,2,4,5-tetraoxane. For cycles comprising 3 oxygen atoms, the calculations showed that the 6-membered counterpart 1,2,4-trioxane is more stable than the 5-membered cycle 1,2,4-trioxolane.

© University of Venda

University of Venda
Creating Future Leaders

CHAPTER 3

OVERVIEW ON COMPUTATIONAL METHODS USED

This chapter gives an overview of the different computational methods used in the current study to elucidate the electronic structures, conformational structures, stability and solvation free energies of withasomnine and other pyrazole alkaloids. In addition, the practical details regarding inputs preparation, calculations and specific instructions to get desired computational information are highlighted.

3.1 Choice of Computational Methods

The choice of the level of theory and of the basis set for molecular calculations is based on the size of the molecules to be studied and the type of their constituent atoms, in an attempt to conciliate the accuracy and cost of the quantum chemical calculations. The study investigates the performance of different quantum chemical methods using different types of Pople basis sets in various environments.

3.1.1. Computations *in vacuo*

The molecules of the alkaloids considered in the current study are of medium size, having a pyrazole ring adjacent to a cyclopentane and a benzene ring bonded trough a single bond. This is the only rotatable bond in the skeleton of the withasomnine and newbouldine structures.

Full optimizations *in vacuo* of withasomnine and newbouldine and their p-hydroxy, p-methoxy derivatives, the nitro-derivatives of withasomnine and p-hydroxywithasomnine, and their corresponding adducts with explicit water molecules, have been performed using wavefunction and density functional methods. In particular, the following methods have been used: Hartree Fock (HF), Møller-Plesset perturbation theory (MP2) and Density Functional Theory (DFT) with the B3LYP functional [61–62], in combination with the 6-31G(d,p), 6-31+G(d,p), 6-31++G(d,p), 6-311G(d,p), 6-311+G(d,p), and 6-311++G(d,p) basis sets. The double and triple zeta basis sets are known to bring acceptable flexibility to the molecular

© University of Venda

University of Venda
Creating Future Leaders

wavefunction leading to a good description of bonds between atoms. The p functions added to hydrogen atoms and the incorporation of diffuse functions in the basis set increase the ability of the molecular total wavefunction to describe hydrogen bonds and long range interactions in the molecular system considered.

Geometry optimizations are first carried out using the less expensive Hartree-Fock method. The HF results are used as inputs for DFT or MP2 calculations. The main drawback of the more affordable Hartree-Fock method is that it does not consider electron correlation. Therefore, the electronic energy obtained with Hartree-Fock may be far away from the true energy. This is the reason for using also other methods. The most widely employed exchange functional, B3LYP, was used in the DFT calculations. The primary problem with this hybrid density functional is the presence of the self electron repulsion, which has been identified as a source of errors [62]. Moreover, both Hartree-Fock and DFT/B3LYP are unable to treat long-range electron correlation effects, such as *dispersion interactions,* which are the main part of weak van der Waals intermolecular forces, and are of great importance in the investigation of hydrogen bonds. Despite the advantage of MP2 in the treatment of electron correlation and dispersion energy, the two-electron integral transformation is the most time-consuming step and prevents its use for very large molecular systems.

On combining the three levels of theory and the different basis sets selected, the following methods have been used for the molecules considered in this study: HF/6-31G(d,p), HF/6-31+G(d,p), HF/6-31++G(d,p), HF/6-311G(d,p), HF/6-311+G(d,p), HF/6-311++G(d,p), MP2/6-31G(d,p), MP2/6-31+G(d,p), MP2/6-31++G(d,p), MP2/6-311G(d,p), MP2/6-311+G(d,p), MP2/6-311++G(d,p), DFT/B3LYP/6-31G(d,p), DFT/B3LYP/6-31+G(d,p), DFT/B3LYP/6-31++G(d,p), DFT/B3LYP/6-311G(d,p), DFT/B3LYP/6-311+G(d,p), and DFT/B3LYP/6-311++G(d,p).

The use of different methods enables a comparison of their performance. The MP2/6-31++G(d,p) results are chosen as reference for the evaluation of the performance of the other methods, as those comprising the best inclusion of effects relevant to the description of H-bonding such as correlation and dispersion effects and diffuse functions in the basis set (section 2.2.4.). Assessing the performance of different methods for molecules of this class is important in view of a future study of many other alkaloid molecules. Larger molecular systems require more computational time. The increase of the size of the basis sets used to

© University of Venda

University of Venda
Creating Future Leaders

describe the wavefunction of the molecular ground state improves the values of the geometrical and chemical properties of the system. However, it is necessary to find a balance between the size of the basis and the size of the molecule, knowing that the larger the system and the basis set, the more expensive the calculation. The evaluation of the performance of different methods and different basis sets is useful in searching for this balance.

The potential energy surface was investigated by scanning the rotation of relevant rotatable bonds, i.e., scanning the rotation of the corresponding relevant dihedral angles. The bond between the two rings, the hydroxy and the bond between C of benzene ring and O of methoxy group were selected in order to have find others mimima. To obtain adequate information, each scan considered 24 steps (15° change of the dihedral angles in each step). The opt=modredundant keyword was used in the route section of the input (flexible scan), and the information about the pace and the number of steps was given in the appropriate section.

The modified GDIIS algorithm (opt= (gdiis) instruction) was used for all the optimisation calculations, because it is more convenient for non-small molecules [144]. All the calculations were performed using the Gaussian03 package [145].

3.1.2. Computation of solvent effects

3.1.2.1. Choice of solvents for calculations with the polarizable continuum model

The conformational preferences of the solute molecule are influenced by the polarity of the solvent molecules and the type of interactions that they establish with the solute molecule. To model the solvation effects of the molecules considered in this study, the polarizable continuum model (PCM) was used, as implemented in the Gaussian 03 program package. In this approach, the solvent is not considered as individual "explicit" solvent molecules, but as a continuum polarizable dielectric (section 2.4.3.). Its dielectric constant is used as the main characteristic property to describe the bulk effect of the solvent. Solvents can be categorized with respect to the magnitude of their dielectric constants.

Three solvents were chosen for this study, namely chloroform, acetonitrile and water. They include polar solvents as well as a non-polar solvent, in order to cover a wide range of

© University of Venda

University of Venda
Creating Future Leaders

polarity of the different media and also to mimic the environments present in a living organism.

Chloroform is an apolar aprotic solvent, characterized by low relative permittivity ($\varepsilon = 4.90$), low dipole moment (μ=1.04 D), and the inability to act as a hydrogen–bond donor or acceptor; therefore, this solvent does not form specific directional interactions with the solute molecule [83]. Acetonitrile is a dipolar aprotic solvent, which possess a large relative permittivity ($\varepsilon = 36.64$) and a high dipole moment (μ=3.92 D). This solvent can act as a hydrogen bond acceptor because of the presence of the N atom, whereas it does not act as hydrogen-bond donor, since its C-H bonds are not sufficiently polarized. Because of the presence of the N atom, it is usually a good electron-pair-donor (EPD) solvent, thus having good ability for cation solvation [83]. Acetonitrile is a good model for the medium in cell membranes. Water is a protic solvent, and can act both as hydrogen-bond donor and as hydrogen-bond acceptor [83]. It has high relative permittivity ($\varepsilon = 78.39$) and sizeable dipole moment (μ=1.83 D).

The geometry optimization is firstly carried out in *vacuo*, and the results in vacuo are used as inputs for the PCM calculations in the solvents considered, at the same level of theory of the calculations in *vacuo*. Re-optimisation in solution at the same level of theory as in vacuo provides information on geometry changes in the solute molecule brought about by the solvent [146]. Compared to calculations in *vacuo,* the PCM re-optimisation in solution requires more computational time. Therefore, only some methods (6-31G (d,p), 6-31+G(d,p) and 6-31++G(d,p) at HF, DFT and MP2 levels) were utilised for calculations in solution.

The default settings of PCM calculations as implemented in the Gaussian03 package [145] were used. These comprise the Integral Equation Formalism model (IEF) [87–91] and an average tesserae area of 0.200 $Å^2$ for the description of the surface of the cavity around the solute. The united atom topological model applied on radii optimized for HF/6-31G(d) level, denoted UAHF radii, were utilized for the interlocking spheres around each atom of the solute molecule. Practically, in the initial input for solvation calculations, the PCM default was combined with the SCFVAC and the radii=UAHF keywords, which allow the consideration of the gaseous phase and the application of the united atom topological model on the radii optimized at HF/6-31G(d).

© University of Venda

University of Venda
Creating Future Leaders

3.1.3. Calculation of adducts with explicit water molecules

Adducts with explicit water molecules were calculated for all the molecules considered in the present work. In withasomnine and newbouldine, there is only one region capable of H-bonding water molecules, namely, the two N atoms in the pyrazole ring. All the other molecules have also atoms or functional groups attached to the benzene ring, defining a second region which can act as H-bond donors or acceptors. However, the two regions are sufficiently separated to prevent any interactions of type solute-solute H-bonds between the water molecules attached to the N atoms and the water molecules attached to the O or OH bound to the benzene ring.

The less computationally demanding method among those used in this work, namely the HF/6-31G(d,p), was employed for the calculations of the adducts with explicit water molecules, because of the bigger size of the supermolecular system. The optimised adducts were, in turn, utilised as solutes for PCM calculations, performed as single point (SP) calculations because of the excessive demands of PCM re-optimisation of the larger supermolecular system.

3.1.4. Frequency calculations

Frequency calculations were carried out at the same level of theory used for geometry optimizations, to predict the IR spectra of the various conformers, in *vacuo* and in the three solvents considered. The *Freq Test* keyword is used for frequency computation if the basis set does not contain diffuse functions, and the *Freq scf=tight* keyword is used if the basis set contains diffuse functions. The vibrational frequencies obtained from frequency calculations need to be scaled by an appropriate factor, for the values to be closer to experimental values. The scaling factor is different for different levels of theory and different basis sets.

Besides the vibrational frequencies, the frequency outputs contain other types of information, such as the ZPE (section 2.3.2.) and the band intensities (although the computed intensities may be less accurate than the frequencies, they are definitely related to the strength of the IR bands). The analysis of data focused on the vibrational frequencies, also because of their importance to evaluate the strength of hydrogen bonds. ZPE corrections were also considered.

© University of Venda

University of Venda
Creating Future Leaders

3.2. Preparation of Inputs

3.2.1. Calculations in vacuo

The inputs for the calculations *in vacuo* were prepared with the help of GaussView program [144].

In order to gain in computation time, the optimized geometries obtained from HF calculations were used as inputs for DFT and MP2 calculations. This is particularly convenient for MP2 calculations, because the zeroth order electronic energy of MP2 calculation corresponds to the HF energy. In fact, HF provides the starting molecular orbitals for MP2 and it contributes in the calculation of the exchange correlation in DFT/B3LYP.

3.2.2. Calculations in solution

According to standard practice, the optimized geometries obtained from calculations *in vacuo* were used as initial geometries for PCM calculations in solution. The change in the geometrical parameters and the molecular properties (dipole moment, HOMO-LUMO gaps, and NBO atomic charges) in solution with respect to *in vacuo* can elucidate the effect of the three solvents considered on the molecules considered.

The analysis of solvent effects was extended to the energy of rotational barriers between conformers. Therefore, the scanning of the rotation of relevant bonds was performed also in each of the solvents considered.

3.2.3. Adducts with explicit water molecules

As stated in section 2.4.3, the PCM model cannot take into account solute-solvent hydrogen bonds. To compensate for this, calculations on adducts comprising explicit water molecules around the solute molecule were also performed (section 2.4.4).

The input geometries of adducts were built by adding water molecules to the optimised geometries *in vacuo*, considering the water molecules that can H-bond directly to the solute molecule and orienting them in the way needed for the formation of these H-bonds. When two of these water molecules can be bridged by another water molecule, these adducts were also considered. The interaction energy of different adducts of the same molecule are compared to

© University of Venda

University of Venda
Creating Future Leaders

identify favourable arrangements and optimum number of water molecules which can H-bond to the central molecule.

Calculations on adducts containing only one water molecule were also performed in order to evaluate the perturbation provoked by that water molecule on the geometrical properties of the central molecule and the strength of the hydrogen bond between the central molecule and that water molecule. This also enables a comparison of the strength with which each of the donor or acceptor sites of the central molecule can bind a water molecule.

3.3. Presentation of Results

The main aspects which need to be mentioned are the units of measure and the acronyms used in the presentation of the obtained results, above all those that are not standard, but are introduced specifically for this study.

3.3.1. Units used

In the Gaussian outputs, most values are given in atomic units. Thus, most energy values are given in hartrees. The values of ΔG_{solv} and its components (G_{el} and $G_{non\text{-}el}$) from PCM calculations are given in kcal/mol.

On reporting results in this work, all the energy values (conformers' relative energies, HOMO-LUMO energy gaps, interaction energies between water molecules and the central molecule in adducts, etc.) are given in kcal/mol, because of the wide use of this unit. To convert a value in hartree to a value in kcal/mol, the value in hartree is multiplied by a factor 627.509. For this reason, all the energy values obtained utilising this conversion factor will have a maximum of 3 decimal positions. Energy values from thermodynamic data expressed in kcal/mol in Gaussian outputs maintain the same number of decimal figures (2 decimal figures) as in the output.

Bond distances are in angstroms (1 Å = 10^{-10} m). Bond angles are given in degrees. Dipole moments are given in Debye (D). The charges on the atoms are given using the atomic unit e, which corresponds to 1.602176 x 10^{-19} Coulombs.

© University of Venda

University of Venda
Creating Future Leaders

3.3.2. Non-Standard Acronyms Utilised

Some non –standard acronyms have been introduced in place of longer standard acronyms, for reason of simplicity and to enable better space organisation in tables and figures. They are listed in table 3.1.

Table 3.1. Standard acronyms and non –standard acronyms utilised in this work.

Standard acronyms	Non-standards acronyms
HF/6-31G(d,p)	HF
HF/6-31+G(d,p)	HF+
HF/6-31++G(d,p)	HF++
HF/6-311G(d,p)	HFb
HF/6-311+G(d,p)	HFb+
HF/6-311++G(d,p)	HFb++
DFT/B3LYP/6-31G(d,p)	DFT
DFT/B3LYP/6-31+G(d,p)	DFT+
DFT/B3LYP /6-31++G(d,p)	DFT ++
DFT/B3LYP /6-311G(d,p)	DFT b
DFT/B3LYP /6-311+G(d,p)	DFT b+
DFT/B3LYP /6-311++G(d,p)	DFT b++
MP2/6-31G(d,p)	MP2
MP2/6-31+G(d,p)	MP2+
MP2/6-31++G(d,p)	MP2++
MP2/6-311G(d,p)	MP2b
MP2/6-311+G(d,p)	MP2b+
MP2/6-311++G(d,p)	MP2b++

For similar reasons, the following acronyms are used in place of the names of the media considered:

vac	for	in *vacuo*
chlrf	for	in chloroform
actn	for	in acetonitrile
aq	for	in water.

© University of Venda

University of Venda
Creating Future Leaders

CHAPTER 4

RESULTS

This chapter presents the results obtained from the calculations of the molecules considered in this study. For better readability of the text, all the tables and the most bulky figures (such as the shapes of the frontier molecular orbitals) are reported at the end of the chapter.

4.1. Conformational Preferences in vacuo

The molecules considered are withasomnine (3-phenyl-5,6-dihydro-4H-pyrrolo[1,2-b]pyrazole), its p-hydroxy and p-methoxy derivatives, newbouldine (3-phenyl-3a,4,5,6-tetrahydro-3H-pyrrolo[1,2-b]pyrazole) and its p-hydroxy and p-methoxy derivatives. They are respectively denoted as A, B, D, E, F and G in this work, for conciseness sake. Their optimised structures are shown in figure 4.1. The main differences between withasomnine and newbouldine, as well as between their p-hydroxy and p-methoxy derivatives, are the fact that withasomnine and its p-hydroxy and p-methoxy derivatives have no asymmetric centres and posses no optical rotation. The nitroderivatives of compounds A and B shown in figure 4.2. have also been calculated. The atom numbering utilized in this work is shown in figure 4.3.

© University of Venda

University of Venda
Creating Future Leaders

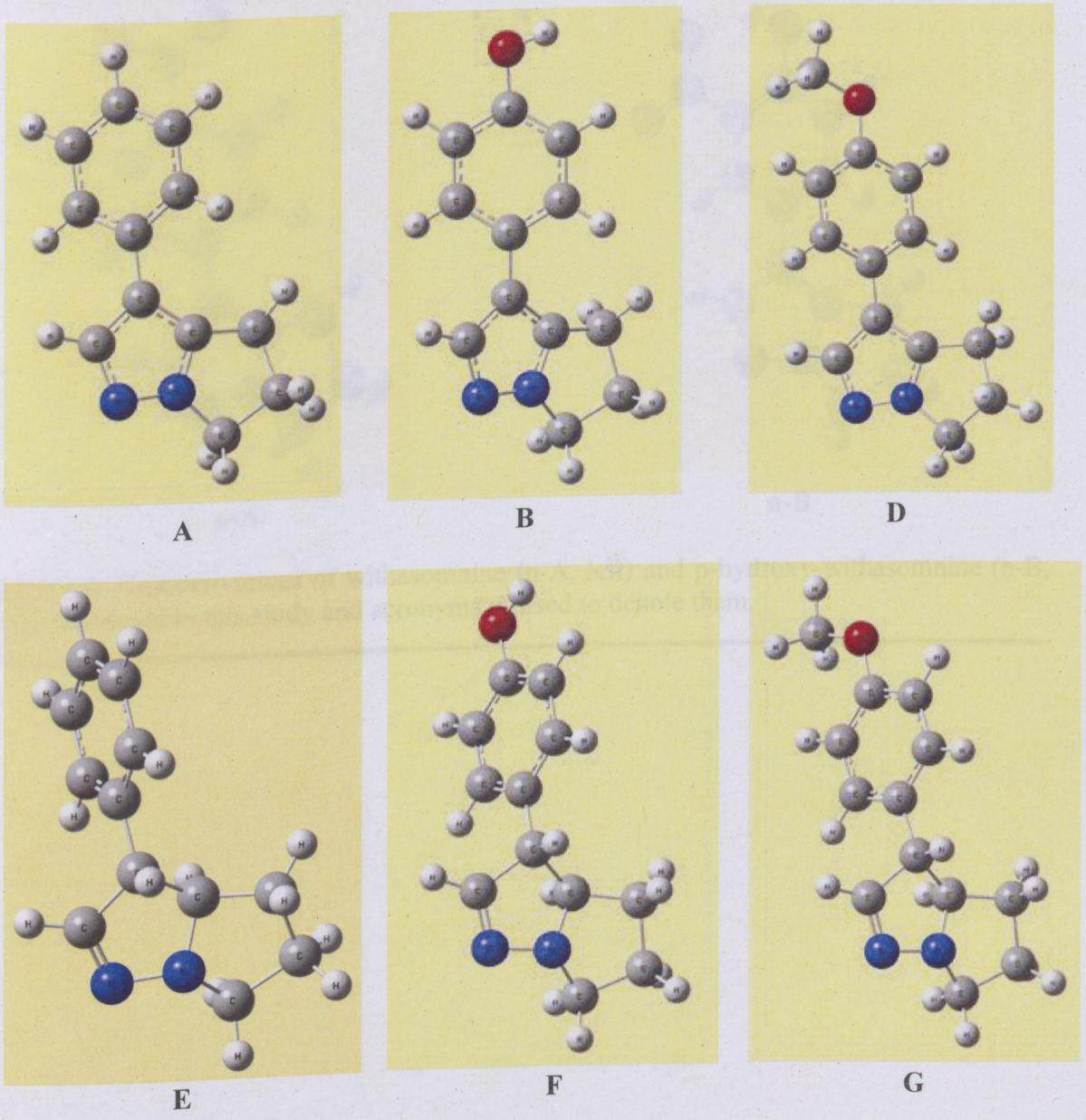

Figure 4.1. Optimized geometries of the pyrazole alkaloids of natural origin considered in this study and acronyms utilised to denote them (A: withasomnine. B: p-hydroxy derivative of withasomnine. D: p-methoxy derivative of withasomnine. E: newbouldine. F: p-hydroxy derivative of newbouldine. G: p-methoxy derivative of newbouldine). Geometries from MP/6-31++G(d,p) results.

© University of Venda

University of Venda
Creating Future Leaders

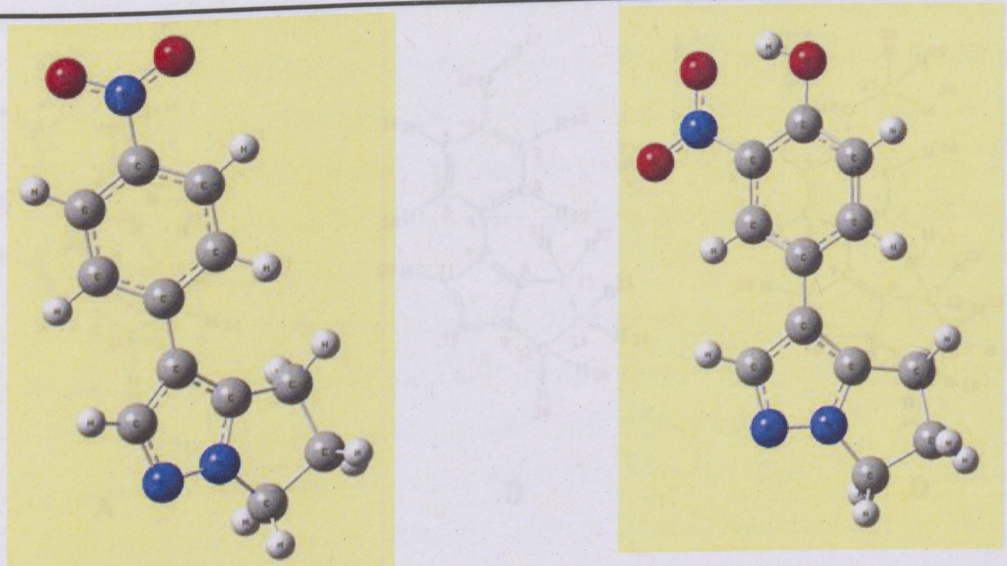

n-A n-B

Figure 4.2. Nitroderivatives of withasomnine (n-A, left) and p-hydroxy-withasomnine (n-B, right) considered in this study and acronyms utilised to denote them.

© University of Venda

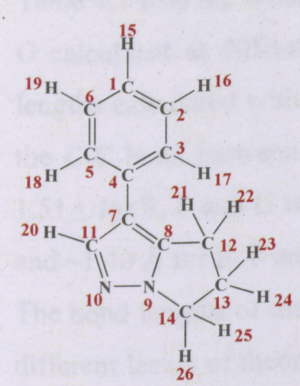

A

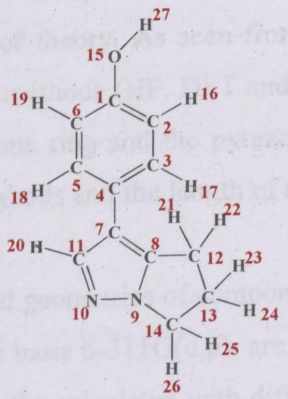

B

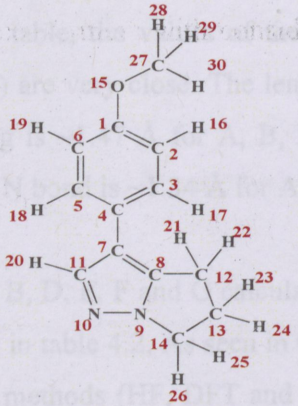

D

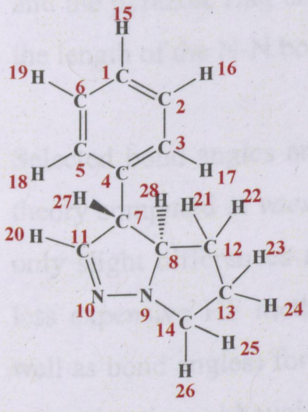

E

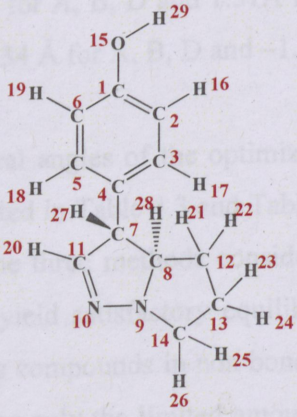

F

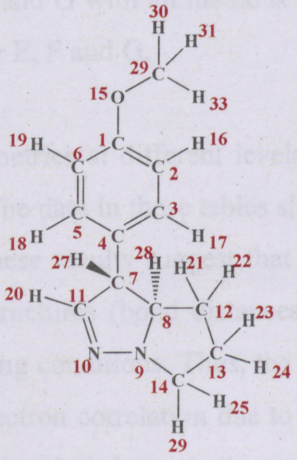

G

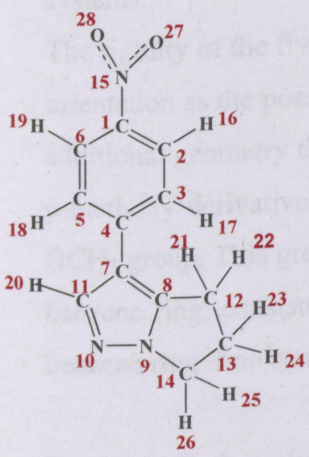

n-A

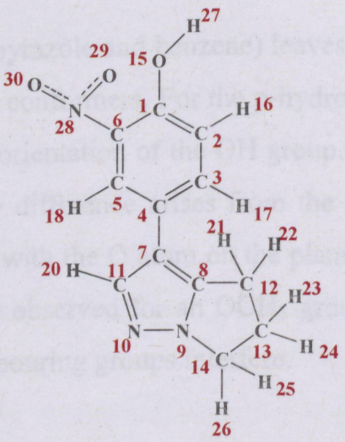

n-B

Figure 4.3. Atom numbering utilised for the compounds considered in this study.

© University of Venda

University of Venda
Creating Future Leaders

Table 4.1 lists the bond lengths of the optimized geometries of compounds A, B, D, E, F and G calculated at different levels of theory. As seen from this table, the values of the bond lengths calculated with different methods (HF, DFT and MP2) are very close. The length of the C-C bond between the benzene ring and the pyrazole ring is ~1.47 Å for A, B, D and 1.51Å for E, F and G with all methods and the length of the N-N bond is ~1.34 Å for A, B, D and ~1.40 Å for E, F and G.

The bond lengths of the optimized geometries of componds A, B, D, E, F and G calculated at different levels of theory with the basis 6-311G(d,p) are given in table 4.2. As seen in this in table, the values of the bond lengths calculated with different methods (HF, DFT and MP2) are very close. The bond lengts calculated with 6-311G(d,p) are close to those calculated with 6-31G(d,p) basis set. In this case also, the length of the C-C bond between the benzene ring and the pyrazole ring is ~1.47 Å for A, B, D and 1.51Å for E, F and G with all methods and the length of the N-N bond is ~1.34 Å for A, B, D and ~1.40 Å for E, F and G.

Selected bond angles and dihedral angles of the optimized geometries at different levels of theory computed *in vacuo* are listed in Table 4.3 and Table 4.4. The data in these tables show only slight differences among the three methods considered. These results suggest that the less expensive HF method can yield satisfactory equilibrium structures (bond distances as well as bond angles) for pyrazole compounds in non bond-breaking conditions. Thus, the HF approximation, although including only the limited amount of electron correlation due to the Pauli exclusion principle, can yield good equilibrium geometries for close shell organic systems.

The rigidity of the five and six member rings (pyrazole and benzene) leaves only their mutual orientation as the possible factor distinguishing conformers. For the p-hydroxy derivatives, an additional geometry difference arises from the orientation of the OH group. Similarly, for the p-methoxy derivatives, an additional geometry difference arises from the orientation of the OCH_3 group. This group prefers to be oriented with the O atom on the plane identified by the benzene ring, consistently with what generally observed for an OCH_3 group attached to the benzene ring if no steric hindrances from neighbouring groups interfere.

For A and E, the only significant geometry difference can be related to the mutual orientation of the two rings. A scan of the rotation of the C4–C7 bond between the rings in A and E was carried out in order to identify possible conformers for those compounds (figure 4.4). For A, two conformers were found which differ by the C11–C7–C4–C5 dihedral angle and have

© University of Venda

University of Venda
Creating Future Leaders

close energy. They are denoted as A-y (with C11–C7–C4–C5 = 32.467°) and A (with C11–C7–C4–C5 = -36.886°). For E, there is only one conformer (the scan rotation gives two minima which correspond to a 180° difference in the dihedral angle and the two minina have a same energy). The height of the barrier between the two conformers is nearly 1 kcal/mol with HF/6-31G(d,p) and MP/6-31G(d,p); 0.2 kcal/mol with DFT/6-31G(d,p) for A and nearly 2 kcal/mol for E with all methods.

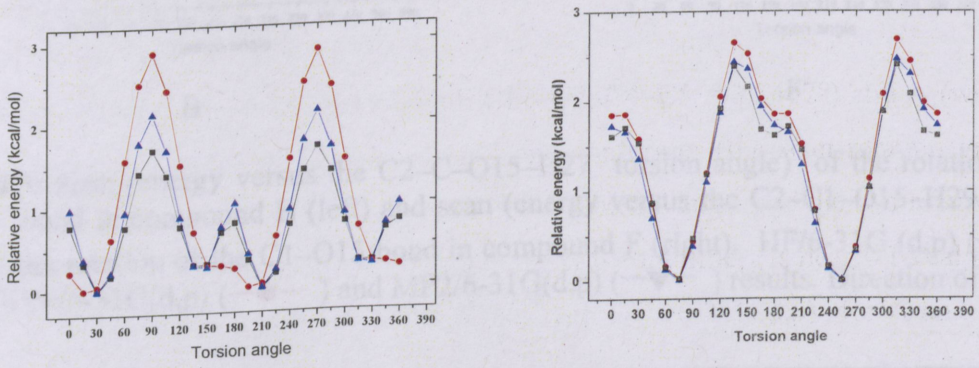

Figure 4.4. Scan (energy versus the C11–C7–C4–C5 torsion angle) of the rotation of the C7–C4 bond between the two rings in compound A (left) and E (right). HF/6-31G (d,p) (—■—), DFT/B3LYP/6-31G (d,p) (—●—) and MP2/6-31G(d,p) (—▼—) results. Direction of rotation ↻

An additional difference due to the orientation of the OH group is present in B and F. The scan of the rotation of the C1–O15 bond (C2–C1–O15–H27 torsion angle, figure 4.5) is very similar for the two compounds. It shows preference for orientation of the OH coplanar to the ring, consistently with what observed for phenols in general ([147,148], fig.4.6). It highlights two conformers, one with the OH oriented to the left and one with the OH oriented to the right, i.e., the equilibrium geometries correspond to 0°and 180° values of the C2–C1–O15–H27 torsion angle, whereas the top of the barrier corresponds to 90° C2–C1–O15–H27. As long as OH is planar, the orientation towards one or another side does not imply significant energy difference. The difference between the two planar orientations is 0.088 kcal/mol/HF, 0.097 kcal/mol/DFT and 0.098 kcal/mol/MP; for phenol (fig.4.6) the computed difference is ~ 10^{-5} kcal/mol, which is tantamount to exactly zero in view of the significant figures of these values. The small energy difference in B and F indicates that the presence of the pyrazole ring

© University of Venda

University of Venda
Creating Future Leaders

does not influence the orientation preferences of the phenol OH significantly.

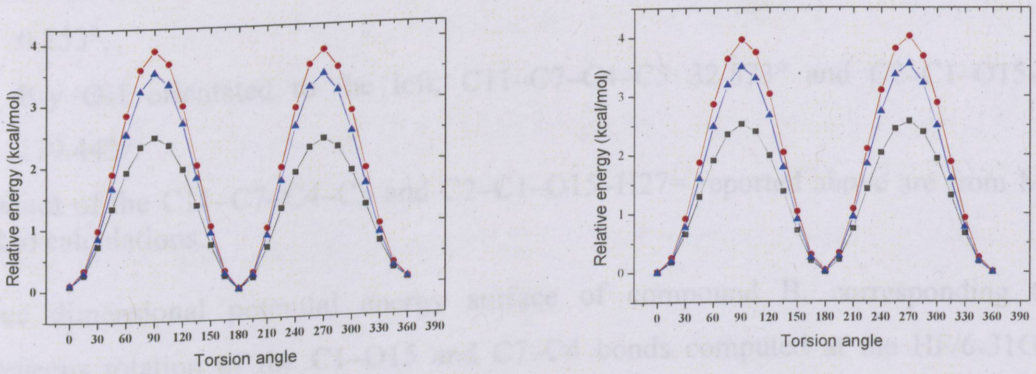

B F

Figure 4.5. Scan (energy versus the C2–C–O15–H27 torsion angle) of the rotation of the C1–O27 bond in compound B (left) and scan (energy versus the C2–C1–O15–H29 torsion angle) of the rotation of the C1–O15 bond in compound F (right). HF/6-31G (d,p) (—■—), DFT/B3LYP/6-31G(d,p) (—●—) and MP2/6-31G(d,p) (—▼—) results. Direction of rotation ↻

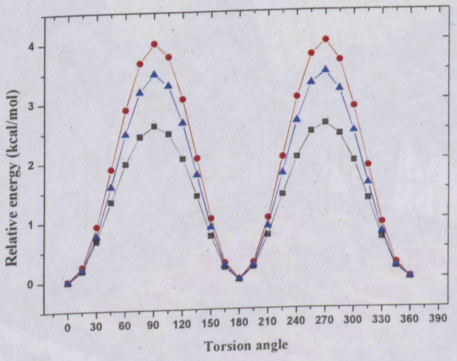

Figure 4.6. Scan the rotation of the OH group in phenol. HF/6-31G (d,p) (—■—), DFT/B3LYP/6-31G(d,p) (—●—) and MP2/6-31G(d,p) (—▼—) results. Direction of rotation ↻

A scan of the rotation of the C4–C7 bond between the two rings was also performed for B and F, and showed two minima. Combining all the information from the scans, four conformers are identified for B, and F, namely:

- B OH orientated to the right, C11–C7–C4–C5=-37.449°and C2–C1–O15–H27=-0.253° ;
- B-x OH orientated to the left, C11–C7–C4–C5=-37.213° and C2–C1–O15–H27=-

UNIVERSITY OF VENDA
LIBRARY

© University of Venda

University of Venda
Creating Future Leaders

179.370 °;

- B-z OH orientated to the right, C11–C7–C4–C5=33.009° and C2–C1–O15–H27= 0.253°;
- B-y OH orientated to the left, C11–C7–C4–C5 32.873° and C2–C1–O15–H27= 179.443°.

The values of the C11–C7–C4–C5 and C2–C1–O15–H27= reported above are from MP2/6-31G(d,p) calculations.

A three dimensional potential energy surface of compound B, corresponding to the simultaneous rotation of the C1–O15 and C7–C4 bonds computed at the HF/6-31G (d,p) level, and a projection of the PES on a plane, is shown in figure 4.7.

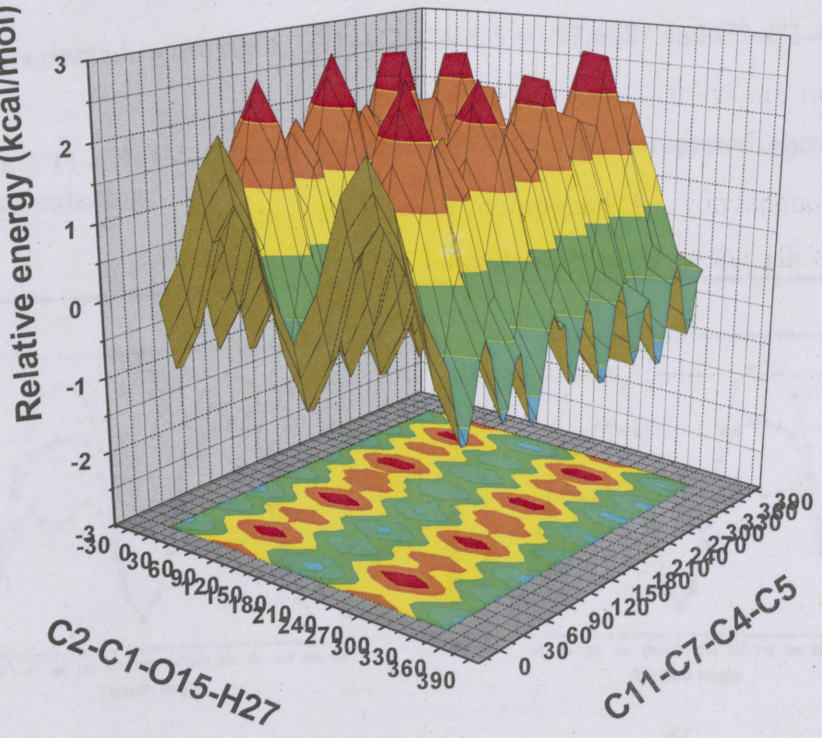

Figure 4.7. Simultaneous scan of the rotation of the C1–O15 and C7–C4 bonds (energy versus C2–C1–O15 –H27 and C11–C7–C4–C5 torsion angles) in compound B, computed at the HF/6-31G (d,p) level. Direction of rotation ↻

For compounds D and G, the additional difference is due to the orientation of OCH_3 group. The scan of the rotation of the C27–O15 bond in D and the C29–O15 bond in G (figure 4.8)

© University of Venda

University of Venda
Creating Future Leaders

gives three conformers, two conformers with OCH_3 oriented to the right, which differ by the dihedral angle between the two rings, and one conformer with OCH_3 oriented to the left. By combining this information with the results of the scan of the C7–C4 bond between the two rings (C11–C7–C4–C5 torsion angle), the three conformers of D are identified as follows:

- D OCH_3 oriented to the left, C11–C7–C4–C5 =32.728°and C2–C1–O15–C27= 179.527°
- D-y OCH_3 oriented to the right, C11–C7–C4–C5 =-37.200° and C2–C1–O15–C27= -0.077°
- D-z OCH_3 oriented to the left, C11–C7–C4–C5 =-37.071° and C2–C1–O15–C27=-179.422°

Similarly, the three conformers of compound G are identified as follows

- G OCH_3 oriented to the left, C11–C7–C4–C5 = -57.686° and C2–C1–O15–C29=-179.827°;
- G-y OCH_3 oriented to the right, C11–C7–C4–C5 = -57.628° and C2–C1–O15–C29=-0.277°;

The values of the C11–C7–C4–C5 and C2–C1–O15–C27 (29) = reported above are from MP2/6-31G(d,p) calculations.

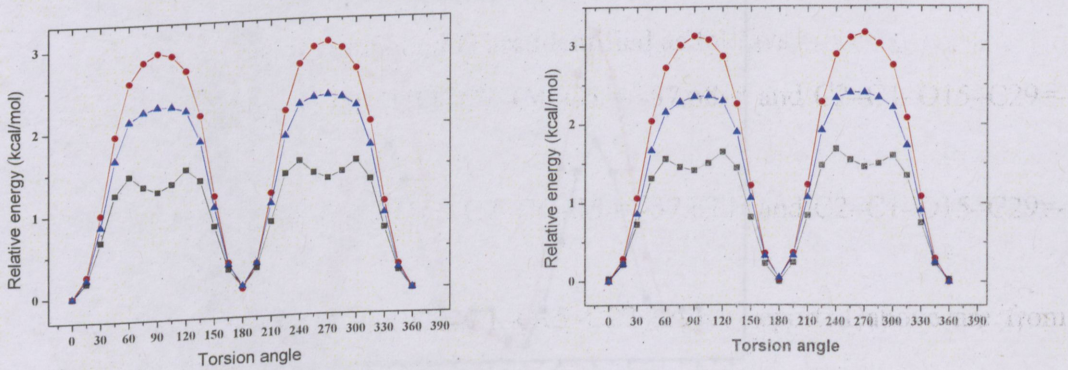

Figure 4.8. Scan (energy versus C6–C1–O15–C27 torsion angle) of the rotation of the C27–O15 bond in compound D (left) and scan (energy versus C6–C1–O15–C29 torsion angle) of the rotation of the C29–O15 bond in compound G (right) in vacuo. HF/6-31G (d,p) (—■—), DFT/B3LYP/6-31G(d,p) (—●—) and MP2/6-31G(d,p) (—▼—) results. Direction of rotation ↻

© University of Venda

University of Venda
Creating Future Leaders

Due to the presence of the chirality in the compounds E, F and G; there are E-R and E-S , F-R and F-S; G-R and G-S,wich are the enantiomers.

Between the two enantiomers, it is not knwon which is responsible for the antimalarial activity. Since, it is unknwon which one of the enantiomers is responsable for the antimalarial activity, the enantiomer R is analyzed in detail in the present study.

In the case of the nitro derivative of A (compound n-A), the scan of the rotation of the C4–C7 bond between the two rings (figure 4.9) gives the same trend as for compound A (figure 4.4). The two minima have very close energies. The scan of the orientation of the nitro group with respect to the benzene ring (rotation of the C6–N28 bond) in n-A (figure 4.10) shows that the equilibrium geometries are characterized by the C2–C1–N15–O27 torsion angle being a multiple of 180°, which means that the NO_2 group prefers to be coplanar to the benzene ring. A similar scan for nitrobenzene (figure 4.11) was carried out as reference, to check for possible influences of the pyrazole ring on the orientation preferences of the nitro group in n-A. Comparison of the two scans shows that the pyrazole ring has no significant influence on the orientation preferences of the NO_2 group in n-A.

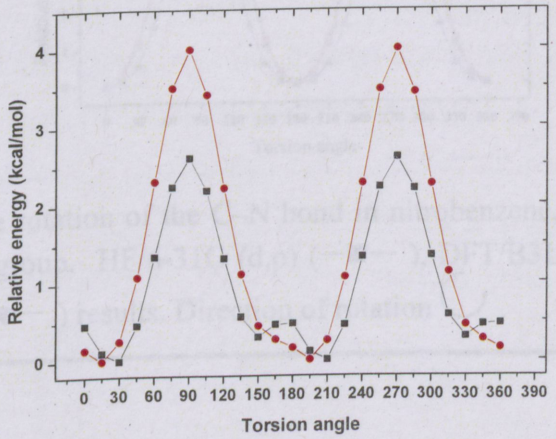

Figure 4.9. Scan (energy versus C11–C7– C4–C5 torsion angle) of the rotation of the C4–C7 bond in compound n-A. HF/6-31G (d,p) (—■—) and DFT/B3LYP/6-31G(d,p) (—●—) results. Direction of rotation ↻

© University of Venda

University of Venda
Creating Future Leaders

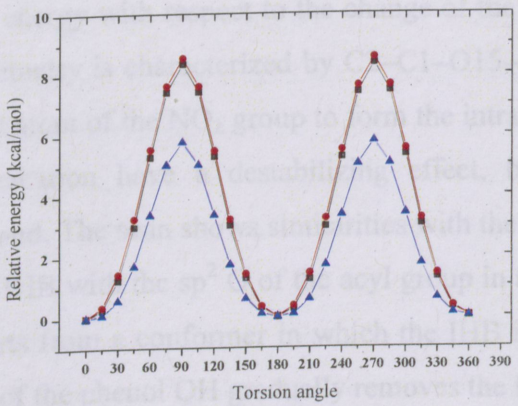

Figure 4.10. Scan (energy versus C2–C1–N15–O27 torsion angle) of the rotation of the C1N15 bond in compound n-A. HF/6-31G (d,p) (—■—), DFT/B3LYP/6-31G(d,p) (—●—) and MP2/6-31G(d,p) (—▼—) results. Direction of rotation ↻

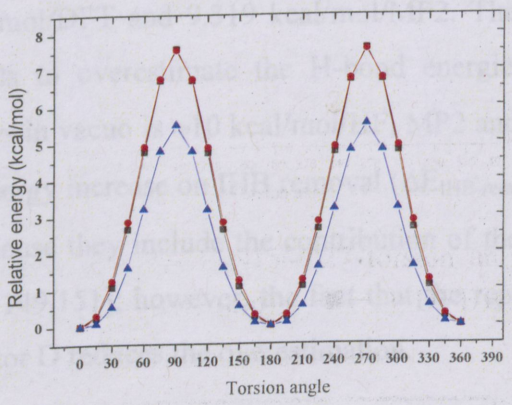

Figure 4.11. Scan of the rotation of the C–N bond in nitrobenzene, to check the orientation preferences of the NO_2 group. HF/6-31G (d,p) (—■—), DFT/B3LYP/6-31G(d,p) (—●—) and MP2/6-31G(d,p) (—▼—) results. Direction of rotation ↻

For nitroderivative n-B, an important geometry difference arises from the possibility of the presence or absence of the intramolecular hydrogen bond (IHB) between the OH group and one of the O atoms of the NO_2 group. This gives rise to two conformers with considerably different energies:

- n-B1 conformer with the intramolecular hydrogen bond.
- n-B2 conformer without the intramolecular hydrogen bond.

© University of Venda

University of Venda
Creating Future Leaders

A scan of the rotation of the OH group in n-B (rotation of the C1–O15 bond, figure 4.12) shows the variation of the energy with respect to the change of the C6–C1–O15–H27 torsion angle. The equilibrium geometry is characterized by C2–C1–O15–H27 being 180°, i.e., H27 being oriented toward an O atom of the NO_2 group to form the intramolecular hydrogen bond. Deviations from this orientation have a destabilizing effect, because they weaken the intramolecular hydrogen bond. The scan shows similarities with the scan of the rotation of the phenol OH engaged in the IHB with the sp^2 O of the acyl group in acylphloroglucinols [149]. In both cases, the scan starts from a conformer in which the IHB is present and has optimal geometry, and the rotation of the phenol OH gradually removes the IHB. The acceptor O atom also rotates "following" the H atom as long as the interaction between the two is not completely removed. In this way, the acceptor O shifts off-plane and remains off-plane in the conformer without the IHB, thus partially smoothing the repulsion between the two O atoms. The height of the barrier for the removal of an IHB by 180° rotation of the donor gives an indication of the IHB strength [150]. In the case of n-B, the height of the barrier is 9.794 kcal/mol/HF, 12.015 kcal/mol/DFT and 9.319 kcal/mol/MP2. The HF and MP2 values are closer, whereas DFT tends to overestimate the H-bond energies. The energy difference between the two conformers in vacuo is ≈10 kcal/mol/HF, MP2 and ≈12kcal/mol/DFT. These values correspond to the energy increase on IHB removal ($\Delta E_{IHB\text{-}removal}$). They are greater than the actual IHB energy, because they include the contribution of the O↔O repulsion ensuing after the IHB is removed [149,151]; however, the fact that the repulsion is smoothed by the off-plane shift of the acceptor O reduces the overestimation.

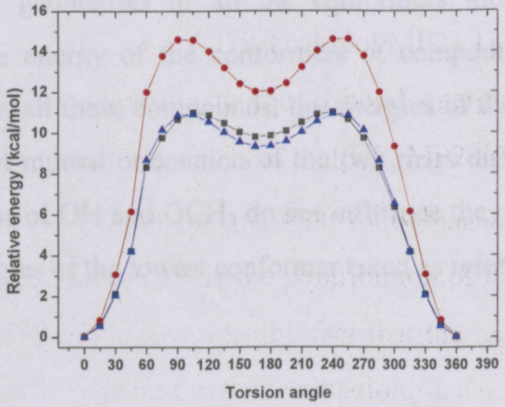

Figure 4.12. Scan (energy versus C6–C1–O15–H27 torsion angle) of the rotation of the OH group in compound n-B. HF/6-31G (d,p) (—■—), DFT/B3LYP/6-31G(d,p) (—●—) and MP2/6-31G(d,p) (—▼—) results. Direction of rotation ↻

© University of Venda

University of Venda
Creating Future Leaders

A comparison of the results of the different methods utilised shows that:

- For compounds A and E, HF and MP2 give similar trends, whereas DFT deviates slightly from the HF and MP2 trends for compound A. Both HF and MP2 show symmetrical trends for the variation of the energy in function of the C11–C7–C4–C5 torsion angle for compound A (figure 4.4). All the methods show asymmetric trends for compound E (figure 4.4).
- All the three methods show similar trends for the rotation of the OH group in compounds B and F (figure 4.5), although DFT overestimates the energy barrier. The same is true for the rotation of the OH group in phenol (figure 4.6).
- DFT and MP2 show similar trends for the rotation of the OCH_3 group in compounds D and G (figure 4.8), although DFT overestimates the energy barrier. HF has a different trend in the high-energy part of the curve. All the methods identify the lowest energy geometry for 0° and 180° values of the C6–C1–O15–C27 torsion angle.
- The three methods show similar trends for the rotation of the NO_2 group in compound n-A (figure 10). HF and DFT also give the same relative energies, whereas MP2 gives smaller values for the relative energies. The same is true for the rotation of the NO_2 group in nitrobenzene (figure 4.11).
- HF and MP2 have very close relative energies for the rotation of the OH group in compound n-B (figure 4.12), whereas DFT considerably overestimates the height of the barrier. This is consistent with the know tendency of DFT to overestimate the energy of hydrogen bonds.

Figure 4.13 shows the geometries of all the conformers identified for the compounds considered. The relative energy of the conformers of compounds A, B, D, F and G are reported in table 4.5. For all these compounds, the energies of the conformers corresponding to minima with different mutual orientation of the two rings differ by less than 2 kcal/mol. The different orientations of OH and OCH_3 do not influence the relative energy significantly. Table 4.6 gives the energies of the lowest conformer taken as reference in Hartree.

© University of Venda

University of Venda
Creating Future Leaders

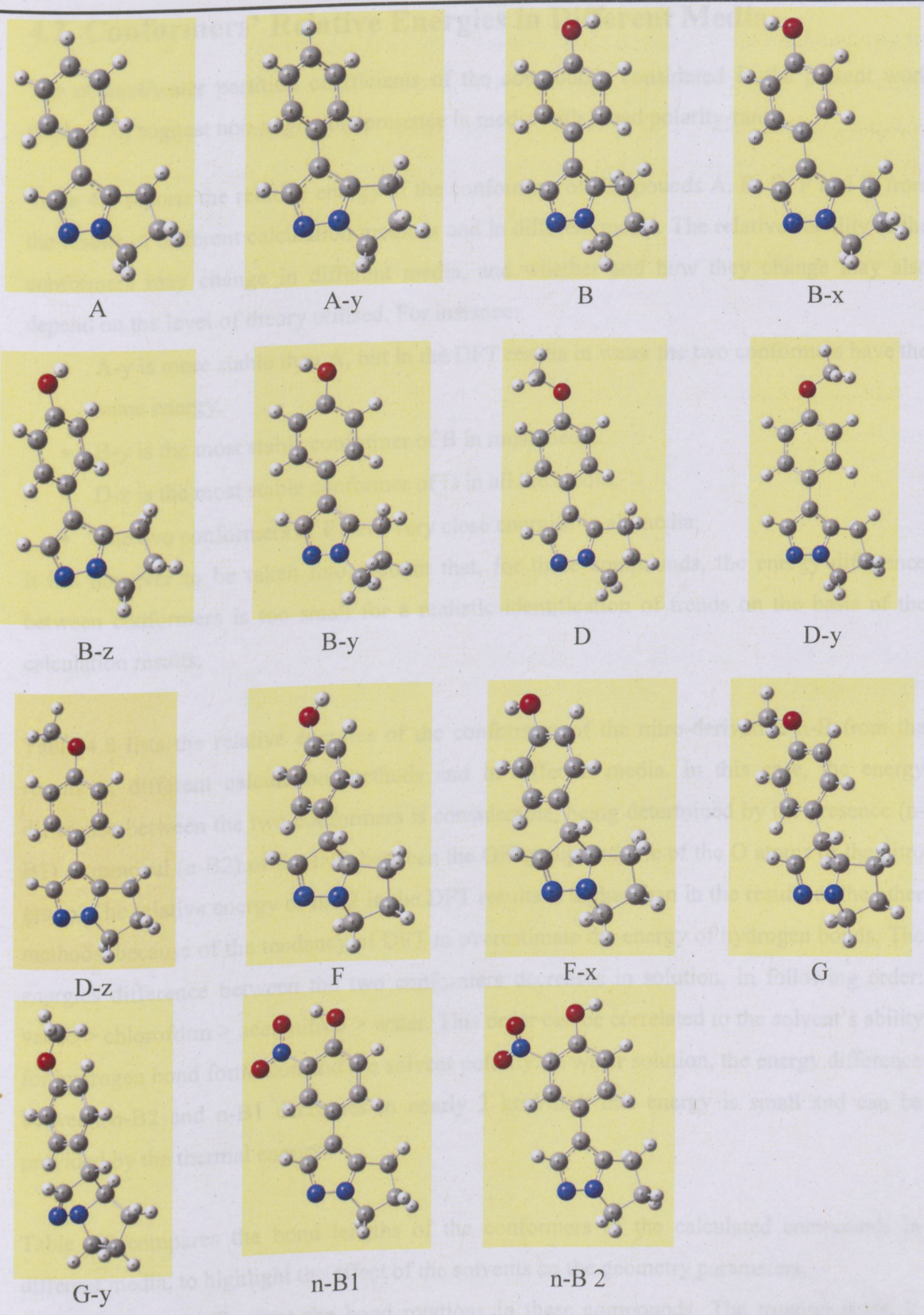

Figure 4.13. Geometries of the conformers of the compounds having more than one conformer.

© University of Venda

University of Venda
Creating Future Leaders

4.2. Conformers' Relative Energies in Different Media

The octanol/water partition coefficients of the compounds considered in the present work (table 4.7.) suggest non-negligible presence in media with broad polarity-range.

Table 4.5 reports the relative energy of the conformers of compounds A, B, D, F and G from the results of different calculation methods and in different media. The relative stability of the conformers may change in different media, and whether and how they change may also depend on the level of theory utilised. For instance:

- A-y is more stable than A, but in the DFT results in water the two conformers have the same energy.
- B-y is the most stable conformer of B in most media.
- D-z is the most stable conformer of D in all the media.
- The two conformers of F have very close energies in all media.

It has however to be taken into account that, for these compounds, the energy difference between conformers is too small for a realistic identification of trends on the basis of the calculation results.

Table 4.8 lists the relative energies of the conformers of the nitro-derivative n-B from the results of different calculation methods and in different media. In this case, the energy difference between the two conformers is considerable, being determined by the presence (n-B1) or removal (n-B2) of the IHB between the OH group and one of the O atoms of the nitro group. The relative energy of n-B2 in the DFT results is higher than in the results of the other methods, because of the tendency of DFT to overestimate the energy of hydrogen bonds. The energies difference between the two conformers decreases in solution, in following order: vacuo > chloroform > acetonitrile > water. This order can be correlated to the solvent's ability for hydrogen bond formation and the solvent polarity. In water solution, the energy difference between n-B2 and n-B1 decreases to nearly 2 kcal/mol; this energy is small and can be provided by the thermal energy.

Table 4.9 compares the bond lengths of the conformers of the calculated compounds in different media, to highlight the effect of the solvents on the geometry parameters.
The solvent also influences the bond rotations in these compounds. The rotation scans in solution were performed using the method which gave results closer to the MP2 results for the

© University of Venda

University of Venda
Creating Future Leaders

corresponding rotation scan in vacuo. In most cases, HF gave results closer to MP2, except for compounds D and G, for which DFT gave results closer to MP2. Figure 4.14 shows the scan of the rotation of the C4–C7 bond between the two rings in compound A, in all the media considered. Figure 4.15 shows the scan of the rotation of the C1–O15 bond in compound B, in all the media considered. In both cases, the rotational barrier increases slightly with the medium polarity and is highest in water.

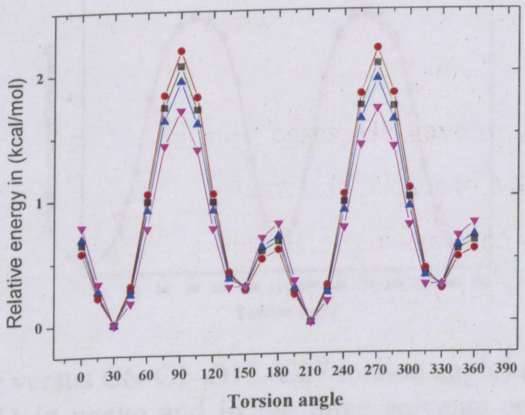

Figure 4.14. Scan (energy versus C11–C7–C4–C5 torsion angle) of the rotation of the C4–C7 bond between the two rings in compound A *in vacuo* and in the three solvents considered. HF/6-31G(d,p) results in vacuo (—▲—), in chloroform (—▼—), in acetonitrile (—■—), and in water (—●—).Direction of rotation ↻

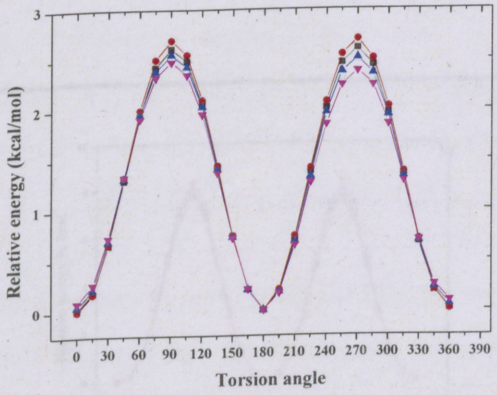

Figure 4.15. Scan (energy versus C2–C1–O15–H27 torsion angle) of the rotation of the C1–O15 bond in compound B *in vacuo* and in the three solvents considered. HF/6-31G(d,p) results in vacuo (—▲—), in chloroform (—▼—), in acetonitrile (—■—) and in water (—●—). Direction of rotation ↻

© University of Venda

University of Venda
Creating Future Leaders

Figure 4.16 shows the scan of the rotation of the O15–C27 bond in compound D, in all the media considered. In this case, there is no significant difference between different media. This may be due to the nature of the group considered in the scan (the OCH_3 group is less polar than the OH group of compound B and, therefore, it interacts less with the solvent) or to the fact that, in this case, the scan is performed at the DFT/B3LYP level.

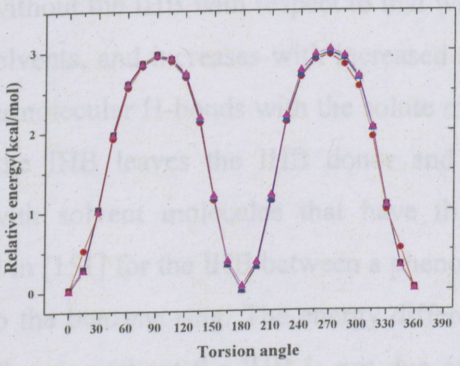

Figure 4.16. Scan (energy versus C6–C1–O15–C27 torsion angle) of the rotation of the C27–O15 bond in compound D *in vacuo* and in the three solvents considered. DFT/B3LYP/6-31G(d,p) results in vacuo (—▲—), in chloroform (—▼—), in acetonitrile (—■—) and in water (—●—).Direction of rotation ↻

Figure 4.17 shows the scan of the rotation of the C1–N15 bond in compound n-A, in all the media considered. In this case, the barrier height decreases as the medium polarity increases, and it is lowest in water solution (the height trend is water < acetonitrile < chloroform < *vacuo*).

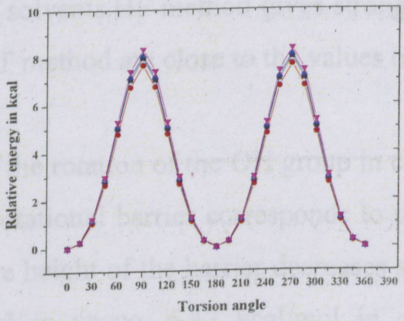

Figure 4.17. Scan (energy versus C2–C1–N15–O27 torsion angle) of the rotation of the C1–N15 group in compound n-A *in vacuo* and in the three solvents considered. HF/6-31G(d,p) results in vacuo (—▲—), in chloroform (—▼—), in acetonitrile (—■—) and in water (—●—).Direction of rotation ↻

© University of Venda

University of Venda
Creating Future Leaders

The case of compound n-B poses the interesting question of the fate of the IHB in solution: whether it is maintained and whether it is weakened or broken. The energy gap between the conformer with the IHB and the conformer without the IHB decreases as the solvent polarity increases (table 4.8). An estimation of the IHB strength in solution cannot be linked to the energy difference between the two conformers, because of the greater stabilization by the solvent of the conformer without the IHB with respect to that with the IHB [152]. This effect is different for different solvents, and increases with increased solvent polarity and with the solvent ability to form intermolecular H-bonds with the solute molecule (an important factor, because the removal of the IHB leaves the IHB donor and acceptor available to form intermolecular H-bonds with solvent molecules that have this ability). The situation is analogous to that discussed in [151] for the IHB between a phenol OH and a sp^2 O attached to an atom in turn attached to the benzene ring. The energy difference between the conformer with the IHB and the conformer without the IHB is not due only to factors "inner" to the molecule (IHB removal, geometry changes like the off-plane rotation of the acceptor O, O↔O repulsion), but also to an "external" factor (the solvent stabilization) that is greater for the conformer without the IHB. This would suggest that the strength of the IHB is greater than the energy difference between the two conformers. The difference between the two conformers is different in different media because the additional solvent stabilization of the conformer without the IHB is different for different media. Thus, it is not easy to find criteria for a reasonable approximation to the IHB energy in solution and the non-availability of experimental techniques [153] further complicates the picture.
Table 4.10 gives differents parameters of the IHB in n-B1 in different media and from different calculation methods. As seen in this table, the strenght of the hydrogen bond increases with the polarity of solvents.HF method gives strongther hydrogen bond than DFT method, and the values of DFT method are close to the values of MP method.

Figure 4.18 shows the scan of the rotation of the OH group in compound n-B, in all the media considered. In this case, the rotational barrier corresponds to the removal of the IHB trough 180° rotation of the donor. The height of the barrier decreases sharply as the medium polarity increases. It is 9.79 kcal/mol in vacuo, 6.47 kcal/mol in chloroform, 5.15 kcal/mol in acetonitrile and 2.34 kcal/mol in water. This trend is similar with the energy difference between the two conformers (9.857 kcal/mol in vacuo, 6.511 kcal/mol in chloroform, 5.156 kcal/mol in acetonitrile and 2.350 kcal/mol in water).

© University of Venda

University of Venda
Creating Future Leaders

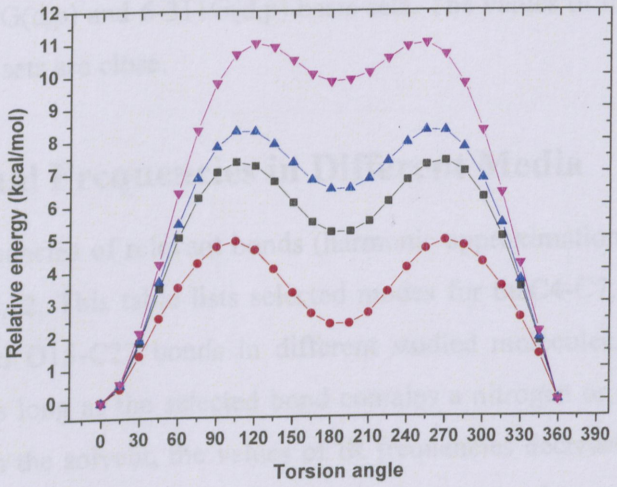

Figure 4.18. Scan (energy versus C6–C1–O15–H27 torsion angle) of the rotation of the OH group in compound n-B *in vacuo* and in the three solvents considered. HF/6-31G(d,p) results *in vacuo* (—▲—), in chloroform (—▼—), in acetonitrile (—■—) and in water (—●—).Direction of rotation ↻.

4.3. Dipole Moments in Different Media

The calculated dipole moments of the conformers of the compounds studied in this work are reported in table 4.11, considering different media and different calculation methods. The dipole moment increases with the solvent polarity. The nitro-derivatives (n-A and n-B) have the largest dipole moments, and B is the most polar molecule among those without a nitro group.

The values of the dipole moment are different in the results of different calculation methods. For the same level of theory, they are higher when the basis set includes diffuse functions. For calculations with the same basis set, MP2 gives higher dipole moments than HF or DFT.
The values of the enantiomers of compound E, F and G are also given in this table and they are named E-S, F-S and G-S respectively. The results in vacuo are identical (as expected); the slight differences in solution are likely due to some spurious effect due to the cavity orientation.

© University of Venda

University of Venda
Creating Future Leaders

The table s-1 gives a comparison of the dipole moment in vacuo at different calculation methods with 6-31G(d,p) and 6-311G(d,p) basis sets. The values of dipole moments obtained from the two basis sets are close.

4.4. Vibrational Frequencies in Different Media

IR calculated frequencies of relevant bonds (harmonic approximation) in different media are reported in table 4.12. This table lists selected modes for theC4-C7, N9-N10, C8-N9, N10-C11, O15-H27 and O15-C27 bonds in different studied molecules. The values change in different media. As long as the selected bond contains a nitrogen or an oxygen atom able to forma H-bond with the solvent, the values of IR frequencies decrease with the increasing of the solvent polarity. For other bonds the values can increase or decrease with the increasing of the solvent polarity. For A compound, the IR frequencies of the C4-C7 bond increase with the polarity of solvent for HF and DFT methods and its decrease for MP2 method; the IR frequencies of the N9-N10 bond decrease with the solvent polarity for all the methods; the IR frequencies of the C8-N9 and N10-C11 bonds increase with the solvent polarity for HF anddecrease with the solvent polarity forDFT and MP2 methods. For B and D compounds, all the IR frequencies of all the bonds selected decrease with the increasing of the solvent polarity.For E compound, the IR frequencies of the C4-C7 bond increase with the solvent polarity for HF and DFTmethodsand decrease with the solvent polarity for MP2 method;the IR frequencies of the N9-N10 decrease with the polarity solvent for all the methods; the IR frequencies of the C8-N9 bond decrease with the solvent polarity for HF and MP2 methods and increase with the solvent polarity for DFTand for N10-C11 bond, IR frequenciesdecrease for HF and increase for DFT and MP2 methods with the solvent polarity. For F and G compounds, the IR frequencies of most of the bonds decrease with the increasing of the solvent polarity.

The calculated IR spectra are shown in figure 4.19.

Table 4.13 reports the frequencies and red shift of the stretching vibrational mode of O-H group in compound n-B in the media considered, from the results of different calculation methods. An H-bond causes a lowering of the IR frequencies of the donor OH, usually termed red-shift. The red shift is greater for stronger H-bonds. It is calculated as difference with the frequency of a conveniently selected free OH. In the case of n-B, the most apt reference is the frequency of the OH in compound B. However, while in vacuo the red shift can be considered

© University of Venda

University of Venda
Creating Future Leaders

an indication of the IHB strength, in solution the solvent effect interferes. The red shift is considerably smaller in solution, decreasing as the solvent polarity increases. The data in this table show a large shift in water.

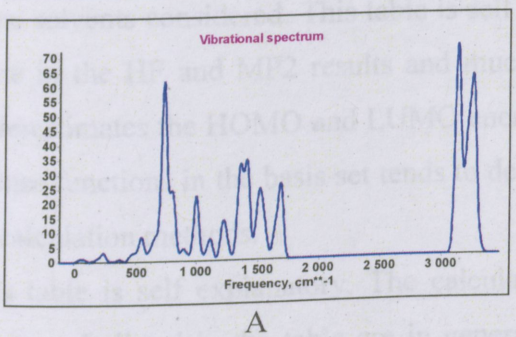

A

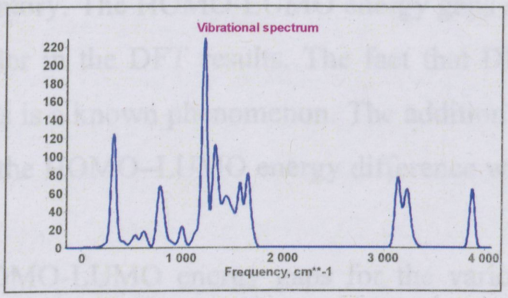

B

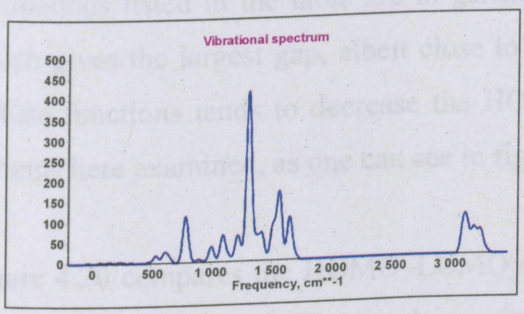

D

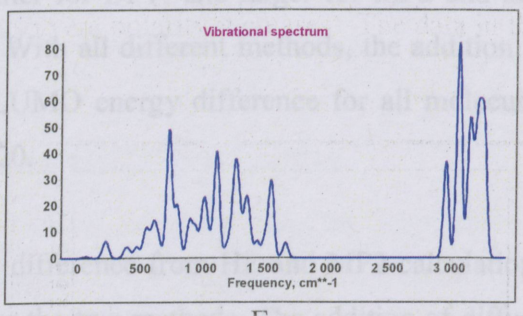

E

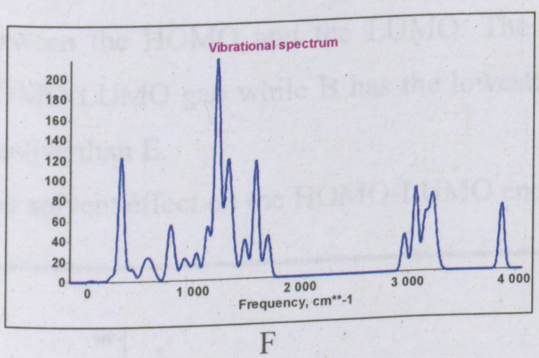

F

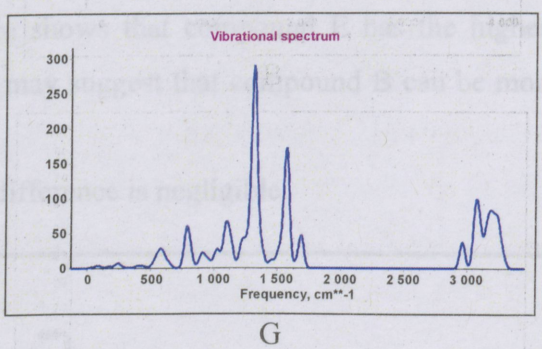

G

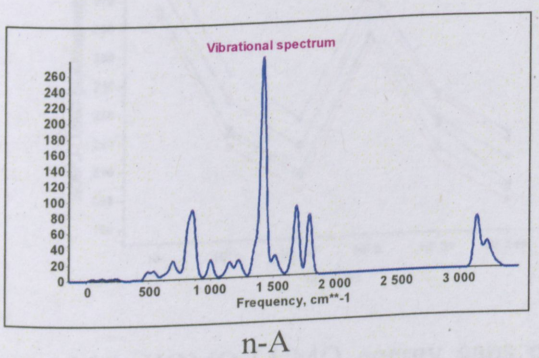

n-A

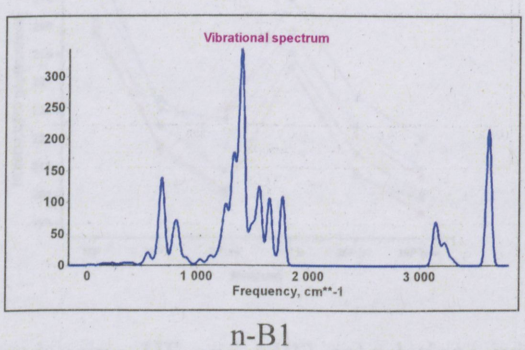

n-B1

Figure 4.19. Calculated IR spectra of compounds A, B, D, E, F, G, n-A and n-B1 at MP2/6-31G(d,p)

© University of Venda

University of Venda
Creating Future Leaders

4.5. HOMO, LUMO and close-to-HOMO Molecular Orbitals in Different Media

Table 4.14 compares the energy difference between HOMO and LUMO in vacuo and in the three solvents considered. This table is self explanatory. The HOMO-LUMO energy gaps are close in the HF and MP2 results and much smaller in the DFT results. The fact that DFT underestimates the HOMO and LUMO energy gaps is a known phenomenon. The addition of diffuse functions in the basis set tends to decrease the HOMO–LUMO energy difference with all calculation methods.

This table is self explanatory. The calculated HOMO-LUMO energy gaps for the various compounds listed in the table are in general smaller for DFT, and larger for MP2 and HF, which gives the largest gap, albeit close to MP2. With all different methods, the addition of diffuse functions tends to decrease the HOMO–LUMO energy difference for all molecular systems here examined, as one can see in figure 4.20.

Figure 4.20 compares the HOMO–LUMO energy difference from HF and MP2 calculations using different basis sets. The trends are similar for the two methods. The addition of diffuse functions and the increase of the size of the basis set tend to lower the energy difference between the HOMO and the LUMO. The figure shows that compound E has the highest HOMO-LUMO gap while B has the lowest; this may suggest that compound B can be more reactive than E.

The solvent effect on the HOMO-LUMO energy difference is negligible.

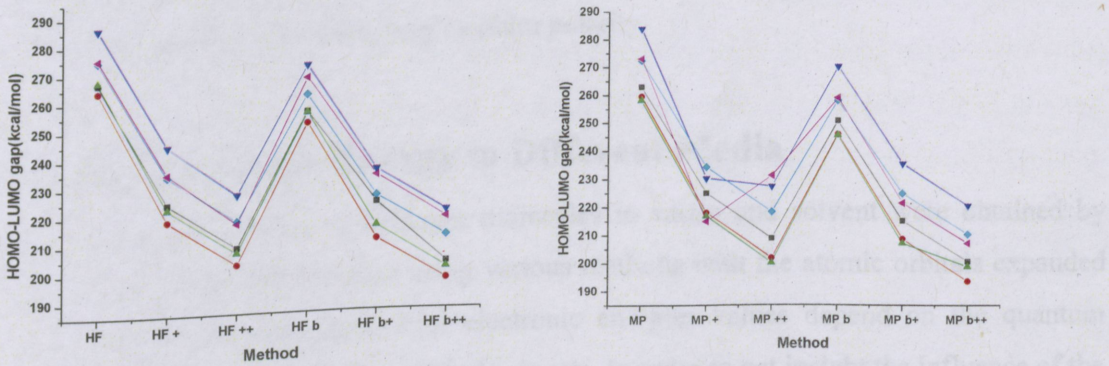

Figure 4.20. HOMO-LUMO energy gaps computed using HF and MP2 calculations with different basis sets for compounds A ( ), B ( ), D ( ), E ( ), F ( ) and G ( ).

© University of Venda

University of Venda
Creating Future Leaders

Tables 4.15 shows the shapes of the frontier molecular orbitals and of selected molecular orbitals close to HOMO (HOMO-1, HOMO-2, HOMO-3), from the results of different calculation methods in vacuo. Table 4.16 shows the shapes of the same molecular orbitals in different media, from HF/6-31G(d,p) results. The figures show that the LUMOs of all these compounds are more localized on the benzene ring, whereas the HOMOs spread on the whole molecule. The LUMOs are of π^* character while the HOMOs in these compounds are of π character following the in phase and out of phase combination of neighbouring p atomic orbitals in these frontier molecular orbitals. The HOMO-1, HOMO-2 and HOMO-3 molecular orbitals have different shapes in different structures. HOMO-1 or HOMO-2 may be more localized on the benzene ring or on the five-member pyrazole ring. HOMO-3 spreads on both rings in most of the compounds considered.

4.6. Natural Charges on the Atoms in Different Media

Table 4.17 shows the natural charges on selected atoms, calculated using the NBO approach, with different calculation methods and in different media. Except for N28 in the nitro compounds n-A and n-B, the hetero atoms and some carbon atoms have negative charge in all the molecules considered. The magnitude of the charges on N10, C8 and C11 in A increase with increasing medium polarity. So do the charges on N10, O15, C8 and in B increase with increasing medium ploarity except C11 which decrease, on N10, O15 and C8 in D increase with increasing medium polarity, on N10 and C11 in E increase with increasing medium polarity, on N10, O15, C8 and C11 in F increase with increasing medium polarity, on N10, O15 and C8 in G increase with increasing medium polarity, N10, O15, N16, C8 and C11 in n-A increase with increasing medium polarity and for both n-B1 and n-B2 N10, O15, N16, O17,O18 C8 increase with increasing medium polarity.

4.7. Total Electronic Energy in Different Media

The total electronic energy of different molecules in vacuo and solvent were obtained by solving the electronic Hamiltonian using various methods with the atomic orbitals expanded in basis sets ϕi. The calculated total electronic energies values depend on the quantum chemical method used and the size of the basis sets. In order to get insight the influence of the basis set on the total electronic energy, the trend of the total energies for the compounds (A, B, D, E, F and G) expressed in term of total electronic energy difference using Hartree-Fock

© University of Venda

University of Venda
Creating Future Leaders

method at different levels with HF/6-31G(d,p) electronic energy as reference is given in figure 4.21 for illustration. According to figure 4.21, large basis sets such as 6-311G(d,p), 6-311+G(d,p) and 6-311++G(d,p) give rise to significantly lower total electronic energies compare to small size basis sets like 6-31G(d,p), 6-31+G(d,p) and 6-31++G(d,p) as expected.

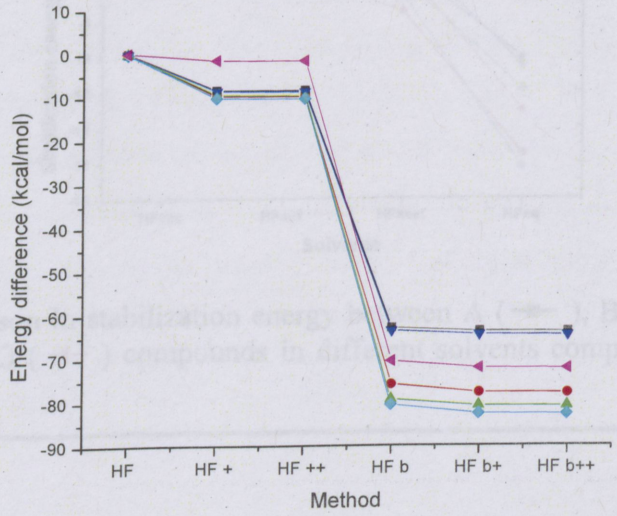

Figure 4.21. Variation of the total electronic energy with respect to the size of the basis set for A ( ), B ( ), D ( ), E ( ), F ( ) and G ( ) using the HF method. The HF energy is set to zero for comparison.

The solvents have also an effect on the energy of the molecules as, one can see in figure 4.22. In this figure the comparaison of the energy of A, B, D, E, F and G was done in acrros medium at HF/6-31G (d,p).

The total electronic energies obtained at HF/6-31G (d,p) in chloroform, acetonitrile and water of the pyrazole molecules are compared with the energy of in vacuo set to zero. This figure shows clearly the decrease of energy with the polarity of solvent. In water, all conformer have lower energy than other medium. The F compound is the most stable in water. This result shows that the pyrazole alkaloids are more stabilized by water than choloroform or acetonitrile.

© University of Venda

University of Venda
Creating Future Leaders

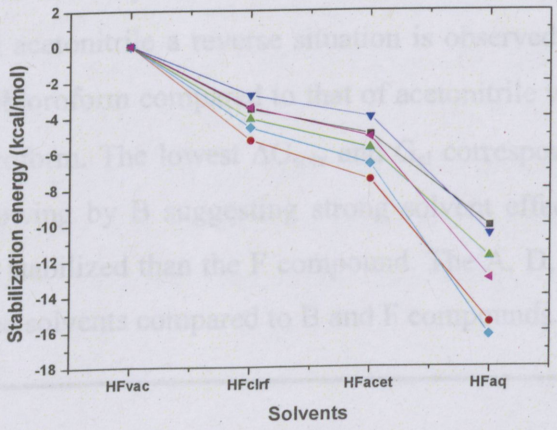

Figure 4.22. Comparison in stabilization energy between A ( ), B ( ), D ( ), E ( ), F ( ) and G ( ) compounds in different solvents computed at HF/6-31G(d,p) using HF.

4.8. The Solvent Effect

Table 4.18 reports the values of the free energy of solvation (solvent effect, ΔG_{solv}) and its electrostatic component (G_{el}) in the solvent considered, obtained from different calculation methods. G_{el} is always negative and its absolute value increases from chloroform to acetonitrile to water. ΔG_{solv} is always negative for chloroform and water, with greater absolute values water; it is often positive in acetonitrile, and, when negative, has small absolute values. These results suggest that the compounds considered are more stabilized by water than by chloroform, and very little or not by acetonitrile.

Figure 4.23 shows the values of ΔG_{solv} for the three solvents considered. This figure itself contains 4 figures with different possibilities.

Figure 4.23(a-b) depict the ΔG_{solv} and G_{el} energies of A, B, D, E, F and G calculated in three solvents at MP++ level. In figure 4.23(c), it a superposition of ΔG_{solv} and G_{el} for comparaison and in figure 4.23(d), it is a superposition of ΔG_{solv} and G_{el} of F compound, the most stable in water, used as a reference to check the performance of different methods in different solvents at different basis set levels.

© University of Venda

University of Venda
Creating Future Leaders

According to the results as illustrated in this figure, the trends are quite similar; the difference is observed in the magnitude of ΔG_{solv} and G_{el} values. In figure 4.23(c), the ΔG_{solv} and G_{el} of compounds in chloroform are very close. The ΔG_{solv} and G_{el} are both important in water, while in chloroform and acetonitrile a reverse situation is observed from the figure. In fact, the ΔG_{solvs} are lower in chloroform compared to that of acetonitrile while G_{els} appear lower in acetonitrile than in chloroform. The lowest ΔG_{solv} and G_{el} correspond to the interaction of F compound in water following by B suggesting strong solvent effects. In chloroform the B compound appears more stabilized than the F compound. The A, D, E and G compounds are less stabilized by the three solvents compared to B and F compounds.

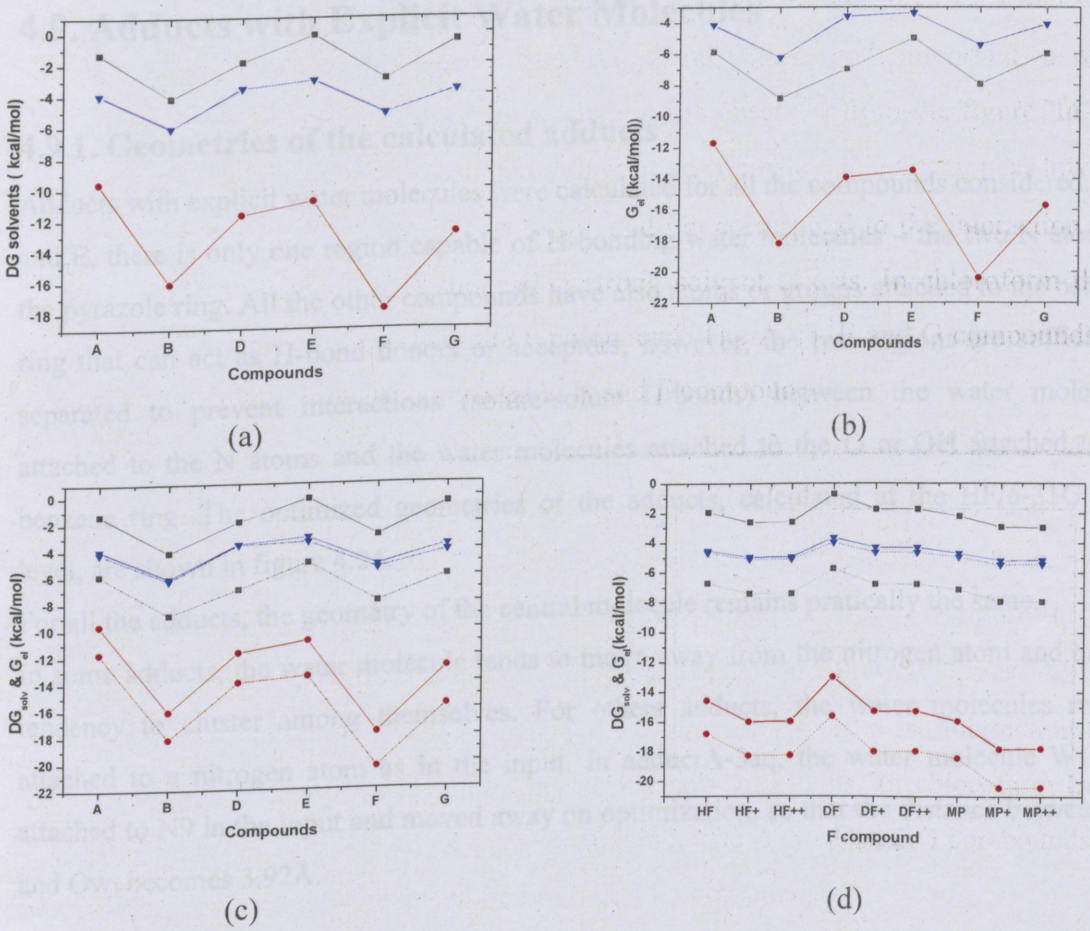

Figure 4.23. ΔG_{solv}(a) and G_{el}(b) energies of A, B, D, E, F and G with various methods in chloroform( ), acetonitrile ( )and water ( )solvent. Solid and doted dashed lines in figures (c-d) correspond to DG solv and DG elec, respectively.

© University of Venda

University of Venda
Creating Future Leaders

Overall speaking, the G_{el} energies are more important than ΔG_{solv} in the three different solvents considered. The MP2 method gives the lowest ΔG_{solv} and G_{el} energies. The insertion of diffuse function decreases the values of ΔG_{solv}. The HF++, DFT++, and MP++ methods yield similar ΔG_{solv} and G_{el} results with HF+, DFT+ and MP+ that can lead to the suggestion that the use of large basis set such as 6-31++G(d,p) may not be nessary the small basis set 6-31+G(d,p) can be sufficient to carry out more reliable solvation effects (fig. 4.23(d)). The ΔG_{solv} energies calculated at different levels of theory in chloroform are approaching that of G_{el} in the same solvent. DFT tends to overestimate ΔG_{solv} and G_{el} energies.

4.9. Adducts with Explicit Water Molecules

4.9.1. Geometries of the calculated adducts

Adducts with explicit water molecules were calculated for all the compounds considered. In A and E, there is only one region capable of H-bonding water molecules – the two N atoms in the pyrazole ring. All the other compounds have also atoms or groups attached to the benzene ring that can act as H-bond donors or acceptors; however, the two regions are sufficiently separated to prevent interactions (solute-solute H-bonds) between the water molecules attached to the N atoms and the water molecules attached to the O or OH attached to the benzene ring. The optimized geometries of the adducts, calculated at the HF/6-31G (d,p) level, are shown in figure 4.24.

For all the adducts, the geometry of the central molecule remains pratically the same.

In some adducts, the water molecule tends to move away from the nitrogen atom and have a tendency to cluster among themselves. For others adducts, the water molecules remain attached to a nitrogen atom as in the input. In adductA-3aq, the water molecule W1 was attached to N9 in the input and moved away on optimization, so that the distance between N9 and Ow_1 becomes 3.92Å.

Furthermore, it appears that, for withasomnine and its derivatives, only one water molecule remains attached to the N region in the optimized adducts, whereas two water molecules remain attached for newbouldine and its derivatives. This could be due to the stereochemistry of the central molecule which is different between withasomnine and newbouldine; the latter and its derivatives contain a chirale carbon.

© University of Venda

University of Venda
Creating Future Leaders

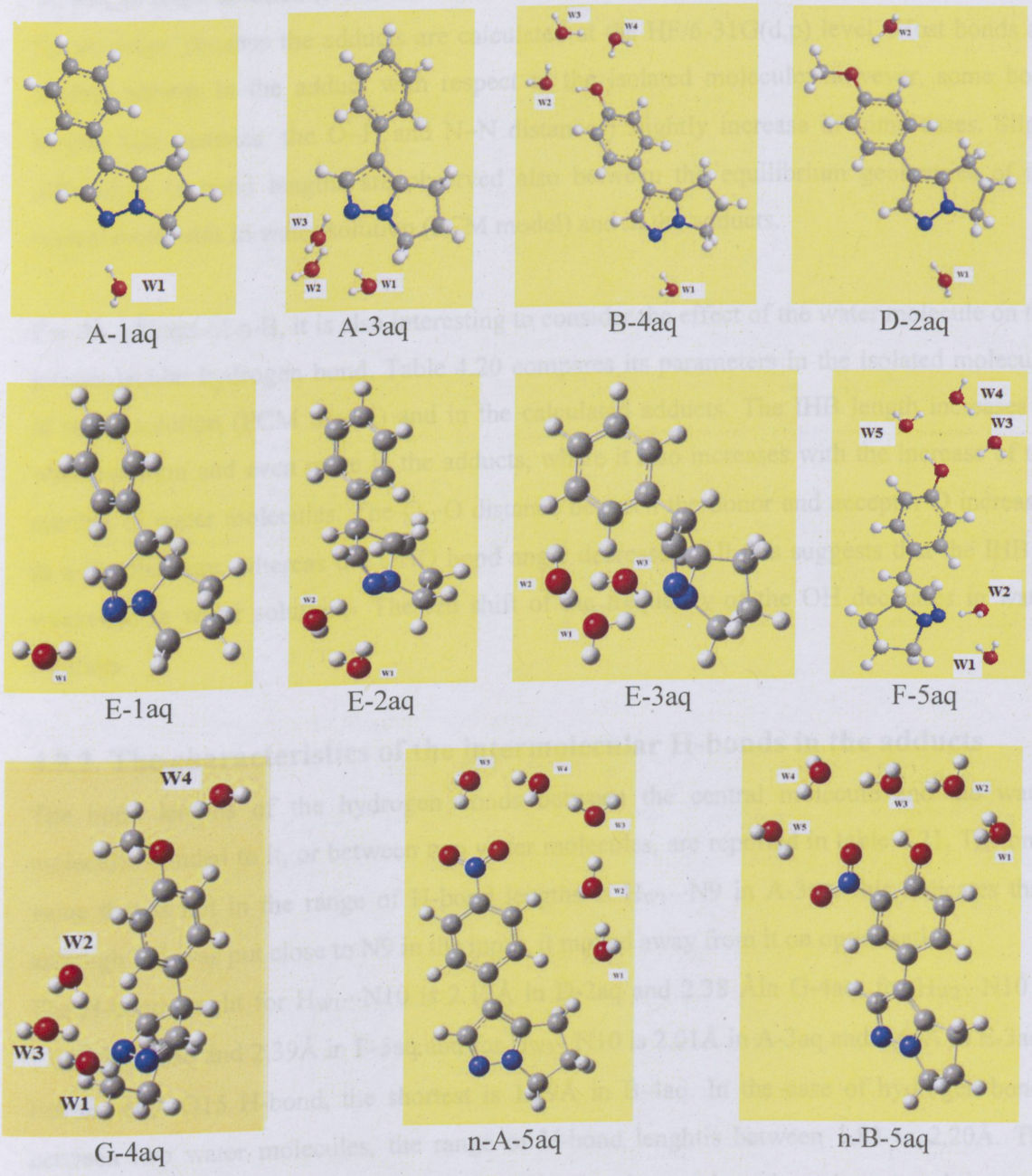

Figure 4.24. Optimized geometries of the calculated adducts with explicit water molecules for the compounds considered.

4.9.2. Geometry characteristics of the central molecule in the adducts

The formation of adducts may cause some changes in the geometry of the central molecule. Table 4.19 compares relevant bond lengths of the central molecule in the gas phase (*in*

UNIVERSITY OF VENDA
LIBRARY

© University of Venda

University of Venda
Creating Future Leaders

vacuo), in water solution (PCM results) and in the adducts, considering HF/6-31G(d,p) results for all cases, because the adducts are calculated at the HF/6-31G(d,p) level. Most bonds are slightly shorter in the adduct with respect to the isolated molecule; however, some bond lengths (for instance, the O–H and N–N distances) slightly increase in some cases. Slight differences in bond lengths are observed also between the equilibrium geometries of the central molecules in water solution (PCM model) and in the adducts.

For the adducts of n-B, it is also interesting to consider the effect of the water molecule on the intramolecular hydrogen bond. Table 4.20 compares its parameters in the isolated molecule, in water solution (PCM model) and in the calculated adducts. The IHB length increases in water solution and even more in the adducts, where it also increases with the increase of the number of water molecules. The O···O distance between the donor and acceptor O increases in a parallel way, whereas the OHO bond angle decreases. All this suggests that the IHB is weakened in water solution. The red shift of the frequency of the OH decreases in water solution.

4.9.2. The characteristics of the intermolecular H-bonds in the adducts

The bond lengths of the hydrogen bonds between the central molecule and the water molecules bonded to it, or between two water molecules, are reported in table 4.21. The only value that is not in the range of H-bond lengths is H_{W1}···N9 in A-3aq; this indicates that, although W1 was put close to N9 in the input, it moved away from it on optimisation.
The H-bond lenght for H_{W1}···N10 is 2.12Å in D-2aq and 2.38 Åin G-4aq; for H_{W2}···N10 is 2.05Å in E-2aq and 2.39Å in F-5aq and for H_{W3}···N10 is 2.01Å in A-3aq and 2.45Å in E-3aq . For the H_W···O15 H-bond, the shortest is 1.99Å in B-4aq. In the case of hydrogen bonds between two water molecules, the range of H-bond lenghtis between 1.83 to 2.20Å. The hydrogen bonds between two water molecules are shorter than those between the central molecule and water molecules because most the hydrogen bonds between a central molecule and a water molecule are between a nitrogen and an hydrogen while the hydrogen bonds between two water molecules are between in an oxygen and an hydrogen.

© University of Venda

University of Venda
Creating Future Leaders

4.9.3. Interaction Energy in the calculated adducts

The interaction energy between the central molecule and the water molecules bonded to it as calculated using equations 2.39 and 2.43. The values are corrected for BSSE. They are reported in figure 4.25, under the image of each adduct.

The interaction energy increases as the number of water molecules in the adduct increases, because the number of intermolecular hydrogen bonds increases. For instance, $E_{interaction}$ is -5.310 kcal/mol in A-1aq and -11.039 kcal/mol in A-3aq. Similarly, it is -12.026 kcal/mol in E-1aq, -14.974 kcal/mol in E-2aq and -15.202 kcal/mol in E-3aq.

The presence of a water molecule bridging two water molecules attached to the central molecule tends to stabilise the adduct. For instance, $E_{interaction}$ is -15.202kcal/mol in E-3aq where one water molecule bridges two water molecules attached to the central molecule and-14.974kcal/mol in E-2aq where the two water molecules attached to the central molecule bridge between them, not through a water molecule.

The case of n-B-5aq is interesting because of the presence of the intramolecular hydrogen bond between the OH and NO_2 groups. Around these groups, the water molecules are distributed in the following way: one water molecule is bonded to the O of the OH group, one water molecule is bonded to the H engaged in the intramolecular hydrogen bond and one water molecule is bonded to the O of NO_2 group which is not engaged in the intramolecular hydrogen bond; each pair of these water molecules is bridged by another water molecule.

It is interesting to note that the H atom engaged in the intramolecular hydrogen bond is simultaneously engaged in the intermolecular hydrogen bond, while the O which is the acceptor of the intramolecular hydrogen bond does not engage in intermolecular hydrogen bonds. It happens often with phenol OH that its atoms may be simultaneously engaged in intermolecular and intramolecular hydrogen bonds.

© University of Venda

University of Venda
Creating Future Leaders

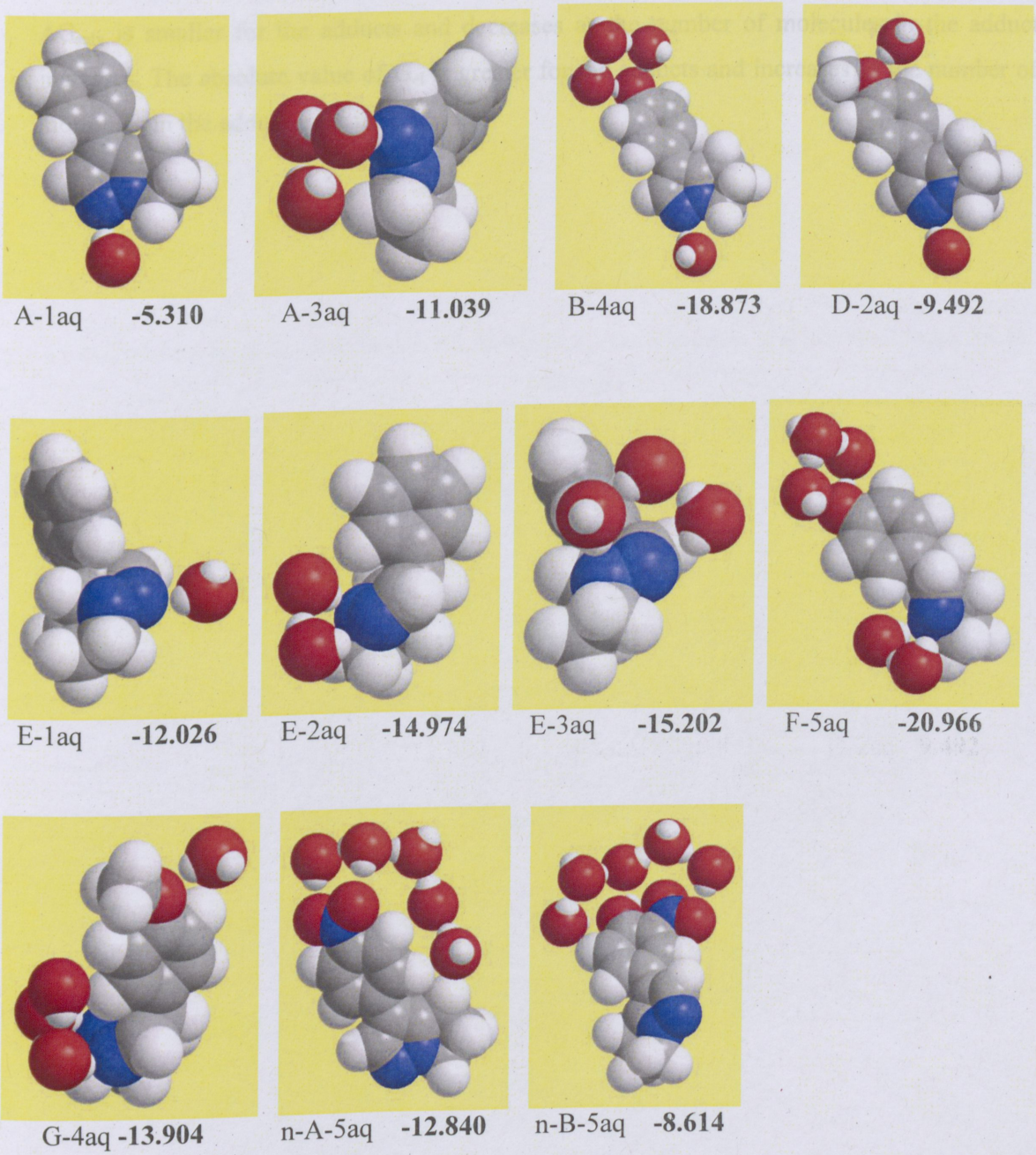

Figure 4.25. Interaction energy (kcal/mol) of the calculated adducts with explicit water molecules.

4.9.4. Solvent effects in adducts with explicit water molecule

The calculated adducts were utilised as solute molecules in single point PCM HF/6-31G (d,p) calculations. Table 4.22 compares the values of ΔG_{solv} and G_{el} thus obtained for the adducts

© University of Venda

University of Venda
Creating Future Leaders

with the corresponding values obtained from full re-optimization PCM HF/6-31G(d,p) calculations on the uncomplexed molecules. The values are all negative. The absolute value of ΔG_{solv} is smaller for the adducts and decreases as the number of molecules in the adduct increases. The absolute value of G_{el} is greater for the adducts and increases as the number of molecules in the adduct increases.

© University of Venda

University of Venda
Creating Future Leaders

Table 4.1. Bond lengths of the skeleton of molecules A, B, D, E, F and G in vacuo, from the results of different calculation methods

Molecule	Bond considered	Bond lengths (Å)								
		HF	HF+	HF++	DFT	DFT+	DFT++	MP	MP+	MP++
A	C1–C2	1.385	1.387	1.387	1.396	1.398	1.398	1.397	1.399	1.399
	C2–C3	1.384	1.386	1.386	1.393	1.396	1.396	1.394	1.397	1.397
	C3–C4	1.394	1.395	1.395	1.406	1.408	1.408	1.404	1.406	1.406
	C4–C5	1.393	1.395	1.395	1.407	1.408	1.408	1.404	1.406	1.406
	C5–C6	1.384	1.386	1.385	1.393	1.395	1.395	1.394	1.397	1.397
	C6–C1	1.385	1.387	1.387	1.396	1.398	1.398	1.397	1.399	1.399
	C4–C7	1.476	1.477	1.477	1.469	1.470	1.470	1.464	1.466	1.466
	C7–C8	1.421	1.376	1.376	1.395	1.396	1.396	1.395	1.396	1.397
	C8–N9	1.307	1.332	1.332	1.355	1.355	1.355	1.359	1.361	1.361
	N9–N10	1.325	1.325	1.325	1.344	1.344	1.344	1.341	1.342	1.342
	N10–C11	1.333	1.309	1.309	1.336	1.338	1.338	1.355	1.359	1.359
	C11–C7	1.374	1.421	1.421	1.426	1.427	1.427	1.416	1.417	1.417
	C8–C12	1.502	1.502	1.502	1.502	1.503	1.503	1.497	1.497	1.497
	C12–C13	1.553	1.553	1.544	1.561	1.562	1.562	1.551	1.552	1.552
	C13–C14	1.543	1.544	1.553	1.549	1.550	1.550	1.540	1.540	1.541
	C14–N9	1.444	1.445	1.445	1.454	1.456	1.456	1.454	1.456	1.456
B	C1–C2	1.384	1.385	1.385	1.398	1.398	1.398	1.398	1.399	1.399
	C2–C3	1.386	1.388	1.388	1.393	1.396	1.396	1.394	1.397	1.397
	C3–C4	1.389	1.390	1.390	1.404	1.405	1.405	1.402	1.404	1.404
	C4–C5	1.396	1.397	1.397	1.408	1.409	1.409	1.402	1.407	1.407
	C5–C6	1.380	1.382	1.382	1.390	1.392	1.392	1.391	1.395	1.394
	C6–C1	1.388	1.388	1.388	1.399	1.398	1.398	1.398	1.398	1.398
	C4–C7	1.477	1.479	1.479	1.469	1.471	1.471	1.464	1.466	1.466
	C7–C8	1.374	1.380	1.375	1.394	1.395	1.395	1.395	1.396	1.397

© University of Venda

University of Venda
Creating Future Leaders

	C8–N9	1.333	1.330	1.333	1.356	1.356	1.356	1.359	1.361	1.361
	N9–N10	1.325	1.324	1.324	1.344	1.343	1.343	1.341	1.342	1.342
	N10–C11	1.307	1.309	1.309	1.337	1.339	1.339	1.355	1.360	1.360
	C11–C7	1.420	1.420	1.421	1.426	1.427	1.427	1.416	1.417	1.417
	C8–C12	1.501	1.502	1.502	1.502	1.502	1.502	1.497	1.497	1.497
	C12–C13	1.553	1.553	1.553	1.561	1.562	1.562	1.551	1.552	1.552
	C13–C14	1.544	1.544	1.544	1.550	1.551	1.551	1.540	1.541	1.541
	C14–N9	1.446	1.445	1.445	1.454	1.456	1.456	1.453	1.456	1.456
	C1–O15	1.352	1.354	1.354	1.369	1.373	1.373	1.374	1.379	1.379
	O15–H27	0.943	0.943	0.943	0.966	0.966	0.966	0.965	0.967	0.967
D	C1–C2	1.384	1.385	1.385	1.402	1.403	1.403	1.399	1.401	1.401
	C2–C3	1.384	1.386	1.386	1.387	1.390	1.390	1.397	1.400	1.400
	C3–C4	1.393	1.394	1.394	1.409	1.410	1.410	1.400	1.402	1.402
	C4–C5	1.393	1.394	1.394	1.402	1.403	1.403	1.407	1.409	1.409
	C5–C6	1.383	1.386	1.386	1.396	1.398	1.398	1.388	1.392	1.391
	C6–C1	1.385	1.386	1.386	1.399	1.400	1.400	1.401	1.403	1.403
	C4–C7	1.477	1.478	1.478	1.469	1.470	1.470	1.462	1.465	1.465
	C7–C8	1.374	1.376	1.376	1.394	1.395	1.395	1.395	1.397	1.397
	C8–N9	1.333	1.333	1.333	1.356	1.355	1.355	1.358	1.360	1.360
	N9–N10	1.325	1.325	1.325	1.344	1.343	1.343	1.341	1.342	1.342
	N10–C11	1.307	1.309	1.309	1.337	1.339	1.339	1.355	1.360	1.360
	C11–C7	1.420	1.421	1.421	1.426	1.427	1.427	1.417	1.418	1.418
	C8–C12	1.502	1.502	1.502	1.502	1.501	1.501	1.495	1.496	1.496
	C12–C13	1.553	1.553	1.554	1.561	1.563	1.563	1.551	1.552	1.553
	C13–C14	1.543	1.544	1.544	1.550	1.551	1.551	1.541	1.541	1.541
	C14–N9	1.444	1.445	1.445	1.454	1.455	1.455	1.453	1.456	1.456
	C1–O15	1.364	1.363	1.363	1.367	1.369	1.369	1.372	1.374	1.374
	O15–C16	1.405	1.408	1.407	1.418	1.421	1.421	1.422	1.427	1.427
E	C1–C2	1.384	1.386	1.386	1.396	1.397	1.397	1.396	1.398	1.399

© University of Venda

University of Venda
Creating Future Leaders

	C2–C3	1.386	1.388	1.388	1.395	1.397	1.397	1.395	1.398	1.398
	C3–C4	1.390	1.391	1.391	1.403	1.403	1.403	1.400	1.403	1.403
	C4–C5	1.392	1.394	1.394	1.401	1.404	1.404	1.402	1.405	1.405
	C5–C6	1.384	1.386	1.386	1.395	1.397	1.397	1.395	1.398	1.398
	C6–C1	1.386	1.388	1.388	1.395	1.398	1.398	1.397	1.399	1.399
	C4–C7	1.512	1.512	1.513	1.511	1.512	1.512	1.501	1.501	1.501
	C7–C8	1.530	1.530	1.530	1.539	1.539	1.539	1.524	1.525	1.525
	C8–N9	1.443	1.443	1.444	1.462	1.462	1.463	1.462	1.464	1.464
	N9–N10	1.377	1.376	1.376	1.379	1.379	1.379	1.394	1.394	1.394
	N10–C11	1.260	1.262	1.262	1.290	1.292	1.292	1.303	1.307	1.307
	C11–C7	1.532	1.532	1.533	1.539	1.539	1.539	1.526	1.527	1.527
	C8–C12	1.518	1.518	1.518	1.524	1.524	1.524	1.513	1.514	1.515
	C12–C13	1.564	1.565	1.565	1.572	1.574	1.574	1.562	1.565	1.566
	C13–C14	1.558	1.557	1.557	1.566	1.566	1.566	1.556	1.556	1.556
	C14–N9	1.439	1.440	1.440	1.450	1.451	1.451	1.452	1.454	1.454
F	C1–C2	1.383	1.384	1.384	1.398	1.398	1.398	1.397	1.398	1.398
	C2–C3	1.387	1.389	1.390	1.395	1.397	1.397	1.395	1.398	1.398
	C3–C4	1.386	1.387	1.387	1.399	1.400	1.400	1.399	1.401	1.401
	C4–C5	1.395	1.396	1.396	1.404	1.406	1.406	1.404	1.406	1.406
	C5–C6	1.379	1.382	1.382	1.391	1.393	1.393	1.392	1.393	1.395
	C6–C1	1.389	1.389	1.389	1.399	1.399	1.399	1.398	1.399	1.399
	C4–C7	1.511	1.512	1.512	1.511	1.511	1.511	1.500	1.501	1.501
	C7–C8	1.529	1.529	1.529	1.539	1.539	1.539	1.524	1.525	1.525
	C8–N9	1.443	1.444	1.444	1.462	1.463	1.463	1.462	1.463	1.464
	N9–N10	1.378	1.376	1.376	1.380	1.379	1.379	1.394	1.394	1.395
	N10–C11	1.261	1.262	1.262	1.290	1.292	1.292	1.303	1.307	1.307
	C11–C7	1.533	1.533	1.533	1.539	1.539	1.539	1.527	1.527	1.527
	C8–C12	1.518	1.518	1.518	1.524	1.524	1.524	1.513	1.515	1.515
	C12–C13	1.564	1.565	1.565	1.572	1.574	1.574	1.562	1.565	1.566
	C13–C14	1.558	1.557	1.557	1.566	1.566	1.566	1.556	1.556	1.556

© University of Venda

University of Venda
Creating Future Leaders

	C14–N9	1.439	1.440	1.440	1.447	1.451	1.451	1.452	1.454	1.454
	C1–O15	1.351	1.352	1.352	1.367	1.372	1.372	1.373	1.378	1.378
	O15–H27	0.943	0.943	0.943	0.966	0.966	0.966	0.966	0.967	0.967
G	C1–C2	1.390	1.393	1.393	1.398	1.398	1.398	1.400	1.402	1.402
	C2–C3	1.379	1.380	1.380	1.399	1.402	1.402	1.390	1.393	1.393
	C3–C4	1.392	1.396	1.396	1.395	1.396	1.396	1.401	1.404	1.404
	C4–C5	1.387	1.386	1.386	1.407	1.408	1.408	1.400	1.401	1.401
	C5–C6	1.388	1.392	1.392	1.387	1.389	1.389	1.397	1.400	1.400
	C6–C1	1.387	1.387	1.387	1.404	1.405	1.405	1.400	1.402	1.402
	C4–C7	1.520	1.512	1.512	1.521	1.521	1.521	1.511	1.512	1.512
	C7–C8	1.544	1.530	1.530	1.550	1.551	1.551	1.538	1.540	1.540
	C8–N9	1.476	1.444	1.444	1.496	1.496	1.496	1.497	1.496	1.495
	N9–N10	1.398	1.376	1.376	1.402	1.399	1.399	1.419	1.417	1.417
	N10–C11	1.253	1.262	1.262	1.282	1.284	1.284	1.294	1.297	1.298
	C11–C7	1.513	1.532	1.532	1.522	1.521	1.521	1.509	1.510	1.510
	C8–C12	1.556	1.518	1.518	1.538	1.538	1.538	1.554	1.555	1.555
	C12–C13	1.540	1.564	1.565	1.539	1.540	1.540	1.537	1.540	1.541
	C13–C14	1.532	1.557	1.557	1.550	1.550	1.550	1.529	1.531	1.531
	C14–N9	1.456	1.439	1.439	1.481	1.483	1.483	1.471	1.472	1.471
	C1–O15	1.349	1.349	1.349	1.367	1.368	1.368	1.372	1.374	1.374
	O15–C27	1.399	1.401	1.401	1.418	1.421	1.421	1.422	1.427	1.427

© University of Venda

University of Venda
Creating Future Leaders

Table 4.2. Bond lengths of the skeleton of molecules A, B, D, E, F and G in vacuo, from the results of different calculation methods with 6-311G (d,p) , 6-311+G(d,p) and 6-311++G(d,p) basis sets.

Molecule	Bond considered	Bond lengths (Å)								
		HF	HF+	HF++	DFT	DFT+	DFT+	MP	MP+	MP++
A	C1–C2	1.384	1.385	1.385	1.393	1.394	1.394	1.400	1.401	1.401
	C2–C3	1.383	1.385	1.385	1.391	1.392	1.392	1.397	1.399	1.399
	C3–C4	1.392	1.393	1.393	1.404	1.404	1.404	1.407	1.408	1.408
	C4–C5	1.392	1.393	1.393	1.404	1.405	1.405	1.407	1.407	1.407
	C5–C6	1.383	1.385	1.385	1.391	1.392	1.392	1.398	1.399	1.399
	C6–C1	1.384	1.385	1.385	1.394	1.394	1.394	1.400	1.401	1.401
	C4–C7	1.476	1.477	1.477	1.468	1.469	1.469	1.466	1.466	1.466
	C7–C8	1.373	1.375	1.375	1.393	1.393	1.393	1.398	1.399	1.399
	C8–N9	1.331	1.331	1.331	1.353	1.353	1.353	1.360	1.361	1.361
	N9–N10	1.322	1.323	1.323	1.341	1.342	1.342	1.334	1.336	1.336
	N10–C11	1.304	1.306	1.306	1.333	1.334	1.334	1.354	1.357	1.357
	C11–C7	1.421	1.421	1.421	1.425	1.425	1.425	1.420	1.420	1.420
	C8–C12	1.501	1.501	1.501	1.501	1.501	1.501	1.499	1.499	1.499
	C12–C13	1.551	1.552	1.552	1.560	1.561	1.561	1.554	1.555	1.555
	C13–C14	1.542	1.543	1.543	1.548	1.548	1.548	1.543	1.543	1.543
	C14–N9	1.444	1.445	1.445	1.455	1.456	1.456	1.455	1.456	1.456
B	C1–C2	1.382	1.383	1.383	1.395	1.395	1.395	1.401	1.401	1.401
	C2–C3	1.385	1.387	1.387	1.392	1.392	1.392	1.397	1.399	1.399
	C3–C4	1.387	1.388	1.388	1.401	1.402	1.402	1.405	1.406	1.406
	C4–C5	1.394	1.395	1.395	1.405	1.405	1.405	1.408	1.408	1.408
	C5–C6	1.379	1.381	1.381	1.388	1.389	1.389	1.394	1.396	1.396
	C6–C1	1.386	1.386	1.386	1.396	1.395	1.395	1.400	1.400	1.400
	C4–C7	1.477	1.478	1.478	1.469	1.470	1.469	1.465	1.466	1.466
	C7–C8	1.372	1.374	1.374	1.392	1.392	1.392	1.398	1.399	1.399
	C8–N9	1.332	1.332	1.332	1.354	1.354	1.354	1.360	1.361	1.361
	N9–N10	1.322	1.323	1.323	1.340	1.341	1.341	1.335	1.336	1.336
	N10–C11	1.305	1.307	1.307	1.334	1.335	1.335	1.354	1.357	1.357
	C11–C7	1.421	1.421	1.421	1.425	1.425	1.425	1.420	1.420	1.420
	C8–C12	1.501	1.501	1.501	1.501	1.501	1.500	1.499	1.499	1.499
	C12–C13	1.552	1.553	1.553	1.560	1.560	1.561	1.554	1.555	1.555
	C13–C14	1.542	1.543	1.543	1.549	1.549	1.549	1.543	1.543	1.543
	C14–N9	1.444	1.445	1.445	1.455	1.456	1.455	1.455	1.456	1.456
	C1–O15	1.351	1.352	1.352	1.368	1.371	1.371	1.367	1.371	1.371
	O15–H27	0.940	0.940	0.940	0.963	0.963	0.963	0.962	0.963	0.963
D	C1–C2	1.383	1.383	1.383	1.400	1.400	1.400	1.405	1.403	
	C2–C3	1.383	1.385	1.385	1.385	1.386	1.386	1.391	1.402	
	C3–C4	1.391	1.392	1.392	1.407	1.407	1.407	1.409	1.403	
	C4–C5	1.392	1.393	1.393	1.399	1.399	1.399	1.403	1.410	
	C5–C6	1.383	1.384	1.384	1.394	1.395	1.395	1.401	1.393	

© University of Venda

University of Venda
Creating Future Leaders

	C6–C1	1.383	1.384	1.384	1.396	1.396	1.396	1.402	1.405	
	C4–C7	1.477	1.477	1.477	1.469	1.469	1.469	1.465	1.465	
	C7–C8	1.373	1.374	1.374	1.392	1.392	1.392	1.398	1.399	
	C8–N9	1.332	1.332	1.332	1.354	1.354	1.354	1.360	1.360	
	N9–N10	1.322	1.323	1.323	1.340	1.341	1.341	1.335	1.336	
	N10–C11	1.305	1.306	1.306	1.334	1.335	1.335	1.355	1.358	
	C11–C7	1.421	1.421	1.421	1.425	1.425	1.425	1.420	1.420	
	C8–C12	1.501	1.501	1.501	1.501	1.501	1.501	1.499	1.498	
	C12–C13	1.552	1.552	1.552	1.560	1.560	1.560	1.554	1.555	
	C13–C14	1.542	1.543	1.543	1.549	1.549	1.549	1.543	1.544	
	C14–N9	1.444	1.445	1.445	1.455	1.455	1.455	1.455	1.456	
	C1–O15	1.361	1.362	1.362	1.365	1.367	1.367	1.364	1.366	
	O15–C27	1.405	1.406	1.406	1.419	1.420	1.420	1.418	1.420	
E	C1–C2	1.385	1.384	1.384	1.393	1.394	1.394			
	C2–C3	1.385	1.386	1.386	1.393	1.394	1.394			
	C3–C4	1.388	1.389	1.389	1.399	1.399	1.399			
	C4–C5	1.391	1.392	1.392	1.401	1.401	1.401			
	C5–C6	1.383	1.385	1.384	1.392	1.393	1.393			
	C6–C1	1.383	1.386	1.386	1.394	1.393	1.393			
	C4–C7	1.511	1.511	1.511	1.510	1.510	1.510			
	C7–C8	1.529	1.529	1.529	1.538	1.538	1.538			
	C8–N9	1.442	1.443	1.443	1.461	1.461	1.461			
	N9–N10	1.375	1.375	1.375	1.375	1.376	1.376			
	N10–C11	1.258	1.259	1.259	1.286	1.287	1.287			
	C11–C7	1.532	1.533	1.533	1.539	1.539	1.539			
	C8–C12	1.517	1.517	1.517	1.522	1.522	1.522			
	C12–C13	1.563	1.564	1.564	1.571	1.572	1.572			
	C13–C14	1.557	1.557	1.557	1.565	1.564	1.564			
	C14–N9	1.439	1.440	1.440	1.449	1.450	1.450			
F	C1–C2	1.382	1.382	1.382	1.395	1.394	1.394	1.399	1.400	1.400
	C2–C3	1.387	1.388	1.388	1.393	1.394	1.394	1.398	1.400	1.400
	C3–C4	1.384	1.385	1.385	1.397	1.397	1.397	1.401	1.402	1.402
	C4–C5	1.394	1.395	1.395	1.402	1.402	1.402	1.406	1.407	1.407
	C5–C6	1.378	1.380	1.380	1.389	1.390	1.390	1.394	1.396	1.396
	C6–C1	1.387	1.388	1.388	1.397	1.396	1.396	1.400	1.400	1.400
	C4–C7	1.510	1.511	1.511	1.510	1.510	1.510	1.501	1.501	1.501
	C7–C8	1.528	1.529	1.529	1.538	1.538	1.538	1.525	1.526	1.526
	C8–N9	1.442	1.443	1.443	1.461	1.461	1.461	1.460	1.462	1.462
	N9–N10	1.375	1.375	1.375	1.376	1.377	1.377	1.387	1.388	1.388
	N10–C11	1.258	1.259	1.259	1.286	1.287	1.287	1.301	1.304	1.304
	C11–C7	1.532	1.533	1.533	1.539	1.538	1.538	1.529	1.530	1.529
	C8–C12	1.517	1.517	1.517	1.522	1.522	1.522	1.515	1.516	1.516
	C12–C13	1.563	1.564	1.564	1.571	1.572	1.572	1.566	1.569	1.569
	C13–C14	1.557	1.557	1.557	1.565	1.564	1.564	1.560	1.559	1.559
	C14–N9	1.439	1.440	1.440	1.449	1.450	1.450	1.452	1.454	1.454
	C1–O15	1.350	1.350	1.351	1.367	1.370	1.370	1.366	1.370	1.370
	O15–H27	0.940	0.941	0.941	0.963	0.963	0.963	0.961	0.963	0.963

© University of Venda

University of Venda
Creating Future Leaders

G	C1–C2	1.382	1.383	1.383	1.400	1.399	1.399	1.403	1.404	1.404
	C2–C3	1.384	1.386	1.386	1.386	1.387	1.387	1.393	1.395	1.395
	C3–C4	1.388	1.389	1.389	1.402	1.402	1.402	1.404	1.405	1.405
	C4–C5	1.391	1.392	1.392	1.396	1.396	1.396	1.401	1.402	1.402
	C5–C6	1.382	1.384	1.384	1.395	1.396	1.396	1.400	1.402	1.402
	C6–C1	1.384	1.385	1.385	1.397	1.397	1.397	1.403	1.404	1.404
	C4–C7	1.511	1.511	1.511	1.510	1.510	1.510	1.512	1.513	1.513
	C7–C8	1.528	1.529	1.529	1.538	1.538	1.538	1.540	1.542	1.542
	C8–N9	1.442	1.443	1.443	1.461	1.461	1.461	1.495	1.494	1.494
	N9–N10	1.375	1.375	1.375	1.376	1.377	1.377	1.410	1.410	1.410
	N10–C11	1.258	1.259	1.259	1.286	1.287	1.287	1.292	1.295	1.295
	C11–C7	1.532	1.533	1.533	1.538	1.538	1.538	1.512	1.513	1.513
	C8–C12	1.516	1.517	1.517	1.522	1.523	1.523	1.557	1.558	1.558
	C12–C13	1.563	1.564	1.564	1.571	1.572	1.572	1.541	1.543	1.543
	C13–C14	1.557	1.557	1.557	1.565	1.564	1.564	1.532	1.534	1.534
	C14–N9	1.439	1.440	1.440	1.449	1.449	1.449	1.470	1.470	1.470
	C1–O15	1.360	1.360	1.360	1.364	1.366	1.366	1.363	1.366	1.366
	O15–C27	1.405	1.406	1.406	1.420	1.421	1.421	1.418	1.420	1.420

© University of Venda

University of Venda
Creating Future Leaders

Table .4.3. Bond angles of the skeleton of molecules A, B, D, E, F and G in vacuo, from the results of different calculation methods

Molecule	Bond angle considered	Bond angle								
		HF	HF+	HF++	DFT	DFT+	DFT++	MP	MP+	MP++
A	C1-C2-C3	120.341	120.353	120.354	120.372	120.369	120.372	120.176	120.158	120.156
	C2-C3-C4	120.927	120.936	120.940	121.095	121.121	121.127	120.638	120.623	120.656
	C3-C4-C5	118.134	118.130	118.123	117.819	117.809	117.798	118.716	118.770	118.714
	C4-C5-C6	120.951	120.966	120.969	121.074	121.082	121.091	120.598	120.581	120.614
	C5-C6-C1	120.322	120.328	120.331	120.392	120.406	120.407	120.213	120.200	120.199
	C6-C1-C2	119.321	119.283	119.279	119.245	119.209	119.204	119.650	119.662	119.650
	C3-C4-C7	120.499	120.519	120.522	121.609	121.576	121.587	120.894	120.750	120.797
	C5-C4-C7	121.367	121.351	121.354	120.572	120.615	120.616	120.390	120.480	120.488
	C4-C7-C8	129.724	129.668	129.680	129.505	129.431	129.442	128.505	128.176	128.214
	C4-C7-C11	127.727	127.722	127.715	127.592	127.576	127.570	127.858	128.022	127.995
	C7-C8-C12	143.499	143.382	143.378	144.017	143.888	143.888	144.760	144.383	144.344
	C7-C8-N9	106.879	106.898	106.900	106.397	106.455	106.457	105.826	105.921	105.920
	C8-N9-N10	113.920	113.877	113.873	114.428	114.280	114.281	115.092	114.879	114.877
	N9-N10-C11	103.929	104.071	104.075	103.012	103.270	103.269	102.386	102.638	102.643
	N10-C11-C7	112.721	112.543	112.543	113.257	112.999	113.002	113.054	112.748	112.755
	C11-C7-C8	102.546	102.605	102.601	102.902	102.991	102.986	103.636	103.802	103.791
	C8-C12-C13	102.019	102.029	102.041	102.361	102.384	102.394	101.581	101.521	101.555
	C12-C13-C14	105.842	105.908	105.901	105.911	105.991	105.995	105.540	105.482	105.504
	C13-C14-N9	101.003	101.024	101.027	101.138	101.119	101.123	100.445	100.390	100.411
	C14-N9-C8	110.941	116.009	116.002	115.541	115.567	115.566	114.857	114.601	114.600
	C14-N9- N10	129.702	129.741	129.733	129.661	129.709	129.702	129.661	129.820	129.761
	N9-C8-C12	109.460	109.545	109.543	109.380	109.423	109.429	109.040	109.187	109.206
B	C1-C2-C3	119.931	119.896	119.896	120.057	119.955	119.950	119.821	119.747	119.743
	C2-C3-C4	121.533	121.535	121.535	121.532	121.530	121.540	121.024	120.990	121.013

© University of Venda

University of Venda
Creating Future Leaders

	C3-C4-C5	117.432	117.427	117.427	117.307	117.325	117.312	118.255	118.298	118.264
	C4-C5-C6	121.684	121.687	121.687	121.736	121.722	121.730	121.155	121.142	121.159
	C5-C6-C1	119.823	119.799	119.799	119.910	119.834	119.831	119.764	119.683	119.682
	C6-C1-C2	119.592	119.651	119.651	119.455	119.630	119.632	119.971	120.132	120.127
	C3-C4-C7	121.735	121.701	121.701	121.841	121.783	121.793	121.115	120.960	120.983
	C5-C4-C7	120.832	120.872	120.872	120.852	120.892	120.895	120.630	120.742	120.751
	C4-C7-C8	129.686	129.607	129.607	129.488	129.379	129.389	128.504	128.163	128.170
	C4-C7-C11	127.784	127.797	127.797	127.618	127.620	127.615	127.878	128.047	128.055
	C7-C8-N9	106.930	106.953	106.953	106.439	106.492	106.494	105.851	105.941	105.949
	C7-C8-C12	143.442	143.320	143.320	143.965	143.825	143.822	144.751	144.359	144.318
	C8-N9-N10	113.877	113.830	113.830	114.390	114.241	114.239	115.078	114.866	114.855
	N9-N10-C11	103.921	104.061	104.061	103.008	103.263	103.267	102.378	102.628	102.632
	N10-C11-C7	112.735	112.555	112.555	113.264	112.996	112.997	113.068	112.760	112.773
	C11-C7-C8	102.528	102.591	102.591	102.894	103.000	102.995	103.617	103.790	103.775
	C8-C12-C13	101.996	102.005	102.005	102.328	102.342	102.355	101.583	101.520	101.561
	C12-C13-C14	105.836	105.902	105.902	105.882	105.962	105.959	105.530	105.477	105.511
	C13-C14-N9	101.000	101.021	101.021	101.127	101.108	101.110	100.446	100.390	100.413
	C14-N9-C8	116.008	115.963	115.963	115.493	115.513	115.513	114.851	114.586	114.589
	C14-N9- N10	129.785	129.834	129.834	129.731	129.789	129.775	129.674	129.820	129.766
	N9-C8-C12	109.484	109.573	109.573	109.380	109.441	109.439	109.040	109.197	109.222
	O15–C1–C2	122.725	122.693	122.693	122.910	122.835	122.830	122.962	122.842	122.839
	O15–C1–C6	117.682	117.656	117.656	117.635	117.535	117.538	117.068	117.026	117.034
	C1–O15– H27	110.890	111.388	111.388	108.954	109.895	109.885	108.371	109.108	109.097
D	C1-C2-C3	119.934	119.960	119.959	120.279	120.231	120.233	119.460	119.457	119.467
	C2-C3-C4	121.278	121.296	121.303	121.578	121.627	121.627	121.518	121.478	121.480
	C3-C4-C5	117.834	117.797	117.789	117.193	117.154	117.154	118.079	118.108	118.084
	C4-C5-C6	121.255	121.273	121.278	121.949	121.943	121.944	121.021	121.047	121.069
	C5-C6-C1	119.946	119.973	119.972	119.739	119.746	119.743	120.146	120.082	120.084
	C6-C1-C2	119.750	119.696	119.693	119.259	119.297	119.296	119.764	119.817	119.801
	C3-C4-C7	121.507	121.501	121.504	121.815	121.609	121.608	120.971	120.975	120.991

© University of Venda

University of Venda
Creating Future Leaders

	C5-C4-C7	120.659	120.702	120.707	120.992	121.238	121.238	120.950	120.917	120.924
	C4-C7-C8	129.708	129.630	129.634	129.472	129.052	129.054	128.048	127.921	127.919
	C4-C7-C11	127.743	127.761	127.762	127.647	128.021	128.017	128.402	128.374	128.397
	C7-C8-N9	106.892	106.917	106.919	106.440	106.561	106.561	105.947	106.012	106.027
	C7-C8-C12	143.474	143.352	143.339	143.980	143.918	143.923	144.816	144.631	144.612
	C8-N9-N10	113.908	113.859	113.859	114.394	114.241	114.240	115.057	114.895	114.886
	N9-N10-C11	103.924	104.063	104.064	102.995	103.247	103.248	102.362	102.594	102.596
	N10-C11-C7	112.723	112.548	112.550	113.285	113.020	113.017	113.092	112.798	112.810
	C11-C7-C8	102.547	102.605	102.600	102.881	102.924	102.927	103.539	103.695	103.675
	C8-C12-C13	102.001	102.011	102.016	102.320	102.254	102.258	101.536	101.477	101.511
	C12-C13-C14	105.839	105.903	105.896	105.880	105.895	105.893	105.557	105.531	105.548
	C13-C14-N9	101.000	101.022	101.026	101.124	101.059	101.061	100.438	100.361	100.380
	C14-N9-C8	116.021	115.978	115.965	115.499	115.505	115.503	114.829	114.652	114.671
	N9-C8-C12	109.479	109.563	109.571	109.372	109.510	109.506	109.191	109.288	109.296
	C14-N9- N10	129.742	129.787	129.781	129.741	130.141	130.142	130.032	130.273	130.247
	O15–C1–C2	119.750	119.968	119.968	115.862	115.967	115.960	124.926	124.702	124.736
	O15–C1–C6	120.221	120.307	120.311	124.879	124.736	124.745	115.310	115.482	115.463
	C1–O15– C16	115.482	115.857	115.835	118.079	118.407	118.411	116.492	116.789	116.797
E	C1-C2-C3	120.135	120.129	120.126	120.222	120.099	120.100	120.066	120.016	120.014
	C2-C3-C4	120.974	121.018	121.016	120.819	121.031	121.024	120.695	120.780	120.775
	C3-C4-C5	118.350	118.312	118.317	118.364	118.305	118.311	118.838	118.774	118.783
	C4-C5-C6	120.819	120.830	120.826	120.970	120.833	120.834	120.543	120.561	120.556
	C5-C6-C1	120.252	120.284	120.284	120.111	120.261	120.257	120.173	120.186	120.183
	C6-C1-C2	119.470	119.428	119.430	119.514	119.469	119.472	119.685	119.683	119.688
	C3-C4-C7	120.238	120.113	120.106	121.167	120.316	120.317	120.547	120.295	120.268
	C5-C4-C7	121.406	121.570	121.572	120.464	121.374	121.367	120.589	120.902	120.920
	C4-C7-C8	116.694	116.596	116.934	116.413	116.692	116.678	115.602	115.752	115.700
	C4-C7-C11	116.443	116.596	116.577	116.645	116.857	116.873	116.145	116.376	116.390
	C7-C8-N9	100.016	101.162	99.9646	100.259	100.168	100.167	100.168	100.038	100.065
	C7-C8-C12	128.932	128.985	128.995	129.06	129.073	129.075	129.172	129.141	129.144

© University of Venda

University of Venda
Creating Future Leaders

	C8-N9-N10	108.232	108.154	108.149	109.250	109.091	109.090	107.761	107.580	107.558
	N9-N10-C11	106.753	106.864	106.866	106.450	106.622	106.617	105.382	105.485	105.482
	N9-C8-C12	100.928	101.162	101.132	100.941	101.205	101.193	100.657	100.956	100.968
	N10-C11-C7	113.824	113.630	113.628	113.820	113.541	113.552	113.849	113.573	113.595
	C11-C7-C8	96.052	96.056	96.052	96.5844	96.623	96.626	96.3411	96.404	96.386
	C8-C12-C13	101.009	101.104	101.111	101.506	101.644	101.638	100.878	101.074	101.072
	C12-C13-C14	106.216	106.250	106.243	106.442	106.478	106.476	106.422	106.4278	106.410
	C13-C14-N9	100.512	100.487	100.484	100.665	100.601	100.599	100.296	100.193	100.178
	C14-N9-C8	107.404	107.283	107.268	107.850	107.765	107.744	105.613	105.444	105.393
	C14-N9- N10	124.173	124.203	124.174	125.628	125.689	125.681	122.622	122.647	122.623
F	C1-C2-C3	119.795	119.752	119.746	119.845	119.736	119.732	119.714	119.604	119.609
	C2-C3-C4	121.608	121.645	121.645	121.473	121.520	121.518	121.112	121.183	121.174
	C3-C4-C5	117.542	117.498	117.502	117.730	117.681	117.684	118.342	118.266	118.278
	C4-C5-C6	121.619	121.620	121.619	121.535	121.534	121.538	121.115	121.136	121.132
	C5-C6-C1	119.793	119.797	119.793	119.802	119.756	119.748	119.740	119.683	119.683
	C6-C1-C2	119.642	119.689	119.694	119.614	119.772	119.779	119.977	120.125	120.124
	C3-C4-C7	120.728	120.598	120.588	120.779	120.620	120.617	120.786	120.529	120.510
	C5-C4-C7	121.726	121.900	121.906	121.486	121.694	121.694	120.846	121.172	121.183
	C4-C7-C8	116.969	117.202	117.205	116.643	116.920	116.903	115.771	115.951	115.899
	C4-C7-C11	116.376	116.524	116.526	116.627	116.834	116.849	116.072	116.312	116.316
	C7-C8-N9	100.078	100.024	100.026	100.311	100.213	100.214	100.194	100.058	100.084
	C7-C8-C12	128.964	129.027	129.029	129.088	129.093	129.091	129.203	129.155	129.164
	C8-N9-N10	108.214	108.144	108.132	109.224	109.086	109.077	107.749	107.570	107.543
	N9-N10-C11	106.726	106.842	106.835	106.418	106.592	106.585	105.355	105.464	105.460
	N10-C11-C7	113.870	113.670	113.676	113.878	113.594	113.600	113.879	113.592	113.615
	C11-C7-C8	96.028	96.035	96.035	96.564	96.614	96.610	96.332	96.401	96.385
	C8-C12-C13	101.020	101.123	101.127	101.518	101.654	101.649	100.870	101.089	101.082
	C12-C13-C14	106.204	106.240	106.230	106.429	106.471	106.467	106.415	106.418	106.401
	C13-C14-N9	100.509	100.484	100.477	100.648	100.587	100.584	100.303	100.184	100.171
	C14-N9-C8	107.405	107.301	107.265	107.833	107.779	107.757	105.614	105.444	105.387

© University of Venda

University of Venda
Creating Future Leaders

	N9-C8-C12	100.913	101.117	101.120	100.932	101.182	101.180	100.644	100.946	100.959
	C14-N9- N10	124.142	124.166	124.146	125.592	125.673	125.659	122.573	122.621	122.586
	O15–C1–C2	122.780	122.768	122.760	122.891	122.830	122.824	123.031	122.921	122.913
	O15–C1–C6	117.578	117.544	117.546	117.494	117.398	117.396	116.992	116.952	116.962
	C1–O15– H27	110.989	111.485	111.470	109.071	110.000	109.992	108.458	109.193	109.178
G	C1-C2-C3	120.091	120.132	120.133	119.442	119.415	119.414	120.006	119.906	119.928
	C2-C3-C4	121.492	121.643	121.642	121.778	121.810	121.809	120.915	121.083	121.062
	C3-C4-C5	117.680	117.367	117.370	117.943	117.855	117.858	118.573	118.410	118.430
	C4-C5-C6	121.627	121.872	121.870	121.065	121.152	121.150	121.121	121.174	121.157
	C5-C6-C1	119.761	119.709	119.711	120.274	120.232	120.232	119.561	119.574	119.589
	C6-C1-C2	119.349	119.277	119.274	119.496	119.535	119.537	119.819	119.849	119.831
	C3-C4-C7	120.880	120.443	120.440	121.029	121.003	120.996	121.155	120.864	120.856
	C5-C4-C7	121.439	122.183	122.183	121.026	121.142	121.146	120.266	120.725	120.715
	C4-C7-C8	115.327	117.129	117.134	114.957	114.964	114.966	113.975	113.903	113.810
	C4-C7-C11	112.660	116.610	116.614	112.765	113.048	113.071	111.056	111.459	111.573
	C7-C8-N9	103.079	100.050	100.047	103.251	103.337	103.344	102.908	102.763	102.732
	C7-C8-C12	116.259	129.063	129.064	117.135	117.439	117.441	115.785	116.022	116.015
	C8-N9-N10	107.618	108.142	108.132	108.139	108.353	108.352	106.956	107.143	107.147
	N9-N10-C11	110.002	106.829	106.824	109.406	109.610	109.609	108.570	108.586	108.562
	N10-C11-C7	114.722	113.711	113.713	114.839	114.711	114.715	114.613	114.345	114.342
	C11-C7-C8	98.655	96.024	96.022	98.9438	99.138	99.137	98.979	99.0803	99.0646
	C8-C12-C13	105.296	101.125	101.130	102.583	102.477	102.481	105.294	105.398	105.417
	C12-C13-C14	102.954	106.239	106.226	104.125	104.151	104.154	102.625	102.953	102.996
	C13-C14-N9	105.065	100.487	100.481	105.845	105.590	105.589	104.457	104.512	104.533
	C14-N9-C8	107.312	107.305	107.270	109.282	109.483	109.488	105.888	106.056	106.072
	C14-N9- N10	111.289	124.166	124.145	113.421	113.792	113.806	108.998	109.873	109.950
	N9-C8-C12	106.049	101.115	101.118	103.907	103.983	103.979	105.927	105.908	105.898
	O15–C1–C2	116.003	116.058	116.066	124.803	124.684	124.688	115.310	115.509	115.511
	O15–C1–C6	124.647	124.665	124.660	115.701	115.781	115.776	124.871	124.642	124.658
	C1–O15– C27	119.751	119.980	119.970	118.156	118.496	118.497	116.522	116.849	116.846

© University of Venda

University of Venda
Creating Future Leaders

Table 4.4 Torsion angles of the skeleton of molecules A, B, D, E, F and G in vacuo, from the results of different calculation methods

Molecule	Dihedral angle considered	Methods								
		HF	HF+	HF++	DFT	DFT+	DFT++	MP	MP+	MP++
A	C1–C2– C3–C4	0.550	0.584	0.591	0.436	0.448	0.441	0.829	0.792	1.062
	C2–C3– C4–C5	-0.102	-0.135	-0.147	-0.222	-0.227	-0.200	-0.411	-0.543	-0.726
	C3–C4– C5–C6	-0.507	-0.493	-0.483	-0.230	-0.252	-0.287	-0.513	-0.251	-0.202
	C4–C5– C6–C1	0.674	0.678	0.674	0.472	0.515	0.537	1.022	0.798	0.797
	C5–C6– C1–C2	-0.219	-0.222	-0.225	-0.256	-0.291	-0.292	-0.600	-0.549	-0.464
	C6–C1– C2–C3	-0.386	-0.401	-0.401	-0.193	-0.184	-0.191	-0.320	-0.241	-0.460
	C3–C4– C7– C8	141.694	140.347	140.663	-24.032	-25.867	-25.321	-36.700	-43.546	-42.194
	C3–C4–C7– C11	-37.535	-38.700	-38.384	156.472	154.787	155.367	143.046	136.299	137.796
	C5–C4– C7– C8	-38.517	-39.904	-39.561	155.982	154.227	154.745	143.368	136.659	138.113
	C5–C4–C7– C11	142.254	141.049	141.392	-23.514	-25.120	-24.567	-36.886	-43.505	-41.897
	C4–C7– C8–C12	-5.200	-5.334	-5.388	-5.869	-6.251	-6.123	-8.662	-10.189	-10.280
	C4–C7– C8– N9	-179.663	-179.567	-179.572	-179.587	-179.568	-179.538	179.896	179.740	179.843
	C7 –C4–C3– C2	179.694	179.623	179.636	179.792	179.864	179.864	179.657	179.658	179.576
	C7 –C4–C5– C6	179.699	179.752	179.736	179.756	179.658	179.650	179.412	179.549	179.497
	C7–C8–N9–N10	0.691	0.773	0.797	0.396	0.549	0.559	0.422	0.827	0.883
	C7–C8-C12–C13	172.454	173.008	173.128	173.399	174.140	174.154	171.708	173.488	173.929
	C7–C8–N9– C14	174.787	174.445	174.320	174.101	173.658	173.612	173.956	172.198	171.878
	C8–N9–N10–C11	-0.783	-0.856	-0.890	-0.624	-0.755	-0.771	-0.756	-1.143	-1.208
	C7–C11–N10 –N9	0.570	0.606	0.636	0.616	0.674	0.690	0.810	1.0282	1.077
	N9–C8 –C12–C13	-13.165	-12.847	-12.778	-12.990	-12.656	-12.549	-17.003	-16.623	-16.381
	N10–C11– C7–C8	-0.184	-0.173	-0.189	-0.401	-0.372	-0.383	-0.590	-0.580	-0.598
	N10–C11– C7– C4	179.209	179.075	179.059	179.200	179.111	179.072	179.615	179.552	179.410
	C11–C7– C8– N9	-0.288	-0.340	-0.345	0.004	-0.099	-0.098	0.102	-0.128	-0.149
	C11–C7– C8–C12	174.175	173.894	173.839	173.722	173.218	173.314	171.544	169.944	169.728
	C12–C8– N9– C14	-1.723	-1.909	-2.002	-1.992	-2.172	-2.275	-0.833	-1.699	-1.894
	C8–C12–C13–C14	22.104	21.773	21.744	22.179	21.822	21.743	27.666	27.847	27.637

© University of Venda

University of Venda
Creating Future Leaders

	C12–C8– N9 –N10	-175.819	-175.581	-175.525	-175.696	-175.280	-175.328	-174.367	-173.070	-172.888
	C12–C13–C14–N9	-22.694	-22.465	-22.483	-22.859	-22.588	-22.563	-27.692	-28.3423	-28.236
	C13–C14 –N9– C8	15.792	15.753	15.822	16.038	15.972	16.019	18.3173	19.251	19.304
	C13–C14 –N9–N10	-171.228	-171.779	-171.887	-171.414	-172.203	-172.220	-169.295	-170.956	-171.342
	C14–N9–N10 –C11	-173.884	-173.455	-173.314	-173.239	-172.667	-172.619	-173.128	-170.913	-170.538
B	C1–C2– C3–C4	0.748	0.757	0.757	0.492	0.548	0.536	0.944	1.107	1.185
	C2–C3– C4–C5	-0.563	-0.558	-0.558	-0.235	-0.271	-0.235	-0.476	-0.733	-0.788
	C3–C4– C5–C6	-0.093	-0.098	-0.098	-0.257	-0.253	-0.314	-0.509	-0.159	-0.196
	C4–C5– C6–C1	0.559	0.554	0.554	0.489	0.497	0.559	1.017	0.670	0.773
	C5–C6– C1–C2	-0.375	-0.356	-0.356	-0.226	-0.214	-0.251	-0.540	-0.295	-0.374
	C6–C1– C2–C3	-0.265	-0.285	-0.285	-0.255	-0.298	-0.286	-0.4283	-0.582	-0.592
	C3–C4– C7– C8	-42.836	-45.737	-45.737	-27.138	-30.155	-29.502	-37.388	-45.073	-43.574
	C3–C4– C7– C11	137.829	135.141	135.141	153.151	150.399	150.957	142.425	134.828	136.606
	C5– C4– C7– C8	137.436	134.578	134.578	153.056	150.086	150.713	142.737	135.292	136.854
	C5– C4– C7– C11	-41.899	-44.545	-44.545	-26.655	-29.370	-28.829	-37.449	-44.807	-42.966
	C4–C7– C8–C12	-5.065	-5.121	-5.121	-6.301	-6.568	-6.666	-8.468	-10.123	-10.022
	C4–C7– C8– N9	-179.837	-179.721	-179.721	-179.867	-179.774	-179.819	179.898	179.735	179.910
	C7 –C4–C3– C2	179.700	179.745	179.745	179.952	179.961	179.971	179.647	179.623	179.630
	C7 –C4–C5– C6	179.647	179.601	179.601	179.558	179.517	179.481	179.369	179.485	179.387
	C7–C8 – N9–N10	0.864	0.950	0.950	0.570	0.723	0.724	0.531	0.958	1.036
	C7–C8 –C12–C13	172.119	172.593	172.593	173.292	173.983	174.118	171.542	173.466	173.848
	C7–C8 –N9 – C14	174.918	174.644	174.644	174.142	173.739	173.615	174.014	172.157	171.867
	C8–N9 –N10– C11	-0.961	-1.0361	-1.036	-0.782	-0.901	-0.929	-0.869	-1.285	-1.353
	C7–C11–N10 –N9	0.687	0.720	0.720	0. 770	0.736	0.781	0.884	1.127	1.159
	N9–C8 –C12–C13	-13.187	-12.890	-12.890	-13.249	-12.926	-12.845	-16.973	-16.572	-16.268
	N10–C11 – C7–C8	-0.203	-0.187	-0.187	-0.386	-0.336	-0.381	-0.604	-0.607	-0.595
	N10–C11– C7– C4	179.274	179.120	179.120	179.385	179.232	179.256	179.547	179.473	179.259
	C11–C7– C8– N9	-0.375	-0.432	-0.432	-0.102	-0.216	-0.192	0.0493	-0.186	-0.236
	C11–C7– C8–C12	174.397	174.168	174.168	173.464	172.990	172.961	171.683	169.957	169.832
	C12–C8– N9– C14	-1.781	-1.936	-1.936	-1.852	-2.015	-2.106	-0.890	-1.780	-2.016

© University of Venda

University of Venda
Creating Future Leaders

	C8–C12–C13–C14	22.188	21.862	21.862	22.460	22.104	22.056	27.667	27.838	27.566
	C12–C8– N9 –N10	-175.835	-175.630	-175.630	-175.423	-175.031	-174.996	-174.373	-172.978	-172.848
	C12–C13–C14–N9	-22.814	-22.574	-22.574	-23.071	-22.796	-22.793	-27.724	-28.377	-28.231
	C13–C14 –N9– C8	15.900	15.834	15.834	16.081	16.001	16.057	18.373	19.323	19.375
	C13–C14–N9–N10	-171.180	-171.685	-171.685	-171.539	-172.295	-172.387	-169.302	-171.091	-171.467
	C14–N9–N10–C11	-174.003	-173.647	-173.647	-173.230	-172.690	-172.572	-173.180	-170.848	-170.488
	C5–C6–C1–O15	179.651	179.674	179.674	179.717	179.722	179.704	179.420	179.501	179.481
	C2–C1–O15–H27	-0.324	-0.3633	-0.363	-0.069	-0.121	-0.150	-0.254	-0.960	-1.008
	O15–C1–C2–C3	179.651	179.684	179.684	179.805	179.770	179.762	179.615	179.635	179.562
	C6–C1–O15–H27	179.650	179.606	179.606	179.990	179.945	179.897	179.789	179.250	179.141
D	C1–C2– C3–C4	0.656	0.749	0.727	0.467	-0.482	-0.458	-1.089	-1.007	-1.383
	C2–C3– C4–C5	-0.289	-0.279	-0.265	-0.239	0.236	0.185	0.600	0.493	0.755
	C3–C4– C5–C6	-0.303	-0.301	-0.317	-0.258	0.283	0.360	0.436	0.544	0.390
	C4–C5– C6–C1	0.526	0.411	0.437	0.523	-0.553	-0.628	-0.968	-1.056	-0.892
	C5–C6– C1–C2	-0.154	0.062	0.029	-0.289	0.2300	0.344	0.469	0.529	0.255
	C6–C1– C2–C3	-0.427	-0.633	-0.601	-0.195	0.206	0.187	0.544	0.487	0.862
	C3–C4– C7– C8	-40.379	-42.556	-42.200	-26.612	25.586	25.544	-145.863	-139.321	-140.390
	C3–C4– C7– C11	140.356	138.353	138.708	153.753	-155.078	-155.097	32.728	39.298	38.309
	C5– C4– C7– C8	139.584	137.415	137.712	153.574	-154.579	-154.586	34.189	40.831	39.599
	C5– C4– C7– C11	-39.681	-41.676	-41.381	-26.061	24.757	24.773	-147.221	-140.551	-141.701
	C4–C7– C8–C12	-5.165	-5.281	-5.336	-6.081	-2.375	-2.378	-4.063	-4.814	-4.780
	C4–C7– C8– N9	-179.734	-179.644	-179.646	-179.766	179.066	179.054	178.924	178.832	178.782
	C7 –C4–C3– C2	179.676	179.693	179.649	179.940	-179.922	-179.941	-179.351	-179.359	-179.255
	C7 –C4–C5– C6	179.733	179.723	179.769	179.565	179.559	-179.515	-179.614	-179.603	-179.600
	C7–C8 – N9–N10	0.769	0.855	0.879	0.526	0.803	0.828	0.308	0.539	0.686
	C7–C8 –C12–C13	172.315	172.837	172.961	173.121	168.172	168.157	166.120	167.132	167.216
	C7–C8 –N9 – C14	174.835	174.5145	174.383	174.261	177.327	177.338	177.352	176.175	176.127
	C8–N9 –N10– C11	-0.860	-0.942	-0.978	-0.753	-0.832	-0.838	-0.538	-0.775	-0.881
	C7–C11–N10 –N9	0.617	0.663	0.697	0.698	0.543	0.528	0.568	0.720	0.744
	N9–C8 –C12–C13	-13.197	-12.886	-12.816	-13.301	-13.293	-13.299	-16.921	-16.581	-16.412

UNIVERSITY OF VENDA
LIBRARY

© University of Venda

University of Venda
Creating Future Leaders

	N10–C11 – C7–C8	-0.187	-0.183	-0.205	-0.412	-0.096	-0.066	-0.407	-0.430	-0.371
	N10–C11– C7– C4	179.234	179.099	179.079	179.299	-179.567	-179.555	-179.265	-179.308	-179.315
	C11–C7– C8– N9	-0.330	-0.381	-0.382	-0.063	-0.397	-0.428	0.061	-0.054	-0.169
	C11–C7– C8–C12	174.240	173.983	173.929	173.622	178.162	178.140	177.074	176.301	176.269
	C12–C8– N9– C14	-1.740	-1.918	-2.015	-1.808	-1.773	-1.768	-0.826	-1.591	-1.688
	C8–C12–C13–C14	22.169	21.842	21.815	22.504	22.452	22.457	27.508	27.671	27.488
	C12–C8– N9 –N10	-175.806	-175.578	-175.520	-175.544	-178.297	-178.278	-177.870	-177.227	-177.130
	C12–C13–C14–N9	-22.771	-22.544	-22.567	-23.092	-23.020	-23.023	-27.546	-28.113	-27.980
	C13–C14 –N9– C8	15.849	15.806	15.880	16.068	16.004	16.003	18.222	19.041	19.020
	C13–C14–N9–N10	-171.211	-171.747	-171.856	-171.357	-168.142	-168.160	-165.276	-166.150	-166.400
	C14–N9–N10–C11	-173.920	-173.519	-173.373	-173.395	-176.728	-176.717	-177.033	-175.574	-175.452
	C5–C6–C1–O15	178.313	178.104	178.138	179.670	-179.657	-179.662	-179.528	-179.473	-179.607
	C2–C1–O15–C16	-92.725	-94.350	-94.304	-179.597	179.554	179.493	-0.469	-0.634	-0.107
	O15–C1–C2–C3	-178.897	-178.682	-178.716	179.842	-179.833	-179.809	-179.460	-179.512	-179.290
	C6–C1–O15–C27	88.813	87.613	87.593	0.443	-0.488	-0.502	179.527	179.364	179.747
E	C1–C2– C3–C4	0.190	0.211	0.206	0.122	0.183	0.187	-0.015	-0.072	0.002
	C2–C3– C4–C5	-0.290	-0.345	-0.357	-0.354	-0.440	-0.463	-0.043	-0.123	-0.186
	C3–C4– C5–C6	0.209	0.258	0.279	0.374	0.416	0.450	-0.032	0.077	0.150
	C4–C5– C6–C1	-0.027	-0.038	-0.050	-0.162	-0.136	-0.161	0.166	0.164	0.071
	C5–C6– C1–C2	-0.078	-0.103	-0.108	-0.078	-0.1330	-0.125	-0.223	-0.359	-0.257
	C6–C1– C2–C3	-0.003	0.017	0.031	0.0978	0.107	0.113	0.148	0.313	0.221
	C3–C4– C7– C8	-108.254	-109.155	-109.069	-70.067	-110.092	-109.780	-108.004	-107.156	-106.264
	C3–C4– C7– C11	139.296	138.104	138.200	43.040	136.374	136.681	140.179	140.669	141.612
	C5– C4– C7– C8	70.820	69.966	70.092	109.083	69.106	69.406	70.138	70.821	71.735
	C5– C4– C7– C11	-41.631	-42.775	-42.639	-137.810	-44.427	-44.134	-41.679	-41.354	-40.389
	C4–C7– C8–C12	90.234	89.342	89.393	-90.721	89.565	89.580	89.079	87.933	87.918
	C4–C7– C8– N9	-156.804	-157.387	-157.374	155.995	-156.863	-156.864	-158.062	-158.931	-158.902
	C7 –C4–C3– C2	178.811	178.804	178.830	178.814	178.784	178.747	178.132	177.897	177.856
	C7 –C4–C5– C6	-178.882	-178.878	-178.896	-178.799	-178.799	-178.751	-178.206	-177.930	-177.879
	C7–C8 – N9–N10	38.981	39.184	39.200	-36.948	37.274	37.268	40.580	41.020	41.017

© University of Venda

University of Venda
Creating Future Leaders

	C7–C8 –C12–C13	150.803	150.186	150.151	-150.440	149.448	149.466	152.180	150.937	150.943
	C7–C8 –N9 – C14	175.284	175.368	175.330	-176.471	176.662	176.624	173.210	173.446	173.363
	C8–N9 –N10– C11	-26.576	-26.614	-26.629	24.301	-24.413	-24.418	-26.717	-26.998	-27.002
	C7–C11–N10 –N9	1.748	1.594	1.607	-0.365	0.192	0.208	1.054	1.0455	1.067
	N9–C8 –C12–C13	38.242	37.441	37.431	-37.455	36.329	36.359	39.534	38.203	38.158
	N10–C11 – C7–C8	21.149	21.425	21.425	-21.256	21.646	21.629	22.805	23.113	23.087
	N10–C11– C7– C4	145.016	145.640	145.644	-145.236	146.095	146.071	145.412	146.046	145.953
	C11–C7– C8– N9	-33.124	-33.415	-33.421	31.843	-32.293	-32.279	-35.045	-35.530	-35.519
	C11–C7– C8–C12	-146.087	-146.685	-146.654	145.127	-145.865	-145.835	-147.905	-148.667	-148.700
	C12–C8– N9– C14	-51.559	-51.338	-51.378	50.118	-49.840	-49.881	-53.417	-53.144	-53.207
	C8–C12–C13–C14	-15.279	-14.125	-14.074	15.438	-13.839	-13.848	-15.184	-13.215	-13.074
	C12–C8– N9 –N10	172.138	172.478	172.492	-170.360	170.773	170.763	173.953	174.430	174.447
	C12–C13–C14–N9	-13.353	-14.385	-14.464	12.614	-14.034	-14.052	-14.968	-16.785	-16.963
	C13–C14 –N9– C8	40.029	40.513	40.599	-38.674	39.379	39.413	41.805	42.753	42.895
	C13–C14 –N9–N10	167.554	167.815	167.850	-169.738	170.145	170.144	165.511	166.062	166.107
	C14–N9–N10 –C11	-153.752	-153.548	-153.508	154.820	-154.663	-154.624	-149.438	-149.326	-149.217
F	C1–C2– C3–C4	0.178	0.203	0.188	0.157	0.164	0.169	-0.107	-0.255	-0.029
	C2–C3– C4–C5	-0.303	-0.363	-0.366	-0.343	-0.392	-0.422	0.017	-0.008	-0.164
	C3–C4– C5–C6	0.230	0.285	0.306	0.308	0.365	0.408	-0.085	-0.052	0.093
	C4–C5– C6–C1	-0.031	-0.046	-0.069	-0.086	-0.109	-0.140	0.241	0.376	0.171
	C5–C6– C1–C2	-0.102	-0.125	-0.120	-0.110	-0.132	-0.128	-0.329	-0.639	-0.368
	C6–C1– C2–C3	0.031	0.048	0.062	0.076	0.105	0.114	0.262	0.580	0.298
	C3–C4– C7– C8	-109.592	-110.523	-110.153	-109.346	-110.365	-109.947	-108.378	-107.512	-106.798
	C3–C4– C7– C11	137.835	136.607	136.974	137.413	135.955	136.380	139.748	140.217	140.988
	C5– C4– C7– C8	69.562	68.681	69.060	69.799	68.813	69.225	69.708	70.368	71.185
	C5– C4– C7– C11	-43.011	-44.189	-43.813	-43.442	-44.868	-44.448	-42.167	-41.902	-41.029
	C4–C7– C8–C12	90.213	89.367	89.352	90.657	89.551	89.527	89.100	87.926	87.917
	C4–C7– C8– N9	-157.337	-157.347	-157.354	-156.007	-156.856	-156.881	-158.018	-158.925	-158.887
	C7 –C4–C3– C2	178.886	178.875	178.882	178.834	178.817	178.782	178.150	177.933	177.876
	C7 –C4–C5– C6	-178.950	-178.943	-178.931	-178.863	-178.836	-178.787	-178.216	-177.980	-177.934

© University of Venda

University of Venda
Creating Future Leaders

	C7–C8 – N9–N10	38.962	39.160	39.178	36.938	37.232	37.246	40.591	41.031	41.035
	C7–C8 –C12–C13	150.894	150.237	150.215	150.474	149.501	149.507	152.291	150.929	150.953
	C7–C8 –N9 – C14	175.210	175.301	175.255	176.372	176.607	176.573	173.153	173.416	173.320
	C8–N9 –N10– C11	-26.601	-26.630	-26.658	-24.346	-24.431	-24.431	-26.755	-27.029	-27.044
	C7–C11–N10 –N9	1.839	1.678	1.7078	0.471	0.282	0.271	1.120	1.099	1.131
	N9–C8 –C12–C13	38.242	37.431	37.401	37.409	36.331	36.337	39.605	38.169	38.139
	N10–C11 – C7–C8	21.040	21.324	21.306	21.143	21.529	21.549	22.742	23.063	23.035
	N10–C11– C7– C4	145.192	145.831	145.818	145.381	146.240	146.243	145.514	146.206	146.105
	C11–C7– C8– N9	-33.058	-33.344	-33.348	-31.780	-32.207	-32.226	-35.020	-35.513	-35.504
	C11–C7– C8–C12	-146.078	-146.629	-146.641	-145.117	-145.801	-145.818	-147.902	-148.662	-148.701
	C12–C8– N9– C14	-51.576	-51.353	-51.394	-50.168	-49.863	-49.898	-53.435	-53.155	-53.223
	C8–C12–C13–C14	-15.265	-14.110	-14.014	-15.325	-13.834	-13.809	-15.280	-13.152	-13.029
	C12–C8– N9 –N10	172.176	172.506	172.529	170.398	170.763	170.775	174.003	174.460	174.491
	C12–C13–C14–N9	-13.377	-14.413	-14.535	-12.755	-14.050	-14.097	-14.883	-16.854	-17.018
	C13–C14 –N9– C8	40.061	40.560	40.660	38.795	39.408	39.457	41.764	42.809	42.943
	C13–C14–N9–N10	167.531	167.832	167.856	169.758	170.168	170.161	165.416	166.084	166.100
	C14–N9–N10–C11	-153.730	-153.546	-153.488	-154.767	-154.681	-154.620	-149.427	-149.325	-149.206
	C5–C6–C1–O15	-179.946	-179.949	-179.939	-179.891	-179.899	-179.887	-179.996	179.903	179.984
	C2–C1–O15–H27	-0.172	-0.233	-0.262	-0.203	-0.312	-0.327	-0.057	-0.106	-0.313
	O15–C1–C2–C3	179.865	179.863	179.871	179.844	179.859	179.860	179.908	-179.996	179.924
	C6–C1–O15–H27	179.665	179.585	179.551	179.570	179.447	179.425	179.599	179.336	179.325
G	C1–C2– C3–C4	-0.004	0.194	0.209	0.021	0.014	0.025	0.268	0.155	0.243
	C2–C3– C4–C5	-0.115	-0.327	-0.359	-0.261	-0.252	-0.254	-0.479	-0.427	-0.388
	C3–C4– C5–C6	0.219	0.243	0.267	0.391	0.360	0.371	0.698	0.686	0.644
	C4–C5– C6–C1	-0.203	-0.027	-0.026	-0.281	-0.230	-0.259	-0.701	-0.668	-0.752
	C5–C6– C1–C2	0.077	-0.115	-0.134	0.030	-0.019	0.019	0.473	0.378	0.591
	C6–C1– C2–C3	0.024	0.033	0.045	0.098	0.125	0.097	-0.261	-0.127	-0.342
	C3–C4– C7– C8	-123.950	-108.068	-107.825	-126.199	-123.021	-123.008	-127.836	-122.410	-121.287
	C3–C4– C7– C11	123.841	139.066	139.304	121.390	124.122	124.118	121.417	126.508	127.635
	C5– C4– C7– C8	56.267	70.968	71.252	54.407	57.306	57.271	53.058	57.855	58.601

© University of Venda

University of Venda
Creating Future Leaders

	C5– C4– C7– C11	-55.943	-41.898	-41.618	-58.005	-55.552	-55.603	-57.689	-53.226	-52.477
	C4–C7– C8–C12	145.274	89.312	89.286	146.319	144.433	144.386	152.121	151.804	151.846
	C4–C7– C8– N9	-99.190	-157.361	-157.385	-100.219	-101.808	-101.855	-92.832	-93.152	-93.144
	C7 –C4–C3– C2	-179.906	178.754	178.762	-179.674	-179.936	-179.984	-179.600	179.832	179.502
	C7 –C4–C5– C6	-179.991	-178.821	-178.837	179.804	-179.957	-179.900	179.827	-179.573	-179.246
	C7–C8 – N9–N10	-24.376	39.112	39.134	-23.433	-22.212	-22.191	-27.885	-28.067	-28.193
	C7–C8 –C12–C13	112.879	150.290	150.261	149.766	149.790	149.786	110.936	112.700	113.101
	C7–C8 –N9 – C14	-144.244	175.256	175.214	-147.333	-146.837	-146.837	-144.029	-145.387	-145.611
	C8–N9 –N10– C11	17.495	-26.604	-26.624	16.599	15.853	15.838	18.585	18.697	18.803
	C7–C11–N10 –N9	-2.325	1.689	1.699	-2.111	-2.159	-2.158	-0.825	-0.764	-0.798
	N9–C8 –C12–C13	-0.980	37.429	37.401	36.672	36.390	36.380	-2.383	-0.482	-0.103
	N10–C11 – C7–C8	-12.628	21.282	21.285	-12.233	-11.452	-11.439	-16.240	-16.386	-16.426
	N10–C11– C7– C4	109.544	145.733	145.744	109.722	110.757	110.781	103.870	103.860	103.751
	C11–C7– C8– N9	21.021	-33.296	-33.312	20.132	19.008	18.989	25.095	25.277	25.370
	C11–C7– C8–C12	-94.516	-146.623	-146.642	-93.330	-94.751	-94.770	-89.952	-89.768	-89.640
	C12–C8– N9– C14	-21.597	-51.348	-51.389	-24.579	-23.671	-23.668	-22.059	-23.226	-23.477
	C8–C12–C13–C14	21.573	-14.113	-14.021	-35.226	-35.736	-35.726	24.633	22.709	22.339
	C12–C8– N9 –N10	98.271	172.508	172.531	99.320	100.954	100.979	94.086	94.094	93.942
	C12–C13–C14–N9	-35.272	-14.407	-14.525	20.799	21.847	21.837	-38.858	-37.524	-37.293
	C13–C14 –N9– C8	35.975	40.555	40.652	2.3505	1.122	1.128	38.297	38.213	38.231
	C13–C14–N9–N10	-81.523	167.829	167.854	-118.379	-120.276	-120.284	-76.455	-77.266	-77.298
	C14–N9–N10–C11	134.807	-153.524	-153.461	137.972	137.877	137.879	132.643	133.485	133.650
	C5–C6–C1–O15	-179.920	-179.920	-179.941	-179.979	-179.965	-179.933	-179.795	-179.769	-179.720
	C2–C1–O15–C27	-179.721	179.855	-179.842	-0.059	-0.166	-0.191	-179.827	-179.340	-179.526
	O15–C1–C2–C3	-179.977	-179.789	179.868	-179.891	-179.934	-179.956	179.982	-179.992	179.941
	C6–C1–O15–C27	0.276	0.022	-0.030	179.951	179.778	179.758	-179.827	0.802	0.773

© University of Venda

University of Venda
Creating Future Leaders

Table 4.5. Relative energies of the conformers of compounds A, B, D, E, F and G in different media, from the results of different calculation methods.

compound	method	conformer	relative energy (kcal/mol)			
			in vacuo	in chloroform	in acetonitrile	in water
A	HF	A-y	0.000	0.000	0.000	0.000
		A	0.233	0.254	0.256	0.249
	HF+	A-y	0.000	0.000	0.000	0.000
		A	0.187	0.213	0.223	0.212
	HF++	A-y	0.000	0.0000	0.000	0.000
		A	0.197	0.224	0.234	0.221
	DFT	A-y	0.000	0.000	0.000	0.000
		A	0.285	0.281	0.275	0.001
	DFT+	A-y	0.000	0.000	0.000	0.000
		A	0.244	0.281	0.244	0.000
	DFT++	A-y	0.000	0.000	0.000	0.000
		A	0.251	0.252	0.000	0.000
	MP	A-y	0.000	0.000	0.000	0.000
		A	0.198	0.2136	0.220	0.213
	MP+	A-y	0.000	0.000	0.000	0.000
		A	0.058	0.092	0.105	0.106
	MP++	A-y	0.000	0.000	0.000	0.000
		A	0.107	0.142	0.153	0.152
B	HF	B-z	0.000	0.051	0.012	0.000
		B-y	0.092	0.000	0.000	0.000
		B- x	0.183	0.192	0.216	0.211
		B	0.273	0.239	0.226	0.213
	HF+	B-z	0.100	0.055	0.041	0.004
		B-y	0.000	0.000	0.000	0.000
		B- x	0.128	0.141	0.055	0.287
		B	0.228	0.197	0.057	0.176
	HF++	B-z	0.089	0.046	0.140	0.000

© University of Venda

University of Venda
Creating Future Leaders

		B-y	0.000	0.000	0.000	0.004
		B- x	0.138	0.151	0.157	0.184
		B	0.227	0.197	0.158	0.182
	DFT	B-z	0.098	0.041	0.000	0.000
		B-y	0.000	0.000	0.000	0.018
		B- x	0.271	0.276	0.272	0.278
		B	0.369	0.322	0.278	0.262
	DFT+	B-z	0.096	0.038	0.000	0.000
		B-y	0.000	0.000	0.007	0.022
		B- x	0.182	0.233	0.242	0.245
		B	0.292	0.280	0.244	0.224
	DFT++	B-z	0.094	0.036	0.000	0.000
		B-y	0.000	0.000	0.009	0.025
		B- x	0.226	0.236	0.244	0.248
		B	0.321	0.245	0.245	0.224
	MP	B-z	0.098	0.050	0.013	0.000
		B-y	0.000	0.000	0.000	0.000
		B- x	0.197	0.217	0.220	0.213
		B	0.000	0.000	0.000	0.222
	MP+	B-z	0.105	0.056	0.014	0.006
		B-y	0.000	0.000	0.000	0.000
		B- x	0.050	0.087	0.094	0.107
		B	0.000	0.000	0.000	0.124
	MP++	B-z	0.250	0.033	0.000	0.000
		B-y	0.000	0.000	0.012	0.018
		B- x	0.215	0.049	0.076	0.082
		B	0.000	0.000	0.000	0.116
D	HF	D-z	0.000	0.000	0.000	0.000
		D-y	0.000	0.026	0.000	0.001
		D	1.259	1.211	1.191	1.163
	HF+	D-z	0.002	0.000	0.000	0.000
		D-y	0.000	0.032	0.005	0.007
		D	0.000	1.139	1.118	1.060
	HF++	D-z	0.002	0.000	0.000	0.000

© University of Venda

University of Venda
Creating Future Leaders

		D-y	0.000	0.030	0.001	0.004
		D	0.000	1.128	1.107	1.049
	DFT	D-z	0.000	0.000	0.031	0.021
		D-y	0.050	0.004	0.000	0.000
		D	0.000	0.000	0.030	0.022
	DFT+	D-z	0.224	0.000	0.036	0.215
		D-y	0.284	0.106	0.000	0.187
		D	0.000	1.285	0.036	0.000
	DFT++	D-z	0.228	0.000	0.035	0.217
		D-y	0.288	0.008	0.000	0.189
		D	0.000	0.000	0.035	0.000
	MP	D-z	0.195	0.000	0.000	0.000
		D-y	0.278	0.042	0.009	0.011
		D	0.000	0.000	0.009	0.011
	MP+	D-z	0.043	0.833	0.091	0.099
		D-y	0.146	0.894	0.095	0.000
		D	0.000	0.833	0.000	0.000
	MP++	D-z	0.129	0.000	0.103	0.120
		D-y	0.000	0.038	0.123	0.000
		D	0.053	0.000	0.000	0.000
F	HF	F	0.000	0.000	0.000	0.000
		F-x	0.003	0.007	0.036	0.022
	HF+	F	0.000	0.000	0.000	0.000
		F-x	0.000	0.017	0.007	0.043
	HF++	F	0.002	0.001	0.000	0.000
		F-x	0.000	0.000	0.006	0.044
	DFT	F	0.025	0.009	0.000	0.000
		F-x	0.000	0.000	0.009	0.014
	DFT+	F	0.034	0.011	0.000	0.000
		F-x	0.000	0.000	0.004	0.027
	DFT++	F	0.037	0.011	0.000	0.000
		F-x	0.000	0.000	0.005	0.015
	MP	F	0.018	0.006	0.000	0.000
		F-x	0.000	0.000	0.003	0.028

© University of Venda

University of Venda
Creating Future Leaders

	MP+	F	0.040	0.016	0.019	0.000
		F-x	0.000	0.000	0.000	0.087
	MP++	F	0.039	0.012	0.002	0.000
		F-x	0.000	0.000	0.000	0.005
G	HF	G-y	0.000	0.000	0.000	0.000
		G	0.030	1.612	1.608	1.477
	HF+	G-y	0.000	0.000	0.000	0.000
		G	1.216	1.335	1.324	1.024
	HF++	G-y	0.000	0.000	0.000	0.000
		G	1.285	1.377	1.366	0.758
	DFT	G-y	0.000	0.000	0.000	0.000
		G	0.361	0.415	0.403	0.361
	DFT+	G-y	0.000	0.000	0.000	0.000
		G	0.201	0.293	0.315	0.185
	DFT++	G-y	0.000	0.000	0.000	0.000
		G	0.189	0.294	0.304	0.177
	MP	G-y	0.047	0.000	0.292	0.209
		G	0.000	0.331	0.000	0.000
	MP+	G-y	0.000	0.287	0.000	0.000
		G	0.056	0.00	0.010	0.020
	MP++	G-y	0.000	0.368	0.043	0.000
		G	0.064	0.000	0.000	0.001

© University of Venda

University of Venda
Creating Future Leaders

Table 4.6. Reference energies in Hartree of the conformers of compounds A, B, D, F and G in different media, from the results of different calculation methods.

Conformer	Method	Lowest energy			
		in vacuo	in chloroform	in acetonitrile	in water
A-y=a	HF	[a]-570.3068834	[a]-570.3125355	[a]-570.3148037	[a]-570.323013
	HF+	[a]-570.3204020	[a]-570.3267193	[a]-570.3292879	[a]-570.3379221
	HF++	[a]-570.3206383	[a]-570.3269564	[a]-570.3295260	[a]-570.3381426
	DFT	[a]-574.0103796	[a]-574.0152100	[a]-574.0171327	[a]-574.0245185
	DFT+	[a]-574.0295154	[a]-574.0352347	[a]-574.0375527	[a]-574.0456187
	DFT++	[a]-574.0297690	[a]-574.0354773	[a]-574.0377920	[a]-574.0458544
	MP	[a]-572.2405631	[a]-572.2453558	[a]-572.2472430	[a]-572.2545475
	MP+	[a]-572.2729711	[a]-572.2786949	[a]-572.2809984	[a]-572.2889785
	MP++	[a]-572.2746133	[a]-572.2803434	[a]-572.2826472	[a]-572.2906188
B=b	HF	[e]-645.1660829	[d]-645.1745848	[d]-645.1780685	[e]-645.1908714
B-x=c	HF+	[d]-645.1819332	[d]-645.1912493	[d]-645.2085720	[d]-645.2085720
B-y=d	HF++	[d]-645.1821285	[d]-645.1914444	[d]-645.2087533	[e]-645.2087597
B-z=e	DFT	[d]-649.2300566	[d]-649.2375461	[d]-649.2406274	[e]-649.2525554
	DFT+	[d]-649.2544626	[d]-649.2631303	[e]-649.2667480	[e]-649.2797779
	DFT++	[d]-649.2547129	[d]-649.2633670	[e]-649.2669831	[e]-649.2800085
	MP	[d]-647.2771048	[d]-647.2846776	[d]-647.2877601	[d]-647.2997619
	MP+	[d]-647.3161510	[d]-647.3249486	[d]-647.3285790	[d]-647.3417008
	MP++	[d]-647.3178621	[d]-647.3263583	[e]-647.3299976	[e]-647.3431054
D=f	HF	[h]-684.1890909	[h-]684.1956523	[h]-684.1982920	[h]-684.2079880
D-y=g	HF+	[h]-684.2044089	[h]-684.2116567	[h]-684.2146130	[h]-684.2248013
D-z=h	HF++	[h]-684.2046445	[h]-684.2118923	[h]-684.2248487	[h]-684.2250199
	DFT	[f]-688.5345290	[h]-688.5402014	[g]-688.5425204	[g]-688.5512332
	DFT+	[f]-688.5577683	[h]-688.5684096	[g]-688.5668826	[f]-688.5767746
	DFT++	[f]-688.5580318	[h]-688.5643444	[g]-688.5671264	[f]-688.5770195
	MP	[f]-686.4446461	[f]-686.4500187	[h]-686.4522721	[h]-686.4610038
	MP+	[f]-686.4836525	[f]-686.4903479	[f]-686.4932008	[f]-686.5028074
	MP++	[g]-686.4851136	[h]-686.4916766	[f]-686.4945826	[f]-686.5041701
F=i	HF	[i]-646.2964400	i-646.3037775	[i]-646.3070414	[i]-646.3223062
F-x=j	HF+	[i]-646.3128036	i-646.3208546	[i]-646.3244987	[i]-646.3408468
	HF++	[j]-646.3131226	[j]-646.3211570	[i]-646.3247995	[i]-646.3411349
	DFT	[j]-650.3975797	[j]-650.4038359	[i]-650.4066077	[i]-650.4212339
	DFT+	[j]-650.4232855	[j]-650.4306196	[i]-650.4339574	[i]-650.4503163
	DFT++	[j]-650.4236206	[j]-650.4309391	[i]-650.4342726	[i]-650.4506319

© University of Venda

University of Venda
Creating Future Leaders

	MP	[j]-648.4218892	[j]-648.4284822	[i]-648.4313281	[i]-648.4463773
	MP+	[j]-648.4637613	[j]-648.4715288	[j]-648.4749938	[i]-648.4920294
	MP++	[j]-648.4656295	[j]-648.4733422	[j]-648.4768441	[i]-648.4938772
G=k	HF	[l]-685.3327293	[l]-685.3382853	[l]-685.3409024	[l]-685.3535989
G-y=l	HF+	[l]-685.3474511	[l]-685.3535529	[l]-685.3564107	[l]-685.3695479
	HF++	[l]-685.3478895	[l]-685.3539824	[l]-685.3568324	[l]-685.3699223
	DFT	[l]-689.7148832	[l]-689.7194984	[l]-689.7215802	[l]-689.7334488
	DFT+	[l]-689.7377531	[l]-689.7432739	[l]-689.7458172	[l]-689.7587736
	DFT++	[l]-689.7380651	[l]-689.7435774	[l]-689.7526119	[l]-689.7590695
	MP	[k]-687.6052753	[l]-687.6099386	[k]-687.6126144	[k]-687.6247700
	MP+	[l]-687.6445626	[k]-687.6507041	[l]-687.6529761	[l]-687.6665673
	MP++	[l]-687.6466462	[k]-687.6529135	[k]-687.6551665	[l]-687.6686442

Table 4. 7. Octanol/water partition coefficients of the compounds considered in this study.
The compounds are denoted by the acronyms explained in fig. 4.1. The partition coefficients (P) have been evaluated with ChemOffice 2004

compound	P	compound	P	compound	P	compound	P
A	2.251	D	2.17	F	0.824	n-A	0.491
B	1.584	E	1.491	G	1.41	n-B	-0.176

© University of Venda

University of Venda
Creating Future Leaders

Table 4.8. Relative energy of the two conformers of compound n-B corresponding to the lowest energy orientation of the rings and differing by the presence or absence of the intramolecular hydrogen bond between the OH group and the NO_2 group. Results from different calculations methods, in vacuo and in the three solvents considered.

Conformer	Method	Relative energy (kcal/mol)			
		in vacuo	in chloroform	in acetonitrile	in water
n-B1	HF	0.000	0.000	0.000	0.000
n-B2		9.857	6.511	5.156	2.350
n-B1	HF+	0.000	0.000	0.000	0.000
n-B2		9.435	6.045	4.668	1.847
n-B1	HF++	0.000	0.000	0.000	0.000
n-B2		9.453	6.063	4.686	1.866
n-B1	DFT	0.000	0.000	0.000	0.000
n-B2		11.783	9.012	7.7336	4.801
n-B1	DFT+	0.000	0.000	0.000	0.000
n-B2		11.19	7.976	6.593	3.556
n-B1	DFT++	0.000	0.000	0.000	0.000
n-B2		11.23	8.049	6.665	3.602
n-B1	MP	0.000	0.000	0.000	0.000
n-B2		9.355	6.479	5.277	2.457
n-B1	MP+	0.000	0.000	0.000	0.000
n-B2		7.782	4.751	2.880	0.565
n-B1	MP++	0.000	0.000	0.000	0.000
n-B2		7.829	5.618	3.518	0.612

© University of Venda

University of Venda
Creating Future Leaders

Table4.9. Bond lengths of the skeleton of the calculated molecules in different media and in the results of different calculation methods

Molecule	Bond considered	Calculation method	Bond lengths (Å)			
			in vacuo	in	in	in Water
A	C1–C2	HF	1.385	1.385	1.386	1.386
		HF+	1.387	1.387	1.388	1.388
		HF++	1.387	1.387	1.388	1.388
		DFT	1.396	1.396	1.396	1.396
		DFT+	1.398	1.398	1.398	1.398
		DFT++	1.398	1.398	1.398	1.399
		MP	1.397	1.397	1.397	1.398
		MP+	1.399	1.400	1.400	1.400
		MP++	1.399	1.400	1.400	1.400
	C2–C3	HF	1.384	1.385	1.385	1.385
		HF+	1.386	1.387	1.387	1.388
		HF++	1.386	1.387	1.387	1.388
		DFT	1.393	1.394	1.394	1.394
		DFT+	1.396	1.396	1.396	1.396
		DFT++	1.396	1.396	1.396	1.397
		MP	1.394	1.394	1.395	1.395
		MP+	1.397	1.397	1.398	1.398
		MP++	1.397	1.397	1.398	1.398
	C3–C4	HF	1.394	1.394	1.394	1.394
		HF+	1.395	1.395	1.395	1.396
		HF++	1.395	1.395	1.395	1.407
		DFT	1.406	1.407	1.407	1.408
		DFT+	1.408	1.408	1.408	1.409
		DFT++	1.408	1.408	1.409	1.409
		MP	1.404	1.404	1.404	1.405
		MP+	1.406	1.406	1.407	1.407
		MP++	1.406	1.406	1.407	1.407
	C4–C5	HF	1.393	1.394	1.394	1.395
		HF+	1.395	1.396	1.396	1.397
		HF++	1.395	1.396	1.396	1.397
		DFT	1.407	1.407	1.408	1.408
		DFT+	1.408	1.409	1.409	1.409
		DFT++	1.408	1.409	1.409	1.410
		MP	1.404	1.404	1.404	1.405
		MP+	1.406	1.406	1.406	1.407
		MP++	1.406	1.406	1.406	1.407
	C5–C6	HF	1.384	1.384	1.385	1.385
		HF+	1.386	1.387	1.387	1.387

© University of Venda

University of Venda
Creating Future Leaders

		HF++	1.38	1.387	1.387	1.387
		DFT	1.393	1.393	1.393	1.393
		DFT+	1.395	1.395	1.395	1.395
		DFT++	1.395	1.395	1.396	1.396
		MP	1.394	1.395	1.395	1.395
		MP+	1.397	1.398	1.398	1.398
		MP++	1.397	1.398	1.398	1.398
	C6–C1	HF	1.385	1.386	1.386	1.386
		HF+	1.387	1.388	1.388	1.388
		HF++	1.387	1.388	1.388	1.388
		DFT	1.396	1.396	1.397	1.397
		DFT+	1.398	1.398	1.399	1.399
		DFT++	1.398	1.398	1.399	1.399
		MP	1.397	1.397	1.397	1.397
		MP+	1.399	1.399	1.400	1.400
		MP++	1.399	1.399	1.400	1.400
	C4–C7	HF	1.476	1.476	1.477	1.477
		HF+	1.477	1.477	1.477	1.478
		HF++	1.477	1.477	1.478	1.478
		DFT	1.469	1.469	1.469	1.469
		DFT+	1.470	1.471	1.471	1.471
		DFT++	1.470	1.471	1.470	1.471
		MP	1.464	1.464	1.464	1.465
		MP+	1.466	1.466	1.466	1.467
		MP++	1.466	1.466	1.466	1.467
	C7–C8	HF	1.374	1.377	1.378	1.381
		HF+	1.376	1.379	1.380	1.383
		HF++	1.376	1.379	1.380	1.383
		DFT	1.395	1.397	1.398	1.398
		DFT+	1.396	1.398	1.400	1.400
		DFT++	1.396	1.398	1.398	1.400
		MP	1.395	1.396	1.396	1.397
		MP+	1.396	1.397	1.398	1.398
		MP++	1.397	1.397	1.398	1.399
	C8–N9	HF	1.333	1.331	1.330	1.328
		HF+	1.332	1.330	1.329	1.327
		HF++	1.332	1.330	1.329	1.327
		DFT	1.355	1.353	1.353	1.353
		DFT+	1.355	1.353	1.352	1.352
		DFT++	1.355	1.353	1.351	1.350
		MP	1.359	1.359	1.358	1.358
		MP+	1.361	1.360	1.360	1.359
		MP++	1.361	1.360	1.360	1.359
	N9–N10	HF	1.325	1.327	1.328	1.330

© University of Venda

University of Venda
Creating Future Leaders

		HF+	1.325	1.327	1.327	1.330
		HF++	1.325	1.327	1.328	1.330
		DFT	1.344	1.346	1.347	1.347
		DFT+	1.344	1.346	1.346	1.346
		DFT++	1.344	1.346	1.347	1.348
		MP	1.341	1.341	1.342	1.342
		MP+	1.342	1.343	1.343	1.343
		MP++	1.342	1.343	1.343	1.343
	N10–C11	HF	1.307	1.309	1.309	1.311
		HF+	1.309	1.311	1.312	1.314
		HF++	1.309	1.311	1.312	1.314
		DFT	1.336	1.337	1.338	1.338
		DFT+	1.338	1.340	1.340	1.340
		DFT++	1.338	1.340	1.341	1.343
		MP	1.355	1.356	1.357	1.358
		MP+	1.359	1.361	1.362	1.363
		MP++	1.359	1.361	1.362	1.363
	C11–C7	HF	1.421	1.419	1.418	1.416
		HF+	1.421	1.419	1.418	1.416
		HF++	1.421	1.419	1.418	1.416
		DFT	1.426	1.425	1.425	1.425
		DFT+	1.427	1.426	1.425	1.425
		DFT++	1.427	1.426	1.425	1.424
		MP	1.416	1.416	1.415	1.415
		MP+	1.417	1.416	1.416	1.416
		MP++	1.417	1.416	1.416	1.416
	C8–C12	HF	1.502	1.502	1.502	1.502
		HF+	1.502	1.502	1.502	1.502
		HF++	1.502	1.502	1.502	1.502
		DFT	1.502	1.502	1.502	1.502
		DFT+	1.503	1.503	1.503	1.503
		DFT++	1.503	1.503	1.501	1.501
		MP	1.497	1.497	1.497	1.498
		MP+	1.497	1.498	1.498	1.498
		MP++	1.497	1.498	1.498	1.498
	C12–C13	HF	1.553	1.552	1.552	1.553
		HF+	1.553	1.5525	1.552	1.552
		HF++	1.544	1.553	1.552	1.552
		DFT	1.561	1.561	1.562	1.562
		DFT+	1.562	1.562	1.562	1.562
		DFT++	1.562	1.562	1.562	1.562
		MP	1.551	1.550	1.550	1.551
		MP+	1.552	1.552	1.551	1.552
		MP++	1.552	1.552	1.552	1.552

© University of Venda

University of Venda
Creating Future Leaders

	C13–C14	HF	1.54	1.543	1.543	1.543
		HF+	1.544	1.5429	1.543	1.543
		HF++	1.543	1.54	1.543	1.543
		DFT	1.549	1.549	1.549	1.549
		DFT+	1.550	1.550	1.549	1.549
		DFT++	1.550	1.550	1.550	1.550
		MP	1.540	1.539	1.539	1.539
		MP+	1.540	1.540	1.540	1.539
		MP++	1.541	1.540	1.540	1.539
	C14–N9	HF	1.444	1.447	1.449	1.452
		HF+	1.445	1.448	1.450	1.453
		HF++	1.445	1.448	1.450	1.453
		DFT	1.454	1.457	1.458	1.458
		DFT+	1.456	1.459	1.460	1.460
		DFT++	1.456	1.459	1.461	1.463
		MP	1.454	1.456	1.457	1.460
		MP+	1.456	1.459	1.461	1.463
		MP++	1.456	1.459	1.460	1.463
B	C1–C2	HF	1.384	1.385	1.385	1.386
		HF+	1.385	1.386	1.386	1.387
		HF++	1.385	1.386	1.386	1.387
		DFT	1.398	1.399	1.399	1.400
		DFT+	1.398	1.399	1.399	1.400
		DFT++	1.398	1.399	1.399	1.400
		MP2	1.398	1.398	1.398	1.399
		MP+	1.399	1.399	1.400	1.400
		MP++	1.399	1.399	1.400	1.400
	C2–C3	HF	1.386	1.386	1.386	1.386
		HF+	1.388	1.388	1.388	1.388
		HF++	1.388	1.388	1.388	1.388
		DFT	1.393	1.393	1.393	1.394
		DFT+	1.396	1.396	1.396	1.396
		DFT++	1.396	1.396	1.396	1.396
		MP	1.394	1.394	1.394	1.395
		MP+	1.397	1.397	1.397	1.398
		MP++	1.397	1.397	1.397	1.398
	C3–C4	HF	1.389	1.390	1.390	1.391
		HF+	1.390	1.391	1.392	1.393
		HF++	1.390	1.391	1.392	1.393
		DFT	1.404	1.405	1.405	1.406
		DFT+	1.405	1.406	1.406	1.407
		DFT++	1.405	1.406	1.406	1.407
		MP	1.402	1.403	1.403	1.404
		MP+	1.404	1.405	1.405	1.406
		MP++	1.404	1.405	1.405	1.406

© University of Venda

University of Venda
Creating Future Leaders

	C4–C5	HF	1.396	1.395	1.395	1.396
		HF+	1.397	1.396	1.396	1.397
		HF++	1.397	1.396	1.396	1.397
		DFT	1.408	1.408	1.408	1.408
		DFT+	1.409	1.409	1.409	1.409
		DFT++	1.409	1.409	1.409	1.409
		MP	1.402	1.405	1.405	1.406
		MP+	1.407	1.407	1.407	1.407
		MP++	1.407	1.407	1.407	1.407
	C5–C6	HF	1.380	1.381	1.381	1.382
		HF+	1.382	1.383	1.384	1.385
		HF++	1.382	1.383	1.384	1.385
		DFT	1.390	1.390	1.391	1.391
		DFT+	1.392	1.393	1.393	1.394
		DFT++	1.392	1.393	1.393	1.394
		MP	1.391	1.391	1.392	1.392
		MP+	1.395	1.395	1.395	1.396
		MP++	1.394	1.395	1.395	1.396
	C6–C1	HF	1.388	1.388	1.388	1.389
		HF+	1.388	1.388	1.388	1.389
		HF++	1.388	1.388	1.388	1.389
		DFT	1.399	1.399	1.400	1.401
		DFT+	1.398	1.399	1.399	1.400
		DFT++	1.398	1.399	1.399	1.400
		MP	1.398	1.398	1.399	1.400
		MP+	1.398	1.399	1.399	1.400
		MP++	1.398	1.399	1.399	1.400
	C4–C7	HF	1.477	1.478	1.478	1.478
		HF+	1.479	1.479	1.479	1.479
		HF++	1.479	1.479	1.479	1.479
		DFT	1.469	1.470	1.470	1.471
		DFT+	1.471	1.472	1.472	1.473
		DFT++	1.471	1.472	1.472	1.473
		MP	1.464	1.464	1.464	1.465
		MP+	1.466	1.466	1.466	1.467
		MP++	1.466	1.466	1.466	1.467
	C7–C8	HF	1.374	1.376	1.377	1.380
		HF+	1.380	1.378	1.377	1.382
		HF++	1.375	1.378	1.379	1.382
		DFT	1.394	1.396	1.396	1.398
		DFT+	1.395	1.397	1.398	1.400
		DFT++	1.395	1.397	1.398	1.400
		MP	1.395	1.396	1.396	1.397
		MP+	1.396	1.397	1.398	1.398

© University of Venda

University of Venda
Creating Future Leaders

		MP++	1.39	1.397	1.398	1.399
	C8–N9	HF	1.333	1.332	1.331	1.329
		HF+	1.330	1.331	1.330	1.328
		HF++	1.333	1.331	1.330	1.328
		DFT	1.356	1.354	1.354	1.352
		DFT+	1.356	1.354	1.354	1.352
		DFT++	1.356	1.354	1.354	1.352
		MP	1.359	1.359	1.359	1.358
		MP+	1.361	1.360	1.360	1.359
		MP++	1.361	1.360	1.360	1.359
	N9–N10	HF	1.325	1.326	1.327	1.329
		HF+	1.324	1.326	1.327	1.329
		HF++	1.324	1.326	1.327	1.329
		DFT	1.344	1.345	1.346	1.347
		DFT+	1.343	1.345	1.346	1.347
		DFT++	1.343	1.345	1.346	1.347
		MP	1.341	1.341	1.342	1.342
		MP+	1.342	1.343	1.343	1.343
		MP++	1.342	1.343	1.343	1.343
	N10–C11	HF	1.307	1.309	1.310	1.312
		HF+	1.309	1.312	1.313	1.316
		HF++	1.309	1.312	1.313	1.315
		DFT	1.337	1.339	1.339	1.341
		DFT+	1.339	1.341	1.342	1.344
		DFT++	1.339	1.341	1.342	1.344
		MP	1.355	1.357	1.357	1.358
		MP+	1.360	1.361	1.362	1.363
		MP++	1.360	1.361	1.362	1.363
	C11–C7	HF	1.420	1.418	1.417	1.416
		HF+	1.420	1.418	1.417	1.415
		HF++	1.421	1.418	1.417	1.415
		DFT	1.426	1.425	1.425	1.424
		DFT+	1.427	1.425	1.424	1.423
		DFT++	1.427	1.425	1.424	1.423
		MP	1.416	1.415	1.415	1.415
		MP+	1.417	1.416	1.416	1.416
		MP++	1.417	1.416	1.416	1.416
	C8–C12	HF	1.501	1.502	1.502	1.502
		HF+	1.502	1.502	1.502	1.502
		HF++	1.502	1.502	1.502	1.502
		DFT	1.502	1.502	1.502	1.502
		DFT+	1.502	1.503	1.503	1.503
		DFT++	1.502	1.503	1.503	1.503
		MP	1.497	1.497	1.497	1.497

© University of Venda

University of Venda
Creating Future Leaders

		MP+	1.49	1.498	1.498	1.498
		MP++	1.497	1.498	1.498	1.498
	C12–C13	HF	1.553	1.553	1.552	1.552
		HF+	1.553	1.553	1.553	1.553
		HF++	1.553	1.553	1.552	1.553
		DFT	1.561	1.561	1.561	1.561
		DFT+	1.562	1.562	1.562	1.562
		DFT++	1.562	1.562	1.562	1.562
		MP	1.551	1.551	1.550	1.551
		MP+	1.552	1.552	1.551	1.552
		MP++	1.552	1.552	1.552	1.552
	C13–C14	HF	1.544	1.543	1.543	1.543
		HF+	1.544	1.543	1.543	1.543
		HF++	1.544	1.543	1.543	1.543
		DFT	1.550	1.549	1.549	1.549
		DFT+	1.551	1.550	1.550	1.550
		DFT++	1.551	1.550	1.550	1.550
		MP	1.540	1.539	1.539	1.539
		MP+	1.541	1.540	1.540	1.540
		MP++	1.541	1.540	1.540	1.540
	C14–N9	HF	1.446	1.447	1.448	1.451
		HF+	1.445	1.448	1.450	1.453
		HF++	1.445	1.448	1.450	1.453
		DFT	1.454	1.457	1.458	1.461
		DFT+	1.456	1.459	1.460	1.463
		DFT++	1.456	1.459	1.460	1.463
		MP	1.453	1.456	1.457	1.460
		MP+	1.456	1.459	1.460	1.463
		MP++	1.456	1.459	1.460	1.463
	C1–O15	HF	1.352	1.352	1.352	1.352
		HF+	1.354	1.354	1.353	1.353
		HF++	1.354	1.354	1.353	1.353
		DFT	1.369	1.367	1.367	1.365
		DFT+	1.373	1.372	1.372	1.371
		DFT++	1.373	1.373	1.372	1.371
		MP	1.374	1.373	1.372	1.370
		MP+	1.379	1.378	1.378	1.377
		MP++	1.379	1.378	1.378	1.377
	O15–H27	HF	0.943	0.946	0.947	0.955
		HF+	0.943	0.946	0.948	0.956
		HF++	0.943	0.946	0.948	0.956
		DFT	0.966	0.969	0.971	0.980
		DFT+	0.966	0.969	0.971	0.981
		DFT++	0.966	0.969	0.971	0.981

© University of Venda

University of Venda
Creating Future Leaders

		MP2	0.96	0.969	0.970	0.980
		MP2+	0.967	0.971	0.972	0.983
		MP2++	0.967	0.971	0.973	0.983
D	C1–C2	HF	1.384	1.384	1.385	1.385
		HF+	1.385	1.385	1.386	1.386
		HF++	1.385	1.386	1.386	1.386
		DFT	1.402	1.402	1.403	1.403
		DFT+	1.403	1.403	1.403	1.404
		DFT++	1.403	1.403	1.403	1.404
		MP	1.399	1.402	1.400	1.400
		MP+	1.401	1.404	1.402	1.402
		MP++	1.401	1.404	1.402	1.402
	C2–C3	HF	1.384	1.384	1.384	1.385
		HF+	1.386	1.387	1.387	1.387
		HF++	1.386	1.387	1.387	1.387
		DFT	1.387	1.388	1.388	1.389
		DFT+	1.390	1.390	1.390	1.391
		DFT++	1.390	1.390	1.390	1.391
		MP	1.397	1.389	1.398	1.398
		MP+	1.400	1.392	1.401	1.401
		MP++	1.400	1.392	1.400	1.401
	C3–C4	HF	1.393	1.393	1.393	1.394
		HF+	1.394	1.394	1.394	1.395
		HF++	1.394	1.394	1.394	1.395
		DFT	1.409	1.409	1.409	1.409
		DFT+	1.410	1.410	1.410	1.411
		DFT++	1.410	1.410	1.410	1.411
		MP	1.400	1.407	1.401	1.401
		MP+	1.402	1.409	1.403	1.403
		MP++	1.402	1.409	1.403	1.403
	C4–C5	HF	1.393	1.394	1.394	1.395
		HF+	1.394	1.395	1.395	1.396
		HF++	1.394	1.395	1.395	1.396
		DFT	1.402	1.403	1.403	1.404
		DFT+	1.403	1.404	1.404	1.405
		DFT++	1.403	1.404	1.404	1.405
		MP	1.407	1.401	1.407	1.407
		MP+	1.409	1.402	1.409	1.409
		MP++	1.409	1.402	1.409	1.409
	C5–C6	HF	1.383	1.384	1.384	1.384
		HF+	1.386	1.386	1.386	1.387
		HF++	1.386	1.386	1.386	1.387
		DFT	1.396	1.396	1.396	1.396
		DFT+	1.398	1.399	1.399	1.399

UNIVERSITY OF VENDA
LIBRARY

© University of Venda

University of Venda
Creating Future Leaders

		DFT++	1.398	1.399	1.399	1.399
		MP	1.388	1.397	1.390	1.390
		MP+	1.392	1.401	1.393	1.393
		MP++	1.391	1.401	1.392	1.393
	C6–C1	HF	1.385	1.385	1.385	1.385
		HF+	1.386	1.386	1.386	1.386
		HF++	1.386	1.386	1.386	1.386
		DFT	1.399	1.399	1.400	1.400
		DFT+	1.400	1.400	1.400	1.401
		DFT++	1.400	1.400	1.400	1.401
		MP	1.401	1.399	1.403	1.403
		MP+	1.403	1.401	1.404	1.404
		MP++	1.403	1.401	1.404	1.404
	C4–C7	HF	1.477	1.477	1.477	1.477
		HF+	1.478	1.478	1.478	1.478
		HF++	1.478	1.478	1.478	1.478
		DFT	1.469	1.470	1.470	1.470
		DFT+	1.470	1.472	1.472	1.472
		DFT++	1.470	1.472	1.472	1.471
		MP	1.462	1.464	1.464	1.464
		MP+	1.465	1.466	1.466	1.466
		MP++	1.465	1.466	1.465	1.466
	C7–C8	HF	1.374	1.377	1.378	1.380
		HF+	1.376	1.378	1.380	1.383
		HF++	1.376	1.379	1.380	1.383
		DFT	1.394	1.396	1.397	1.399
		DFT+	1.395	1.397	1.398	1.400
		DFT++	1.395	1.397	1.39	1.400
		MP	1.395	1.396	1.397	1.397
		MP+	1.397	1.397	1.399	1.399
		MP++	1.397	1.397	1.398	1.399
	C8–N9	HF	1.333	1.331	1.330	1.328
		HF+	1.333	1.330	1.330	1.327
		HF++	1.333	1.330	1.330	1.327
		DFT	1.356	1.354	1.354	1.352
		DFT+	1.355	1.354	1.354	1.351
		DFT++	1.355	1.354	1.354	1.351
		MP	1.358	1.359	1.358	1.358
		MP+	1.360	1.360	1.358	1.358
		MP++	1.360	1.360	1.359	1.358
	N9–N10	HF	1.325	1.327	1.327	1.329
		HF+	1.325	1.327	1.327	1.329
		HF++	1.325	1.327	1.327	1.329
		DFT	1.344	1.345	1.346	1.347

© University of Venda

University of Venda
Creating Future Leaders

		DFT+	1.343	1.345	1.346	1.347
		DFT++	1.343	1.345	1.346	1.347
		MP	1.341	1.341	1.342	1.342
		MP+	1.342	1.343	1.343	1.343
		MP++	1.342	1.343	1.343	1.343
	N10–C11	HF	1.307	1.309	1.310	1.312
		HF+	1.309	1.312	1.312	1.315
		HF++	1.309	1.311	1.312	1.315
		DFT	1.337	1.338	1.339	1.341
		DFT+	1.339	1.341	1.342	1.344
		DFT++	1.339	1.341	1.342	1.344
		MP	1.355	1.357	1.358	1.358
		MP+	1.360	1.361	1.363	1.363
		MP++	1.360	1.361	1.362	1.363
	C11–C7	HF	1.420	1.418	1.418	1.416
		HF+	1.421	1.418	1.417	1.416
		HF++	1.421	1.418	1.417	1.416
		DFT	1.426	1.425	1.425	1.424
		DFT+	1.427	1.425	1.424	1.424
		DFT++	1.427	1.425	1.424	1.424
		MP	1.417	1.416	1.415	1.415
		MP+	1.418	1.416	1.416	1.416
		MP++	1.418	1.416	1.416	1.416
	C8–C12	HF	1.502	1.502	1.502	1.502
		HF+	1.502	1.502	1.502	1.502
		HF++	1.502	1.502	1.502	1.502
		DFT	1.502	1.502	1.502	1.502
		DFT+	1.501	1.503	1.503	1.502
		DFT++	1.501	1.503	1.503	1.502
		MP	1.495	1.497	1.497	1.497
		MP+	1.496	1.498	1.497	1.497
		MP++	1.496	1.498	1.497	1.497
	C12–C13	HF	1.553	1.553	1.552	1.553
		HF+	1.553	1.553	1.552	1.553
		HF++	1.554	1.553	1.552	1.553
		DFT	1.561	1.561	1.561	1.561
		DFT+	1.563	1.562	1.562	1.562
		DFT++	1.563	1.562	1.562	1.562
		MP	1.551	1.550	1.551	1.551
		MP+	1.552	1.552	1.552	1.552
		MP++	1.553	1.552	1.552	1.552
	C13–C14	HF	1.543	1.543	1.543	1.543
		HF+	1.544	1.543	1.543	1.543
		HF++	1.544	1.543	1.543	1.543

© University of Venda

University of Venda
Creating Future Leaders

		DFT	1.5	1.549	1.549	1.549
		DFT+	1.551	1.550	1.550	1.550
		DFT++	1.551	1.550	1.550	1.550
		MP	1.541	1.539	1.539	1.539
		MP+	1.541	1.540	1.540	1.540
		MP++	1.541	1.540	1.541	1.540
	C14–N9	HF	1.444	1.447	1.449	1.452
		HF+	1.445	1.449	1.450	1.453
		HF++	1.445	1.449	1.450	1.453
		DFT	1.454	1.457	1.458	1.461
		DFT+	1.455	1.459	1.460	1.463
		DFT++	1.455	1.459	1.460	1.463
		MP	1.453	1.456	1.460	1.460
		MP+	1.456	1.459	1.463	1.463
		MP++	1.456	1.459	1.460	1.463
	C1–O15	HF	1.364	1.365	1.365	1.366
		HF+	1.363	1.364	1.365	1.366
		HF++	1.363	1.364	1.365	1.366
		DFT	1.367	1.367	1.367	1.368
		DFT+	1.369	1.369	1.370	1.371
		DFT++	1.369	1.369	1.370	1.371
		MP	1.372	1.372	1.372	1.372
		MP+	1.374	1.374	1.376	1.376
		MP++	1.374	1.374	1.375	1.376
	O15–C16	HF	1.405	1.408	1.410	1.413
		HF+	1.408	1.411	1.412	1.416
		HF++	1.407	1.411	1.412	1.416
		DFT	1.418	1.421	1.423	1.426
		DFT+	1.421	1.425	1.427	1.430
		DFT++	1.421	1.425	1.427	1.430
		MP	1.422	1.425	1.430	1.430
		MP+	1.427	1.430	1.436	1.436
		MP++	1.427	1.430	1.432	1.435
E	C1–C2	HF	1.384	1.385	1.385	1.385
		HF+	1.386	1.386	1.386	1.387
		HF++	1.386	1.386	1.387	1.387
		DFT	1.396	1.396	1.396	1.397
		DFT+	1.397	1.397	1.398	1.398
		DFT++	1.397	1.397	1.398	1.398
		MP	1.396	1.397	1.397	1.398
		MP+	1.398	1.399	1.400	1.400
		MP++	1.399	1.399	1.400	1.400
	C2–C3	HF	1.386	1.386	1.386	1.387
		HF+	1.388	1.388	1.389	1.390

© University of Venda

University of Venda
Creating Future Leaders

		HF++	1.388	1.389	1.390	
		DFT	1.395	1.396	1.396	1.397
		DFT+	1.397	1.398	1.398	1.399
		DFT++	1.397	1.398	1.398	1.399
		MP	1.395	1.395	1.395	1.396
		MP+	1.398	1.398	1.398	1.399
		MP++	1.398	1.398	1.398	1.399
	C3–C4	HF	1.390	1.390	1.390	1.390
		HF+	1.391	1.391	1.392	1.392
		HF++	1.391	1.391	1.392	1.392
		DFT	1.403	1.401	1.401	1.402
		DFT+	1.403	1.403	1.403	1.403
		DFT++	1.403	1.403	1.403	1.404
		MP	1.400	1.402	1.403	1.403
		MP+	1.403	1.405	1.405	1.406
		MP++	1.403	1.405	1.405	1.406
	C4–C5	HF	1.392	1.392	1.393	1.393
		HF+	1.394	1.394	1.394	1.395
		HF++	1.394	1.394	1.394	1.395
		DFT	1.401	1.403	1.403	1.404
		DFT+	1.404	1.405	1.405	1.406
		DFT++	1.404	1.405	1.405	1.406
		MP	1.402	1.400	1.401	1.401
		MP+	1.405	1.403	1.403	1.404
		MP++	1.405	1.403	1.403	1.404
	C5–C6	HF	1.384	1.385	1.385	1.385
		HF+	1.386	1.387	1.387	1.388
		HF++	1.386	1.387	1.387	1.388
		DFT	1.395	1.395	1.395	1.396
		DFT+	1.397	1.397	1.397	1.398
		DFT++	1.397	1.397	1.397	1.398
		MP	1.395	1.396	1.396	1.397
		MP+	1.398	1.398	1.399	1.399
		MP++	1.398	1.398	1.399	1.399
	C6–C1	HF	1.386	1.386	1.386	1.387
		HF+	1.388	1.388	1.388	1.389
		HF++	1.388	1.388	1.388	1.388
		DFT	1.395	1.396	1.397	1.397
		DFT+	1.398	1.398	1.399	1.399
		DFT++	1.398	1.398	1.399	1.399
		MP	1.397	1.396	1.396	1.397
		MP+	1.399	1.399	1.399	1.400
		MP++	1.399	1.399	1.399	1.400
	C4–C7	HF	1.512	1.512	1.512	1.511

© University of Venda

University of Venda
Creating Future Leaders

		HF+	1.512	1.512	1.513	1.511
		HF++	1.513	1.512	1.513	1.511
		DFT	1.511	1.512	1.512	1.510
		DFT+	1.512	1.512	1.512	1.510
		DFT++	1.512	1.512	1.512	1.510
		MP	1.501	1.501	1.501	1.499
		MP+	1.501	1.501	1.501	1.499
		MP++	1.501	1.501	1.502	1.499
	C7–C8	HF	1.530	1.529	1.529	1.529
		HF+	1.530	1.529	1.529	1.529
		HF++	1.530	1.530	1.529	1.529
		DFT	1.539	1.539	1.539	1.538
		DFT+	1.539	1.539	1.539	1.538
		DFT++	1.539	1.539	1.539	1.538
		MP	1.524	1.524	1.5239	1.523
		MP+	1.525	1.525	1.525	1.524
		MP++	1.525	1.525	1.525	1.524
	C8–N9	HF	1.443	1.445	1.446	1.450
		HF+	1.443	1.446	1.447	1.450
		HF++	1.444	1.446	1.447	1.450
		DFT	1.462	1.464	1.465	1.468
		DFT+	1.462	1.465	1.466	1.469
		DFT++	1.463	1.465	1.466	1.469
		MP	1.462	1.464	1.465	1.468
		MP+	1.464	1.466	1.467	1.470
		MP++	1.464	1.466	1.467	1.470
	N9–N10	HF	1.377	1.381	1.383	1.388
		HF+	1.376	1.380	1.382	1.387
		HF++	1.376	1.380	1.382	1.387
		DFT	1.379	1.383	1.384	1.390
		DFT+	1.379	1.382	1.384	1.390
		DFT++	1.379	1.382	1.384	1.390
		MP	1.394	1.396	1.398	1.401
		MP+	1.394	1.397	1.398	1.402
		MP++	1.394	1.397	1.397	1.402
	N10–C11	HF	1.260	1.261	1.262	1.263
		HF+	1.262	1.263	1.263	1.265
		HF++	1.262	1.263	1.264	1.265
		DFT	1.290	1.291	1.291	1.292
		DFT+	1.292	1.293	1.293	1.294
		DFT++	1.292	1.293	1.293	1.510
		MP	1.303	1.304	1.304	1.304
		MP+	1.307	1.308	1.308	1.308
		MP++	1.307	1.308	1.308	1.308

© University of Venda

University of Venda
Creating Future Leaders

	C11–C7	HF	1.532	1.532	1.531	1.529
		HF+	1.532	1.532	1.531	1.528
		HF++	1.533	1.532	1.531	1.528
		DFT	1.539	1.538	1.538	1.534
		DFT+	1.539	1.538	1.537	1.532
		DFT++	1.539	1.538	1.537	1.532
		MP	1.526	1.526	1.525	1.522
		MP+	1.527	1.526	1.525	1.521
		MP++	1.527	1.526	1.525	1.521
	C8–C12	HF	1.518	1.518	1.518	1.517
		HF+	1.518	1.518	1.518	1.518
		HF++	1.518	1.518	1.518	1.518
		DFT	1.524	1.523	1.523	1.523
		DFT+	1.524	1.524	1.524	1.524
		DFT++	1.524	1.524	1.524	1.524
		MP	1.513	1.513	1.513	1.513
		MP+	1.514	1.514	1.514	1.514
		MP++	1.515	1.514	1.514	1.
	C12–C13	HF	1.564	1.564	1.564	1.564
		HF+	1.565	1.565	1.565	1.565
		HF++	1.565	1.565	1.565	1.565
		DFT	1.572	1.572	1.572	1.572
		DFT+	1.574	1.574	1.574	1.575
		DFT++	1.574	1.574	1.574	1.575
		MP	1.562	1.562	1.562	1.563
		MP+	1.565	1.565	1.565	1.566
		MP++	1.566	1.566	1.566	1.566
	C13–C14	HF	1.558	1.558	1.558	1.558
		HF+	1.557	1.557	1.557	1.557
		HF++	1.557	1.557	1.557	1.557
		DFT	1.566	1.566	1.566	1.566
		DFT+	1.566	1.565	1.565	1.565
		DFT++	1.566	1.565	1.565	1.565
		MP	1.556	1.556	1.556	1.556
		MP+	1.556	1.556	1.556	1.556
		MP++	1.556	1.556	1.556	1.556
	C14–N9	HF	1.439	1.441	1.442	1.445
		HF+	1.440	1.441	1.443	1.446
		HF++	1.440	1.442	1.443	1.446
		DFT	1.450	1.452	1.453	1.456
		DFT+	1.451	1.454	1.455	1.458
		DFT++	1.451	1.454	1.455	1.458
		MP	1.452	1.455	1.456	1.458
		MP+	1.454	1.457	1.458	1.461
		MP++	1.454	1.457	1.458	1.461

© University of Venda

University of Venda
Creating Future Leaders

F	C1–C2	HF	1.383	1.384	1.385	1.386
		HF+	1.384	1.385	1.385	1.386
		HF++	1.384	1.385	1.385	1.386
		DFT	1.398	1.398	1.399	1.399
		DFT+	1.398	1.398	1.399	1.399
		DFT++	1.398	1.398	1.399	1.399
		MP	1.397	1.397	1.398	1.399
		MP+	1.398	1.399	1.399	1.399
		MP++	1.398	1.399	1.399	1.399
	C2–C3	HF	1.387	1.387	1.387	1.387
		HF+	1.389	1.389	1.389	1.390
		HF++	1.390	1.389	1.389	1.390
		DFT	1.395	1.395	1.395	1.395
		DFT+	1.397	1.397	1.397	1.398
		DFT++	1.397	1.397	1.397	1.398
		MP	1.395	1.395	1.395	1.396
		MP+	1.398	1.398	1.398	1.399
		MP++	1.398	1.398	1.398	1.399
	C3–C4	HF	1.386	1.387	1.387	1.388
		HF+	1.387	1.388	1.388	1.389
		HF++	1.387	1.388	1.388	1.389
		DFT	1.399	1.399	1.400	1.401
		DFT+	1.400	1.401	1.401	1.402
		DFT++	1.400	1.401	1.401	1.402
		MP	1.399	1.399	1.399	1.400
		MP+	1.401	1.401	1.402	1.402
		MP++	1.401	1.401	1.402	1.402
	C4–C5	HF	1.395	1.394	1.394	1.395
		HF+	1.396	1.396	1.396	1.396
		HF++	1.396	1.396	1.396	1.396
		DFT	1.404	1.404	1.404	1.405
		DFT+	1.406	1.405	1.406	1.406
		DFT++	1.406	1.405	1.405	1.406
		MP	1.404	1.404	1.404	1.404
		MP+	1.406	1.406	1.406	1.406
		MP++	1.406	1.406	1.406	1.406
	C5–C6	HF	1.379	1.380	1.381	1.382
		HF+	1.382	1.383	1.383	1.384
		HF++	1.382	1.383	1.383	1.384
		DFT	1.391	1.391	1.392	1.392
		DFT+	1.393	1.394	1.394	1.395
		DFT++	1.393	1.394	1.394	1.395
		MP	1.392	1.392	1.392	1.393
		MP+	1.393	1.395	1.396	1.396

© University of Venda

University of Venda
Creating Future Leaders

		MP++	1.395	1.395	1.396	1.396
	C6–C1	HF	1.389	1.38	1.389	1.390
		HF+	1.389	1.389	1.390	1.390
		HF++	1.389	1.389	1.390	1.390
		DFT	1.399	1.400	1.400	1.401
		DFT+	1.399	1.400	1.400	1.401
		DFT++	1.399	1.400	1.400	1.401
		MP	1.398	1.399	1.399	1.400
		MP+	1.399	1.399	1.399	1.400
		MP++	1.399	1.399	1.399	1.400
	C4–C7	HF	1.511	1.512	1.512	1.511
		HF+	1.512	1.512	1.512	1.512
		HF++	1.512	1.512	1.512	1.512
		DFT	1.511	1.511	1.511	1.510
		DFT+	1.511	1.512	1.512	1.511
		DFT++	1.511	1.512	1.512	1.511
		MP	1.500	1.501	1.501	1.500
		MP+	1.501	1.501	1.501	1.500
		MP++	1.501	1.501	1.501	1.500
	C7–C8	HF	1.529	1.529	1.529	1.529
		HF+	1.529	1.529	1.529	1.529
		HF++	1.529	1.529	1.529	1.529
		DFT	1.539	1.539	1.539	1.538
		DFT+	1.539	1.539	1.539	1.538
		DFT++	1.539	1.539	1.539	1.538
		MP	1.524	1.524	1.524	1.523
		MP+	1.525	1.525	1.525	1.524
		MP++	1.525	1.525	1.525	1.524
	C8–N9	HF	1.443	1.445	1.446	1.450
		HF+	1.444	1.446	1.447	1.450
		HF++	1.444	1.446	1.447	1.450
		DFT	1.462	1.465	1.46	1.469
		DFT+	1.463	1.465	1.466	1.470
		DFT++	1.463	1.465	1.466	1.470
		MP	1.462	1.464	1.465	1.468
		MP+	1.463	1.466	1.467	1.471
		MP++	1.464	1.466	1.467	1.471
	N9–N10	HF	1.378	1.382	1.383	1.388
		HF+	1.376	1.380	1.382	1.387
		HF++	1.376	1.380	1.382	1.387
		DFT	1.380	1.383	1.385	1.391
		DFT+	1.379	1.383	1.385	1.391
		DFT++	1.379	1.383	1.385	1.391
		MP	1.394	1.397	1.398	1.402

© University of Venda

University of Venda
Creating Future Leaders

		MP+	1.394	1.397	1.399	1.403
		MP++	1.395	1.397	1.399	1.403
	N10–C11	HF	1.261	1.261	1.262	1.263
		HF+	1.262	1.263	1.264	1.265
		HF++	1.262	1.263	1.264	1.265
		DFT	1.290	1.291	1.291	1.292
		DFT+	1.292	1.293	1.293	1.294
		DFT++	1.292	1.293	1.293	1.294
		MP	1.303	1.304	1.304	1.304
		MP+	1.307	1.307	1.308	1.308
		MP++	1.307	1.307	1.308	1.308
	C11–C7	HF	1.533	1.532	1.531	1.529
		HF+	1.533	1.532	1.531	1.529
		HF++	1.533	1.532	1.531	1.529
		DFT	1.539	1.538	1.538	1.534
		DFT+	1.539	1.538	1.537	1.533
		DFT++	1.539	1.538	1.537	1.533
		MP	1.527	1.526	1.525	1.523
		MP+	1.527	1.526	1.525	1.522
		MP++	1.527	1.556	1.525	1.522
	C8–C12	HF	1.518	1.518	1.517	1.517
		HF+	1.518	1.518	1.518	1.518
		HF++	1.518	1.518	1.518	1.518
		DFT	1.524	1.523	1.523	1.523
		DFT+	1.524	1.524	1.524	1.523
		DFT++	1.524	1.524	1.524	1.523
		MP	1.513	1.513	1.513	1.513
		MP+	1.515	1.514	1.514	1.514
		MP++	1.515	1.514	1.514	1.514
	C12–C13	HF	1.564	1.564	1.564	1.564
		HF+	1.565	1.565	1.565	1.565
		HF++	1.565	1.565	1.565	1.565
		DFT	1.572	1.572	1.572	1.573
		DFT+	1.574	1.574	1.574	1.575
		DFT++	1.574	1.574	1.574	1.575
		MP	1.562	1.562	1.562	1.563
		MP+	1.565	1.565	1.565	1.566
		MP++	1.566	1.566	1.566	1.566
	C13–C14	HF	1.558	1.558	1.558	1.558
		HF+	1.557	1.557	1.557	1.557
		HF++	1.557	1.557	1.557	1.557
		DFT	1.566	1.566	1.566	1.566
		DFT+	1.566	1.565	1.565	1.565
		DFT++	1.566	1.565	1.565	1.565

© University of Venda

University of Venda
Creating Future Leaders

		MP	1.556	1.556	1.556	1.556
		MP+	1.556	1.556	1.556	1.556
		MP++	1.556	1.556	1.556	1.556
	C14–N9	HF	1.439	1.441	1.442	1.445
		HF+	1.440	1.442	1.443	1.446
		HF++	1.440	1.442	1.443	1.446
		DFT	1.447	1.452	1.453	1.456
		DFT+	1.451	1.454	1.455	1.458
		DFT++	1.451	1.454	1.455	1.458
		MP	1.452	1.454	1.456	1.458
		MP+	1.454	1.457	1.458	1.461
		MP++	1.454	1.457	1.458	1.461
	C1–O15	HF	1.351	1.351	1.350	1.350
		HF+	1.352	1.352	1.352	1.352
		HF++	1.352	1.352	1.352	1.352
		DFT	1.367	1.366	1.366	1.365
		DFT+	1.372	1.371	1.371	1.371
		DFT++	1.372	1.371	1.371	1.371
		MP	1.373	1.372	1.372	1.371
		MP+	1.378	1.378	1.378	1.378
		MP++	1.378	1.378	1.378	1.378
	O15–H27	HF	0.943	0.946	0.947	0.955
		HF+	0.943	0.946	0.948	0.956
		HF++	0.943	0.946	0.948	0.956
		DFT	0.966	0.969	0.971	0.980
		DFT+	0.966	0.970	0.971	0.981
		DFT++	0.966	0.970	0.971	0.981
		MP	0.966	0.969	0.970	0.979
		MP+	0.967	0.971	0.972	0.983
		MP++	0.967	0.971	0.972	0.983
G	C1–C2	HF	1.390	1.382	1.382	1.383
		HF+	1.393	1.383	1.383	1.383
		HF++	1.393	1.383	1.383	1.383
		DFT	1.398	1.402	1.402	1.402
		DFT+	1.398	1.402	1.402	1.403
		DFT++	1.398	1.402	1.403	1.403
		MP	1.400	1.402	1.402	-
		MP+	1.402	1.403	1.403	-
		MP++	1.402	1.403	1.403	-
	C2–C3	HF	1.379	1.387	1.388	1.388
		HF+	1.380	1.390	1.390	1.391
		HF++	1.380	1.390	1.390	1.391
		DFT	1.399	1.390	1.391	1.392
		DFT+	1.402	1.393	1.393	1.394

© University of Venda

University of Venda
Creating Future Leaders

		DFT++	1.392	1.393	1.394	1.394
		MP	1.390	1.390	1.390	-
		MP+	1.393	1.393	1.393	-
		MP++	1.393	1.393	1.393	-
	C3–C4	HF	1.392	1.387	1.387	1.388
		HF+	1.396	1.388	1.389	1.389
		HF++	1.396	1.388	1.389	1.389
		DFT	1.395	1.402	1.402	1.403
		DFT+	1.396	1.404	1.404	1.404
		DFT++	1.396	1.404	1.405	1.404
		MP	1.401	1.403	1.403	-
		MP+	1.404	1.405	1.405	-
		MP++	1.404	1.405	1.405	-
	C4–C5	HF	1.387	1.394	1.394	1.394
		HF+	1.386	1.395	1.395	1.396
		HF++	1.386	1.395	1.395	1.396
		DFT	1.407	1.400	1.400	1.401
		DFT+	1.408	1.401	1.401	1.402
		DFT++	1.408	1.401	1.401	1.402
		MP	1.400	1.399	1.399	-
		MP+	1.401	1.401	1.401	-
		MP++	1.401	1.401	1.401	-
	C5–C6	HF	1.388	1.382	1.382	1.383
		HF+	1.392	1.382	1.384	1.385
		HF++	1.392	1.384	1.384	1.385
		DFT	1.387	1.396	1.396	1.397
		DFT+	1.389	1.399	1.399	1.400
		DFT++	1.389	1.399	1.400	1.400
		MP	1.397	1.398	1.398	-
		MP+	1.400	1.401	1.401	-
		MP++	1.400	1.401	1.401	-
	C6–C1	HF	1.387	1.388	1.387	1.388
		HF+	1.387	1.389	1.389	1.389
		HF++	1.387	1.389	1.389	1.389
		DFT	1.404	1.401	1.401	1.401
		DFT+	1.405	1.402	1.402	1.402
		DFT++	1.405	1.402	1.402	1.402
		MP	1.400	1.400	1.400	-
		MP+	1.402	1.401	1.401	-
		MP++	1.402	1.401	1.401	-
	C4–C7	HF	1.520	1.520	1.521	1.521
		HF+	1.512	1.520	1.521	1.521
		HF++	1.512	1.521	1.521	1.521
		DFT	1.521	1.522	1.522	1.522

© University of Venda

University of Venda
Creating Future Leaders

		DFT+	1.521	1.522	1.523	1.523
		DFT++	1.521	1.522	1.522	1.523
		MP	1.511	1.500	1.501	-
		MP+	1.512	1.501	1.501	-
		MP++	1.512	1.501	1.501	-
	C7–C8	HF	1.544	1.542	1.543	1.542
		HF+	1.530	1.543	1.543	1.543
		HF++	1.530	1.543	1.543	1.543
		DFT	1.550	1.550	1.550	1.550
		DFT+	1.551	1.552	1.552	1.551
		DFT++	1.551	1.552	1.551	1.551
		MP	1.538	1.524	1.524	-
		MP+	1.540	1.525	1.525	-
		MP++	1.540	1.525	1.525	-
	C8–N9	HF	1.476	1.479	1.481	1.485
		HF+	1.444	1.481	1.482	1.487
		HF++	1.444	1.480	1.482	1.487
		DFT	1.496	1.500	1.501	1.505
		DFT+	1.496	1.500	1.502	1.507
		DFT++	1.496	1.500	1.505	1.507
		MP	1.497	1.464	1.465	-
		MP+	1.496	1.466	1.467	-
		MP++	1.495	1.466	1.467	-
	N9–N10	HF	1.398	1.395	1.397	1.401
		HF+	1.376	1.394	1.395	1.399
		HF++	1.376	1.394	1.395	1.399
		DFT	1.402	1.405	1.407	1.410
		DFT+	1.399	1.402	1.404	1.409
		DFT++	1.399	1.402	1.407	1.409
		MP	1.419	1.397	1.398	-
		MP+	1.417	1.397	1.399	-
		MP++	1.417	1.397	1.399	-
	N10–C11	HF	1.253	1.254	1.254	1.255
		HF+	1.262	1.256	1.256	1.257
		HF++	1.262	1.256	1.256	1.257
		DFT	1.282	1.282	1.282	1.283
		DFT+	1.284	1.284	1.284	1.285
		DFT++	1.284	1.284	1.285	1.285
		MP	1.294	1.304	1.304	-
		MP+	1.297	1.307	1.308	-
		MP++	1.298	1.308	1.308	-
	C11–C7	HF	1.513	1.513	1.512	1.511
		HF+	1.532	1.513	1.512	1.511
		HF++	1.532	1.513	1.512	1.511

© University of Venda

University of Venda
Creating Future Leaders

		DFT	1.522	1.520	1.520	1.518
		DFT+	1.521	1.520	1.519	1.516
		DFT++	1.521	1.520	1.518	1.516
		MP	1.538	1.523	1.525	-
		MP+	1.540	1.525	1.525	-
		MP++	1.540	1.525	1.525	-
	C8–C12	HF	1.556	1.530	1.530	1.530
		HF+	1.518	1.530	1.530	1.530
		HF++	1.518	1.530	1.530	1.530
		DFT	1.538	1.537	1.537	1.536
		DFT+	1.538	1.537	1.536	1.536
		DFT++	1.538	1.537	1.536	1.536
		MP	1.554	1.513	1.513	-
		MP+	1.555	1.514	1.514	-
		MP++	1.555	1.514	1.514	-
	C12–C13	HF	1.540	1.530	1.530	1.530
		HF+	1.564	1.531	1.530	1.530
		HF++	1.565	1.531	1.530	1.530
		DFT	1.539	1.538	1.538	1.537
		DFT+	1.540	1.539	1.538	1.538
		DFT++	1.540	1.539	1.538	1.538
		MP	1.537	1.562	1.562	-
		MP+	1.540	1.565	1.565	-
		MP++	1.541	1.566	1.566	-
	C13–C14	HF	1.532	1.538	1.536	1.535
		HF+	1.557	1.536	1.535	1.534
		HF++	1.557	1.536	1.535	1.534
		DFT	1.550	1.548	1.547	1.545
		DFT+	1.550	1.547	1.546	1.544
		DFT++	1.550	1.547	1.545	1.544
		MP	1.529	1.556	1.556	-
		MP+	1.531	1.556	1.556	-
		MP++	1.531	1.556	1.556	-
	C14–N9	HF	1.456	1.471	1.472	1.475
		HF+	1.439	1.472	1.474	1.476
		HF++	1.439	1.472	1.473	1.476
		DFT	1.481	1.485	1.486	1.489
		DFT+	1.483	1.487	1.489	1.492
		DFT++	1.483	1.487	1.490	1.492
		MP	1.471	1.455	1.456	-
		MP+	1.472	1.457	1.459	-
		MP++	1.471	1.457	1.459	-
	C1–O15	HF	1.349	1.364	1.364	1.366
		HF+	1.349	1.364	1.364	1.366

© University of Venda

University of Venda
Creating Future Leaders

		HF++	1.349	1.364	1.364	1.366
		DFT	1.367	1.367	1.367	1.368
		DFT+	1.368	1.369	1.369	1.371
		DFT++	1.368	1.369	1.371	1.371
		MP	1.372	1.371	1.371	-
		MP+	1.374	1.374	1.375	-
		MP++	1.374	1.374	1.375	-
	O15–C16	HF	1.399	1.409	1.410	1.413
		HF+	1.401	1.411	1.413	1.416
		HF++	1.401	1.411	1.413	1.416
		DFT	1.418	1.422	1.423	1.426
		DFT+	1.421	1.426	1.427	1.430
		DFT++	1.421	1.426	1.429	1.430
		MP	1.422	1.426	1.423	-
		MP+	1.427	1.431	1.432	-
		MP++	1.427	1.431	1.432	-

Table 4.10. Parameters of the intramolecular hydrogen bond in the lowest energy conformer of compound n-B, from the results of different calculation methods and in the media considered.

method	medium	Parameters of the IHB		
		H···O (Å)	O···O (Å)	OĤO
HF	vac	1.825	2.601	136.976
	chlrf	1.833	2.606	136.520
	actn	1.838	2.608	136.282
	aq	1.862	2.618	134.619
HF+	vac	1.833	2.604	136.278
	chlrf	1.843	2.608	135.725
	actn	1.848	2.611	135.452
	aq	1.875	2.622	133.610
HF++	vac	1.833	2.604	136.289
	chlrf	1.842	2.609	135.751
	actn	1.847	2.611	135.483
	aq	1.876	2.623	133.621
DFT	vac	1.689	2.561	144.946
	chlrf	1.693	2.563	144.702
	actn	1.695	2.564	144.554
	aq	1.716	2.574	143.150
DFT+	vac	1.707	2.567	143.427
	chlrf	1.712	2.570	143.102
	actn	1.714	2.570	142.931
	aq	1.740	2.582	141.141
DFT++	vac	1.688	2.561	144.977
	chlrf	1.712	2.569	143.148

© University of Venda

University of Venda
Creating Future Leaders

	actn	1.71	2.569	142.979
	aq	1.740	2.582	141.181
MP	vac	1.747	2.599	143.493
	chlrf	1.751	2.601	143.189
	actn	1.754	2.603	142.996
	aq	1.773	2.611	141.562
MP+	vac	1.747	2.599	143.493
	chlrf	1.751	2.601	143.189
	actn	1.755	2.603	142.996
	aq	1.773	2.611	141.562
MP++	vac	1.747	2.599	143.493
	chlrf	1.751	2.601	143.189
	actn	1.754	2.603	142.996
	aq	1.773	2.611	141.562

Table 4.11. Dipole moments of the calculated compounds in vacuo and in the three solvents considered. Results from different calculation methods.

compound	method	dipole moment (debye)			
		in vacuo	in chloroform	in acetonitrile	in water
A	HF	3.116	3.720	3.952	4.314
	HF+	3.312	4.015	4.291	4.679
	HF++	3.306	4.100	4.289	4.674
	DF	3.015	3.640	3.878	4.236
	DF+	3.235	3.985	4.281	4.681
	DF++	3.225	3.974	4.271	4.673
	MP	3.174	3.801	4.043	4.417
	MP+	3.386	4.122	4.418	4.820
	MP++	3.380	4.119	4.415	4.820
B	HF	4.191	5.035	5.384	5.928
	HF+	4.360	5.332	5.734	6.316
	HF++	4.357	5.331	5.736	6.314

© University of Venda

University of Venda
Creating Future Leaders

	DF	4.146	5.029	5.403	5.976
	DF+	4.401	5.439	5.891	6.497
	DF++	4.393	5.432	5.883	6.502
	MP	4.332	5.197	5.561	6.119
	MP+	4.433	5.424	5.852	6.454
	MP++	4.447	5.448	5.860	6.458
D	HF	2.359	2.932	3.177	3.539
	HF+	2.432	3.100	3.387	3.811
	HF++	2.437	3.108	3.380	3.808
	DF	2.034	2.450	2.582	2.801
	DF+	2.168	2.782	2.977	3.129
	DF++	2.160	2.765	2.958	3.121
	MP	2.183	2.900	2.988	3.135
	MP+	2.493	3.218	3.227	3.479
	MP++	2.477	3.186	3.214	3.471
E-R	HF	2.325	2.753	2.931	3.187
	HF+	2.441	2.947	3.165	3.456
	HF++	2.436	2.944	3.163	3.453
	DF	2.172	2.534	2.699	2.928
	DF+	2.362	2.881	3.106	3.382
	DF++	2.358	2.879	3.105	3.382
	MP	2.470	2.927	3.112	3.382
	MP+	2.584	3.127	3.360	3.669
	MP++	2.580	3.125	3.358	3.667
E-S	HF	2.267	2.690	2.872	3.119
	HF+	2.440	2.946	3.165	3.376

© University of Venda

University of Venda
Creating Future Leaders

	HF++	2.436	2.944	3.098	3.373
	DF	2.137	2.535	2.624	2.841
	DF+	2.362	2.881	3.108	3.278
	DF++	2.358	2.879	3.107	3.275
	MP	2.471	2.928	3.116	3.384
	MP+	2.584	3.127	3.360	3.671
	MP++	2.580	3.125	3.358	3.669
F-R	HF	3.060	3.676	3.945	4.355
	HF+	3.175	3.865	4.176	4.638
	HF++	3.177	3.868	4.182	4.639
	DF	3.001	3.645	3.931	4.391
	DF+	3.165	3.905	4.248	4.746
	DF++	3.169	3.911	4.258	4.751
	MP	3.111	3.766	4.053	4.528
	MP+	3.238	3.983	4.303	4.831
	MP++	3.243	3.984	4.313	4.836
F-S	HF	3.067	3.667	3.948	4.375
	HF+	3.172	3.866	4.177	4.638
	HF++	3.163	3.869	4.181	4.639
	DF	3.009	3.543	3.734	4.745
	DF+	3.165	3.904	4.248	4.750
	DF++	3.169	3.912	4.258	4.752
	MP	3.121	3.757	4.037	4.520
	MP+	3.165	3.979	4.292	4.827
	MP++	3.244	3.981	4.310	4.828

© University of Venda

University of Venda

G-R	HF	2.640	2.887	3.031	3.192
	HF+	2.668	3.121	3.308	3.553
	HF++	2.661	3.113	3.300	3.530
	DF	2.477	2.777	2.915	3.017
	DF+	2.616	3.110	3.322	3.398
	DF++	2.619	3.095	3.306	3.410
	MP	2.578	2.938	3.084	3.226
	MP+	2.709	3.153	3.380	3.547
	MP++	2.697	3.140	3.332	3.572
G-S	HF	2.659	2.887	3.031	3.191
	HF+	2.763	3.121	3.171	3.528
	HF++	2.764	3.113	3.301	3.518
	DF	2.400	2.766	2.923	3.019
	DF+	2.617	3.108	3.320	3.412
	DF++	2.602	3.092	3.308	3.408
	MP	2.577	2.942	3.085	3.225
	MP+	2.709	3.154	3.345	3.553
	MP++	2.695	3.142	3.329	3.449
n-A	HF	6.982	7.980	8.286	8.681
	HF+	7.189	8.278	8.623	9.048
	HF++	7.191	8.289	8.636	9.059
	DF	7.011	8.275	8.683	9.250
	DF+	7.528	9.034	9.542	10.234
	DF++	7.521	9.025	9.533	10.224
	MP	7.087	8.026	8.305	8.666
	MP+	7.300	8.324	8.632	9.019
	MP++	7.299	8.325	8.634	9.021

© University of Venda

University of Venda
Creating Future Leaders

n-B1	HF	6.465	7.477	7.836	8.336
	HF+	6.656	7.805	8.209	8.765
	HF++	6.661	7.810	8.215	8.773
	DF	6.489	7.677	8.090	8.673
	DF+	7.064	8.495	9.014	9.702
	DF++	6.488	8.497	9.019	9.705
	MP	6.969	8.047	8.413	8.919
	MP+	7.236	8.446	8.867	9.423
	MP++	7.234	8.446	8.868	9.424
n-B2	HF	8.870	10.343	10.917	11.707
	HF+	9.008	10.660	11.313	12.170
	HF++	9.013	10.669	11.316	12.179
	DF	8.731	10.405	11.056	11.992
	DF+	9.249	11.225	12.026	13.124
	DF++	9.240	11.235	12.037	13.133
	MP	9.287	10.777	11.337	12.114
	MP+	9.543	11.206	11.843	12.679
	MP++	9.541	11.205	11.843	12.679



© University of Venda

University of Venda
Creating Future Leaders

Table 4.12. IR frequencies of relevant bonds (harmonic approximation) in different media.
The frequencies have been scaled by the following factors: 0.9024[a], 0.92[b], 0.961[a] , 0.9857[b] and 0.9356[a] for respectively HF, HF+, DFT, DFT+ and MP.

compound	method	medium	bond considered					
			C4–C7	N9–N10	C8–N9	N10–C11	O15–H27	O15–C16
A	HF	vac	309.70	1359.25	1509.07	1427.24	-	-
		chlrf	310.43	1353.99	1509.79	1423.25	-	-
		actn	310.76	1351.84	1510.58	1421.57	-	-
		aq	311.38	1345.86	1511.75	1416.10	-	-
	HF+	vac	315.84	1366.34	1542.43	1439.05	-	-
		chlrf	316.07	1367.92	1541.55	1439.20	-	-
		actn	315.64	1374.23	1536.83	1441.96	-	-
		aq	316.22	1368.25	1538.32	1436.16	-	-
	DFT	vac	311.12	1392.30	1483.21	1550.48	-	-
		chlrf	311.48	1302.15	1453.95	1343.91	-	-
		actn	311.85	1301.04	1453.24	1343.07	-	-
		aq	315.46	1295.02	1471.28	1340.28	-	-
	DFT+	vac	316.13	1331.97	1514.89	1375.04	-	-
		chlrf	317.94	1332.04	1484.53	1422.55	-	-
		Actn	316.96	1334.31	1508.01	1427.41	-	-
		aq	321.70	1324.59	1502.23	1420.62	-	-
	MP	vac	300.60	1324.63	1422.61	1288.50	-	-
		chlrf	300.19	1322.56	1421.50	1288.11	-	-
		actn	299.80	1321.83	1420.93	1287.80	-	-
		aq	298.91	1320.04	1426.31	1289.71	-	-
B	HF	vac	271.25	1359.12	1492.56	1424.62	3786.26	-

© University of Venda

University of Venda
Creating Future Leaders

		chlrf	272.10	1353.76	1508.68	1420.42	3731.81	-
		actn	272.88	1351.62	1509.36	1418.74	3703.69	-
		aq	272.99	1345.97	1509.97	1413.15	3526.24	-
	HF+	vac	276.99	1371.30	1536.99	1438.81	3793.62	-
		chlrf	277.79	1375.74	1534.62	1440.35	3797.96	-
		actn	277.96	1373.52	1535.52	1438.40	3767.17	-
		aq	278.79	1370.89	1535.15	1438.18	3589.72	-
	DFT	vac	269.08	1306.01	1482.64	1389.54	3674.36	-
		chlrf	268.65	1302.72	1478.81	1389.36	3622.96	-
		actn	268.25	1301.42	1476.47	1342.12	3622.96	-
		aq	268.18	1296.49	1469.16	1338.57	3390.18	-
	DFT+	vac	316.70	1331.44	1513.38	1421.22	3713.23	-
		chlrf	316.96	1335.34	1508.35	1423.48	3718.80	-
		Actn	316.46	1334.04	1507.01	1423.24	3689.83	-
		aq	316.02	1328.86	1499.74	1420.20	3472.25	-
	MP	vac	262.26	1324.81	1421.21	1295.96	3628.73	-
		chlrf	260.33	1322.97	1419.69	1294.55	3574.54	-
		Actn	259.47	1322.25	1418.93	1293.88	3546.42	-
		aq	257.45	1321.00	1425.71	1290.31	3340.49	-
D	HF	vac	267.47	1357.76	1508.33	1427.57	-	1048.97
		chlrf	280.77	1352.89	1508.32	1423.44	-	1055.46
		actn	266.41	1350.86	1509.22	1422.59	-	1037.75
		aq	261.64	1345.07	1509.92	1403.85	-	1030.06
	HF+	vac	270.97	1370.70	1537.11	1444.01	-	1050.78
		chlrf	284.74	1374.35	1534.32	1437.05	-	1069.44
		actn	270.91	1372.73	1535.39	1443.19	-	1049.85

© University of Venda

University of Venda
Creating Future Leaders

		aq	265.31	1367.16	1536.33	1463.66	-	1041.58
	DFT	vac	283.02	1306.45	1482.20	1342.78	-	1035.29
		chlrf	283.91	1303.33	1477.67	1340.16	-	1028.75
		actn	284.32	1301.19	1476.04	1339.00	-	1026.17
		aq	284.48	1297.77	1469.52	1336.51	-	1020.20
	DFT+	vac	288.94	1337.67	1466.70	1415.94	-	1052.35
		chlrf	289.59	1332.64	1507.33	1415.24	-	1044.46
		Actn	290.02	1331.29	1505.81	1414.86	-	1041.35
		aq	289.59	1327.14	1500.25	1362.47	-	1034.69
	MP	vac	273.44	1329.07	1417.19	1292.12	-	1021.30
		chlrf	274.90	1322.67	1419.21	1287.90	-	1014.82
		Actn	274.41	1321.96	1418.82	1287.59	-	1012.80
		aq	272.84	1320.35	1425.13	1286.78	-	1007.39
E	HF	vac	276.85	1272.17	1290.76	1671.79	-	-
		chlrf	277.23	1266.86	1268.28	1671.69	-	-
		actn	277.61	1265.82	1267.62	1632.13	-	-
		aq	278.03	1259.18	1261.99	1669.55	-	-
	HF+	vac	317.10	1153.26	1443.16	1289.95	-	-
		chlrf	316.58	1154.74	1441.87	1290.09	-	-
		actn	316.20	1153.56	1442.08	1311.26	-	-
		aq	315.36	1147.58	1441.79	1355.02		-
	DFT	vac	309.98	1233.75	1298.19	1554.26	-	-
		chlrf	310.06	1283.76	1297.12	1554.87	-	-
		actn	272.72	1227.29	1301.34	1556.95	-	-
		aq	310.36	1200.38	1431.53	1553.96	-	-
	DFT+	vac	316.38	1256.36	1399.25	1577.18	-	-

© University of Venda

University of Venda
Creating Future Leaders

		chlrf	316.11	1258.51	1398.12	1581.62	-	-
		actn	315.86	1255.42	1398.39	1581.71	-	-
		aq	315.52	1254.52	1398.67	1590.21	-	-
	MP	vac	305.09	1194.98	1282.02	1466.47	-	
		chlrf	303.23	1190.88	1281.12	1466.54	-	-
		actn	302.16	1209.99	1280.93	1471.84	-	-
		aq	298.78	1180.29	1276.55	1474.83	-	-
F	HF	vac	278.52	1264.52	1344.61	1668.78	3786.16	-
		chlrf	279.17	1262.44	1343.98	1669.32	3729.89	-
		actn	279.60	1261.33	1344.00	1669.43	3702.10	-
		aq	279.80	1256.18	1307.55	1668.27	3525.07	-
	HF+	vac	284.50	1153.55	1382.30	1681.27	3792.04	-
		chlrf	283.70	1154.63	1382.53	1686.46	3795.62	-
		actn	283.86	1153.71	1382.87	1686.65	3765.12	-
		aq	284.26	1148.30	1380.20	1683.84	3574.25	-
	DFT	vac	277.75	1233.48	1298.32	1555.13	3673.48	-
		chlrf	277.52	1230.53	1297.18	1555.66	3622.50	-
		actn	277.93	1229.13	1296.61	1555.64	3596.17	-
		aq	278.91	1226.04	1292.00	1554.91	3392.57	-
	DFT+	vac	284.26	1256.21	1399.72	1577.94	3773.93	-
		chlrf	285.66	1257.91	1398.49	1574.22	3713.75	-
		Actn	283.58	1257.31	1398.83	1582.53	3682.80	-
		aq	284.20	1253.40	1403.57	1581.19	3455.38	-
	MP	vac	273.48	1195.01	1289.46	1466.66	3628.57	-
		chlrf	270.45	1190.62	1288.56	1467.29	3573.96	-
		Actn	268.90	1188.42	1288.26	1472.18	3545.89	-

© University of Venda

University of Venda
Creating Future Leaders

		aq	266.82	1179.17	1276.42	1475.69	3342.48	-
G	HF	vac	246.11	1198.75	1350.35	1705.64	-	1049.08
		chlrf	266.51	1196.75	1350.66	1707.21	-	1041.33
		actn	266.88	1196.09	1350.65	1707.90	-	1039.12
		aq	276.35	1198.93	1337.21	1669.17	-	1030.07
	HF+	vac	271.17	1172.43	1408.18	1722.34		1049.48
		chlrf	270.08	1217.65	1401.46	1725.94	-	1050.82
		actn	270.47	1216.82	1407.05	1726.71	-	1047.93
		aq	279.02	1218.24	1429.53	1684.47	-	1041.35
	DFT	vac	275.91	1233.88	1299.27	1554.54	-	1035.34
		chlrf	275.69	1230.60	1297.98	1554.65	-	1028.34
		actn	274.93	1229.83	1297.28	1554.98	-	1025.70
		aq	277.00	1225.89	1292.23	1554.45	-	1019.84
	DFT+	vac	280.12	1255.73	1399.24	1577.76	-	1039.56
		chlrf	279.56	1313.15	1398.09	1582.17	-	1043.53
		Actn	279.08	1312.92	1398.62	1582.27	-	1040.53
		aq	281.92	1304.31	1398.21	1581.36	-	1033.40
	MP	vac	251.29	1194.81	1285.09	1466.65	-	1022.19
		chlrf	250.28	1190.60	1284.01	1467.42	-	1019.20
		actn	248.87	1183.58	1274.75	1472.10	-	1014.18
		Aq	248.92	1178.36	1267.31	1476.60	-	1178.36

LIBRARY

© University of Venda

University of Venda
Creating Future Leaders

Table 4.13. Frequency (harmonic approximation) and Red shifts of the IR frequency (in parentheses) of the OH group in compound n-B in different media.
The reference is the frequency of the OH group in compound B.
The frequencies have been scaled by the following factors: 0.9024[a], 0.92[b], 0.961[b], 0.9857[b] and 0.9356[a] for respectively HF, HF+, DFT, DFT+ and MP2.

Method	Frequencies and Red shift in (cm^{-1})			
	in vacuo	in chloroform	in acetonitrile	in water
HF	3786.26 (128.65)	3731.42 (70.81)	3703.69 (43.27)	3526.24 (-114.87)
HF+	3793.62 (57.98)	3797.96 (66.78)	3767.17 (36.22)	3589.72 (-116.94)
DFT	3674.36 (400.97)	3622.96 (342.14)	3622.96 (338.61)	3390.18 (95.36)
DFT+	3713.23 (314.17)	3718.80 (324.72)	3689.78 (293.00)	3472.25 (61.14)
MP	3628.73 (243.32)	3574.54 (186.59)	3546.42 (156.98)	3340.49 (-48.66)

[a] K. Irikura. R. D. Johnson III. and R. N. Kacker. Uncertainties in scaling factors for ab initio vibrational frequencies. J. Phys. Chem. A 2005. 109. 8430-8437.
[b] J. P. Merrick. D. Moran. and L. Radom. An Evaluation of Harmonic Vibrational Frequency Scale Factors. J. Phys. Chem. A 2007. 111. 11683-11700.

Table 4.14. HOMO-LUMO energy difference of the calculated compounds in vacuo and in the three solvents considered. Results from different calculation methods.

compound	method	HOMO-LUMO energy difference (kcal/mol)			
		in vacuo	In chloroform	in acetonitrile	in water
A	HF	266.892	266.334	266.107	265.662
	HF+	224.121	228.858	229.882	230.930
	HF++	208.182	211.966	212.895	213.541
	DFT	123.776	123.355	122.760	123.638
	DFT+	121.115	120.695	119.898	120.883
	DFT++	120.964	120.538	121.015	120.877
	MP	262.870	262.945	262.989	263.102
	MP+	225.024	230.076	231.249	232.492
	MP++	208.747	212.870	213.830	214.846

© University of Venda

University of Venda
Creating Future Leaders

B	HF	263.912	263.560	263.440	263.159
	HF+	218.085	222.464	223.568	224.184
	HF++	202.171	206.099	207.172	207.649
	DFT	121.662	121.561	121.480	121.404
	DFT+	117.940	117.903	117.858	118.015
	DFT++	117.451	117.789	117.783	117.758
	MP	259.419	259.619	259.701	259.852
	MP+	217.996	223.010	224.240	225.018
	MP++	201.731	206.268	207.674	208.339
D	HF	267.726	267.074	266.716	266.189
	HF+	222.483	227.133	228.169	229.066
	HF++	206.525	210.190	211.125	211.759
	DFT	121.573	121.172	120.858	120.550
	DFT+	117.293	117.614	117.482	116.923
	DFT++	116.986	117.513	117.369	116.892
	MP	258.339	259.638	258.891	259.255
	MP+	217.042	222.627	223.782	225.382
	MP++	200.125	205.126	205.597	206.946
E-R	HF	286.213	288.359	288.993	289.049
	HF+	244.446	248.154	249.190	249.717
	HF++	226.944	230.233	231.249	231.299
	DFT	127.755	124.196	124.724	124.761
	DFT+	118.021	119.672	120.324	120.337
	DFT++	118.021	119.678	120.331	120.419
	MP	283.841	285.554	286.000	285.773
	MP+	230.364	248.273	249.158	249.359
	MP++	227.278	230.364	231.174	230.810
E-S	HF	286.213	289.607	290.285	290.436
	HF+	244.446	248.148	249.190	252.133
	HF++	226.944	230.227	233.371	233.578
	DFT	122.785	124.178	125.614	126.292
	DFT+	118.003	119.653	120.324	122.057
	DFT++	118.009	119.666	120.324	121.956
	MP	283.834	285.585	285.987	285.780
	MP+	244.697	248.273	249.158	249.365
	MP++	227.271	230.364	231.187	230.822
F-R	HF	275.037	275.414	275.489	275.188

© University of Venda

University of Venda
Creating Future Leaders

	HF+	234.011	238.414	238.489	238.188
	HF++	217.758	220.952	238.723	238.497
	DFT	117.758	120.952	121.516	120.996
	DFT+	115.518	117.846	118.724	119.283
	DFT++	115.574	117.890	118.762	119.258
	MP	273.279	272.709	272.753	272.665
	MP+	234.443	238.466	239.169	238.667
	MP++	218.279	212.404	212.937	212.103
F-S	HF	275.991	276.481	275.489	275.244
	HF+	234.789	238.083	238.716	238.503
	HF++	218.492	220.952	221.516	221.002
	DFT	117.394	122.558	123.255	120.394
	DFT+	115.524	117.846	118.737	119.339
	DFT++	115.574	117.890	118.756	119.270
	MP	272.514	272.797	272.803	272.652
	MP+	234.619	237.387	238.102	238.880
	MP++	216.974	212.628	213.327	213.381
G-R	HF	275.301	283.094	283.219	283.352
	HF+	234.449	243.950	245.450	246.322
	HF++	216.616	226.826	227.968	228.388
	DFT	124.585	125.457	125.841	125.244
	DFT+	119.804	120.827	121.247	120.978
	DFT++	119.709	120.764	121.674	120.908
	MP	272.928	272.797	272.803	272.652
	MP+	234.619	237.387	238.102	260.880
	MP++	216.974	212.628	213.327	213.381
G-S	HF	281.400	282.549	282.987	283.307
	HF+	241.904	244.929	245.802	246.416
	HF++	224.385	227.296	228.187	228.388
	DFT	121.441	122.753	123.110	124.027
	DFT+	116.691	118.147	118.706	120.167
	DFT++	116.798	118.235	118.756	120.162
	MP	272.100	272.414	272.545	273.010
	MP+	234.613	237.392	238.090	238.691
	MP++	216.967	219.628	220.362	220.526
n-A	HF	234.613	229.191	227.547	225.683
	HF+	227.622	222.019	220.206	218.065

© University of Venda

University of Venda
Creating Future Leaders

	HF++	218.454	221.724	219.955	217.859
	DFT	91.666	86.671	85.134	83.1709
	DFT+	87.769	81.958	80.114	77.754
	DFT++	87.763	81.965	80.126	77.754
	MP	228.212	223.167	221.712	220.206
	MP+	222.050	216.879	215.348	213.616
	MP++	220.858	216.810	215.304	213.573
n-B1	HF	224.623	221.422	220.526	219.778
	HF+	219.170	215.637	214.727	213.591
	HF++	213.340	215.298	214.438	213.315
	DFT	75.188	72.302	71.548	70.940
	DFT+	72.521	69.083	68.141	67.212
	DFT++	75.188	69.032	68.065	67.174
	MP	210.516	207.266	206.475	206.036
	MP+	205.220	201.857	201.022	200.332
	MP++	205.132	201.794	200.960	200.270
n-B2	HF	238.008	232.761	230.930	228.701
	HF+	225.859	226.393	224.290	221.667
	HF++	211.351	216.497	218.304	217.695
	DFT	87.380	82.140	80.427	78.212
	DFT+	84.431	77.861	75.759	72.985
	DFT++	84.293	77.792	75.683	72.917
	MP	228.940	223.192	221.272	218.988
	MP+	221.774	216.158	214.131	211.590
	MP++	208.521	214.470	213.848	211.376

© University of Venda

Table 4.15. Shapes of the frontier orbitals (LUMO and HOMO) and close-to-HOMO molecular orbitals (HOMO-1, HOMO-2, and HOMO-3) for the calculated compounds *in vacuo*, from the results of different calculation methods.

Structure. conformer and MO						
A	HF	HF+	DFT	DFT+	MP	MP+
LUMO	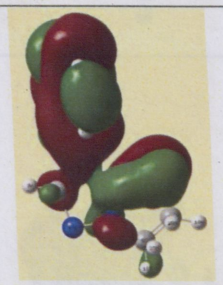	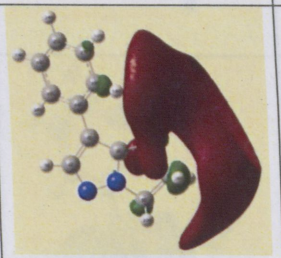	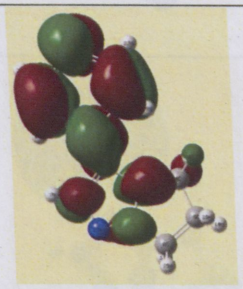	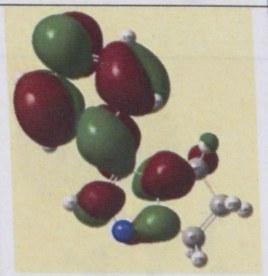	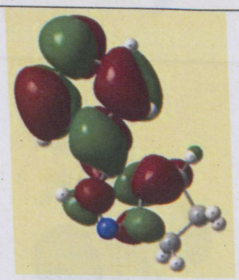	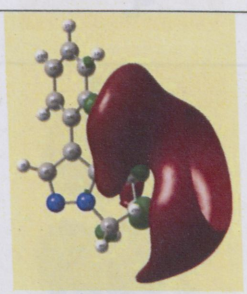
HOMO	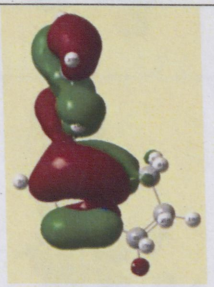			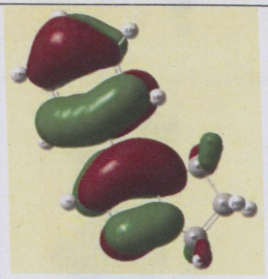	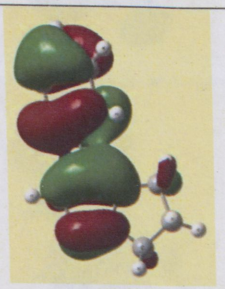	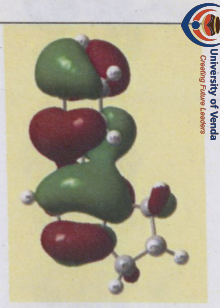

© University of Venda

University of Venda
Creating Future Leaders

© University of Venda

University of Venda
Creating Future Leaders

© University of Venda

University of Venda
Creating Future Leaders

© University of Venda

University of Venda
Creating Future Leaders

© University of Venda

University of Venda
Creating Future Leaders

	E						
LUMO							
HOMO							
HOMO-1							

© University of Venda

University of Venda
Creating Future Leaders

© University of Venda

University of Venda
Creating Future Leaders

HOMO						
HOMO-1						
HOMO-2						
HOMO-3						

© University of Venda

LIBRARY

University of Venda
Creating Future Leaders

	G					
LUMO						
HOMO						
HOMO-1						

© University of Venda

University of Venda
Creating Future Leaders

© University of Venda

University of Venda
Creating Future Leaders

© University of Venda

University of Venda
Creating Future Leaders

© University of Venda

University of Venda
Creating Future Leaders

© University of Venda

University of Venda
Creating Future Leaders

© University of Venda

University of Venda
Creating Future Leaders

© University of Venda

University of Venda
Creating Future Leaders

Table4.16. Shapes of the frontier orbitals (HOMO and LUMO) and close-to-HOMO molecular orbitals (HOMO-1, HOMO-2, and HOMO-3) for the calculated compounds in different media. HF/6-31G (d,p) results.

Structure, conformer and MO's				
A	*in vacuo*	in chloroform	in acetonitrile	in water
LUMO			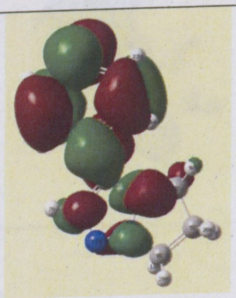	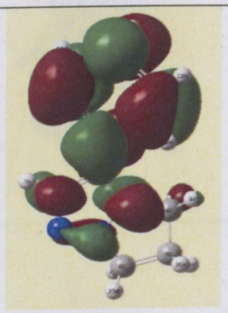
HOMO	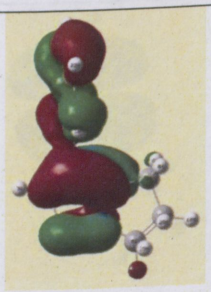	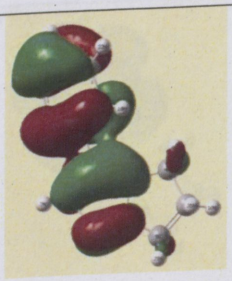		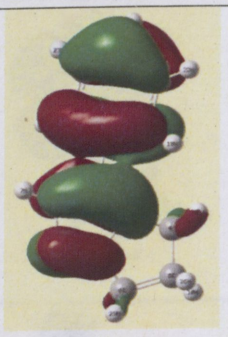
HOMO-1	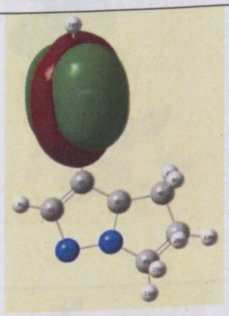	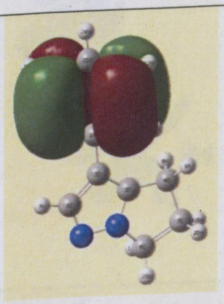	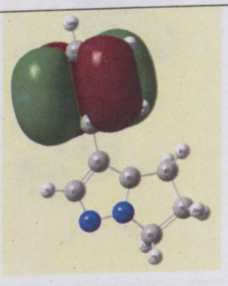	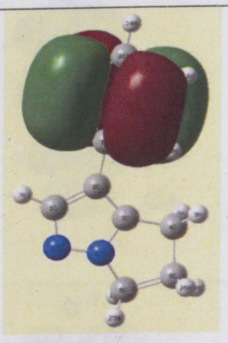

© University of Venda

University of Venda
Creating Future Leaders

HOMO-2	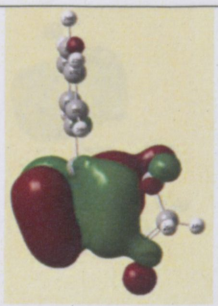		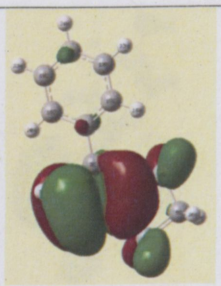	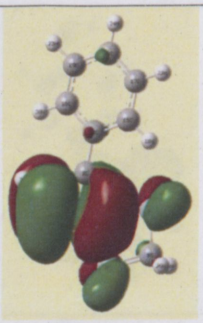
HOMO-3	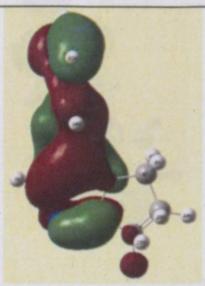			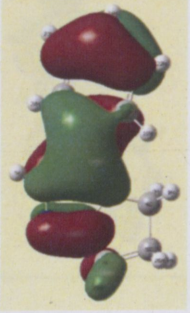
B				
LUMO	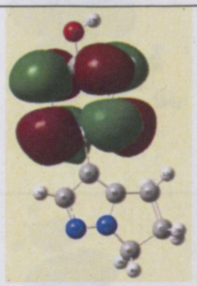	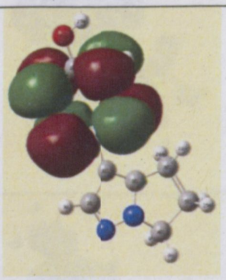	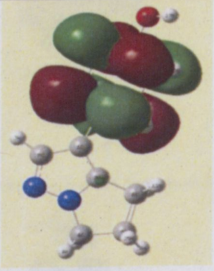	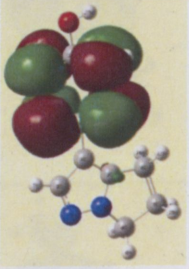
HOMO	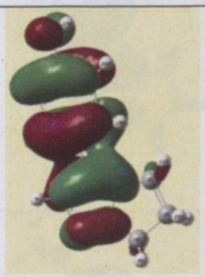	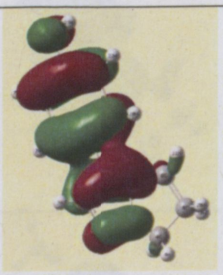	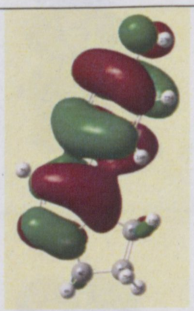	
HOMO-1	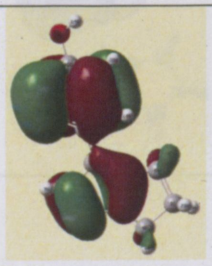	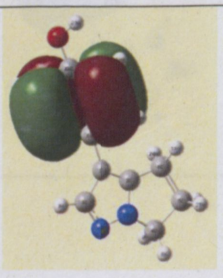	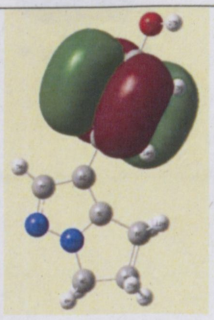	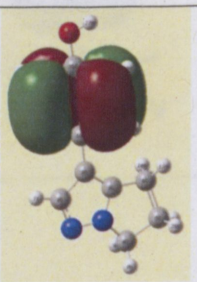

© University of Venda

University of Venda
Creating Future Leaders

HOMO-2	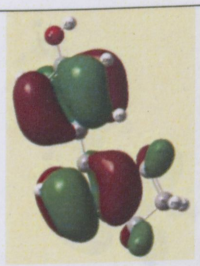	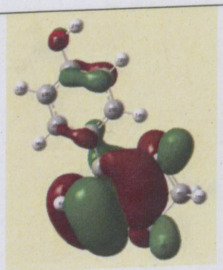		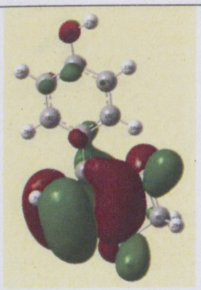
HOMO-3	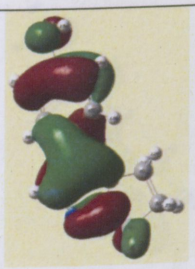	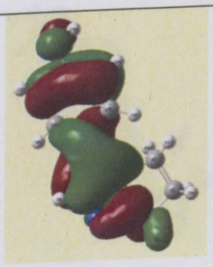	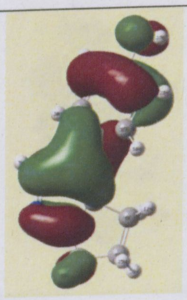	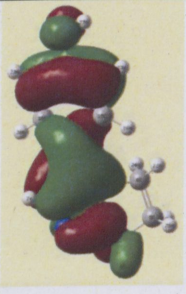
D				
LUMO		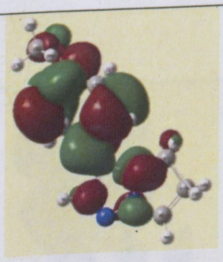	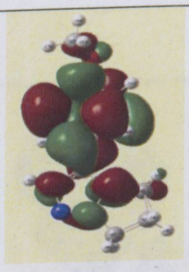	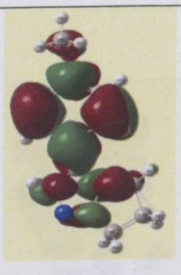
HOMO	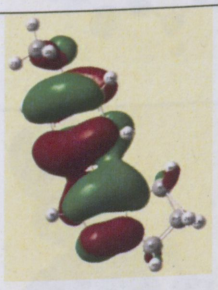	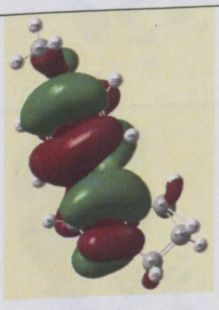	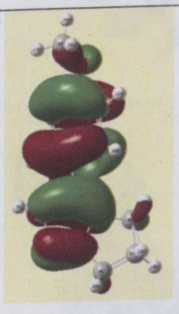	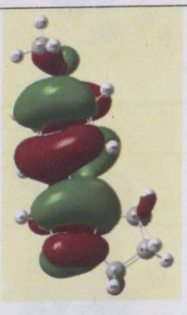
HOMO-1	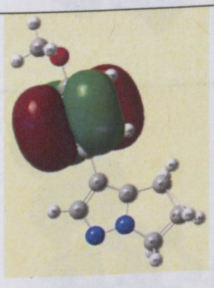	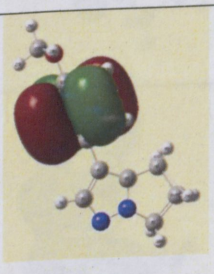	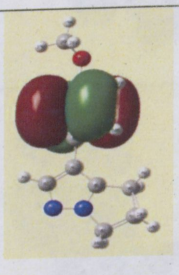	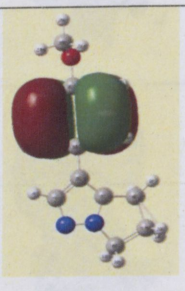

© University of Venda

University of Venda
Creating Future Leaders

HOMO-2	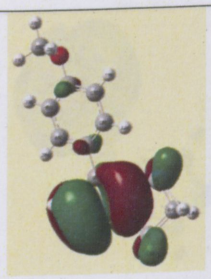	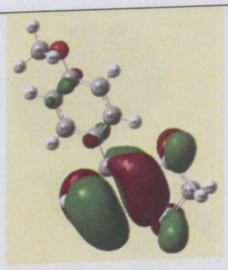		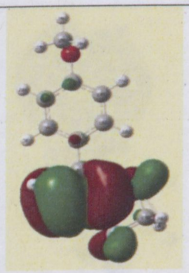
HOMO-3	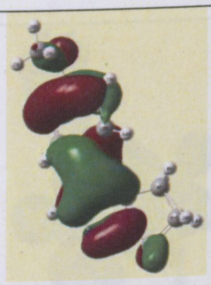	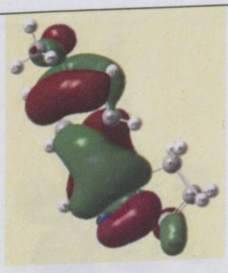		
E				
LUMO	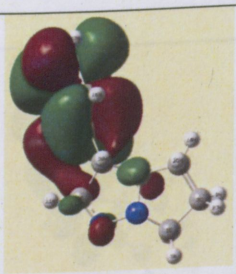	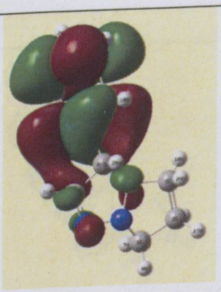	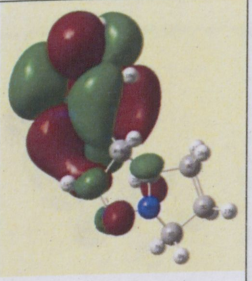	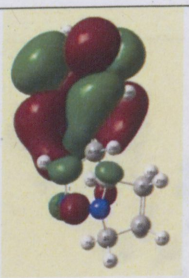
HOMO	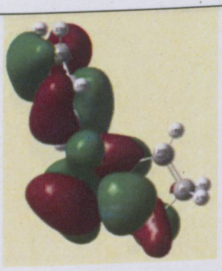	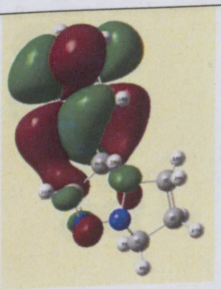	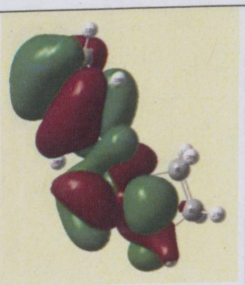	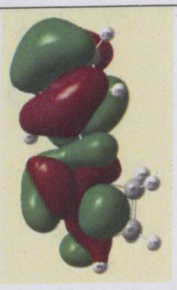
HOMO-1	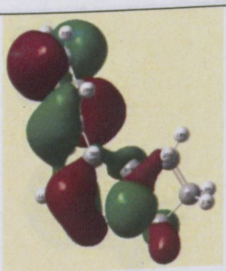	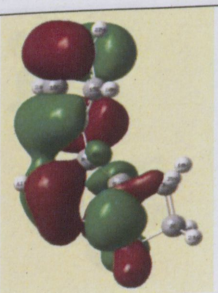	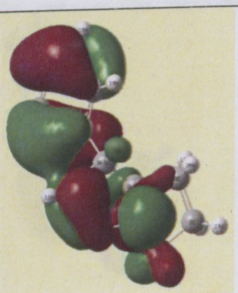	

© University of Venda

University of Venda
Creating Future Leaders

HOMO-2	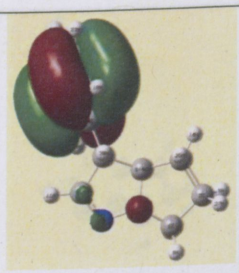	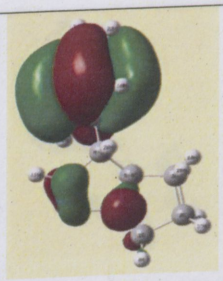	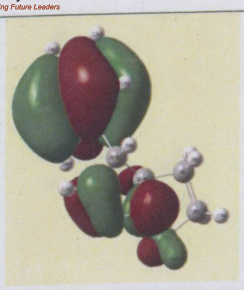	
HOMO-3	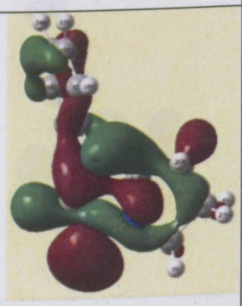	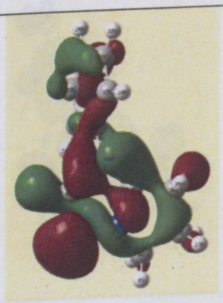	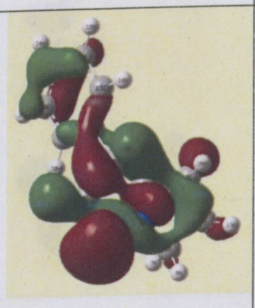	
F				
LUMO	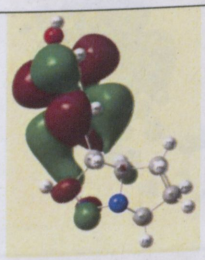	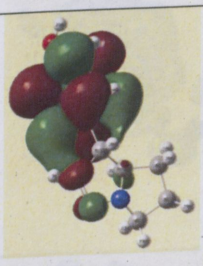	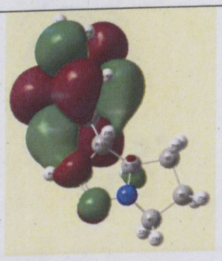	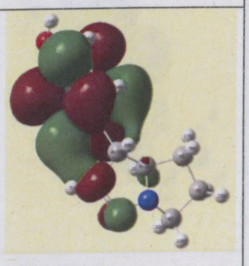
HOMO	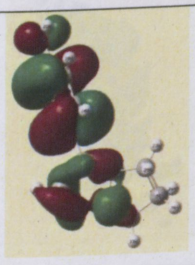	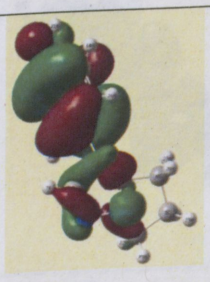	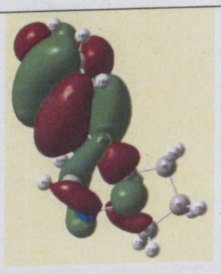	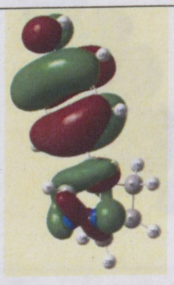
HOMO-1	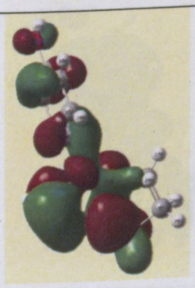		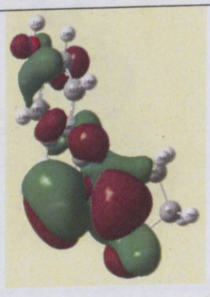	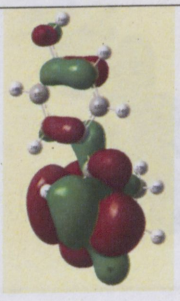

© University of Venda

University of Venda
Creating Future Leaders

HOMO-2	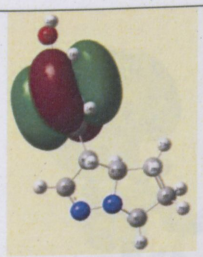	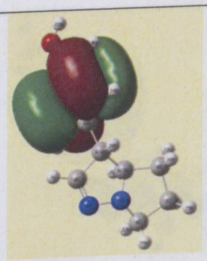	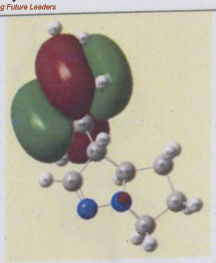	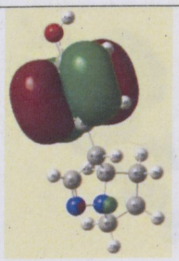
HOMO-3		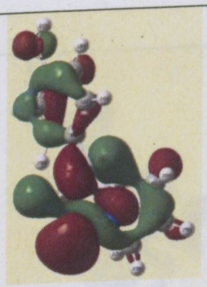	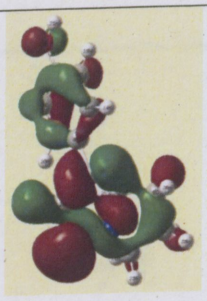	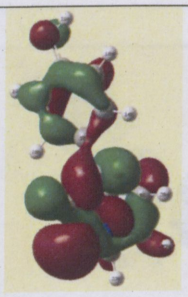
G				
LUMO	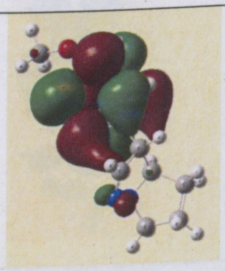	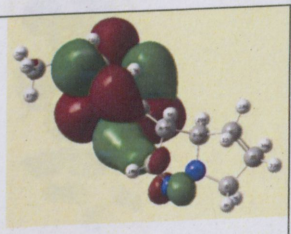	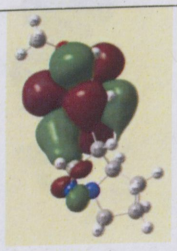	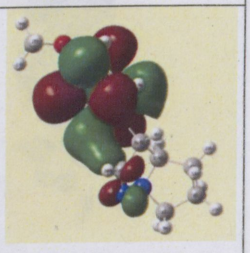
HOMO	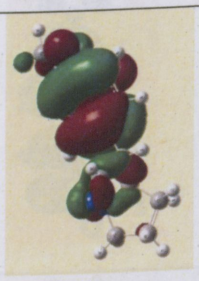	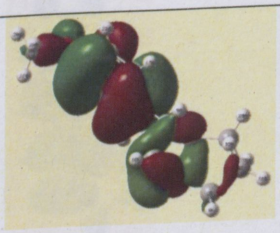	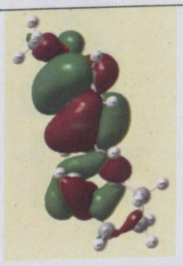	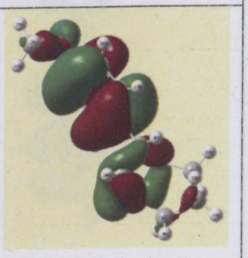
HOMO-1		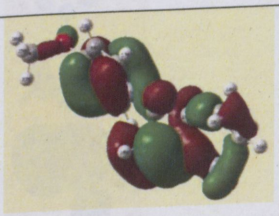	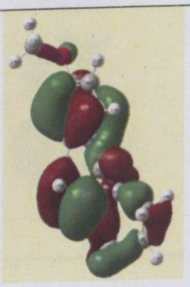	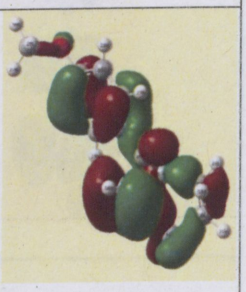

© University of Venda

University of Venda
Creating Future Leaders

HOMO-2	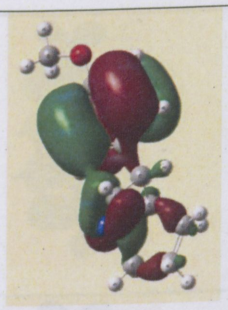	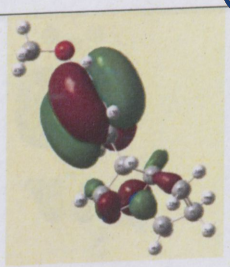	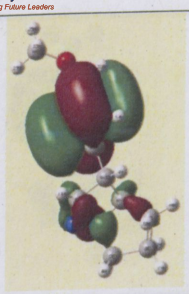	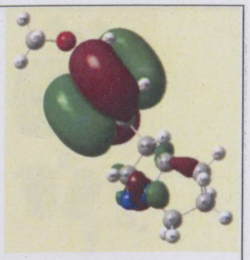
HOMO-3		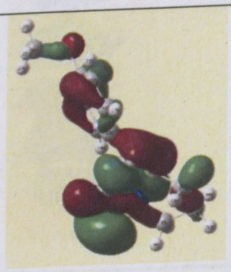		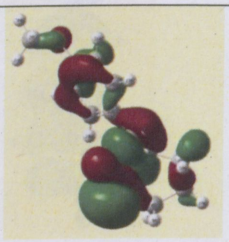
n-A				
LUMO		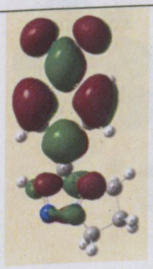	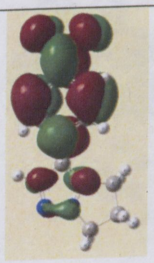	
HOMO				
HOMO-1	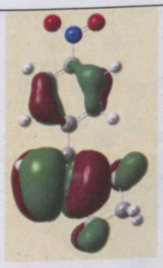			

© University of Venda

University of Venda
Creating Future Leaders

HOMO-2	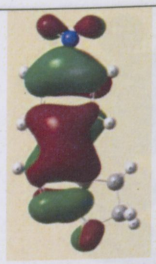			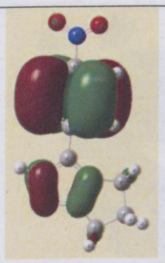
HOMO-3		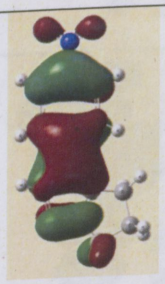	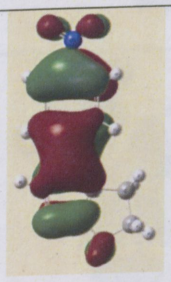	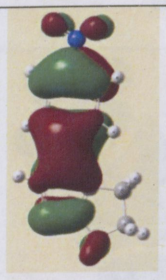
n-B1				
LUMO	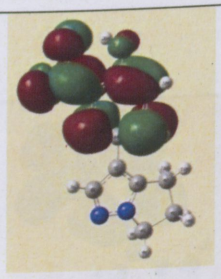	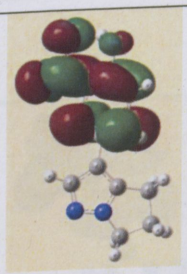	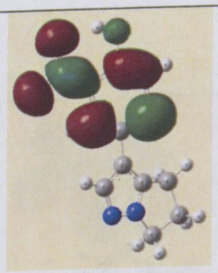	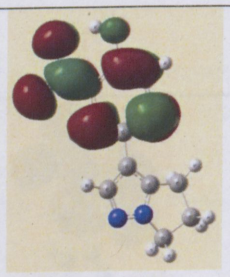
HOMO			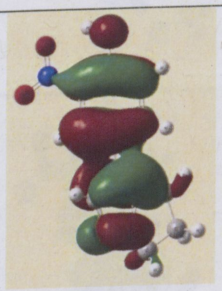	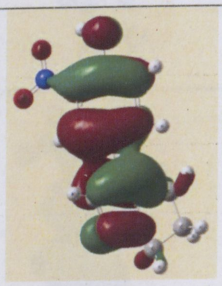
HOMO-1	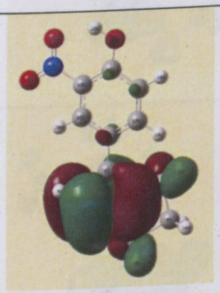		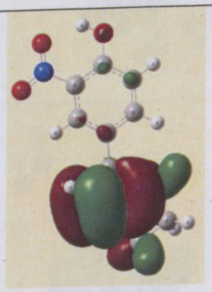	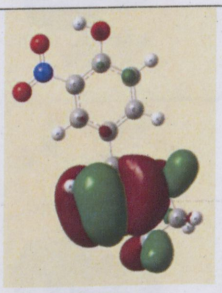

© University of Venda

University of Venda
Creating Future Leaders

HOMO-2	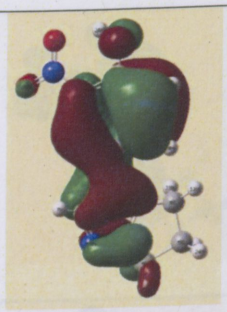	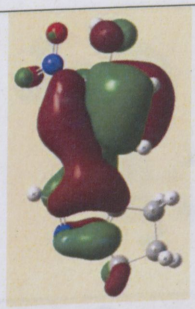	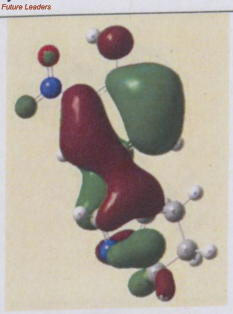	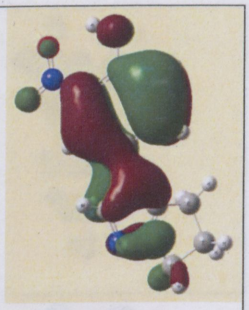
HOMO-3	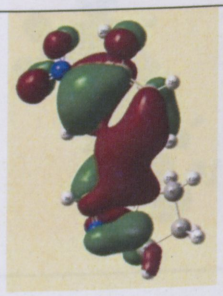	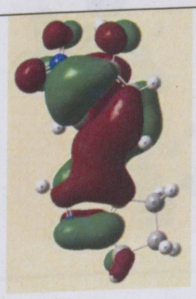	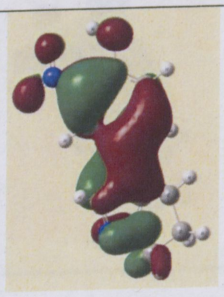	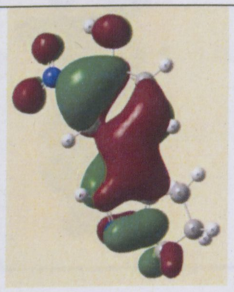
n-B2				
LUMO	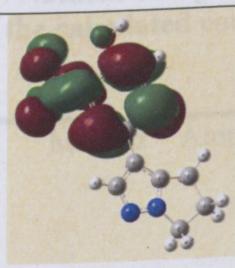	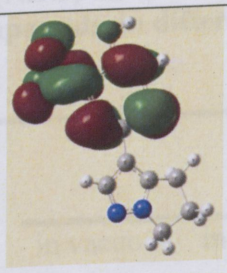	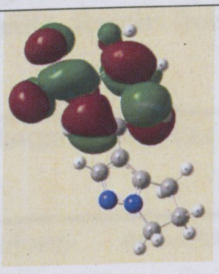	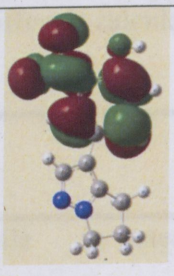
HOMO	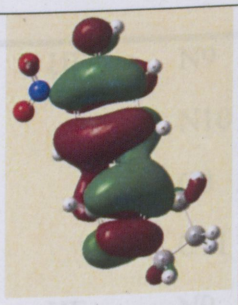	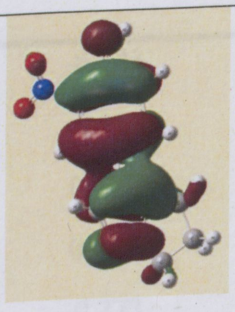	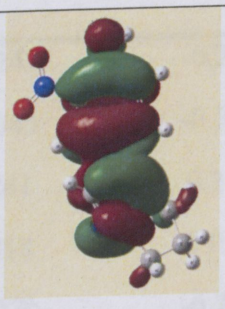	
HOMO-1	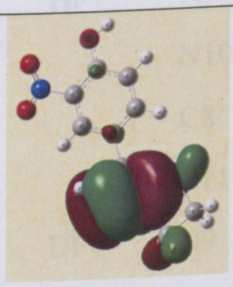	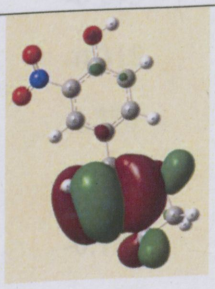	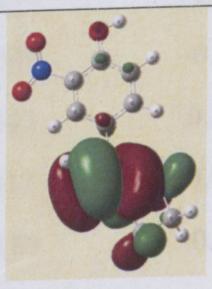	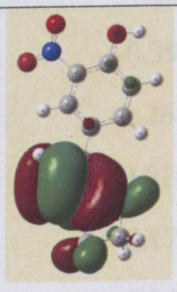

© University of Venda

University of Venda
Creating Future Leaders

HOMO-2	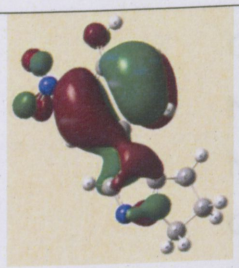	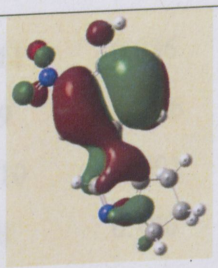	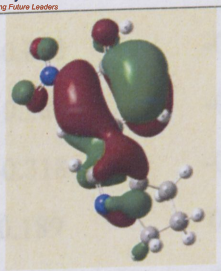	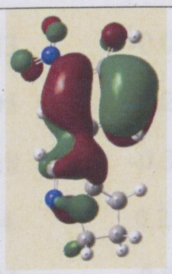
HOMO-3	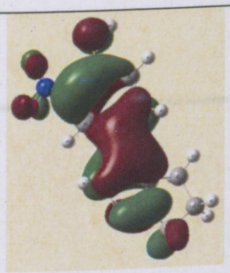	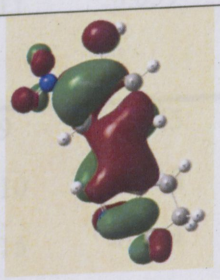	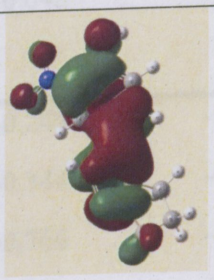	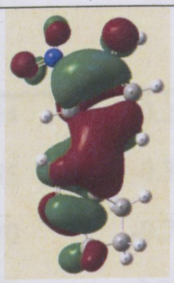

Table 4.17. Natural charges (NBO) on the electronegative atoms and the atoms adjacent to them in the calculated compounds, in different media. Results from different calculation methods.

Compound	Method	Atom	Natural charge (a.u.)			
			in vacuo	in chloroform	in acetonitrile	in water
A	HF	N9	-0.243	-0.243	-0.243	-0.242
		N10	-0.318	-0.343	-0.354	-0.382
		C8	0.231	0.241	0.244	0.253
		C11	0.019	0.018	0.017	0.018
	HF+	N9	-0.273	-0.270	-0.270	-0.268
		N10	-0.318	-0.349	-0.361	-0.391
		C8	0.236	0.247	0.252	0.261
		C11	0.018	0.017	0.017	0.018
	DFT	N9	-0.182	-0.180	-0.179	-0.172
		N10	-0.288	-0.309	-0.317	-0.343
		C8	0.180	0.188	0.191	0.192

© University of Venda

University of Venda
Creating Future Leaders

		C11	0.036	-0.041	-0.043	-0.044
	DFT+	N9	-0.206	-0.204	-0.205	-0.203
		N10	-0.291	-0.318	-0.328	-0.354
		C8	0.180	0.189	0.194	0.200
		C11	0.039	-0.043	-0.044	-0.050
B	HF	N9	-0.245	-0.244	-0.244	-0.244
		N10	-0.318	-0.344	-0.355	-0.376
		O15	-0.754	-0.766	-0.770	-0.791
		C1	0.384	0.381	0.380	0.378
		C8	0.225	0.235	0.238	0.243
		C11	0.015	0.014	0.013	0.012
	HF+	N9	-0.273	-0.271	-0.271	-0.269
		N10	-0.319	-0.350	-0.363	-0.393
		O15	-0.763	-0.776	-0.781	-0.800
		C1	0.366	0.363	0.362	0.360
		C8	0.229	0.241	0.245	0.254
		C11	0.014	0.013	0.012	0.012
	DFT	N9	-0.182	-0.181	-0.180	-0.173
		N10	-0.289	-0.311	-0.321	-0.345
		O15	-0.693	-0.703	-0.707	-0.716
		C1	0.321	0.319	0.319	0.318
		C8	0.174	0.181	0.184	0.186
		C11	-0.040	-0.046	-0.048	-0.049
	DFT+	N9	-0.207	-0.207	-0.206	-0.204
		N10	-0.292	-0.320	-0.332	-0.357
		O15	-0.712	-0.725	-0.731	-0.750
		C1	0.301	0.300	0.299	0.297
		C8	0.173	0.184	0.187	0.193

© University of Venda

University of Venda
Creating Future Leaders

		C11	-0.043	-0.048	-0.050	-0.056
D	HF	N9	-0.245	-0.243	-0.243	-0.243
		N10	-0.318	-0.343	-0.354	-0.375
		O15	-0.630	-0.637	-0.640	-0.647
		C1	0.337	0.332	0.331	0.325
		C8	0.229	0.239	0.242	0.248
		C11	0.017	0.016	0.016	0.015
		C27	-0.228	-0.230	-0.232	-0.234
	HF+	N9	-0.273	-0.271	-0.270	-0.268
		N10	-0.318	-0.351	-0.362	-0.391
		O15	-0.650	-0.633	-0.662	-0.670
		C1	0.333	0.373	0.327	0.322
		C8	0.233	0.241	0.249	0.258
		C11	0.016	0.013	0.015	0.016
		C27	-0.230	-0.245	-0.235	-0.241
	DFT	N9	-0.183	-0.243	-0.180	-0.172
		N10	-0.289	-0.343	-0.320	-0.343
		O15	-0.521	-0.637	-0.528	-0.575
		C1	0.313	0.332	0.310	0.289
		C8	0.175	0.239	0.184	0.191
		C11	-0.040	0.016	-0.047	-0.045
		C27	-0.327	-0.230	-0.332	-0.314
	DFT+	N9	-0.208	-0.207	-0.206	-0.204
		N10	-0.292	-0.320	-0.332	-0.356
		O15	-0.541	-0.546	-0.548	-0.557
		C1	0.308	0.306	0.305	0.302
		C8	0.174	0.184	0.187	0.194
		C11	-0.043	-0.048	-0.049	0.055

© University of Venda

University of Venda
Creating Future Leaders

		C27	-0.335	-0.339	-0.340	-0.346
E	HF	N9	-0.395	-0.397	-0.396	-0.324
		N10	-0.251	-0.278	-0.295	-0.408
		C8	-0.023	-0.024	-0.038	-0.033
		C11	0.062	0.075	0.091	0.098
	HF+	N9	-0.434	-0.436	-0.439	-0.448
		N10	-0.244	-0.275	-0.289	-0.325
		C8	-0.021	-0.024	-0.025	-0.034
		C11	0.068	0.082	0.089	0.106
	DFT	N9	-0.319	-0.323	-0.324	0.335
		N10	-0.230	-0.251	-0.265	-0.288
		C8	-0.060	-0.061	-0.072	-0.069
		C11	0.000	0.006	0.021	0.018
	DFT+	N9	-0.356	-0.361	-0.364	-0.374
		N10	-0.224	-0.251	-0.263	-0.293
		C8	-0.062	-0.063	-0.064	-0.073
		C11	0.004	0.013	0.017	0.027
F	HF	N9	-0.388	-0.398	-0.400	-0.409
		N10	-0.267	-0.280	-0.292	-0.326
		O15	-0.753	-0.764	-0.769	-0.034
		C1	0.389	0.387	0.386	0.098
		C8	-0.038	-0.024	-0.025	-0.787
		C11	0.066	0.076	0.082	0.382
	HF+	N9	-0.426	-0.437	-0.440	-0.449
		N10	-0.258	-0.277	-0.291	-0.27
		O15	-0.760	-0.774	-0.760	-0.800
		C1	0.372	0.370	0.369	0.365

© University of Venda

University of Venda
Creating Future Leaders

		C8	-0.037	-0.024	-0.025	-0.035
		C11	0.067	0.082	0.089	0.107
	DFT	N9	-0.320	-0.323	-0.326	-0.336
		N10	-0.231	-0.253	-0.263	-0.291
		O15	-0.692	-0.702	-0.707	-0.723
		C1	0.25	0.324	0.323	0.319
		C8	-0.060	-0.061	-0.061	-0.070
		C11	0.000	0.006	0.010	0.019
	DFT+	N9	-0.357	-0.362	-0.367	-0.376
		N10	-0.226	-0.252	-0.267	-0.296
		O15	-0.711	-0.724	-0.732	-0.750
		C1	0.306	0.305	0.304	0.300
		C8	0.062	-0.063	-0.066	-0.074
		C11	0.005	0.013	0.020	0.028
G	HF	N9	-0.384	-0.398	-0.398	-0.409
		N10	-0.281	-0.302	-0.300	-0.331
		O15	-0.606	-0.641	-0.640	-0.648
		C1	0.382	0.336	0.337	0.331
		C8	-0.041	-0.040	-0.040	-0.048
		C11	0.074	0.082	0.080	0.099
		C29	-0.240	-0.232	-0.232	-0.237
	HF+	N9	-0.434	-0.398	-0.434	-0.409
		N10	-0.246	-0.302	-0.295	-0.331
		O15	-0.626	-0.641	-0.661	-0.648
		C1	0.382	0.336	0.334	0.331
		C8	-0.021	-0.040	-0.039	-0.048
		C11	0.068	0.082	0.087	0.099
		C29	-0.242	-0.232	-0.235	-0.237

© University of Venda

University of Venda
Creating Future Leaders

	DFT	N9	-0.319	-0.332	-0.326	-0.345
		N10	-0.231	-0.270	-0.262	-0.300
		O15	-0.521	-0.526	-0.528	-0.536
		C1	0.318	0.315	0.315	0.309
		C8	-0.060	-0.077	-0.061	-0.086
		C11	0.000	0.022	0.010	0.028
		C29	-0.328	-0.331	-0.333	-0.338
	DFT+	N9	-0.357	-0.362	-0.365	-0.375
		N10	-0.227	-0.253	-0.265	-0.294
		O15	-0.540	-0.545	-0.548	-0.557
		C1	0.313	0.311	0.310	0.305
		C8	-0.062	-0.063	-0.064	-0.075
		C11	0.005	0.013	0.018	0.027
		C29	-0.335	-0.339	-0.340	-0.346
n-A	HF	N9	-0.241	-0.240	-0.466	-0.465
		N10	-0.312	-0.349	-0.349	-0.384
		O15	-0.470	-0.490	-0.494	-0.505
		N28	0.663	0.675	0.522	0.529
		C1	0.015	0.004	0.112	0.116
		C8	0.247	0.265	0.378	0.382
		C11	0.027	0.031	0.119	0.112
	HF+	N9	-0.268	-0.266	-0.266	-0.265
		N10	-0.312	-0.340	-0.352	-0.382
		O15	-0.466	-0.478	-0.483	-0.493
		N28	0.646	0.651	0.652	0.659
		C1	0.017	0.007	0.004	0.002
		C8	0.252	0.268	0.274	0.284
		C11	0.027	0.030	0.032	0.034

© University of Venda

University of Venda
Creating Future Leaders

	DFT	N9	-0.178	-0.175	-0.174	-0.173
		N10	-0.280	-0.298	-0.306	-0.330
		O15	-0.392	-0.407	-0.412	-0.421
		N28	0.510	0.511	0.510	0.514
		C1	0.045	0.040	0.039	0.038
		C8	0.196	0.207	0.211	0.218
		C11	-0.026	-0.028	-0.029	-0.031
	DFT+	N9	-0.201	-0.198	-0.201	-0.199
		N10	-0.281	-0.305	-0.315	-0.340
		O15	-0.392	-0.410	-0.417	-0.490
		N28	0.490	0.490	0.490	0.494
		C1	0.048	0.043	0.041	0.041
		C8	0.196	0.211	0.233	0.240
		C11	-0.028	-0.028	-0.029	-0.031
n-B1	HF	N9	-0.242	-0.240	-0.241	-0.240
		N10	-0.312	-0.375	-0.349	-0.378
		O15	-0.751	-0.759	-0.754	-0.760
		O29	-0.522	-0.531	-0.528	-0.529
		O30	-0.437	-0.462	-0.454	-0.467
		N28	0.670	0.681	0.675	0.680
		C1	0.448	0.450	0.449	0.450
		C6	-0.064	-0.064	-0.065	-0.063
		C8	0.230	0.252	0.246	0.253
		C11	0.019	0.018	0.018	0.018
	HF+	N9	-0.270	-0.268	-0.267	-0.266
		N10	-0.313	-0.344	-0.357	-0.387
		O15	-0.762	-0.765	-0.762	-0.769
		O29	-0.518	-0.523	-0.524	-0.525

© University of Venda

University of Venda
Creating Future Leaders

		O30	-0.434	-0.448	-0.453	-0.468
		N28	0.655	0.658	0.660	0.665
		C1	0.439	0.440	0.438	0.439
		C6	-0.057	-0.058	-0.058	-0.055
		C8	0.234	0.247	0.252	0.261
		C11	0.017	0.017	0.017	0.018
	DFT	N9	-0.179	-0.177	-0.177	-0.176
		N10	-0.281	-0.304	-0.311	-0.336
		O15	-0.676	-0.679	-0.679	-0.684
		O29	-0.444	-0.448	-0.453	-0.457
		O30	-0.362	-0.379	-0.381	-0.393
		N28	0.513	0.514	0.514	0.517
		C1	0.360	0.361	0.362	0.362
		C6	-0.013	-0.012	-0.011	-0.008
		C8	0.179	0.191	0.192	0.198
		C11	-0.035	-0.038	-0.041	-0.044
	DFT+	N9	-0.203	-0.201	-0.201	-0.199
		N10	-0.283	-0.310	-0.321	-0.348
		O15	-0.689	-0.692	-0.693	-0.699
		O29	-0.444	-0.454	-0.457	-0.461
		O30	-0.364	-0.380	-0.387	-0.402
		N28	0.495	0.495	0.495	0.499
		C1	0.348	0.350	0.351	0.353
		C6	-0.004	-0.002	-0.001	0.003
		C8	0.179	0.191	0.196	0.202
		C11	-0.037	-0.041	-0.042	-0.046
n-B2	HF	N9	-0.242	-0.241	-0.241	-0.240
		N10	-0.312	-0.375	-0.350	-0.378

© University of Venda

University of Venda
Creating Future Leaders

	O15	-0.725	-0.756	-0.742	-0.758
	O29	-0.432	-0.464	-0.454	-0.466
	O30	-0.479	-0.500	-0.494	-0.501
	N28	0.661	0.675	0.668	0.674
	C1	0.421	0.428	0.428	0.432
	C6	-0.013	-0.031	-0.028	-0.032
	C8	0.231	0.252	0.246	0.253
	C11	0.019	0.018	0.018	0.018
HF+	N9	-0.270	-0.268	-0.268	-0.267
	N10	-0.313	-0.344	-0.355	-0.388
	O15	-0.732	-0.745	-0.748	-0.768
	O29	-0.426	-0.444	-0.451	-0.464
	O30	-0.473	-0.485	-0.492	-0.498
	N28	0.643	0.649	0.652	0.659
	C1	0.404	0.410	0.415	0.418
	C6	-0.002	-0.014	-0.021	-0.024
	C8	0.234	0.247	0.252	0.261
	C11	0.017	0.017	0.017	0.017
DFT	N9	-0.179	-0.177	-0.177	-0.179
	N10	-0.282	-0.303	-0.312	-0.336
	O15	-0.654	-0.663	-0.667	-0.681
	O29	-0.362	-0.381	-0.388	-0.401
	O30	-0.399	-0.413	-0.419	-0.429
	N28	0.511	0.512	0.512	0.515
	C1	0.343	0.348	0.350	0.354
	C6	0.014	0.009	0.007	0.005
	C8	0.179	0.188	0.192	0.196
	C11	-0.034	-0.040	-0.042	-0.046
DFT+	N9	-0.203	-0.201	-0.201	-0.200

© University of Venda

University of Venda
Creating Future Leaders

N10	-0.284	-0.311	-0.323	-0.349
O15	-0.672	-0.685	-0.686	-0.701
O29	-0.357	-0.378	-0.387	-0.403
O30	-0.393	-0.412	-0.420	-0.432
N28	0.493	0.495	0.495	0.496
C1	0.325	0.332	0.335	0.341
C6	0.026	0.019	0.016	0.014
C8	0.179	0.190	0.195	0.200
C11	-0.037	-0.041	-0.043	-0.048

© University of Venda

University of Venda
Creating Future Leaders

Table 4.18. Solvent effect (ΔG_{solv}) and its electrostatic component (G_{el}) for the calculated compounds in the three solvents considered. Results from different calculation methods.

compound	method	ΔG_{solv} (kcal/mol)			G_{el} (kcal/mol)		
		in chloroform	in acetonitrile	in water	in chloroform	in acetonitrile	in water
A	HF	-3.54	-0.71	-8.49	-3.55	-5.00	-10.27
	HF+	-3.94	-1.29	-9.36	-3.55	-5.60	-11.17
	HF++	-3.94	-1.29	-9.35	-3.97	-5.61	-11.16
	DF	-3.03	0.02	-7.13	-3.05	-4.30	-8.99
	DF+	-3.56	-0.78	-8.36	-3.61	-5.12	-10.25
	DF++	-3.56	-0.73	-8.34	-3.61	-5.08	-10.24
	MP	-3.59	-0.78	-8.77	-3.73	-5.23	-10.76
	MP+	-3.92	-1.30	-9.60	-4.15	-5.85	-11.71
	MP++	-3.94	-1.33	-9.63	-4.16	-5.87	-11.72
B	HF	-5.46	-3.21	-14.19	-5.41	-7.64	-15.91
	HF+	-5.94	-3.93	-15.34	-5.93	-8.40	-17.11
	HF++	-5.94	-3.93	-15.33	-5.92	-8.40	-17.10
	DF	-4.80	-2.29	-12.64	-4.78	-6.78	-14.49

© University of Venda

University of Venda
Creating Future Leaders

	DF+	-5.50	-3.32	-14.37	-5.51	-7.86	-16.28
	DF++	-5.49	-3.31	-14.38	-5.51	-7.85	-16.28
	MP	-5.62	-3.47	-14.92	-5.68	-8.05	-16.85
	MP+	-6.05	-4.16	-16.11	-6.22	-8.86	-18.20
	MP++	-6.09	-4.17	-16.11	- 6.25	-8.86	-18.19
D	HF	-3.86	-0.72	-9.85	-4.20	-5.91	-12.17
	HF+	-4.30	-1.37	-10.87	-4.68	-6.60	-13.24
	HF++	-4.31	-1.37	-10.86	-4.68	-6.60	-13.22
	DF	-3.44	-0.03	-8.52	-3.58	-5.03	-10.62
	DF+	-4.04	-0.91	-9.97	-4.23	-5.97	-12.11
	DF++	-4.04	-0.90	-9.96	-4.22	-5.96	-12.10
	MP	-4.20	-1.23	-10.69	-4.41	-6.30	-12.88
	MP+	-4.57	-1.84	-11.70	-4.90	-6.95	-13.94
	MP++	-3.56	-1.87	-11.71	-3.61	-6.97	-13.94
E	HF	-2.58	0.63	-8.64	-2.81	-4.06	-11.00
	HF+	-2.93	0.10	-9.73	-3.17	-4.61	-12.13

LIBRARY

© University of Venda

University of Venda
Creating Future Leaders

	HF++	-2.93	0.11	-9.71	-3.17	-4.61	-12.11
	DF	-1.90	1.60	-7.26	-2.28	-3.30	-9.94
	DF+	-2.37	0.86	-8.97	-2.78	-4.07	-11.71
	DF++	-2.36	0.87	-8.97	-2.77	-4.06	-11.70
	MP	-2.69	0.43	-9.51	-3.00	-4.38	-12.07
	MP+	-3.05	-0.14	-10.87	-3.40	-4.99	-13.51
	MP++	-3.05	-0.14	-10.85	-3.40	-4.99	-13.50
E-a	HF	-2.84	0.32	-9.23	-2.97	-4.30	-11.56
	HF+	-2.93	0.10	-10.40	-3.17	-4.61	-12.77
	HF++	-2.92	-0.25	-10.39	-3.17	-4.90	-12.76
	DF	-1.90	1.35	-7.97	-2.28	-3.51	-10.65
	DF+	-2.37	0.86	-9.81	-2.78	-4.07	-12.55
	DF++	-2.36	0.87	-9.80	-2.77	-4.06	-12.54
	MP	-2.69	-0.43	-9.51	-3.00	-4.37	-12.06
	MP+	-3.05	-0.13	-10.86	-3.40	-4.99	-13.50
	MP++	-3.05	-0.14	-10.85	-3.39	-4.99	-13.49

© University of Venda

University of Venda
Creating Future Leaders

F	HF	-4.52	-1.93	-14.58	-4.64	-6.71	-16.83
	HF+	-4.95	-2.60	-16.01	-5.09	-7.41	-18.30
	HF++	-4.94	-2.59	-15.99	-5.08	-7.40	-18.28
	DF	-3.66	-0.71	-13.01	-3.97	-5.74	-15.63
	DF+	-4.32	-1.73	-15.31	-4.65	-6.79	-18.01
	DF++	-4.32	-1.72	-15.29	-4.65	-6.78	-17.99
	MP	-4.72	-2.21	-15.95	-4.96	-7.14	-18.47
	MP+	-5.20	-2.95	-17.84	-5.48	-7.94	-20.45
	MP++	-5.17	-2.96	-17.81	-5.44	-7.94	-20.42
F-a	HF	-4.80	-1.91	-14.58	-4.82	-6.69	-16.83
	HF+	-4.95	-2.61	-16.01	-5.09	-7.41	-18.30
	HF++	-4.94	-2.59	-15.99	-5.08	-7.40	-18.28
	DF	-3.65	-0.69	12.97	-3.95	-5.71	-15.60
	DF+	4.32	-1.73	-15.26	-4.65	-6.79	-17.96
	DF++	-4.32	-1.72	-15.24	-4.65	-6.78	-17.94
	MP	-4.72	-2.20	-15.92	-4.95	-7.13	-18.43
	MP+	-5.18	-2.95	-17.80	-5.46	-7.93	-20.41

© University of Venda

University of Venda
Creating Future Leaders

	MP++	-5.15	-2.93	-17.78	-5.42	-7.92	-20.38
G	HF	-2.89	0.15	-11.14	-3.44	-5.24	-13.78
	HF+	-3.54	-0.38	-12.21	-3.95	-5.81	-14.89
	HF++	-3.53	-0.37	-11.51	-3.94	-5.79	-14.46
	DF	-2.51	1.17	-9.54	-2.83	-4.17	-12.17
	DF+	-3.08	0.35	-11.46	-3.44	-5.05	-14.17
	DF++	-3.07	0.25	-11.41	-3.43	-5.13	-14.12
	MP	-3.28	0.11	-11.43	-3.69	-5.33	-14.18
	MP+	-3.69	-0.53	-12.88	-4.13	-6.02	-15.73
	MP++	-3.68	-0.49	-12.89	-4.12	-5.99	-15.74
G-a	HF	-2.88	0.59	-10.27	-3.42	-4.99	-13.17
	HF+	-3.26	-0.01	-11.51	-3.82	-5.62	-14.46
	HF++	-3.25	0.00	-11.51	-3.81	-5.61	-14.46
	DF	-2.32	1.54	-8.68	-2.79	-4.00	-11.57
	DF+	-2.89	0.65	-10.62	-3.40	-4.93	-13.59
	DF++	-2.89	0.66	-10.61	-3.40	-4.92	-13.57

© University of Venda

University of Venda
Creating Future Leaders

	MP	-3.28	0.10	-11.61	-3.68	-5.33	-14.37
	MP+	-3.70	-0.52	-12.93	-4.13	-6.01	-15.79
	MP++	-3.68	-0.50	-12.78	-4.13	-5.99	-15.62
n-A	HF	-4.51	-1.70	-11.07	-5.42	-7.43	-14.00
	HF+	-5.01	-2.44	-12.20	-5.94	-8.19	-15.14
	HF++	-5.02	-2.45	-12.20	-5.94	-8.19	-15.13
	DF	-3.66	-0.54	-9.10	-4.73	-6.48	-12.30
	DF+	-4.61	-1.89	-11.22	-5.69	-7.86	-14.45
	DF++	-4.60	-1.88	-11.20	-5.68	-7.84	-14.43
	MP	-4.44	-1.64	-11.17	-5.66	-7.74	-14.55
	MP+	-4.95	-2.39	-12.27	-6.18	-8.49	15.65
	MP++	4.95	-2.39	-12.26	-6.18	-8.48	-15.64
n-B1	HF	-3.77	-0.68	-10.68	-4.85	-6.72	-13.73
	HF+	-4.27	-1.39	-11.87	-5.39	-7.47	-14.96
	HF++	-4.27	-1.40	-11.86	-5.39	-7.47	-14.95
	DF	-2.95	0.46	-8.50	-4.12	-5.71	-11.74

© University of Venda

University of Venda
Creating Future Leaders

	DF+	-3.81	-0.78	-10.60	-5.02	-6.99	-13.89
	DF++	-3.80	-0.77	-10.59	-5.01	-6.98	-13.88
	MP	-3.88	-0.86	-11.02	-5.16	-7.13	-14.36
	MP+	-4.40	-1.62	-12.22	-5.69	-7.89	-15.56
	MP++	-4.40	-1.62	-12.20	-5.68	-7.88	-15.54
n-B2	HF	-7.06	-5.34	-18.21	-8.24	-11.51	-21.46
	HF+	-7.58	-6.10	-19.46	-8.82	-12.33	-22.78
	HF++	-7.59	-6.10	-19.45	-8.82	-12.33	-22.77
	DF	-6.00	-3.86	-15.88	-7.19	-10.09	-19.25
	DF+	-7.02	-5.39	-18.42	-8.29	-11.70	-21.86
	DF++	-7.02	-5.40	-18.41	-8.28	-11.69	-21.85
	MP	-7.25	-5.64	-19.00	-8.70	-12.13	-22.68
	MP+	-7.81	-6.47	-20.29	-9.26	-12.96	-23.97
	MP++	-7.81	-6.46	-20.27	-9.26	-12.96	-23.95

© University of Venda

University of Venda
Creating Future Leaders

Table 4.19. Comparison of the geometries of the isolated molecule, of the same molecule in water solution, and when it is the central molecule in an adduct with explicit water molecules. HF/6-31G (d,p) results.

a) Relevant bond lengths for the central molecule

	Where	bond length considered (Å)								
		C3–C4	C4–C5	C4–C7	C7–C8	N9–N10	C11–C7	C1–O15	O15–H27	O15–C27
A	in vacuo	1.394	1.393	1.476	1.421	1.325	1.374	-	-	-
	in water	1.394	1.395	1.477	1.381	1.330	1.416	-	-	-
	A-1aq	1.393	1.394	1.475	1.377	1.326	1.417	-	-	-
	A-3aq	1.393	1.393	1.476	1.379	1.326	1.414	-	-	-
B	in vacuo	1.389	1.396	1.477	1.374	1.325	1.420	1.352	0.943	-
	in water	1.391	1.396	1.478	1.380	1.329	1.416	1.352	0.955	-
	B-4aq	1.393	1.391	1.477	1.376	1.325	1.417	1.352	0.957	-
D	in vacuo	1.393	1.393	1.477	1.374	1.325	1.420	1.364	-	1.405
	in water	1.394	1.395	1.477	1.380	1.329	1.416	1.366	-	1.413
	D-2aq	1.397	1.386	1.476	1.377	1.326	1.417	1.358	-	1.402
E	in vacuo	1.390	1.392	1.512	1.530	1.377	1.532	-	-	-
	in water	1.390	1.393	1.511	1.529	1.388	1.529	-	-	-
	E-1aq	1.387	1.393	1.520	1.542	1.393	1.512	-	-	-

© University of Venda

University of Venda
Creating Future Leaders

	E-2aq	1.388	1.393	1.521	1.544	1.400	1.511	-	-	-
	E-3aq	1.388	1.394	1.521	1.543	1.4018	1.513	-	-	-
F	in vacuo	1.386	1.395	1.511	1.529	1.378	1.533	1.351	0.943	-
	in water	1.388	1.395	1.511	1.529	1.388	1.529	1.350	0.955	
	F-2aq	1.384	1.397	1.520	1.544	1.400	1.511	1.350	0.943	
	F-5aq	1.386	1.395	1.520	1.544	1.401	1.511	1.350	0.957	

© University of Venda

University of Venda
Creating Future Leaders

Table 4.20. Comparison of the parameters of the intramolecular hydrogen bond of the lowest energy conformer of compound n-B (conformer n-B1) in the isolated molecule. in water solution and in adducts with explicit water molecules. HF/6-31G (d,p) results.

where	O···H bond length (Å)	O···O distance (Å)	$\hat{OHO}$ bond angle
in vacuo	1.825	2.601	136.976
in water	1.862	2.618	134.619
n-B-4aq	1.949	2.642	127.799
n-B-5aq	1.957	2.637	126.468

Table 4.21. Bond length of the intermolecular hydrogen bonds in the calculated adducts with explicit water molecules. HF/6-31G (d,p) results.

Adduct	molecule-water H-bonds		water-water H-bonds	
	H-bond	H-bond	H-bond	H-bond
A-1aq	H_{W1}···N10	2.120		
A-3aq	H_{W1}···N9	3.924	H_{W2}···O_{W1}	2.169
	H_{W3}···N10	2.007	H_{W2}···O_{W3}	2.057
B-4aq	H_{W1}···N10	2.124	H_{W2}···O_{W3}	1.890
	H_{W4}···O15	1.994	H_{W3}···O_{W4}	1.903
			H_{27}···O_{W2}	1.836
D-2aq	H_{W1}···N10	2.118		
	H_{W2}···O15	2.103		
E-1aq	H_{W1}···N10	2.147		
E-2aq	H_{W1}···N9	2.395	H_{W1}···O_{W2}	2.174
	H_{W2}···N10	2.045		
E-3aq	H_{W1}···N9	2.052	H_{W2}···O_{W1}	1.981
	H_{W3}···N10	2.446	H_{W3}···O_{W2}	2.039
F-5aq	H_{W1}···N9	2.040	H_{W2}···O_{W1}	2.174
	H_{W2}···N10	2.385	H_{W4}···O_{W3}	1.901
	H_{W3}···O15	2.006	H_{W5}···O_{W4}	1.886
G-4aq	H_{W1}···N10	2.376	H_{W2}···O_{W1}	2.202
	H_{W3}···N9	2.055	H_{W2}···O_{W3}	2.203
	H_{W4}···O15	2.098		

© University of Venda

University of Venda
Creating Future Leaders

n-A-5aq	$H_{W4}\cdots N17$	2.366	$H_{W1}\cdots O_{W2}$	1.944
	$H_{W5}\cdots N18$	2.161	$H_{W2}\cdots O_{W3}$	1.878
			$H_{W3}\cdots O_{W4}$	1.868
			$H_{W4}\cdots O_{W5}$	1.998
n-B-5aq	$O_{W3}\cdots H27$	2.133	$H_{W1}\cdots O_{W2}$	2.064
	$H_{W1}\cdots O15$	2.398	$H_{W2}\cdots O_{W3}$	2.004
	$H_{W5}\cdots N28$	2.149	$H_{W3}\cdots O_{W4}$	1.859
			$H_{W4}\cdots O_{W5}$	1.918

Table 4.22. Comparison of the bulk solvent effect (DG_{solv}) and its electrostatic component (G_{el}) for the calculated adducts with explicit water molecules and for the corresponding uncomplexed molecules in water solution. HF/6-31G (d,p) results.

compound	what is considered	ΔG_{solv} (kcal/mol)	G_{el} (kcal/mol)
A	isolated molecule	-8.49	-10.27
	A-1aq	-7.12	-11.29
	A-3aq	-5.41	-14.17
B	isolated molecule	-14.19	-15.91
	B-4aq	-11.44	-20.70
D	isolated molecule	-9.85	-12.17
	D-2aq	-9.58	-16.56
E	isolated molecule	-8.64	-11.00
	E-1aq	-8.82	-13.19
	E-2aq	-7.52	-15.42
	E-3aq	-7.14	-17.15
F	isolated molecule	-14.58	-16.83
	F-2aq	-13.04	-20.80
	F-5aq	-11.61	-24.56
n-A	isolated molecule	-12.20	-15.14
	n-A-2aq	-11.42	-18.73
	n-A-3aq	-12.68	-22.47
	n-A-4aq	-7.96	-19.85

© University of Venda

University of Venda
Creating Future Leaders

	n-A-5aq	-7.68	-21.13
n-B1	isolated molecule	-10.68	-13.73
	n-B-4aq	-13.05	-24.10
	n-B-5aq	-11.89	-24.86

Table S 1 Results in vacuo for calculations with the 6-311G (d.p) basis set. The results are compared with the corresponding results from using the 6-31G (d.p) basis sets, with the same methods (HF, MP2 and DFT/B3LYP). considering also the addition of diffuse functions only on the heavy atoms or on both the heavy atoms and the hydrogen atoms.

Dipole moment

compound	method	6-31 basis sets	6-311 basis sets
		in vacuo	
A	HF	3.116	3.128
	HF+	3.312	3.279
	HF++	3.306	3.277
	DF	3.015	3.033
	DF+	3.235	3.209
	DF++	3.225	3.204
	MP	3.174	3.181
	MP+	3.386	3.346
	MP++	3.380	3.343
B	HF	4.191	4.155
	HF+	4.360	4.315
	HF++	4.357	4.313
	DF	4.146	4.133
	DF+	4.401	4.353
	DF++	4.393	4.347
	MP	4.332	4.301
	MP+	4.433	4.392
	MP++	4.447	4.409
D	HF	2.359	2.337
	HF+	2.432	2.418
	HF++	2.437	2.410
	DF	2.034	2.108
	DF+	2.168	2.265
	DF++	2.160	2.259
	MP	2.183	2.333
	MP+	2.493	2.395
	MP++	2.477	-
E-S	HF	2.325	2.268

© University of Venda

University of Venda
Creating Future Leaders

	HF+	2.441	2.398
	HF++	2.436	2.394
	DF	2.172	2.123
	DF+	2.362	2.335
	DF++	2.358	2.329
	MP	2.470	2.400
	MP+	2.584	2.528
	MP++	2.580	2.524
E-R	HF	2.267	2.268
	HF+	2.440	2.398
	HF++	2.436	2.394
	DF	2.137	2.123
	DF+	2.362	2.335
	DF++	2.358	2.329
	MP	2.471	2.337
	MP+	2.584	2.449
	MP++	2.580	2.448
F-R	HF	3.060	3.024
	HF+	3.175	3.122
	HF++	3.177	3.121
	DF	3.001	3.010
	DF+	3.165	3.129
	DF++	3.169	3.126
	MP	3.111	3.077
	MP+	3.238	3.182
	MP++	3.243	3.182
F-S	HF	3.067	3.024
	HF+	3.172	3.113
	HF++	3.163	3.126
	DF	3.009	3.059
	DF+	3.165	3.129
	DF++	3.169	3.121
	MP	3.121	-
	MP+	3.165	-
	MP++	3.244	-
G-R	HF	2.640	2.653
	HF+	2.668	2.727
	HF++	2.661	2.729
	DF	2.477	2.421
	DF+	2.616	2.568
	DF++	2.619	2.560
	MP	2.578	2.583
	MP+	2.709	2.665
	MP++	2.697	2.669
G-S	HF	2.659	2.653
	HF+	2.763	2.726
	HF++	2.764	2.727
	DF	2.400	2.421
	DF+	2.617	2.568

© University of Venda

University of Venda
Creating Future Leaders

DF++	2.602	2.560
MP	2.577	2.584
MP+	2.709	2.657
MP++	2.695	2.657

© University of Venda

University of Venda
Creating Future Leaders

CHAPTER 5

DISCUSSION AND CONCLUSION

The study of pyrazole alkaloids, as a sub-class of alkaloids compounds, with the comprehensive approach utilised in this work, is to my knowledge the first of its kind for alkaloids. In view of this, the work considered the aspects that may be relevant in studying these molecules both *in vacuo* and in solution – the study in solution being particularly important for the investigation of the activity of biologically active molecules. The results provide interesting indications for future studies of alkaloids, whose general interest is enhanced by the consideration that many of these compounds are promising biologically active molecules. Their schematic representation with names and acronyms is reported in figure 5.1.

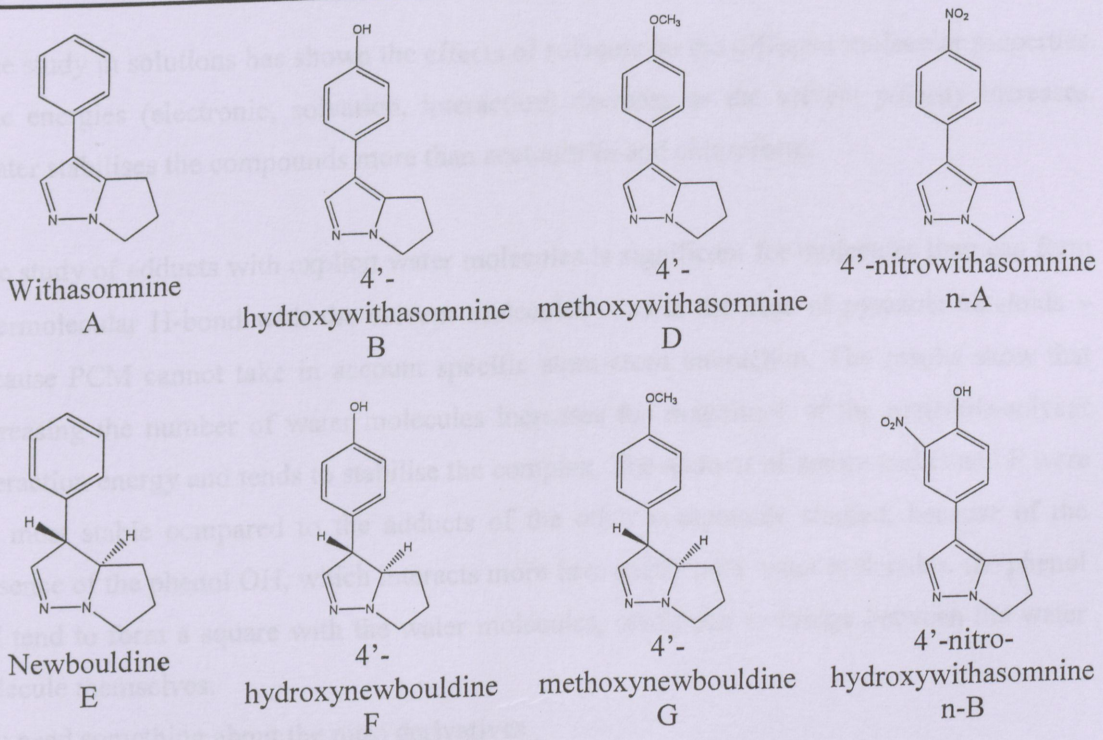

Figure 5.1. Schemes, names and acronyms of all alkaloids and nitroderivatives investigated.

© University of Venda

University of Venda
Creating Future Leaders

The study *in vacuo* of pyrazole alkaloids focused first on their conformers, obtained by optimising geometries with different calculation methods. The geometry parameters were analysed. The average value of the bond length of the C4-C7 bond between the two rings is 1.4 Å and that of the N-N bond in the pyrazole ring is 1.34 Å with all the methods. The factors influencing conformational preferences are the following:

- the mutual orientation of the two rings. The energy difference between the stable orientations is very small.
- The orientation of the phenol OH group, when present. The orientation coplanar to the benzene ring is the most stable.
- The orientation of the methoxy (OCH_3) group, when present. The orientation for which the C atom is coplanar to the benzene ring is the most stable.
- The orientation of the nitro group in n-A. The orientation coplanar to the benzene ring is the most stable.
- The presence of an intramolecular hydrogen bond in n-B. The conformer where it is present is much more stable than the conformer in which it is not present.

The study in solutions has shown the effects of solvents on the different molecular properties. The energies (electronic, solvation, interaction) decrease as the solvent polarity increases. Water stabilises the compounds more than acetonitrile and chloroform.

The study of adducts with explicit water molecules is significant for molecules than can form intermolecular H-bond with the solvent molecules – as is the case of pyrazole alkaloids – because PCM cannot take in account specific atom-atom interaction. The results show that increasing the number of water molecules increases the magnitude of the molecule-solvent interaction energy and tends to stabilise the complex. The adducts of compound B and F were the most stable compared to the adducts of the other compounds studied, because of the presence of the phenol OH, which interacts more favourably with water molecules. the phenol OH tend to form a square with the water molecules, result due to bridge between the water molecule themselves.

You need something about the nitro derivatives

For compound n-B, the length of the IHB increases in the adduct, and its bond angle decreases.

MP2 results were taken as reference to assess the performance of the other methods. The results show that, for the study of pyrazole alkaloids, the less expensive HF level with the

© University of Venda

University of Venda
Creating Future Leaders

addition of diffuse functions, is sufficiently reliable. In most cases, HF has given results closer to MP2 than DFT has. Compared to MP2, DFT tends to overestimate the energy barriers and HF underestimates the energy barriers. DFT also overestimates the strength of hydrogen bonds.

The results of the current work are important because is the first time that a systematic computational study of pyrazole alkaloids has been carried out and, therefore, it makes available new information on these molecules. This information can be utilised for analyses pertaining to drug design, e.g., for the study of quantitative structure-activity relationship (QSAR), where the computational information obtained may be used to try and identify patterns that assist in correlating the physico-chemical and molecular characteristics of alkaloids with their biological activities. It can also be useful as a starting point for other computational studies aimed both at expanding the information related to individual molecules (e.g., by complementing the already performed quantum mechanical studies in solution with Molecular Dynamic studies) and at investigating possible reaction pathways (or modes of action), to try and understand the mechanisms of their biological activity at the molecular level.

© University of Venda

University of Venda
Creating Future Leaders

REFERENCES

1. Snow R. W., Guerra C. A., Noor A. M., Myint H. Y., Hay S. I., *Nature*, 2005, **434** (7030): 214–217.
2. http://www.who.int/malaria/world_malaria_report_2010/malaria2010_summary_keypoints_fr.pdf
3. World Health Organization (2011). World Malaria Report 2011 summary. http://www.who.int/malaria/world_malaria_report_2011/wmr2011_summary_keypoints
4. World Health Organization (2013). World Malaria Report 2013 summary. http://www.who.int/malaria/publications/world_malaria_report_2013/en/
5. WHO, 2008. http://rbm.who.int/wmr.2008.
6. Singh B., Kim S. L., Matusop A., Radhakrishnan A., Shamsul S. S., Cox-Singh J., Thomas A., Conway D. J., A large focus of naturally acquired *Plasmodium knowlesi* infections in human beings, *Lancet* , 2004, **363** (9414) : 1017–1024.
7. Dondorp A. M., Fanello C. I., Hendriksen I. C., Gomes E., Seni A., Chhaganlal K. D., Bojang K., Olaosebikan R., Anunobi N., Maitland K., Kivaya E., Agbenyega T., Nguah S. B., Evans J., Gesase S., Kahabuka C., Mtove G., Nadjm B., Deen J., Mwanga-Amumpaire J., Nansumba M., Karema C., Umulisa N., Uwimana A., Mokuolu O. A., Adedoyin O. T., Johnson W. B. R., Tshefu A. K., Onyamboko M. A., Sakulthaew T., Ngum W. P., Silamut K., Stepniewska K., Woodrow C. J., Bethell D., Wills B., Oneko M., Peto T. E, von Seidlein L., Day N. P. J., White N. J., Artesunate versus quinine in the treatment of severe falciparum malaria in African children (AQUAMAT) : an open-label, randomised trial, *Lancet*, 2010, **376** (9753) : 1647–1657.
8. Foley M., Tilley L., Quinoline antimalarials: Mechanisms of action and resistance and prospects for new agents, *Pharmacology & Therapeutics*, 1998, **79**: 55.
9. Ouellette M., Biochemical and molecular mechanisms of drug resistance in parasites, *Tropical Medicine & International Health,* 2001, **6** (11) : 874-882.
10. Wellems T. E, Plasmodium chloroquine resistance and the search for a replacement antimalarial drug, *Science,* 2002, **298** (5591) : 124–126.
11. Chinappi M., Via A., Marcatili P. and Tramontano A., On the Mechanism of Chloroquine Resistance in *Plasmodium falciparum*, *PloS One,* 2010, **5** (11) : 14064.
12. Olliaro P., Mode of action and mechanisms of resistance for antimalarial drugs, *Pharmacology &Therapeutics,* 2001, **89** (2) : 207–219.

© University of Venda

University of Venda
Creating Future Leaders

13. White N. J, Assessment of the pharmacodynamic properties of antimalarial drugs in vivo, *Antimicrob Agents Chemother*, 1997, **41** (7) : 1413–1422.
14. Buttler A., Hensman T., Artemisinin and a new generation of antimalarial drugs, *Education in Chemistry,* 2000, **37** (6): 151.
15. Artemisinin and a new generation of antimalarial drugs, http://www.rsc.org/Education/EiC/issues/2006July/Artemisinin.asp, Brown G., 2006.
16. Napolitano J. G., Lankin D. C., Graf T.N., Friesen J. B., Chen S.-N., McAlpine J. B., Oberlies N.H., Pauli G. F., HiFSA Fingerprinting Applied to Isomers with near-Identical NMR Spectra: The Silybin/Isosilybin Case. *The Journal of Organic Chemistry*, 2013, **78**: 2827-2839.
17. Batista R., Júnior A. J. S., Oliveira A. B., Plant-Derived Antimalarial Agents: New Leads and Efficient Phytomedicines. Part II. Non-Alkaloidal Natural Products, *Molecules,* 2009, **14:** 3037-3072.
18. Taba K. M, Paulus J., Kayembe J. S, Novel plant remedies show great promise in treating the deadly disease, Global Journal of Research on medicinal plants and ingeniuous medecine, 2012, **1**(3): 62-68.
19. Eyong O. K., Krohn K., Hussain H., Folefoc G. N., Nkengfack A. E., Schulz B., Hu Q., Newbouldiaquinone and newbouldiamide: a new naphthoquinone–anthraquinone coupled pigment and a new ceramide from Newbouldia laevis. *Chemical and Pharmaceutical Bulletin*, 2005, **53**(6): 616–619.
20. Adesanya S. A., Nia R., Fontaine C., Pays M., Pyrazole alkaloids from *Newbouldza laevis*, *Phytochemistry*, 1994, **35** (4): 1053-1055.
21. Nsiama T., Etude comparative de l'activité antipaludique *in vitro* des extraits alcaloïdiques des plantes: *Carica papaya, Newbouldia laevis, Ocimum gratissimum* et *Tithonia diversifolia*, Mémoire de licence, Faculté des Sciences, Université de Kinshasa. (1999) Unpublished.
22. Mifundu N., Etude *in vitro* de l'activité antipaludique des alcaloïdes de *Newbouldia laevis*, Mémoire de licence, Faculté des Sciences, Université de Kinshasa, 2001, Unpublished.
23. Mudimba M., Activité antipaludique des alcaloïdes nitrés de *Newbouldia laevis*, Mémoire de licence, Faculté des Sciences, Université de Kinshasa, 2004, Unpublished.
24. Bosange L. L., Evaluation in vitro de l'activité antipaludique des alcaloïdes nitrés de *Newbouldia laevis*, Mémoire de licence, Faculté des Sciences, Université de Kinshasa, 2008, Unpublished.

© University of Venda

University of Venda
Creating Future Leaders

25. Roy Mc.Weeny, Atoms, *Molecules and Matter: the stuff of chemistry*, 2011, Basic Books in Science, Pisa, Italy.
26. Essén H., Svensson M., Calculation of coordinates from molecular geometric parameters and the concept of a geometric calculator, *Computers and Chemistry* 1996, **20**, 389-395.
27. Daley R. F. and Daley S. J., *Organic Chemistry,* eds. Daley, 2005, 911-977. www.ochem4free.com
28. Lewars, E. G., Computational Chemistry, introduction to the theory and Applications of Molecular and Quantum Mechanics, Springer, 2011, 9-43.
29. Hratchian H. P. and Schlegel H. B., Finding minima, transition states and following reaction pathways on a*b initio* potential energy surfaces, in *Theory and Applications of Computational Chemistry*: *The First 40 Years*, eds. Dykstra C. E., Kim K. S., Frenking G., Scuseria G. E., Elsevier, 2005, 195-259.
30. Schlegel H. B., *Tools for Exploring Potential Energy Surfaces*, in *Modern Electronic Structure Theory*, World Scientific, Singapore, (1994): 459-500.
31. Foresman J. B., Frisch A., *Exploring Chemistry with Electronic Structure Methods,* Gaussian, Inc., Pittsburg, PA (USA), 1995, 39-59.
32. Kraka E., Dunning Jr T. H., Characterization of Molecular Potential Energy Surfaces: Critical Points, Reaction Paths and Reaction Valleys, *Advances in Molecular Electronic Structure Theory,* JAI Press, Greenwich, USA, 1990, **1**:129-173.
33. Fletcher R., *Practical Methods of Optimizations,* Wiley, Chichester, UK, 1987.
34. Murrell J. N., The Potential Energy Surfaces of Polyatomic Molecules, *Structure and Bonding* 1977, **3:** 93.
35. Schrodinger E., Quantisierung als Eigenwertproblem (Erste Mitteilung), *Annals of Physics,* 1926, **79:** 361–376.
36. Schrödinger E., Quantisierung als Eigenwertproblem (Zweiter Mitteilung), *Annals of Physics* ,1926, **79:** 489-527.
37. Schrodinger E., Über das Verhältnis der Heisenberg-Born-Jordanschen Quantenmechanik zu der meinen, *Annals of Physics,* 1926, **79** : 734–756.
38. Szabo A., Ostlund N., *Modern Quantum Chemistry, Introduction to Advanced Electronic Structure theory*, Dover Publications, New York,1996.
39. Born M. and Oppeinheimer R., *Zur Quantentheorie der molekeln*, Annalen der Phyisik, 1927, **84**, 457-484.
40. Lukačević I., The Hartree-Fock approximation: Quantum mechanics 2-Lecture 7, UJJS, Dept. of Physics, Osijek, 2012.

© University of Venda

University of Venda
Creating Future Leaders

41. Fock V., Näherungsmethode zur Lösung des quantenmechanischen Mehrkörperproblems, *Zeitschrift für Physik, Physik Z.*, 1930, **61:** 126-148.
42. Hartree D.R., The wave mechanics of an atom with a non-Coulomb central field. Part I. Theory and methods. *Proceedings of the Cambridge Philosophical Society* , 1928, **24**: 89–110.
43. http://www.physics.sc.edu/~knight/502s08/spin.pdf
44. http://www.tcm.phy.cam.ac.uk/~bds10/aqp/handout_operator.pdf
45. http://eg.bucknell.edu/~koutslts/Ph332/Text/Chap9_JQPMaster.pdf
46. http://www.phys.sinica.edu.tw/TIGP-NANO/Course/2011_Spring/classnotes/CMS_20110511.pdf
47. Lennard-Jones J., The electronic structure of some diatomic molecules, *Transactions of the Faraday Society* ,1929, **25**: 668-686.
48. Jean Y., Volatron F., An Introduction to Molecular Orbitals, Oxford University Press, 1993.
49. Balabin R. M., Communications: Intramolecular basis set superposition error as a measure of basis set incompleteness: can one reach the basis set limit without extrapolation?, *Journal of Chemical Physics*, 2010, **132** (21): 211103.
50. McQuarrie D. A., Simon J. D., *Physical chemistry*: *Molecular Approach*, University Science Books, USA, 1997.
51. Boys S. F., Electronic wave functions. I. A General method of calculation for the stationary states of any molecular system, *Proceedings the Royal Society A,* 1950, **200**: 542-554.
52. Hanninen V., *Introduction to Computational Chemistry*, Laboratory of Physical Chemistry, Helsinki, 2012. http://www.helsinki.fi/kemia/fysikaalinen/opetus/jlk/luennot/Lecture5.pdf
53. Ahlrichs R., Taylor P. R., The choice of gaussian basis sets for molecular electronic structure calculations, *Journal of Chemical Physics*, 1981 **78**: 315-324.
54. Andzelm J., Klobukowski M., Radzio-Andzelm E., Saski Y., Tatewaki H., *Gaussian Basis Sets for Molecular Calculations,* Elsevier, Amsterdam ,1984.
55. Dunning T. H., Hay P. J., Gaussian basis sets for molecular calculations, in: "Modern Theoretical Chemistry, Plenum Press, New York, 1977, **3**: 1-28.
56. Feller D., Davidson E. R., Basis set selection for molecular calculations, *Chemical Reviews*, 1986, **86**: 681-696.

© University of Venda

University of Venda
Creating Future Leaders

57. Feller D., Davidson E. R., Basis Sets for *Ab Initio* Molecular Orbital Calculations and Intermolecular Interactions, *Reviews in Computational Chemistry* VCH, New York , 1990, 1-43.

58. Møller C., Plesset M. S., Note on an approximation treatment for many electron systems, *Physical Review,* 1934, **46 (7)**: 618-622.

59. Bell S., Dines T. J., Chowdhry B. Z. and R. Withnall, Computational Chemistry Using Modern Electronic Structure Methods, *Journal of Chemical Education*, 2007, **84**: 1364-1370.

60. Parr R. G., Yang W., *Density Functional Theory of Atoms and Molecules*. Oxford University Press, 1989.

61. Hohenberg P., Kohn W., Inhomogeneous electron gas, *Physical Review,* 1964, **136**: B864-B871. Becke A. D., Density functional thermochemistry. III. The role of exact exchange, *Journal of Chemical Physics,* 1993, **98**: 5648-5652.

62. Lee C., Yang W., Parr R. G., Development of the Colle-Salvetti correlation-energy formula into a functional of the electron density, *Phys. Rev. B (*1988) **37:** 785–789.

63. Landau L. D., Lifshitz E. M., *Quantum Mechanics* (3rd ed.), 1976, Pergamon Press, Exeter, England.

64. Cotton F. A., *Chemical Applications of Group Theory* (2nd ed.), 1971, New York: Wiley.

65. Wilson, E. B., Decius, J. C., Cross, P. C., *Molecular Vibrations*, 1995, New York: Dover.

66. Baiz C. R., Reppert M., Tokmakoff A., *Introduction to Protein 2D IR Spectroscopy*, Massachusetts Institute of Technology, Cambridge Massachusetts, 2012, 1-38.

67. Walther M. M., Plochocka P., Fischer B., Helm H., Uhd Jepsen P., Collective vibrational modes in biological molecules investigated by terahertz time-domain spectroscopy *Biopolymers (Biospectroscopy),* 2002, **67**(4-5): 310-313.

68. Dan Dill, *Harmonic oscillator Notes on Quantum Mechanics*. http://quantum.bu.edu/notes/QuantumMechanics/HarmonicOscillator.pdf, 2006.

69. Ogilvie J. F., *The Vibrational and Rotational Spectrometry of Diatomic Molecules*, Academic Press, San Diego ,1998.

70. Drees M., *Introduction to Computational Chemistry for Experimental Chemist* (Part 1/2), 11th PhD seminar, Garching, September 12th 2008, Technische Universitate München.

71. HyperChem *Computational Chemistry: Part 1: Practical Guide, Part 2: Theory and Methods*, Hypercube, Inc., 1996.

72. Fukui K., Yonezawa T., Shingu H., A Molecular Orbital Theory of Reactivity in Aromatic Hydrocarbons. *The Journal of Chemical Physics,* 1952, **20** (4): 722-725.

© University of Venda

University of Venda
Creating Future Leaders

73. Klopman G., Chemical reactivity and the concept of charge and frontier controlled reactions, *Journal of the American Chemical Society,* 1968, **90**: 223-234.

74. Salem L., Intermolecular orbital theory of the interaction between conjugated systems. I. General theory. *Journal of the American Chemical Society,* 1968, **90 (3)**: 543-552.

75. Bevan D.R., *QSAR and Drug Design* http://www.netsci.org/Science/Compchem/feature12.html

76. Young D. C., *Computational Chemistry: A Practical Guide for Applying Techniques to Real-World Problems*, John Wiley & Sons, New York, 2001.

77. Kabak M., Elmali A., The Influence of Solvents on Formation of the Molecular Geometry of [{Fe(salphen)}$_2$O] , *Turkish Journal of Physics*, 1998, **22**: 797–801.

78. Kirschner K. N., Woods R. J., Solvent interactions determine carbohydrate conformation, *Proceedings of the National Academy of Sciences*, 2001, **98** (19): 10541–10545.

79. Homocianu M., Airinei A., Dorohoi D. O., Solvent Effects on the Electronic Absorption and Fluorescence Spectra, *Journal of Advanced Research in Physics* ,2011, **2** (1): 1-9.

80. Fawcett W. R., Charge distribution effects in the solution chemistry of polyatomic ions, *Condensed Matter Physics*, 2005, **8**(2): 413–424.

81. Valdebenito S., Zanocco R., Günther G., Lemp E. and Zanocco A. L., Solvent and compartmentalization effectson the photophysics of 4-(benzothiazol-2-yl)-N,N-diphenylaniline, AFINIDAD LXVIII ,2011, **553**: 226-233.

82. Da Silva O., Mennuci B., Vreven T., Density functional study of the optical rotation of glucose in aqueous solution, *Journal of Organic Chemistry*, 2004, **69**(23): 8161–8164.

83. Reichardt C., *Solvents Effects in Organic Chemistry*, 3rd Ed., Willey-VCH Verlag GmBHB& Co., ,2003, 82.

84. Miertus S., Scrocco E., Tomasi J., Electrostatic Interaction of a Solute with a Continuum. A Direct Utilization of *Ab Initio* Molecular Potentials for the Prevision of Solvent Effects, *Chemical Physics*, 1981, **55**:117–129.

85. Goldblum A., Perahia C., Pullman A., Hydration Scheme of Complementary Base-pairs of DNA, *Federation* of *European Biochemical Societies Letters* ,1979, **91**: 213–215.

86. Miertus S., Tomasi J., Approximate Evaluations of the Electrostatic Free-Energy and Internal Energy Changes in Solution Processes, *Chemical Physics*, 1982 **65**: 239–235.

87. Barone V., Cossi M., A New Definition of Cavities for the Computation of Solvation Free Energies by the Polarizable Continuum Model, *Journal of Chemical Physics,* 1997, **107**: 3210–3221.

88. Tomasi J., Mennucci B., Cammi R., Quantum Mechanical Continuum Solvation Models,

© University of Venda

University of Venda
Creating Future Leaders

Chemical Reviews, 2005, **105**: 2999–3093.

89. Barone V., Cossi M., Tomasi J., Geometry Optimization of Molecular Structures in Solution by the Polarizable Continuum Model, *Journal of Computational Chemistry* , 1998,**19**: 404–417.
90. Cossi M., Scalmani G., Rega N., Barone V., New developments in the polarizable continuum model for quantum mechanical and classical calculations on molecules in solution, *Journal of Chemical Physics,* 2002, **117**: 43–54.
91. Cancès E., Mennucci B., Tomasi J., A New Integral Equation Formalism for the Polarizable Continuum Model: Theoretical Background and Applications to Isotropic and Anisotropic Dielectrics, *Journal of Chemical Physics,* 1997, **107**: 3032–3041.
92. Tomasi J., Mennucci B., and Cancès E., The IEF version of the PCM solvation method: an overview of a new method addressed to study molecular solutes at the QM ab initio level. *Journal of Molecular Structure (Theochem.)*, 1999, **464**: 211.
93. Alagona G, Ghio C, Conformational Landscape of (R,R)-Pterocarpans with biological activity in vacuo and in aqueous solution (PCM and/or water clusters), *Journal of Physical Chemistry A*, 2006, **110**: 647-659.
94. Salvador P., Szczęśniak M. M., Counterpoise-corrected geometries and harmonic frequencies of N-body clusters: Application to (HF)n (n=3,4), *Journal of Chemical Physics,* 2003, **118** (2): 537-549.
95. Sedano P. S. Implementation and Application of the Basis Set Superposition Error Correction Schemes to the Theoretical Modelling of Weak Intermolecular Interactions, Doctoral Thesis at the University of Girona, 2001.
96. Boys S. F., Bernardi F. The Calculation of Small Molecular Interactions by the Differences of Separate Total Energies. Some Procedures with Reduced Errors, *Molecular Physics*, 1970, **19:** 553–566.
97. Arunan E., Desiraju G. R., Klein R. A., Sadlej J., Scheiner S., Alkorta I., Clary D. C., Crabtree R. H., Dannenberg J. J., Hobza P., Kjaergaard H. G., Legon A. C., Mennucci B. , Nesbitt D. J., *Definition of the hydrogen bond*, IUPAC Provisional Recommendation, submitted by the IUPAC task group, 2004-026-2-2 100.
98. Smith D. A. (Ed.), *Modelling the Hydrogen Bond*, American Chemical Society, Washington, DC ,1994.
99. Steiner T. The Hydrogen Bond in the Solid State, *Angewandte Chemie International Edition* ,2002, **41**: 48–76.

© University of Venda

University of Venda
Creating Future Leaders

100. Poater J., Fradera X., Solà M., Duran M., Simon S. On the Electron-pair of the Hydrogen Bond in the Framework of the Atoms in Molecules Theory, *Chemical Physics Letters,* 2003, **369**: 248–255.

101. Cornilescu G., Jin-Shan Hu, Bax A., Identification of the Hydrogen Bonding Network in a Protein by Scalar Couplings, *Journal of the American Chemical Society,* 1999, **121**: 2949-2950.

102. Joesten M. D., Schaad L. J., *Hydrogen Bonding*, Marcel Dekker, New York (1974).

103. Schuster P., Zundel G., Sandorfy C. (Eds.). *The Hydrogen Bond: Recent Developments in Theory and Experiments*, North-Holland, Amsterdam, 1976.

104. Scheiner S., Maksic Z. B. (Eds.), *Theoretical Models of Chemical Bonding*, vol.4, Springer Verlag, Berlin, 1991.

105. Naray-Szabo G., Surjan P. R., Angyan, J. G. *Applied Quantum Chemistry*, Akademiai Kiado, Budapest, 1987.

106. Langoor H. M., van der Maas H. J., On the Competitive Intramolecular H-bonding in Alcohols with two Accepting Sites, *Journal of Molecular Structure*, 1997, **403**: 213–229.

107. Lipkowski P., Koll A., Karpfen A., Wolschann P. An Approach to Estimate the Energy of the Intramolecular Hydrogen Bond, *Chemical Physics Letters*, 2002, **360**: 256–263.

108. Latimer W. M., Rodebush W. H., Polarity and Ionisation from the Standpoint of the Lewis Theory of Valence, *Journal of the American Chemical Society*, 1920, **42**: 1419–1433.

109. Pimentel G. C., McClellan A. L. *The Hydrogen Bond*, Freeman, San Francisco (1960).

110. Kojić-Prodić B., Molčanov K., The Nature of Hydrogen Bond: New Insights Into Old Theories, *Acta Chim. Slov.*, 2008, **5**: 692–708.

111. Jeffrey G. A. *An Introduction to Hydrogen Bonding*, Oxford University Press, New York, 1997.

112. Bioactive Compounds http /www.chalmers.se/chem/fbac-en/bioactive-compounds, Guaadaoui A., 2012.

113. Agrawal V. K., Sharma R. and Khadikarb P.V., QSAR Studies on Antimalarial Substituted Phenyl Analogues and Their N^{ω} -Oxides, *Bioorganic & Medicinal Chemistry* , 2002, **10**: 1361–1366.

114. Merz K. M., Ringe D, Reynolds C. H, *Drug design: structure- and ligand-based approaches*, Cambridge University Press., New York, USA , 2010.

115. Batista R., Júnior A. J. S., Oliveira A. B., Plant-Derived Antimalarial Agents: New Leads and Efficient Phytomedicines. Part II. Non-Alkaloidal Natural Products, *Molecules,* 2009,

© University of Venda

University of Venda
Creating Future Leaders

14: 3037-3072.

116. Oliveira A. B., Dolabela M. F., Braga F. C., Jácome L. R. P., Varotti F. C. and Póvoa M. M., Plant-derived antimalarial agents: new leads and efficient phythomedicines,Part I. Alkaloids, Annals of the Brazilian Academy of Sciences, 2009, **81**(4): 715-740

117. Angerhofer C. K, Guinaudeau H, Wongpanich V, Pezzuto J. M and Cordell G. A, Antiplasmodial and cytotoxic activity of natural bisbenzylisoquinoline alkaloids, *Journal of Natural Products*,1999, **62**: 59–66.

118. Lin L. Z, Hu S. F, Chu M., Chan T. M, Chai H, Angerhofer C. K, Pezzuto J. M and Cordell G. A, Phenolic aporphine-benzylisoquinoline alkaloids from *Thalictrum faberi*, *Phytochemestry* , 1999, **50**: 829–834.

119. Carraz M. et al., A plant-derived morphinan as a novel lead compound active against malaria liver stages, *PLoS Medicine* , 2006, **3**: 2392–2402.

120. Bringmann G., Feineis D., Stress-related polyketide metabolism of Diocophyllaceae and Ancistrocladaceae, J Exp Bot , 2001, **52**: 2015–2022.

121. Bringmann G., Messer K., Schwöbel B., Brun R .and Assi L. A, Habropetaline A, an antimalarial naphthylisoquinoline alkalaoid from *Triphyophyllum peltatum*. *Phytochemistry* ,2003, **62**: 345–349.

122. François G., Timperman G., Eling W., Assi L. A and Bringmann G., Naphtylisoquinoline alkaloids against malaria: Evaluation of the curative potential of dioncophylline C and Dioncopeltine A against *Plasmodium berghei in vivo*, Antimicrob Agents Chemother, 1997, **41**: 2533–2539.

123. Cimanga K., Bruyne T. D, Pieters L. and Vlietinck A. J., *In vitro* and *in vivo* antiplasmodial activity ofcryptolepine and related alkaloids from *Cryptolepis sanguinolenta*, *Journal of Natural Products*,1997, **60**: 688–691.

124. Wright C. W, Addae-Kyereme J., Breen A .G, Brown J. E, Cox M. F, Croft S. L, Gok E. K. Y., Kendrick H., Phillips R. M., Pollet P. L., Synthesis and evaluation of cryptolepine analogues for their potential as new antimalarial agents. *Journal of Medicine and Chemistry*, 2001, **44**: 3187–3194.

125. Frederich M., Tits M., Angenot L., Potential antimalarial activity of indole alkaloids, Trans Royal SocTrop Med Hyg, 2008, **102**: 11–19.

126. Frederich M., Jacquier M. J, Thépenier P., Mol P. D, Tits M., Philippe G., Delaude C., Angenot L., Zèches-Hanrot M., Antiplasmodial activity of alkaloids from various *Strychnos* species, *Journal of Natural Products*, 2002, **65**: 1381–1386.

© University of Venda

University of Venda
Creating Future Leaders

127. Frederich M., Tits M., Angenot L., Indole alkaloids from *Strychnos* species and their antiplasmodial and cytotoxic activities, *Chemistry of Natural Compounds*, 2003, **39**: 513–519.

128. Steele J. C. P, Veitch N. C, Kit G. C, Simmonds M. S. J and Warhurst D. C., Indole and β-caboline alkaloids from *Geissospermum sericeum, Journal of Natural Products,* 2002, **65**: 85–88.

129. Julian V., Bourdy G., Georges S., Maurel S. and Sauvain M., Validation of use a traditional antimalarial remedy from French Guiana, *Zanthoxylum rhoifolium* Lam, *Journal of Ethnopharmacol*, 2006, **106**: 348–352.

130. Randrianarivelojosia M., Rasidimanana V. T, Rabarison H., Cheplogoi P. K, Ratsimbason M., Mulholland D., Mauclère P., Plants traditionally prescribed to treat *tazo* (malaria) in the eastern region of Madagascar, *Malaria Journal*, 2003, **2**: 25–35.

131. Fujioka H., Nishiyama Y., Furukawa H., Kumada N., *In vitro* and *in vivo* activities of atalaphilline and related acridone alkaloids against rodent malaria, *Antimicrobial Agents and Chemotherapy*, 1989, **33**: 6–9.

132. Basco L. K, Mitaku S., Tsounis S. A. L, Ravelomanantsoa N., Tillequin F., Koch M. and Bras J. L., *In vitro* activities of furoquinoline and acridone alkaloids against *Plasmodium falciparum*, *Antimicrobial Agents and Chemotherapy*, 1994,**38**: 1169–1171.

133. Jacquemond-Collet I., Benoit-Vical F., Valentin A., Stanislas E., Mallie M., Fouraste I., Antiplasmodial and cytotoxic activity of galipinine and other tetrahydroquinolines from *Galipea officinalis*, *Planta Medica*, 2002, **68**: 68–69.

134. Silva T. H. A., Oliveira A. B. and Almeida W. B., Conformational analysis of the antimalarial agent Quinine, *Structural Chemistry*, 1997, **8**(2): 95-107.

135. Julı´nek O., Krupicˇka M., Lindnerc W., Urbanova M., Enantioselective interaction of carbamoylated quinine and (S)-3,5-dinitrobenzoyl alanine: theoretical and experimental circular dichroism study, *Physical Chemistry Chemical Physics,* 2010, **12**: 11487–11497.

136. Joshi S. and Pant D., Solvatochromic Shift and Estimation of Dipole Moment of Quinine Sulphate Dication, *International Journal of Chemical and Biological Engineering*, 2012, **6**: 225-229.

137. Bhattacharjee A. K. Electrostatic potential profiles may guide cation–pi interaction in antimalarials chloroquine and mefloquine: an *ab initio* quantum chemical study, *Journal of Molecular Structure* (*THEOCHEM*), 2000 **529**:193–201.

138. Bhattacharjee A. K., Kyle D. E, Vennerstrom J. L. and W. K. Milhous, A 3D QSAR Pharmacophore Model and Quantum Chemical Structure-Activity Analysis of

© University of Venda

University of Venda
Creating Future Leaders

Chloroquine (CQ)-Resistance Reversal, *Journal of Chemical Information and Computer Sciences*, 2002, **42**: 1212-1220.

139. Nguyen-Cong V. and Rode B. M., Quantum Pharmacological Analysis of Structure-Activity Relationships for Mefloquine Antimalarial Drugs Using Optimal Transformations, *Journal of Chemical Information and Computer Sciences*, 1996, **36**: 114-117.

140. Cardoso F. J. B., Da Costa R. B., De Figueiredo A. F., Barbosa J. P., Nava I. Jr., Pinheiro J. C., Romero O. A. S., Modeling Artemisinin Derivatives with Potent Activity against *P. falciparum* Malaria with *Ab Initio* and PLS Method, *Internet Electronic Journal of Molecular Design*, 2007, **6**: 122–134.

141. Pinheiro J. C., Kiralj R., Ferreira M. M. C., Romero O. A. S., Artemisinin Derivatives with Antimalarial Activity against Plasmodium falciparum Designed with the Aid of Quantum Chemical and Partial Least Squares Methods, *QSAR & Combinatorial Science*, 2003, **22**: 830-842.

142. Sullivan D. J. Jr, Kaludov N. and Martinov M. N., Discovery of potent, novel, non- toxic anti-malarial compounds via quantum modelling, virtual screening and in vitro experimental validation, *Malaria Journal*, 2011, **10**: 274-282.

143. Fernandez I. and Robert A., Peroxide bond strength of antimalarial drugs containing an endoperoxidecycle. Relation with biological activity, *Organic &Biomolecular Chemistry* , 2011, **9**: 4098–4107.

144. Gaussian 03 User's Reference Manual Version 7, Gaussian Inc., 2003, Pittsburgh, Pennsylvania.

145. Császár C., Pulay P., Geometry optimization by direct inversión in the iterative subspace, *Journal of Molecular Structure*, 1984, **114**, 31-34.

146. Saracino G. A. A., Improta R., Barone V. Absolute pKa determination for carboxylic acids using density functional theory and the polarizable continuum model, *Chemical Physics Letters*, 2003), **373:** 411–415.

147. Spoliti M., Bencivenni L., Quirante J. J, Ramondo F., Molecular conformations and harmonic force field of 1,3,5-benzenetriol molecule from ab initio and density functional theory investigations, *Journal of Molecular Structure (THEOCHEM)*, 1997, **390**: 139–148.

148. Rudyk R., Molina M. A. A, Yurquina A., Gómez M. I, Blanco S. E, Ferretti F. H J, A theoretical and experimental study on the structure and dipole moment of phloroglucinol in ethanol, *Journal of Molecular Structure (THEOCHEM)*, 2004, **673**: 231–238.

© University of Venda

University of Venda
Creating Future Leaders

149. Mammino L., Kabanda M. M, A study of the intramolecular hydrogen bond in acylphloroglucinols, *Journal of Molecular Structure (THEOCHEM)*, 2009, **901**: 210–219.

150. Buemi G., Zuccarello F., Is the intramolecular hydrogen bond energy vbaluable from internal rotation barriers?, *Journal of Molecular Structure (THEOCHEM)*, 2002, **581**: 71-85.

151. Mammino L., Kabanda M. M, A computational study of the effects of different solvents on the charactertics of the intramolecular hydrogen bond in acylphloroglucinols, *Journal of Physical Chemistry A*, 2009, **113** (52): 15064–15077.

152. Alagona, G., Ghio C., Interplay of intra- and intermolecular H-bonds for the addition of a water molecule to the neutral and N-proronated forms of noradrenaline, *International Journal of Quantum Chemistry,* 2002, **90**: 641-656.

153. Korth H-G., de Herr M. I., Mulder P. A DFT study on intramolecular hydrogen bonding in 2-substituted phenols: conformations, enthalpies, and correlation with solute parameters, *Journal of Physical Chemistry A*, 2002, **106 (37)**: 8779-8789.

© University of Venda